



National Library
of Canada

Bibliothèque nationale
du Canada

Canadian Theses Service

Service des thèses canadiennes

Ottawa, Canada
K1A 0N4

NOTICE

The quality of this microform is heavily dependent upon the quality of the original thesis submitted for microfilming. Every effort has been made to ensure the highest quality of reproduction possible.

If pages are missing, contact the university which granted the degree.

Some pages may have indistinct print especially if the original pages were typed with a poor typewriter ribbon or if the university sent us an inferior photocopy.

Reproduction in full or in part of this microform is governed by the Canadian Copyright Act, R.S.C. 1970, c. C-30, and subsequent amendments.

AVIS

La qualité de cette microforme dépend grandement de la qualité de la thèse soumise au microfilmage. Nous avons tout fait pour assurer une qualité supérieure de reproduction.

S'il manque des pages, veuillez communiquer avec l'université qui a conféré le grade.

La qualité d'impression de certaines pages peut laisser à désirer, surtout si les pages originales ont été dactylographiées à l'aide d'un ruban usé ou si l'université nous a fait parvenir une photocopie de qualité inférieure.

La reproduction, même partielle, de cette microforme est soumise à la Loi canadienne sur le droit d'auteur, SRC 1970, c. C-30, et ses amendements subséquents.



National Library
of Canada

Bibliothèque nationale
du Canada

Canadian Theses Service Service des thèses canadiennes

Ottawa, Canada
K1A 0N4

The author has granted an irrevocable non-exclusive licence allowing the National Library of Canada to reproduce, loan, distribute or sell copies of his/her thesis by any means and in any form or format, making this thesis available to interested persons.

The author retains ownership of the copyright in his/her thesis. Neither the thesis nor substantial extracts from it may be printed or otherwise reproduced without his/her permission.

L'auteur a accordé une licence irrévocable et non exclusive permettant à la Bibliothèque nationale du Canada de reproduire, prêter, distribuer ou vendre des copies de sa thèse de quelque manière et sous quelque forme que ce soit pour mettre des exemplaires de cette thèse à la disposition des personnes intéressées.

L'auteur conserve la propriété du droit d'auteur qui protège sa thèse. Ni la thèse ni des extraits substantiels de celle-ci ne doivent être imprimés ou autrement reproduits sans son autorisation.

ISBN 0-315-56089-4

Canada

Stability Analysis and Directional Response Characteristics
of Heavy Vehicles Carrying Liquid Cargo

Raman Ranganathan

A thesis
in
The Faculty
of
Engineering
and
Computer Science

Presented in Partial Fulfillment of the Requirements
for the Degree of Doctor of Philosophy at
Concordia University
Montréal, Québec, Canada

February 1990

© Raman Ranganathan, 1990

ABSTRACT

Stability Analysis and Directional Response Characteristics of Heavy Vehicles Carrying Liquid Cargo

Raman Ranganathan
Concordia University, 1990

Liquid motion within a partially filled tank generates slosh forces and moments of considerable magnitude. The stability and the directional dynamics of partially filled tank vehicles are adversely influenced by the dynamic loads due to liquid movement within the tank. The stability analysis and directional response characteristics of heavy vehicles carrying liquid cargo are carried out in four phases: (i) kineto-static stability analysis of tank vehicles; (ii) directional stability analysis of tank vehicles assuming steady-state fluid motion; (iii) directional stability analysis of tank vehicles using a dynamic liquid slosh model; and (iv) validation of computer simulation results through field testing.

A kineto-static roll plane model of a tractor-semitrailer equipped with a partially filled tank of arbitrary cross-section is developed. Roll stability limits of partially filled tank vehicles are determined via computer simulation for typical cornering manoeuvres. Influence of various vehicle and tank design factors on roll stability limits is investigated. A quasi-dynamic directional response model of a partially filled tank vehicle is developed by integrating the steady-state roll plane model of fluid with three-dimensional model of the vehicle, assuming constant forward speed. Computer simulation is carried out to determine the directional response of tank vehicles subject to both open- and closed-loop steer inputs. The directional response characteristics of tank vehicles are compared to those of

equivalent rigid cargo vehicles to demonstrate the adverse influence of liquid motion on the directional stability of heavy vehicles. The directional behaviour of tank vehicles is further investigated in view of variations in vehicle speed, fill level and fluid density.

A comprehensive tank vehicle model is formulated by integrating a two-dimensional non-linear fluid slosh model of a partially filled cylindrical tank with the three-dimensional vehicle model. The dynamic slosh forces and moments are computed from dynamic fluid slosh model of the partially filled tank. The directional response characteristics of the partially filled tank vehicle are then evaluated, incorporating dynamic slosh loads and compared to those attained from the quasi-dynamic vehicle model. The analytical tank vehicle models are validated through field tests. The directional response characteristics of the tank vehicle from field testing compared well to those obtained from computer simulations to demonstrate a high degree of confidence in the analytical simulation in predicting the stability and directional behaviour of tank vehicles.

ACKNOWLEDGEMENTS

The author wishes to thank the supervisors, Dr. S. Sankar and Dr. S. Rakheja for their guidance and encouragement during the course of this investigation. The author wishes to acknowledge CONCAVE Research Centre for the financial support provided to him to undertake this investigation. The cooperation extended by the members of the CONCAVE Research Centre and of the Department of Mechanical Engineering is gratefully acknowledged. The author is thankful to the staff of Ontario Ministry of Transportation for their technical support during the investigation.

The author also wishes to thank Mr. Gennady Popov, Mr. Moses Levy and Mr. Ramesh Rajagopalan for their technical and moral support provided during the preparation of this dissertation.

Finally, the author is deeply indebted to his parents and family members for their continued support and understanding.

TABLE OF CONTENTS

	<u>Page</u>
LIST OF FIGURES	xi
LIST OF TABLES	xix
NOMENCLATURE	xx
CHAPTER 1	
INTRODUCTION	
1 1 Problem Background	1
1.2 Tank Vehicle Accidents	4
1.3 Scope and Layout of the Thesis	11
REFERENCES FOR CHAPTER 1	14
CHAPTER 2	
KINETO-STATIC ROLL PLANE MODEL OF A PARTIALLY FILLED TANK VEHICLE	
2.1 General	15
2.2 State-of-the-Art Investigations on the Rollover Threshold of Heavy Vehicles	16
2.3 Stability of Liquid Tank Vehicles during Steady Turning	19
2.4 Selection of Candidate Tank Vehicle Configurations	20
2.5 Selection of Tank Cross-sections	23
2.6 Computation of the Gradient of Free Surface of Liquid within a Tank	26
2.7 Roll Plane Steady State Fluid Model of a Partially Filled Tank	31
2.7.1 Circular Cross-section	31
2.7.2 Modified Oval Cross-section	33
2.7.3 Modified Square Cross-section	37
2.7.4 Elliptical Cross-section	37

	<u>Page</u>
2.8 Kineto-Static Roll Plane Model of an Articulated Tank Vehicle	38
2.9 Equations of Kineto-Static Roll Equilibrium	47
2.9.1 Roll Moments Acting on Sprung Weights	47
2.9.2 Roll Moments Acting on Unsprung Weights	49
2.9.3 Forces Acting through the Suspension Springs	50
2.9.4 Vertical Forces Generated by the Tires	50
2.9.5 Lateral Forces Generated by the Tires	51
2.10 Summary	51
REFERENCES FOR CHAPTER 2	52

CHAPTER 3

ROLLOVER THRESHOLD LIMITS OF LIQUID TANK VEHICLES

3.1 General	53
3.2 Method of Solution	53
3.3 Load Shift during Steady Turning	55
3.4 Rollover Acceleration Limits of Tank Vehicles	63
3.4.1 Rollover Threshold of Tank Vehicles (Variable Axle Loads)	63
3.4.2 Rollover Threshold of Tank Vehicles (Constant Axle Loads)	66
3.5 Rollover Threshold Limits of Compartmented Tank Vehicles	68
3.6 Summary	76
REFERENCES FOR CHAPTER 3	79

CHAPTER 4

QUASI-DYNAMIC DIRECTIONAL RESPONSE MODEL OF A PARTIALLY FILLED TANK VEHICLE

4.1 General	80
4.2 Review of Previous Investigations	81
4.3 Development of a Quasi-Dynamic Tank Vehicle Model	83
4.3.1 Steady State Roll Plane Model of Fluid Motion in a Partially Filled Circular Tank	84

	<u>Page</u>
4.3.2 Steady State Roll Plane Model of Fluid Motion in a Partially Filled Modified-Oval Tank	87
4.4 Modeling of a Tractor-Semitrailer Tank Vehicle	89
4.5 Modeling of a B-Train Tank Vehicle	92
4.6 Model Assumptions	92
4.7 Equations of Motion of an Articulated Tank Vehicles	94
4.7.1 Axis Systems	97
4.7.2 Equations of Motion	97
4.7.3 Computation of Liquid Mass Acceleration	100
4.7.4 Constraint Equations	100
4.8 Summary	102
REFERENCES FOR CHAPTER 4	103

CHAPTER 5

DIRECTIONAL RESPONSE OF TANK VEHICLE COMBINATIONS

5.1 General	104
5.2 Method of Solution	104
5.3 Directional Response of Tractor-Semitrailer Tank Vehicle	106
5.3.1 Open-Loop Constant Steer Manoeuvre	106
5.3.1.1 Directional Response of Five-Axle Tractor-Semitrailer Combination (Variable Axle Loads)	106
5.3.1.2 Directional Response of Five-Axle Tractor-Semitrailer Combination (Constant Axle Loads)	113
5.3.1.3 Directional Response of Six-Axle Tractor-Semitrailer Combination (Constant Axle Loads)	117
5.3.2 Closed-Loop Transient Steer Manoeuvre	119
5.3.2.1 Directional Response of Five-Axle Tractor-Semitrailer Combination (Variable Axle Loads)	119
5.3.2.2 Directional Response of Five-Axle Tractor-Semitrailer Combination (Constant Axle Loads)	124
5.3.2.3 Directional Response of Six-Axle Tractor-Semitrailer Combination (Constant Axle Loads)	127
5.3.3 Directional Response of a Compartmented Tank Vehicle	127
5.4 Directional Response of a B-Train Tank Vehicle	135
5.4.1 Open-Loop Constant Steer Manoeuvre (Constant Axle Loads)	135
5.4.2 Closed-Loop Transient Steer Manoeuvre (Constant Axle Loads)	144
5.4.2.1 Lane Change Manoeuvre	144

	<u>Page</u>
5.4.2.2 Evasive Manoeuvre	146
5.4.3 Roll and Lateral Acceleration Amplification	150
5.5 Summary	153
REFERENCES FOR CHAPTER 5	155

CHAPTER 6

DYNAMIC STABILITY ANALYSIS OF LIQUID TANK VEHICLES SUBJECT TO LIQUID SLOSH FORCES

6.1 General	156
6.2 Survey of Past Investigations on Dynamic Behaviour of Liquid within a Moving Vehicle	157
6.3 Development of the Tank Vehicle Model	161
6.3.1 Development of the Liquid Slosh Model	162
6.3.2 Dynamic Model of the Tank Vehicle	166
6.4 Equations of Motion	167
6.5 Method of Solution	168
6.6 Directional Response of the Tank Vehicle	169
6.6.1 Constant Steer Manoeuvre	171
6.6.2 Transient Steer Manoeuvre	177
6.7 Summary	183
REFERENCES FOR CHAPTER 6	184

CHAPTER 7

FIELD TESTING OF A TANK VEHICLE

7.1 General	185
7.2 Description of the Test Vehicle	185
7.3 Description of the Test Program	190
7.3.1 Test Manoeuvres	195
7.3.2 Instrumentation	197
7.4 Comparison of Simulation with Field Test Results	198
7.4.1 30m Constant Radius Turn	198
7.4.2 Lane Change Manoeuvre	207

	<u>Page</u>
7.5 Summary	213
REFERENCES FOR CHAPTER 7	215

CHAPTER 8

CONCLUSIONS AND SUGGESTIONS FOR FUTURE RESEARCH

8.1 General	216
8.2 Highlights of the Investigation and Conclusions	217
8.2.1 Steady-Turning Stability Analysis	217
8.2.2 Directional Stability Analysis	218
8.2.3 Directional Stability Analysis incorporating Dynamic Fluid Slosh	219
8.2.4 Validation of Analytical Models	220
8.3 Suggestions for Future Research	221

APPENDIX I

DERIVATION OF EQUATIONS OF MOTION FOR THE KINETO-STATIC ROLL PLANE MODEL OF AN ARTICULATED TANK VEHICLE

APPENDIX II

DERIVATION OF EQUATIONS OF MOTION FOR THE DYNAMIC YAW/ROLL MODEL

LIST OF FIGURES

<u>Figure</u>		<u>Page</u>
2.1	Schematic of various vehicle configurations	22
2.2	Tank cross-sections commonly used in liquid bulk transportation	25
2.3	Roll plane model of an articulated vehicle	27
2.4	Translation of centre of gravity (C.G) of liquid due to tank tilt	28
2.5	Translation of C.G of liquid due to tank tilt and lateral acceleration	28
2.6	Equilibrium of a fluid element within a partially filled tank subject to tilt and lateral acceleration	30
2.7	Roll plane steady state fluid model of a partially filled circular tank cross-section	32
2.8	Cross-section of a modified oval tank	34
2.9	Roll plane steady state fluid model of a partially filled modified-oval tank cross-section	34
2.10	Roll plane steady state model of a partially filled elliptical tank cross-section	39
2.11	Composite axle representation of a tractor-semitrailer	40
2.12	Representation of the tractor-tank semitrailer and the axles	42
2.13	Typical torque-deflection characteristics of the tractor frame	43
2.14	Kineto-static roll plane model of a tank vehicle	45
2.15	Force deflection characteristics of the suspension springs	46
3.1	Lateral translation of C.G of liquid due to tank roll alone	57
3.2	Lateral translation of C.G of liquid due to tank roll and lateral acceleration	59
3.3	Comparison of lateral translation of C.G of liquid in various tanks	60
3.4	Vertical translation of C.G of liquid due to tank roll and lateral acceleration	61

<u>Figure</u>		<u>Page</u>
3.5	Comparison of vertical translation of C.G of liquid in various tanks	62
3.6	Rollover threshold acceleration of equivalent rigid cargo and circular tank vehicles (Variable axle loads)	64
3.7	Rollover threshold acceleration of equivalent rigid cargo and modified-oval tank vehicles (Variable axle loads)	64
3.8	Rollover threshold acceleration of equivalent rigid cargo and modified-square tank vehicles (Variable axle loads)	65
3.9	Rollover threshold acceleration of equivalent rigid cargo and elliptic tank vehicles (Variable axle loads)	65
3.10	Comparison of rollover acceleration limits of tank vehicles with various tank cross-sections (Variable axle loads)	67
3.11	Rollover threshold acceleration of equivalent rigid cargo and circular tank vehicles (Constant axle loads)	69
3.12	Rollover threshold acceleration of equivalent rigid cargo and modified-oval tank vehicles (Constant axle loads)	69
3.13	Rollover threshold acceleration of equivalent rigid cargo and modified-square tank vehicles (Constant axle loads)	70
3.14	Rollover threshold acceleration of equivalent rigid cargo and elliptic tank vehicles (Constant axle loads)	70
3.15	Comparison of rollover acceleration limits of tank vehicles with various tank cross-sections (Constant axle loads)	71
3.16	Schematic of a compartmented tank vehicle	73
3.17	Rollover acceleration limits of a compartmented tank vehicle with partial load in one of the compartments	74
3.18	Rollover acceleration limits of a compartmented tank vehicle with an empty compartment and partial load in one of the other compartments	75
3.19	Rollover acceleration limits of a compartmented tank vehicle with two empty compartments and partial load in one of the other compartments	77
4.1	Roll plane model of a circular tank cross-section	85
4.2	Computation of the moment of inertias of the liquid mass	88
4.3	Roll plane model of the tank vehicle	90

<u>Figure</u>		<u>Page</u>
4.4	Pitch plane of the tractor-semitrailer tank vehicle and the various coordinate systems	91
4.5	Pitch plane of the B-train tank vehicle and the various coordinate systems	93
4.6	Idealized representation of the axles and suspension in the roll plane of the tank vehicle	95
4.7	Cornering force and aligning moment characteristics of the tires under various normal loads	96
5.1	Roll response of a two-axle semitrailer with liquid and equivalent rigid cargo loads	108
5.2	Lateral acceleration response of a two-axle semitrailer with liquid and equivalent rigid cargo loads	108
5.3	Dynamic vertical load factor on the left track of the last axle of the five-axle tractor semitrailer	110
5.4	Comparison of path followed by a partially filled tank and equivalent rigid cargo five-axle tractor semitrailer vehicle	110
5.5	Roll response of a two-axle semitrailer with liquid and equivalent rigid cargo loads	112
5.6	Lateral acceleration response of a two-axle semitrailer with liquid and equivalent rigid cargo loads	112
5.7	Roll response of a two-axle semitrailer with liquid and equivalent rigid cargo loads	115
5.8	Lateral acceleration response of a two-axle semitrailer with liquid and equivalent rigid cargo loads	115
5.9	Dynamic vertical load factor on the left track of the last axle of the five-axle tractor semitrailer	116
5.10	Roll response of a two-axle semitrailer with liquid and equivalent rigid cargo loads	116
5.11	Roll response of a three-axle semitrailer with liquid and equivalent rigid cargo loads	118
5.12	Lateral acceleration response of a three-axle semitrailer with liquid and equivalent rigid cargo loads	118
5.13	Vehicle path during typical lane change and evasive manoeuvres	121

<u>Figure</u>		<u>Page</u>
5.14	Front wheel steer angles required to perform a typical lane change and an evasive manoeuvre	122
5.15	Lateral load shift in a partially filled two-axle tank trailer during a lane change manoeuvre	122
5.16	Roll angle response of a partially filled liquid and equivalent rigid cargo two-axle semitrailers during a lane change manoeuvre	123
5.17	Roll angle response of a partially filled liquid and equivalent rigid cargo two-axle semitrailers during an evasive manoeuvre	123
5.18	Roll angle response of a partially filled liquid and equivalent rigid cargo two-axle semitrailers during an evasive manoeuvre	125
5.19	Vertical load on the left track of the rearmost axle of a five-axle tractor semitrailer carrying liquid and equivalent rigid cargo, during an evasive manoeuvre	126
5.20	Vertical load on the right track of the rearmost axle of a five-axle tractor semitrailer carrying liquid and equivalent rigid cargo, during an evasive manoeuvre	126
5.21	Roll response of a partially filled liquid and equivalent rigid cargo three-axle semitrailers, during a lane change manoeuvre	128
5.22	Lateral acceleration response of a partially filled liquid and equivalent rigid cargo three-axle semitrailers, during a lane change manoeuvre	128
5.23	Roll response of a partially filled liquid and equivalent rigid cargo three-axle semitrailers, during an evasive manoeuvre	129
5.24	Four compartmented modified oval tank	132
5.25	Comparison of roll response of a compartmented and cleanbore modified oval tank vehicle	133
5.26	Comparison of lateral acceleration response of a compartmented and cleanbore modified oval tank vehicle	134
5.27	Roll response of semitrailer B of a 7-axle B-train with liquid and equivalent rigid cargo loads	138
5.28	Lateral acceleration response of semitrailer B of a 7-axle B-train with liquid and equivalent rigid cargo loads	138

<u>Figure</u>		<u>Page</u>
5.29	Roll rate response of semitrailer B of a 7-axle B-train with liquid and equivalent rigid cargo loads	140
5.30	Roll response of semitrailer B of a 7-axle B-train with liquid and equivalent rigid cargo loads	141
5.31	Roll response of semitrailer B of a 7-axle B-train with liquid and equivalent rigid cargo loads	141
5.32	Comparison of vehicle path followed by a partially filled and an equivalent rigid cargo B-train tank vehicles	143
5.33	Roll response of semitrailer B of a 7-axle B-train with liquid and equivalent rigid cargo loads	143
5.34	Roll response of semitrailer B of a 7-axle B-train with liquid and equivalent rigid cargo loads, during a lane change manoeuvre	145
5.35	Lateral acceleration response of semitrailer B of a 7-axle B-train with liquid and equivalent rigid cargo loads, during a lane change manoeuvre	145
5.36	Roll response of semitrailer B of a 7-axle B-train with liquid and equivalent rigid cargo loads, during a lane change manoeuvre	147
5.37	Roll response of semitrailer B of a 7-axle B-train with liquid and equivalent rigid cargo loads, during an evasive manoeuvre	149
5.38	Lateral acceleration response of semitrailer B of a 7-axle B-train with liquid and equivalent rigid cargo loads, during an evasive manoeuvre	149
5.39	Dynamic vertical load ratio on the left track of the rearmost axle of a B-train tank vehicle, during an evasive manoeuvre	151
5.40	Roll response of semitrailer B of a 7-axle B-train with liquid and equivalent rigid cargo loads, during an evasive manoeuvre	151
6.1	Natural frequency of liquid as a function of fill condition within a cylindrical tank cross-section	159
6.2	Coordinate system and mesh arrangement of a circular tank cross-section	163
6.3	Computation of the directional response of a tank vehicle	170

<u>Figure</u>		<u>Page</u>
6.4	Comparison of roll response of dynamic slosh and quasi-dynamic tank vehicle models	172
6.5	Comparison of lateral acceleration response of dynamic slosh and quasi-dynamic tank vehicle models	172
6.6	Comparison of roll rate response of dynamic slosh and quasi-dynamic tank vehicle models	174
6.7	Comparison of roll angle response of dynamic slosh and quasi-dynamic tank vehicle models	174
6.8	Comparison of roll angle response of dynamic slosh models, under various fill conditions	176
6.9	Height of the liquid free surface at the centre, right and left walls of the tank, during a constant steer manoeuvre	176
6.10	Comparison of roll angle response of dynamic slosh and quasi-dynamic tank vehicle models, during a lane change manoeuvre	178
6.11	Comparison of lateral acceleration response of dynamic slosh and quasi-dynamic tank vehicle models, during a lane change manoeuvre	178
6.12	Comparison of roll rate response of dynamic slosh and quasi-dynamic tank vehicle models, during a lane change manoeuvre	180
6.13	Comparison of roll angle response of dynamic slosh model under various fill conditions, during a lane change manoeuvre	180
6.14	Comparison of roll angle response of dynamic slosh and quasi-dynamic tank vehicle models, during an evasive manoeuvre	182
6.15	Comparison of lateral acceleration response of dynamic slosh and quasi-dynamic tank vehicle models, during an evasive manoeuvre	182
7.1	Schematic of the test vehicle tank	189
7.2	Tank mounting frame assembly	191
7.3	Rear view of the tank assembly	192
7.4	Side view of the tank assembly	193
7.5	Typical 30m radius turn manoeuvre path	196
7.6	Typical 15m lane change manoeuvre path	196

<u>Figure</u>		<u>Page</u>
7.7	Pictorial views of the tank truck used in the field test	200
7.8	Repeatability of the test runs	202
7.9	Comparison of experimental and simulation response of the 50% filled tank vehicle at a vehicle speed of 39 km/h, during a 30m radius turn	203
7.10	Comparison of experimental and simulation response of the 50% filled tank vehicle at a vehicle speed of 29 km/h, during a 30m radius turn	205
7.11	Comparison of experimental and simulation response of the 70% filled tank vehicle at a vehicle speed of 39 km/h, during a 30m radius turn	206
7.12	Comparison of experimental and simulation response of the 50% filled tank vehicle at a vehicle speed of 45 km/h, during a 15m lane change manoeuvre	208
7.13	Comparison of experimental and simulation response of the 50% filled tank vehicle at a vehicle speed of 35 km/h, during a 15m lane change manoeuvre	210
7.14	Comparison of experimental and simulation response of the 50% filled tank vehicle at a vehicle speed of 45 km/h, during a 21m lane change manoeuvre	211
7.15	Comparison of experimental and simulation response of the 50% filled tank vehicle at a vehicle speed of 35 km/h, during a 21m lane change manoeuvre	212
7.16	Comparison of experimental and simulation response of the 70% filled tank vehicle at a vehicle speed of 45 km/h, during a 15m lane change manoeuvre	214
I.1	Representation of the tractor-tank semitrailer and the axles	224
I.2	Forces and moments acting on the roll plane of a tank vehicle	225
II.1	Pitch plane and the coordinate system attached to an articulated tank vehicle	233
II.2	Euler angle representation of the sprung mass axis system	234
II.3	Euler angle representation of the unsprung mass axis system	236
II.4	Roll plane model of a tank vehicle	238
II.5	Coordinate system attached to the fifth wheel arrangement	245

<u>Figure</u>	<u>Page</u>
II.6 Typical path geometry used in the preview control driver model	251
II.7 Representation of the preview control driver model	253
II.8 Implementation of the driver model in the vehicle simulation	253

LIST OF TABLES

<u>Table</u>		<u>Page</u>
1.1	Dangerous occurrences in transit during 1981-83	6
1.2	Dangerous occurrences during 1981-83 by class of dangerous goods	6
1.3	Causal factors related to dangerous occurrences	7
1.4	Fatalities and injuries incurred during 1981-83 involving single and multi-vehicle accidents	9
1.5	Property damage incurred during 1981-83 involving single and multi-vehicle accidents	9
2.1	Rollover threshold limits of heavy vehicles	17
2.2	Population of the various vehicle combinations present in various centres across Canada	21
2.3	Most commonly used tank vehicle configurations in Canada	24
3.1	Specifications of the tank vehicle used in simulation	56
5.1	Comparison of the directional characteristics of 5- and 6-axle tractor semitrailer tank vehicle	120
5.2	Comparison of the directional characteristics of 5- and 6-axle tractor semitrailer tank vehicle	130
5.3	Load distribution sequences in a four compartmented modified oval tank vehicle	132
5.4	Specifications of the B-train tank vehicle used in the simulation	137
5.5	Roll and lateral acceleration amplification factors for the B-train subject to lane change and evasive manoeuvre at various vehicle speeds.	153
7.1	Specifications of the front and rear axles and force deflection characteristics of the suspension springs	187
7.2	Specifications of the tank used in field test	189
7.3	Liquid load data corresponding to various fill conditions	194
7.4	Axle loads under various fill conditions	194
7.5	Test vehicle instrumentation list	199

NOMENCLATURE

a_f :	Lateral acceleration of the sprung mass f (m/s^2)
a_ℓ :	Lateral acceleration imposed on the liquid during steady turning (m/s^2)
$a_{\ell f}$:	Lateral acceleration imposed on the fluid in unit f (m/s^2)
a_y :	Vehicle lateral acceleration during steady turning (m/s^2)
A_a :	Lateral acceleration amplification factor
A_θ :	Roll amplification factor
AT_{ij} :	Aligning moment of tire j on axle i (N.m)
b_i :	Dual tire spacing of tires on axle i (m)
C_{tr} :	Torsional coulumb friction in the tractor frame (N.m)
F_{rl} :	Lateral forces acting through the roll centre (N)
F_{yf} :	Horizontal fluid slosh forces (N)
F_{zf} :	Vertical fluid slosh forces (N)
F_{yl} :	Total lateral forces generated at the tire-road interface (N)
FS_{ij} :	Force due to spring j on axle i (N)
FT_{ij} :	Vertical force due to tire j on axle i (N)
FY_{ij} :	Lateral forces acting on tire j on axle i (N)
g :	Acceleration due to gravity (m/s^2)
h_0 :	Fill height of liquid in a cleanbore tank (m)
$h_0^{(k)}$:	Fill height of liquid in a compartment k of the tank vehicle (m)
H_{rl} :	Height of the roll centre from the ground plane (m)
H_l :	Height of unsprung mass centre of gravity from the ground plane (m)
k :	Number of equations of motion
K_{tr} :	Torsional compliance of the tractor frame (N.m/rad)
K_{ij} :	Spring constant for spring j on axle i

K_{sf} :	Torsional compliance of fifth wheel connecting sprung units f and $f + 1$ (Nm/rad)
$KOVT_{ij}$:	Overturning stiffness of tire j on axle i (N.m/rad)
KRS_i :	Auxiliary roll stiffness of the suspension spring on axle i (N.m/rad)
KT_{ij} :	Vertical spring rate of tire j on axle i (N/m)
KY_{ij} :	Lateral spring rate of tire j on axle i (N/m)
m_f :	Mass of the sprung mass unit f (N.s ² /m)
m_{ui} :	Mass of the unsprung mass i (N.s ² /m)
m_{lf} :	Mass of liquid bulk in the sprung unit f (N.s/m ²)
n :	Number of compartments
N :	Number of circular arcs defining the modified-oval tank cross-section
OM_f :	Overturning moment due to vertical and horizontal slosh forces about the tank-trailer C.G (N.m)
P :	Pressure (N/m ²)
R_f :	Radius of the circular tank on unit f (m)
R_{ti} :	Effective radius of tires on axle i (m)
s_i :	Half the lateral suspension spread (m)
T_i :	Half of the lateral distance between inner tires on axle i (m)
W_f :	Sprung weight of the sprung unit f (N)
W_f :	Sprung weight on the front axle due to tractor alone (N)
W_r :	Sprung weight on the tractor rear composite axle (N)
W_{lf} :	Weight of liquid in the cleanbore tank on sprung unit f (N)
$W_{lf}^{(k)}$:	Weight of liquid in compartment k of the sprung unit f (N)
W_{si} :	Sprung weight on the composite axle i (N)
W_{fr} :	Vertical shear force acting through the tractor frame (N)
W_{sf} :	Load on the fifth wheel attached to the sprung unit f (N)

- X_{ui} : Longitudinal location of axle i from the sprung mass C.G. (m)
- X_{5f} : Longitudinal location of the fifth wheel constraint from the sprung mass unit f (m)
- y_1 : Lateral displacement of tires (m)
- Z_{r1} : Height of the tractor frame from the sprung mass C.G. on unit i (m)
- Z_{r1} : Height of the roll centre on axle i from the sprung mass C.G. (m)
- Z_{ui} : Vertical height of roll centre from unsprung mass C.G. (m)
- Z_{5f} : Vertical height of the fifth wheel from the sprung mass C.G. on unit f (m)
- (X_{lf}, Y_{lf}, Z_{lf}) : Location of the liquid C.G. within a cleanbore tank with respect to the sprung weight C.G. (m)
- $(X_{lf}^{(k)}, Y_{lf}^{(k)}, Z_{lf}^{(k)})$: Location of the liquid C.G. within compartment k with respect to the sprung weight C.G. (m)
- (R_1, R_2, R_3) : Radius of the various circular arcs forming the modified-oval tank cross-section (m)
- (H_2, H_1) : Height and width of the modified oval tank cross-section (m)
- (I_{xf}, I_{yf}, I_{zf}) : Moment of inertias of the sprung mass f about the body-fixed coordinates (i_s, j_s, k_s) (kg.m^2)
- $(I_{xlf}, I_{ylf}, I_{zlf})$: Moment of inertias of liquid mass in unit f about the coordinates attached to its C.G. (i_ℓ, j_ℓ, k_ℓ) (kg.m^2)
- $(I_{x\ell_0}, I_{y\ell_0}, I_{z\ell_0})$: Moment of inertias of liquid mass in unit f about the coordinates attached to its C.G. (i_ℓ, j_ℓ, k_ℓ) when the free surface gradient is zero (kg.m^2)
- $(I'_{x\ell}, I'_{y\ell}, I'_{z\ell})$: Moment of inertias of the defected shape of liquid within a modified-oval tank about the coordinates attached to its C.G. (i_ℓ, j_ℓ, k_ℓ) (kg.m^2)

- $(I_{xui}, I_{yui}, I_{zui})$: Moment of inertias of the unsprung mass i about the body-fixed coordinates (i_u, j_u, k_u) (kg.m^2)
- (p_f, q_f, r_f) : Roll rate, pitch rate and yaw rate of the sprung mass unit f (rad/s)
- (p_{ui}, q_{ui}) : Roll rate and pitch rate of the unsprung mass i (rad/s)
- (u_f, v_f, w_f) : Longitudinal, lateral and vertical velocities of the sprung mass unit f (m/s)
- α_{sf} : Pitch angle of the sprung mass f (deg)
- δ_i : Steer Input (deg)
- Δ_{ij} : Vertical deflection of tire j on axle i (m)
- Δ_{ij}^0 : Static deflection of tire j on axle i (m)
- ϕ_f : Gradient of free surface of liquid in sprung unit f (rad)
- γ_{ij} : Slip angle of tire j on axle i (rad)
- η_a : Number of axles
- η_s : Number of sprung mass units
- η_ℓ : Number of liquid masses
- ψ_{sf} : Yaw angle of the sprung mass f (deg)
- ρ : Mass density of liquid (N/m^3)
- θ_{sf} : Roll angle of the sprung mass f (deg)
- θ_{ui} : Roll angle of the unsprung mass i (deg)
- ξ_{ij} : Vertical deflection of spring j on axle i (m)
- ξ_{ij}^0 : Static vertical deflection of spring j on axle i (m)

CHAPTER 1

INTRODUCTION

1.1 Problem Background

For reasons of economy, the trucking industry has indicated a continuing interest in increasing vehicle sizes and load carrying capacities. In the last few years, vehicle weights and dimensions regulations have been mostly relaxed in Canada. The maximum gross vehicle weight has increased quite significantly. Variations in the size and weight of heavy freight vehicles, specifically the tank vehicles have resulted in significant changes in handling and manoeuvrability characteristics. The rollover immunity levels of conventional articulated highway vehicles are known to be so low compared to that of other road vehicles and have been shown to be distinctly sensitive to certain size and weight variables [1]. Research efforts on heavy vehicle dynamics have been increased considerably, since accidents involving high inertia heavy vehicles pose unreasonable risk to safety on highways, driver/passengers of light weight vehicles, and property in commerce.

Cargo tank trucks are the prime movers of dangerous goods on our highways. Safe highway transportation of such hazardous products requires highly skilled drivers and safe equipments. The transportation of dangerous goods via tank trucks presents the greatest potential risk of catastrophic accidents on the highways. The variety of factors to be considered for safe transportation of bulk liquids include, loading and unloading procedures, structural integrity to withstand stresses due to liquid surge, containability in the event of an accident, and stability and controllability of the vehicle influenced by the mobility of liquid

cargo within a partially filled tank [2]. Hence, it is vital that cargo tank trucks have handling and control characteristics that are either comparable to or better than those of other highway vehicles.

General design standards and safety regulations for vehicles carrying dangerous goods in Canada have been outlined by the CSA (Canadian Standards Association) B338-1982 [3]. This standard applies to highway tanks used for transportation of dangerous goods by road and portable tanks used for transportation of dangerous goods through other modes. The standard describes the design, construction, testing, inspection and re-testing, maintenance, and identification aspects of such tanks. Highway tanks are designated as TC 306, TC 307, TC 312, or TC 331. TC 306 tanks are generally used to haul petroleum products, while the majority of the chemicals are hauled by TC 307 and TC 312 tanks and TC 331 tanks are used to haul compressed gases at high pressures such as anhydrous ammonia and propane.

Some of the general design and construction requirements applicable to TC 306, TC 307, and TC 312 cargo tanks include:

- (a) Construction Practices: The general construction practices for single and compartmented tanks are listed in section 173 of the U.S. DOT (Department of Transportation) code [4];
- (b) Material: All sheet and plate materials required for shell, heads, bulkheads and baffles are designated by ASME Boiler and Pressure Vessel's Code. Additional material requirements, however, apply to those parts which are exempted from the above code; and
- (c) Structural Integrity: Maximum calculated stress must be less than 20% of the minimum ultimate strength except when ASME code for pressure vessel design requirements apply. Additional structural

integrity is necessary for cases where applicable such as, change in dynamic loading, internal pressure, and temperature gradient.

The standard also addresses the design requirements for joints, supports, circumferential reinforcements, and accident damage protection. The standard, however, does not address the adverse influence of liquid slosh forces on the stability and handling of tank trucks. The magnitude of slosh forces arising due to partial filling of tank trucks depends on various tank and liquid parameters such as type of tank truck, tank cross-section, and type of liquid cargo.

Bulk liquid goods include a broad range of densities and viscosities. The recognition of various groups of liquid cargos is necessary as different types of equipment are generally chosen for safe and economic transportation. CSA have classified the dangerous goods in nine classes, based upon their flammability, toxicity and other chemical properties. Most tank vehicles are designed for a particular group of liquid cargo products, in order to avoid partial filling of tanks. The tanks and their handling equipments are primarily designed for the following three groups of cargo, based upon their weight densities and chemical properties.

- (a) Fuels such as gasoline, diesel oil, and domestic type fuel oil;
- (b) Industrial acids; and
- (c) Highly viscous petrochemical products, and asphalt products.

In view of the transport economy, the tanks are designed for the lightest possible chemical, consequently partial fill condition is achieved while hauling heavier chemicals. The vehicle size, axle loads, and the gross vehicle weight used in transportation of dangerous goods are regulated by federal and provincial laws. The environmental hazards

posed by the spillage of dangerous goods either during or after a vehicle accident prompted a great interest among the researchers to analyze the influence of tank design factors on vehicle accidents.

1.2 Tank Vehicle Accidents

With the increase in the volume of motor vehicles carrying dangerous liquids, accidents involving bulk carriers have gained increased attention due to the associated unreasonable risks to health, safety, and property in commerce. This necessitates critical examination of the accident experiences in order to ratify the problem and avert the potential environmental hazards, loss of human life, and property damage. In the U.S., significant attempts have been made to collect all the data pertaining to tank vehicle accidents, carrying hazardous materials. The collected accident data are analyzed in order to revise the regulations (49 CFR 171.8) [4], so as to ensure safe transportation of hazardous materials. In Canada, there have been problems associated with the collection of accident data due to the absence of centralized accident reporting and data collection mechanism. The necessity of a centralized accident data collection agency has been emphasized [5].

A dangerous occurrence is a transportation incident leading to discharge, emission or escape of dangerous goods or an emission of radiation exceeding permissible levels. The occurrence of accidents during loading, unloading and temporary storage are also considered to be reportable dangerous occurrences. The compiled data from the dangerous occurrences is neither comprehensive, nor is considered to be representative, specifically for road mode of transportation. This is attributed to the fact that the reporting system is governed by the

provincial or territorial governments and there exists a lack of uniform accident reporting. Moreover, the carriers attempt to avoid the accident reporting due to fear of a legal reprisal. Due to lack of a uniform reporting mechanism for the road mode, the accident reports on files provide only limited information on the cause of the accident. The information on dangerous goods accidents in the rail mode is considered to include all major accidents, while the information regarding the accidents in storage houses and during handling is far from complete. Of the total number of dangerous occurrences accounted for during 1981-83, dangerous occurrences in transit were estimated to be around 56%, while in storage and during handling accounted for 34%. In 10% of the dangerous occurrences no information regarding the accident phase was reported [5]. Various modes of transportation involving dangerous occurrences in transit in Canada during 1981-83 are listed in Table 1.1 [5].

Dangerous goods are classified by nine classes as defined under the transportation of dangerous goods act. Of these, the dangerous goods, flammable liquids and fuel oils, grouped under Class 3, have the highest frequency of involvement in dangerous occurrences (Table 1.2), of which 70% occurred in the road and 14% in the rail mode of transportation. The available data has been reviewed to establish the primary and secondary causal factors associated with the tank vehicle accident. The most probable factors associated with the type of dangerous occurrence via the road mode are listed in Table 1.3. The reporting mechanisms lack in reasoning out the causal factors, such as longitudinal fluid surge during sudden braking, lateral surge of the fluid during highway manoeuvres. Although majority of the accidents have been attributed to

TABLE 1.1

DANGEROUS OCCURRENCES IN TRANSIT DURING 1981-83 [5]

MODE OF TRANSPORT	% OF DANGEROUS OCCURRENCES
ROAD	76
RAIL	18
AIR	2
MARINE	4

TABLE 1.2

DANGEROUS OCCURRENCES DURING 1981-83 BY CLASS OF DANGEROUS GOODS [5]

CLASS OF DANGEROUS GOODS	% OF DANGEROUS OCCURRENCES *
1	0.3
2	11
3	58
4	3
5	3
6	8
7	0.1
8	11
9	3
UNKNOWN	3

* Percentages may not add to 100% due to rounding off.

TABLE 1.3

CAUSAL FACTORS RELATED TO DANGEROUS OCCURRENCES [5]

Causal Factors	NATURE OF OCCURRENCE (%) *		
	Vehicle Overturn	Collision with other Vehicles	Handling
Human Factors	85	67	100
Weather Conditions	6	5	-
Poor Roads	4	-	-
Equipment Failure	2	2	-
Human Error	-	13	-
Unknown	2	13	-

* Percentages may not add up to 100%, due to round off.

human factors, the influence of longitudinal and lateral slosh has been emphasized in limited number of accident reports.

The tank vehicle accident data are classified into two types: single vehicle and multi-vehicle accidents. A total of 85 accident investigation reports involving tank vehicles were reviewed, in which 59 reports deal with single vehicle accidents, and the rest involved multiple vehicles [6]. In case of single vehicle accidents, the cause of accident is related to the driver's negligence and due to the liquid slosh. In case of multi-vehicle accidents, however, involvement of other vehicles on the road also contributed towards the accident.

The review and analysis of the single vehicle accident reports conclude that the human factors are the primary cause of vehicle accidents; however, there exist various contributing factors [6], such as lateral liquid surge, instability during braking on a downgrade and driver's unfamiliarity with the road. The review of the accident reports also reveal that most of the accidents occurred while negotiating a curve. This may be due to the excessive liquid surge occurring during simultaneous curving and braking of the vehicle. Multi-vehicle accidents, similar to the single vehicle accidents reveal human factors as the primary cause of accidents. The various other contributing factors include the weather and road conditions. Information pertaining to liquid surge are not available from the multi-vehicle accident data.

The magnitude of fatalities and injuries encountered during single and multi-vehicle accidents (1981-83) are summarized in Table 1.4. Table 1.5 presents the property damage incurred during the single and multi-vehicle accidents [6]. Nearly 50% of single vehicle accidents and

TABLE 1.4

**FATALITIES AND INJURIES INCURRED DURING 1981-83 INVOLVING SINGLE
AND MULTI-VEHICLE ACCIDENTS [6]**

FATALITIES	% OF TOTAL ACCIDENTS		INJURIES	% OF TOTAL ACCIDENTS	
	SINGLE VEHICLE	MULTI- VEHICLE		SINGLE VEHICLE	MULTI- VEHICLE
One or more	47	81	One or more	51	65
Two or more	24	54	Two or more	22	38
Three or more	10	31	Three or more	12	31
Four or more	7	19	Four or more	10	19
Five or more	-	11.5	Five or more	-	15
Unknown	-	4	Unknown	-	4

TABLE 1.5

**PROPERTY DAMAGE INCURRED DURING 1981-83 INVOLVING SINGLE
AND MULTI-VEHICLE ACCIDENTS [6]**

PROPERTY DAMAGES	% OF TOTAL ACCIDENTS	
	SINGLE VEHICLE	MULTI- VEHICLE
Less than \$25000	36	35
\$25000 - \$50000	32	23
\$50000 - \$100000	5	19
More than \$100000	17	11.5
Unknown	10	11.5

nearly 80% of the multi-vehicle accidents involved more than one fatality. Also, 17% of the single and 11.5% of multi-vehicle accidents caused a property damage in excess of 100,000 dollars. Due to the high levels of risk associated with the tank vehicle accidents, the need to study stability and control performance of such vehicles has been strongly emphasized.

An investigation by Rohm and Haas Company to determine influence of truck design changes on vehicle accidents [7], indicated truck rollover as the primary cause when large spills occurred during highway accidents. Analysis of the Hazardous Material Incident Reports (HMIR) for the period 1983 to 1987 indicates that 554 of the 624 reports are actual vehicle accidents of which 452 or 81.6% are vehicle rollovers.

Most of the investigations conducted during the past two decades have concentrated on the directional stability of the heavy commercial vehicles carrying rigid cargo [1,8,9]. Studies on stability of liquid tank vehicles [10,11], concentrated primarily on liquid slosh forces and lacked complete integration of vehicle and fluid slosh models. This dissertation is the outcome of the research carried out at the CONCAVE Research Centre, to investigate the stability of liquid tank vehicles. The steady turning and dynamic stability of partially filled tank vehicles are investigated using a steady state fluid model. The study also verified the results of the steady state fluid model using a comprehensive model of the tank vehicle formed by integrating a finite-difference fluid code with a three-dimensional model of a tank vehicle. The study also validated the analytical models through field tests. Since a variety of topics have been addressed in this

dissertation, each chapter reviews the literature relevant to the topic that is being addressed in the chapter.

1.3 Scope and Layout of the Thesis

The main objective of this research thesis is to investigate the stability of liquid tank vehicles during various types of manoeuvres and to evaluate the impact of changes in the vehicle weights and dimensions on their handling and manoeuvrability characteristics. The detailed objectives of this dissertation can be summarized as follows:

1. To develop a computer simulation model capable of predicting the rollover threshold limits of liquid tank vehicles;
2. To investigate the influence of tank and vehicle design factors on the vehicle rollover stability;
3. To develop a quasi-dynamic yaw/roll model of tank vehicles capable of predicting their directional response characteristics during various highway manoeuvres;
4. To develop a comprehensive stability model by integrating a finite-difference based fluid slosh model with the three-dimensional tank vehicle and to compare the results with quasi-dynamic model.
5. To validate tank vehicle models through field test results.

In chapter 2, a Kineto-static roll plane model of a tank vehicle is developed, assuming steady state fluid motion, to calculate the rollover threshold acceleration limit of the vehicle. A steady state fluid motion model in the roll plane of a partially filled arbitrarily shaped tank cross-section is derived and integrated into the vehicle model to investigate the influence of the destabilizing roll moments of the liquid cargo on the rollover threshold of the vehicle.

The influence of various tank design factors, such as cross-section, size and compartments on the steady turning stability of tank vehicles is investigated in Chapter 3. The influence of specific changes in vehicle design, such as suspension properties, axle locations, compartmenting of the tanks, etc., on the steady turning roll stability of tank vehicles are also investigated. The rollover threshold acceleration of a liquid tank vehicle equipped with tanks of varying geometry are compared to that of an equivalent rigid cargo vehicle.

A dynamic model for investigating directional stability of tank vehicles capable of simulating steering response characteristics at highway speeds is presented in Chapter 4. The lateral and roll dynamics of partially filled tank vehicles are investigated by integrating a three-dimensional model of a tank vehicle with the dynamics associated with the movement of free surface of liquid within the tank, assuming inviscid fluid flow conditions (quasi-dynamic fluid model).

In Chapter 5, the influence of various tank and vehicle design factors on the directional response of tank vehicles are investigated. The directional dynamics of tank vehicles are evaluated under various tank fill, vehicle speed, and loading conditions. The dynamic response characteristics of a partially filled tank vehicle are compared to those of an equivalent rigid cargo vehicle to demonstrate the destabilizing effects of the liquid movement within the tank vehicle.

The steady-state fluid model is replaced by a dynamic fluid slosh model and the vehicle response to dynamic steering inputs is investigated in Chapter 6. The directional response of the tank vehicle incorporating the dynamic slosh model are compared to those of the

vehicle model incorporating the quasi-dynamic model in order to demonstrate the influence of dynamic fluid slosh.

The computer simulation models are validated through the field tests. A comparison of simulation results with the field measured vehicle response characteristics is presented in Chapter 7, for various vehicle manoeuvres.

Conclusions drawn from this study are summarized in Chapter 8, and recommendations for future studies on tank vehicle stability are proposed.

REFERENCES FOR CHAPTER 1

1. Ervin, Robert C., "The influence of Size and Weight Variables on the Roll Stability of Heavy Duty Trucks", SAE Paper No. 831163, 1983.
2. Botkin, L.A., "Safe Highway Transportation of Bulk Liquids", SAE Paper No. 700872, 1970.
3. Canadian Standards Association, "Highway Tanks and Portable Tanks for the Transportation of Dangerous Goods", CSA preliminary Standard B338-1982, March 1982.
4. Code of Federal Regulations, Title 49 - Transportation, U.S. Government Printing Office, Washington D.C., 1975.
5. Transport Dangerous Goods, "Dangerous Occurrences Reports 1981-1983, Summary of Reports on File", Evaluation and Analysis, Transport Dangerous Goods, Report TP 5695E, 1984.
6. Rakheja, S. and Sankar, S., "Tank Vehicle Accidents: A survey of Reports on File", CONCAVE Report No. 14-87, Concordia University, Oct. 1987.
7. Murnane, Timothy J., "Vehicle Accident Statistics Producing Rollover and Spills involving Tank Semi-Trailers", SAE Truck and Bus Meet, Charlotte, NC, Nov. 1989.
8. Miller, D.W.G. and Barter, N.F., "Rollover of Articulated Vehicles", I. Mech. E. Conf. on Vehicle Safety Legislation, Paper No. C203/73, 1973.
9. Fancher, Paul S., "The Static Stability of Articulated Commercial Vehicles", Veh. Sys. Dyn., Vol. 14, pp. 210-227, 1985.
10. Strandberg, L., "Lateral Stability of Road Tankers", VTI Rapport No. 138A, Sweden.
11. Slibar, A. and Troger, H., "The Steady State Behaviour of a Tank Trailer System Carrying Rigid or Liquid Load", VSD-IUTAM Symp. on Dynamics of Vehicles on Roads and Tracks, Vienna, 1977.

CHAPTER 2

KINETO-STATIC ROLL PLANE MODEL OF A PARTIALLY FILLED TANK VEHICLE

2.1 General

The dynamic interactions associated with movement of liquid cargo within a partially filled tank vehicle affect the control and handling of the vehicle. Safe highway transportation of hazardous chemicals and fuel oils has drawn significant attention due to associated unreasonable risks to health, safety, and property in commerce. The economic and environmental impact of any accidents involving dangerous liquids can be catastrophic, consequently the safe transportation of liquid bulk deals with factors other than normal trucking practices.

The rollover immunity levels of heavy commercial vehicles are known to be so low that a moderately severe manoeuvre can cause considerable lateral forces and roll moments leading to vehicle rollover [1]. The rollover immunity and stability of tank vehicles are further deteriorated due to sloshing effect of liquid cargo. The degradation of rollover immunity of tank vehicles is primarily attributed to the motion of the free surface of liquid within a partially filled tank. Liquid tank vehicles, employed in general purpose chemical transportation, are often partially filled due to regulatory limitations on axle loads, and variations in weight density of various chemicals transported. The motion of the free surface of liquid within a partially filled tank coupled with fluid-structure interactions and vehicle dynamics yield significant slosh forces. The longitudinal and lateral slosh forces caused by abrupt vehicle manoeuvres can adversely affect the controllability and stability of tank vehicle [2].

In this chapter, a brief overview on the state-of-the-art

investigations into the rollover threshold limits of heavy vehicles is presented. A kineto-static roll plane model of a tank vehicle is developed for computing the rollover threshold limits of liquid tank vehicles. The roll plane model of a partially filled arbitrarily shaped tank is developed to determine the motion of the free surface of the liquid and the corresponding load shift encountered during steady turning. The rollover immunity of a tank vehicle can be computed by integrating the roll plane model of the vehicle with a steady state fluid model of the partially filled tank, assuming inviscid fluid flow conditions.

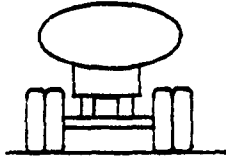
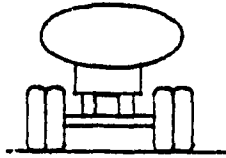
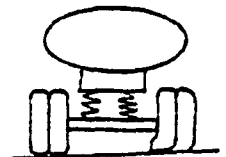
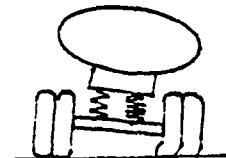
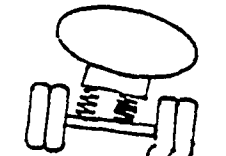

2.2 State-of-the-Art Investigations on the Rollover Threshold of Heavy Vehicles

The likelihood of vehicle rollover is strongly related to the rollover threshold acceleration, also referred to as the overturning limit of the vehicle in steady turning. The rollover threshold of heavy vehicles, in general, depends upon the vehicle geometry and inertia, suspension characteristics, and tire properties.

The rollover threshold limits of a rigid heavy vehicle with negligible suspension and tire deflections can be estimated from the ratio of half of the effective track width to the trailer centre of gravity height. The rollover threshold acceleration level of such vehicles is of the order of 0.6g [3]. Introduction of compliant tires can reduce the rollover threshold value to approximately 0.5g. The rollover threshold is further decreased to approximately 0.44g due to compliant tires and suspensions. Spring lash can lead to even lower value (approximately 0.34g) of vehicle rollover threshold, as shown in Table 2.1. Dynamic interactions of the free surface of the liquid in a partially filled tank vehicle further reduce the rollover threshold

TABLE 2.1

ROLLOVER THRESHOLD LIMITS OF HEAVY VEHICLES [3]

Vehicle Characteristics	Schematic	Rollover Threshold
Rigid Vehicle		0.58 g
Compliant Tires Only		0.495 g
Compliant Tires and Suspensions		0.435 g
Compliant Tires and Springs plus Spring Lash (Typical Vehicle)		0.34 g
Typical Vehicle in Dynamic Lane Change		0.24 g
Typical Vehicle in Dynamic Lane Change with 50% Liquid Load		0.20 g

value; a 50% filled elliptic tank vehicle can rollover at a lateral acceleration of 0.20g during a lane change manoeuvre [3].

Isermann [4] was the first to develop a roll plane model of an articulated vehicle carrying rigid or liquid loads and investigated the sensitivity of the rollover threshold to design and loading conditions. The lateral load shift due to movement of liquid cargo in a partially filled tank trailer, however, was neglected in the analysis. Although the suspension characteristics and the torsional properties of the tractor frame and the fifth wheel arrangement were represented appropriately in the model, the representation of the dual tires and the tire properties lacked accuracy. The simulation results were verified through tests performed on a tilt-table arrangement.¹

Miller and Barter [5], in 1973, developed a model following the work of Isermann, to compute the rollover threshold limits of articulated vehicles carrying rigid cargo. The computer simulation model solves a set of differential equations for small increments of the lateral acceleration and the corresponding roll angles of the various vehicle units are computed, until the roll instability is encountered. The simulation results are compared to the tilt-table test data which revealed that an average error was present in the prediction of the rollover threshold. This error is presumably due to the over simplified assumptions about how the trailer will rollover [5].

A roll plane model of articulated vehicles with rigid cargo was:

¹ A tilt-table arrangement is a device used for measuring the rollover threshold of a vehicle. In the test, the vehicle is mounted on the platform which is gradually tilted until a roll instability is identified through the lift-off of the tires at the trailer and tractor rear axles on one side. The rollover threshold acceleration a_y , in g units, is then approximated as : $a_y = \tan(\text{maximum tilt angle})$.

developed by Gillespie and Verma [6] to compute the dynamic roll response. In this model, all the axles on the vehicle are lumped together and represented by a single composite axle. The roll plane model provided an overestimate of the threshold values due to the lumped-axle representation.

Mallikarjunarao [7] developed a comprehensive "static roll-plane model" to calculate the rollover threshold limits of articulated vehicles during steady turning manoeuvres. The multi-axled vehicle is represented by three composite axles by grouping the axles with similar suspension properties. The model lacks representation of the liquid slosh forces within the partially filled tank vehicle. The model results were compared with tilt-table tests.

Strandberg [8] investigated the lateral stability of tank vehicles due to the liquid motion within the tanks assuming negligible roll and yaw motion of the vehicle. The measurement of liquid forces was performed on a laterally oscillated scale model tank. Strandberg *et al* [9] investigated the dynamic behaviour of heavy vehicle combinations to propose regulations on the handling performance of vehicle combinations in Sweden. The study proposed regulations on risk variable limits in different simulated manoeuvres, and suggested the minimum steady state overturning limit as 4 m/s^2 (0.408 g) for all the commercial vehicles.

2.3 Stability of Liquid Tank Vehicles during Steady Turning

Heavy vehicles, in general, begin to exhibit unstable behaviour at lateral acceleration levels of 0.3 to 0.4 g [1]. In the case of vehicles carrying rigid cargo, the cargo is often attached to the trailer bed, thus the dynamic movements of the cargo with respect to the vehicle are assumed insignificant. The dynamics associated with the

motion of liquid within a partially filled tank, however, are quite significant and thus cannot be neglected.

Partial loads in a tank yield low sprung weight centre of gravity height and thus an improved rollover threshold value, when the cargo movement is considered insignificant. The rollover threshold for partially filled tank vehicles, however, is rather deteriorated due to roll moments arising from motion of the free surface of the liquid. Although bulk transporters make every possible attempt to avoid partial fill conditions in order to achieve safety of the driver and the equipment, cylindrical tanks used in general purpose chemical fleet, however, often carry partial loads due to variations in weight density of various chemicals transported and due to provincial regulations on permissible axle loads. Gasoline and fuel oil tankers are often partially filled during their delivery routes around the city.

While a comprehensive fluid-vehicle dynamic model may be highly complex, the rollover limits of liquid tank vehicles can be established by interfacing a kineto-static fluid model to a static roll plane model of an articulated vehicle. A computer simulation model of an articulated vehicle with partially filled arbitrarily shaped tank is developed to investigate the steady turning behaviour of the vehicle, assuming inviscid fluid flow conditions.

2.4 Selection of Candidate Tank Vehicle Configurations

A large number of commercial vehicle configurations, such as straight trucks, tractor-semitrailers, tractor-trailers, and B-trains are used in general purpose transportation of the liquid bulk across Canada. Table 2.2 presents the percentage population of the various vehicle combinations currently in use across Canada [10]. Figure 2.1

TABLE 2.2

POPULATION OF THE VARIOUS HEAVY VEHICLE COMBINATIONS PRESENT
IN VARIOUS CENTRES ACROSS CANADA [10]

Vehicle Combination	% Distribution of Vehicle Combination					
	Vancouver	Calgary	Winnipeg	Toronto	Montreal	Moncton
Tractor- Semitrailers	60	80	60	70	90	98
A-Doubles	32	8	25	25	8	1
B-Doubles	8	10	14	5	2	1
C-Doubles	0	<2	<1	<1	<1	0
Triples	0	<1	<1	0	<1	0
Total	100	100	100	100	100	100

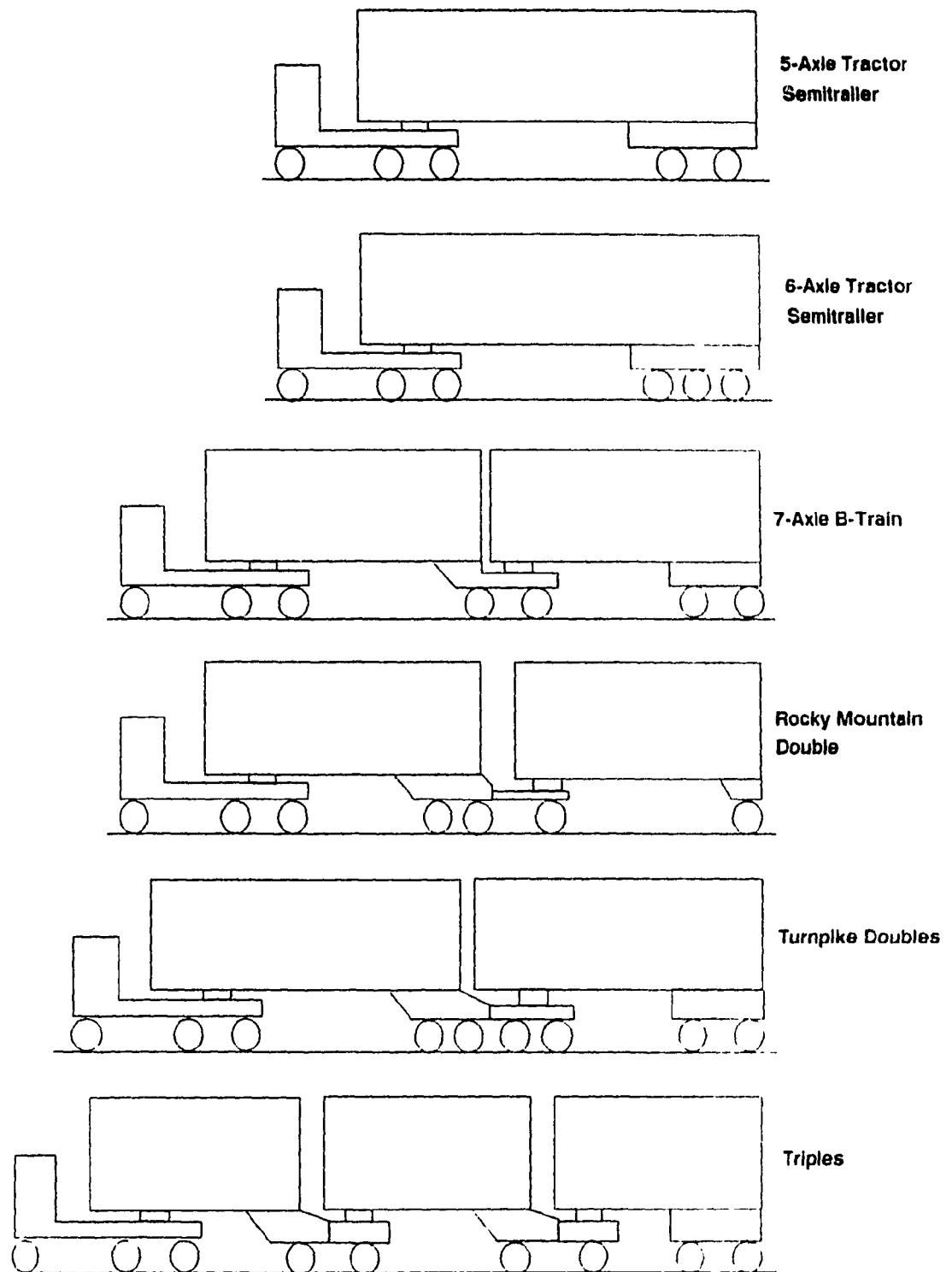


Figure 2.1 Schematic of various vehicle configurations

presents a schematic of some of these vehicle configurations. Based on the research conducted by the University of Michigan Transport Research Institute (UMTRI) [10], approximately 77% of all heavy vehicles operating in Canada are tractor-semitrailers, 17% are A-doubles, 5% are B-doubles, and remaining are C-doubles and triples [10]. A survey of road transporters across Canada was conducted to determine the vehicle configurations used most frequently for transportation of bulk liquids. The results of the survey are summarized in Table 2.3. The findings of the UMTRI and the bulk liquid carriers survey reveal that a tractor with either a tandem or tri-axle semitrailer is most often used on the Canadian Highways. The second popular vehicle in gasoline or chemical transportation is either a 7-axle or 8-axle B-train combination. Thus tractor-semitrailer and B-train configurations are selected as the candidate vehicles for this investigation. Initial study is based on modeling a tractor-semitrailer vehicle. This analytical model is further extended to study the dynamic response characteristics of the B-train tank vehicle combination.

2.5 Selection of Tank Cross-sections

Tanks of various cross-sections have been designed for bulk transportation of gasoline and chemicals. Of these, tanks with circular, elliptical, modified oval, and modified square cross-sections are used widely in transportation of gasoline, fuel oils, and chemicals. Figure 2.2 presents typical cross-sections of some of the tanks used in the industry. The liquid load shift within a tank vehicle and the sprung weight centre of gravity height are dependent on the tank cross-section and the fill level. Hence, the overturning threshold limits of tank vehicles are thus influenced by the tank cross-section.

TABLE 2.3

MOST COMMONLY USED TANK VEHICLE CONFIGURATIONS IN CANADA [11]

CARRIER	VEHICLE CONFIGURATIONS IN USE
Shell Canada	7-axle B-train
Provost Inc.	Tandem Semitrailer Triaxle Semitrailer
Ultramar Canada	Triaxle Semitrailer
Canadian Liquid-Air Ltd.	C-train Triaxle Semitrailer
Fruehauf Inc.	Tandem Semitrailer Triaxle Semitrailer 8-axle B-train
Bulk Carriers Ltd.	Tandem Semitrailer Triaxle Semitrailer Quadaxle Semitrailer
Westank Ltd.	B-train A-train
Hutchinson Inc.	Tandem Semitrailer Triaxle Semitrailer
Gulf Canada	8-axle B-train Triaxle Semitrailer
Trimac Inc.	8-axle B-train Quadaxle Semitrailer

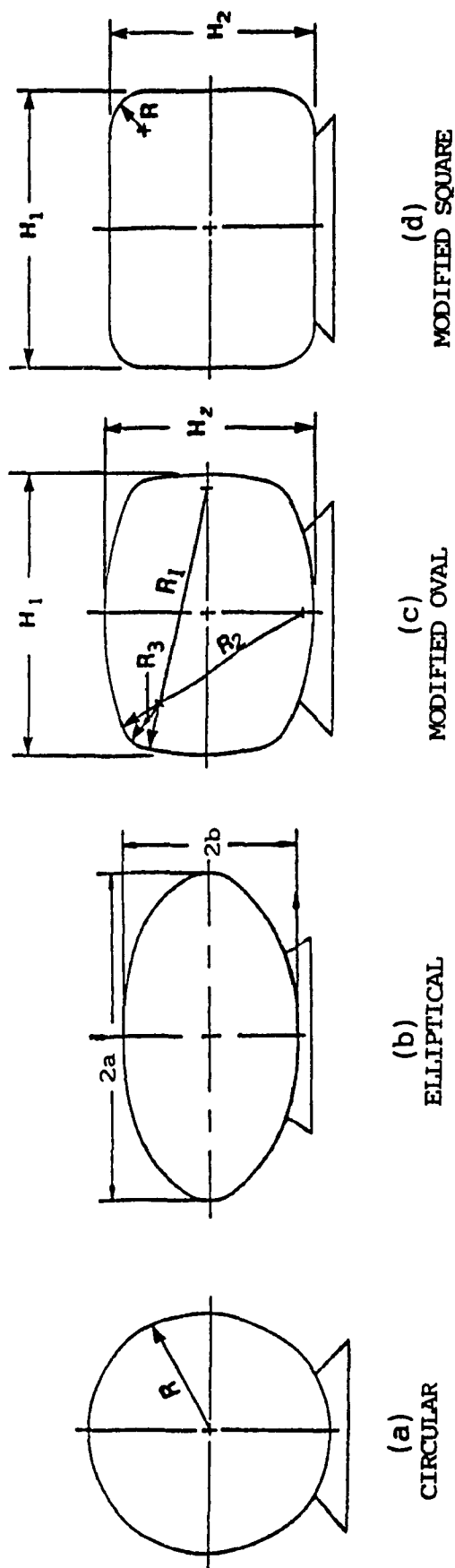


Figure 2.2 Tank cross-sections commonly used in liquid bulk transportation

Although a rectangular cross-section tank can provide least overall height of the vehicle, for a given cross-sectional area and payload, the sharp corners can impose high stresses in the tank walls. Bends of small radius are introduced to join the various arcs to improve the structural integrity of the tank. The results of the survey conducted on the bulk carriers [11] reveal that circular and modified-oval cross-section tanks are most commonly used for transportation of chemicals and fuel oils. A general computer model is developed to study liquid motion within arbitrarily shaped tanks.

2.6 Computation of the Gradient of Free Surface of Liquid within a Tank

The magnitude of liquid motion within a tank depends on the tank cross-section, and hence the rollover immunity levels of the vehicle are significantly affected by the tank geometry. The most common tank cross-sections used in transportation of chemicals and fuel oils include circular and modified oval shapes. The elliptical and modified square tanks are also used for certain specific applications [11].

The sprung and unsprung masses of an articulated vehicle experience roll as well as lateral (centrifugal) acceleration during a steady turning manoeuvre. A schematic diagram for the roll plane model of an articulated vehicle is shown in Figure 2.3. Assuming steady state conditions, the entire fluid bulk in the tank trailer is considered to move as a rigid body. The vehicle tilt causes the motion of the free surface of the liquid, as shown in Figure 2.4. The centre of mass of the liquid experiences a shift due to motion of the free surface of liquid and thus a load transfer occurs from the inner to the outer tires. The lateral acceleration experienced by the sprung mass of the vehicle during the manoeuvre imposes an equal and opposite acceleration

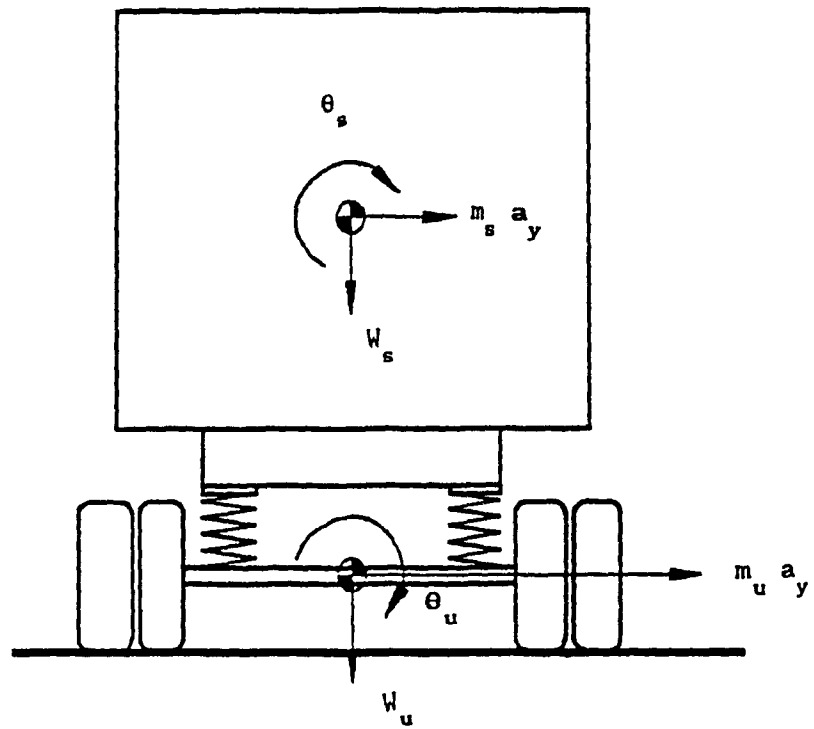


Figure 2.3 Roll plane model of an articulated vehicle

- a. C.G. of solid load
- b. C.G. due to tank tilt alone
- c. C.G. due to tank tilt & lateral acceleration

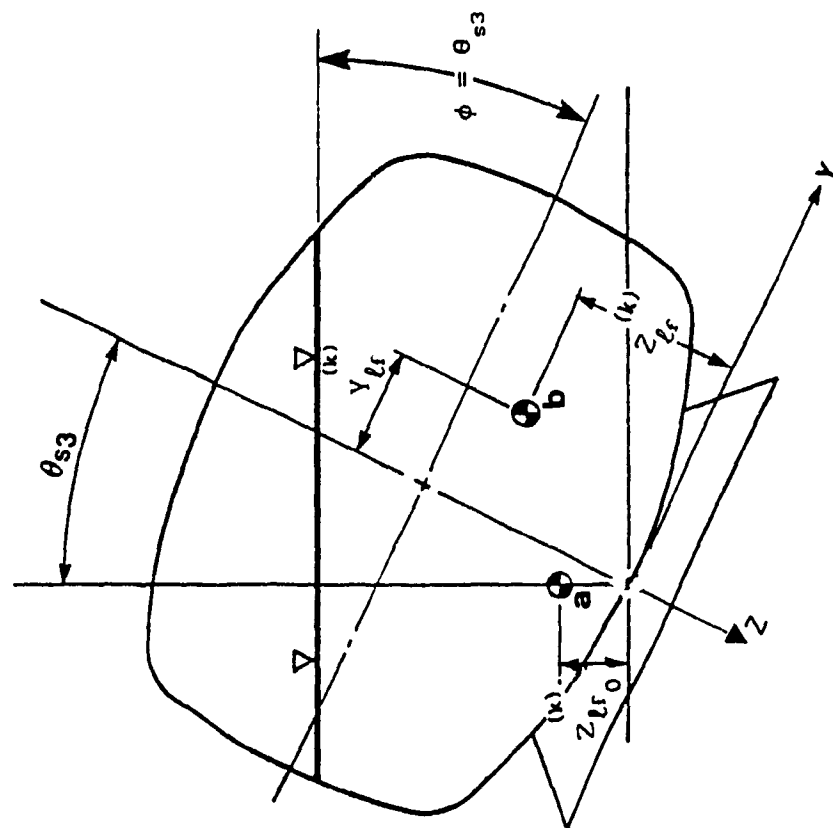


Figure 2.4
Translation of centre of gravity (C.G.) of liquid due to tank tilt

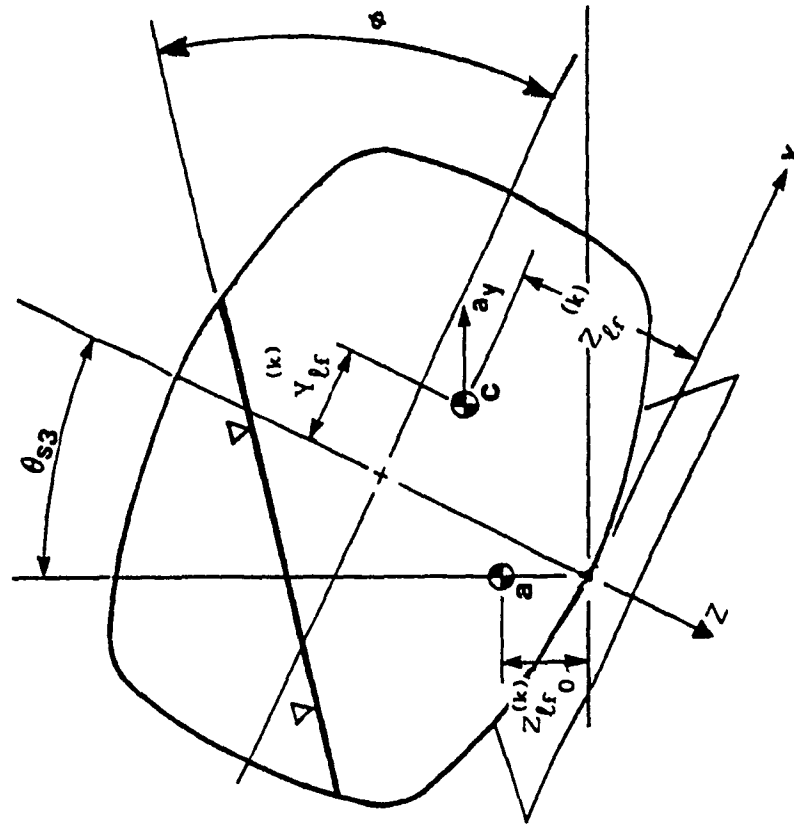


Figure 2.5
Translation of C.G. of liquid due to tank tilt and lateral acceleration

on the liquid bulk and thus causes further motion of the free surface of liquid and the centre of mass of liquid as shown in Figure 2.5.

The translation of the centre of liquid bulk due to the motion of the free surface leads to considerable load shift from the inner to the outer track of the vehicle. The magnitude of the translation of centre of mass is a function of tank cross-section, fill level, and gradient of the free surface due to tank tilt and lateral acceleration. The gradient of the free surface can be determined assuming inviscid fluid motion, from the pressure variations in a static fluid. Consider the equilibrium of forces for a fluid element inside a partially filled tank vehicle subject to tank tilt and lateral acceleration, as shown in Figure 2.6(a). The body and surface forces acting on the fluid element at rest in the axes system (Y and Z) are shown in Figure 2.6(b). The pressure variation, dP at the free surface must vanish [12]:

$$dP = \frac{\partial P}{\partial y} dy + \frac{\partial P}{\partial z} dz = 0 \quad (2.1)$$

where

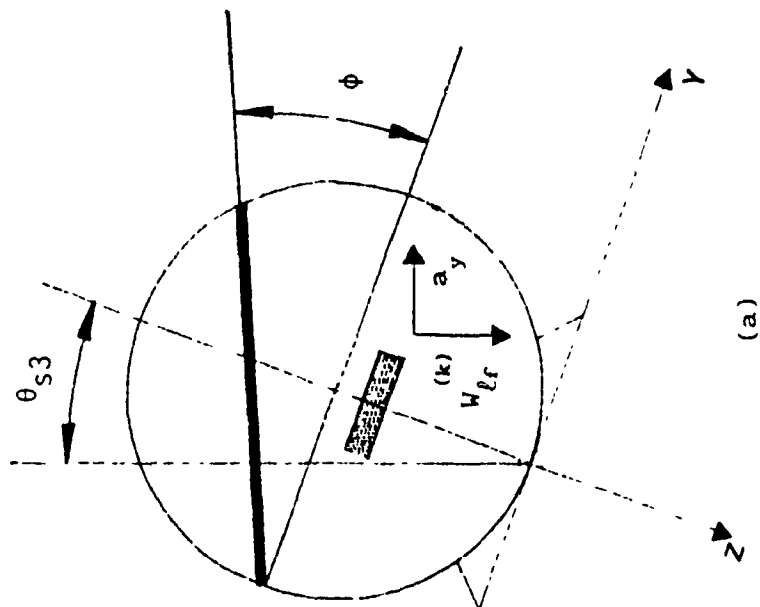
$$\frac{1}{\rho} \frac{\partial P}{\partial y} = a_l \cos \theta_{s3} + g \sin \theta_{s3} \quad (2.2)$$

and

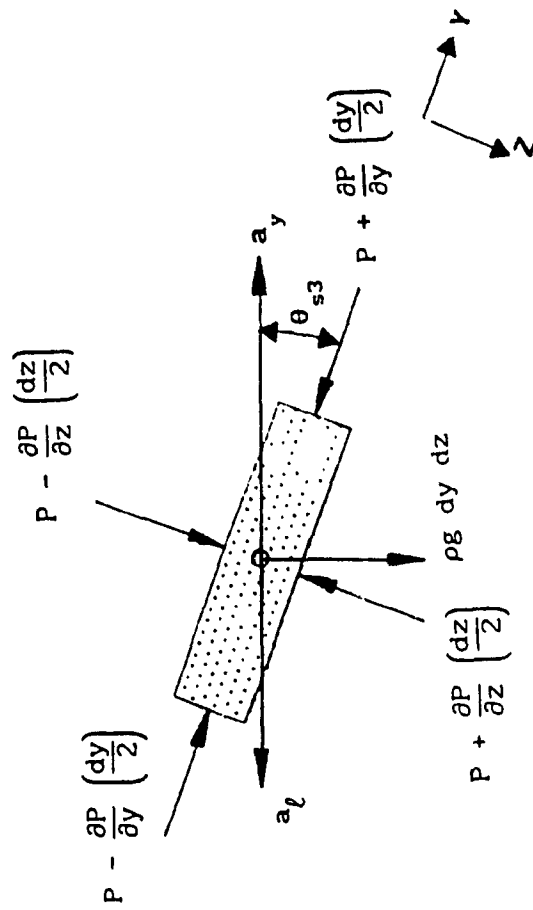
$$\frac{1}{\rho} \frac{\partial P}{\partial z} = -a_l \sin \theta_{s3} + g \cos \theta_{s3} \quad (2.3)$$

where a_l is the lateral acceleration imposed on the fluid due to the centrifugal acceleration of the tank, g is the acceleration due to gravity, ρ is the mass density of the liquid, and θ_{s3} is the tank roll angle. The gradient of the free surface of liquid is given by:

$$\tan \phi = - \frac{dz}{dy} = \frac{\partial P / \partial y}{\partial P / \partial z} \quad (2.4)$$



(a)



(b)

Figure 2.6 Equilibrium of a fluid element within a partially filled tank subject to tilt and lateral acceleration

Assuming roll angles of the sprung mass, θ_{s3} to be small, the gradient of the free surface due to vehicle roll and lateral acceleration can be expressed as:

$$\tan \phi = \frac{\theta_{s3} - a_y}{(1 + a_y \theta_{s3})} \quad (2.5)$$

where the vehicle lateral acceleration, $a_y = -a_x/g$ and ϕ is the gradient of the free surface of liquid. The free surface gradient reduces to tank roll angle in the absence of lateral acceleration.

2.7 Roll Plane Steady State Fluid Model of a Partially Filled Tank

2.7.1 Circular Cross-section

The vertical and lateral translation of the centre of mass of liquid bulk in the partially filled tank are computed from the gradient of free surface, the tank cross-section, and the fill level. The roll plane steady state fluid model of a partially filled tank of circular cross-section tank is presented in Figure 2.7. The circular tanks are normally cleanbore (uncompartmented), however, the analysis presented here is applicable to both cleanbore and compartmented tanks. The lateral and vertical translation of the centre of mass of liquid within a compartment are then computed from the following equations, derived from the tank geometry:

$$Z_{\ell f}^{(k)} = R - \left(R - Z_{\ell f 0}^{(k)} \right) \cos \phi \quad ; \quad k = 1, 2, \dots, n \quad (2.6)$$

$$Y_{\ell f}^{(k)} = \left(R - Z_{\ell f 0}^{(k)} \right) \sin \phi \quad ; \quad k = 1, 2, \dots, n \quad (2.7)$$

where R is the tank radius, n is the number of compartments (for cleanbore tank, $n = 1$), $Z_{\ell f 0}^{(k)}$ is the height of the centre of mass of

The superscript (k) is dropped for the notation representing the centre of mass of liquid within a cleanbore tank.

- a - C.G of solid load
- b - C.G due to tank tilt alone
- c - C.G due to tank tilt and lateral acceleration

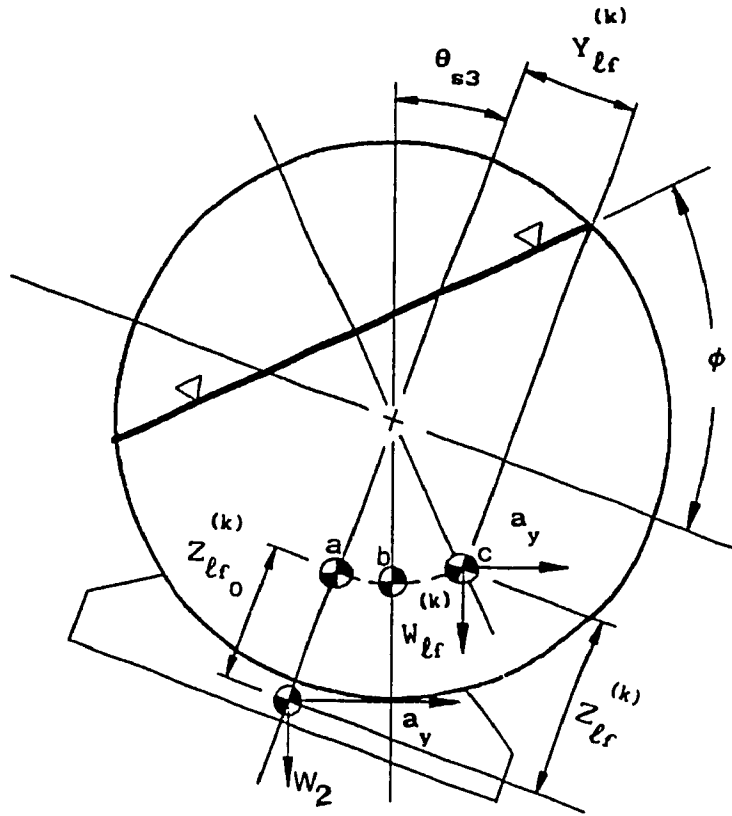


Figure 2.7 Roll plane steady state fluid model of a partially filled circular tank cross-section

liquid in compartment k for $\theta_{s3} = 0$ and $a_y = 0$, $Z_{lf}^{(k)}$ and $Y_{lf}^{(k)}$ are the lateral and vertical locations of the centre of mass of liquid in compartment k , respectively due to tank roll and lateral acceleration encountered during steady turning. In case of tanks of arbitrary cross-section, such as modified oval, the computation of instantaneous centre of mass of liquid, however, yields significant complexities.

2.7.2 Modified Oval Cross-section

Figure 2.8 shows the cross-section of a modified oval tank of width H_1 and height H_2 , enclosed by circular arcs of radii R_1 , R_2 , and R_3 . The tank periphery can be observed as a combination of 8 circular arcs and is symmetric about the vertical axis. The origin of the body fixed axis system, Y-Z is assumed to be located at the centre of gravity of the trailer. A numerical algorithm is developed to compute the coordinates of the centre of curvature for each arc which enclose the cross-section of the tank. The equation for each circular arc, is expressed in terms of its radius and coordinates of the centre of curvature:

$$(y - b_s)^2 + (z - c_s)^2 = r_s^2 ; \quad s = 1, 2, \dots, N \quad (2.8)$$

where b_s and c_s are the coordinates of the centre of curvature of arc s , r_s is the radius of the arc s , and N is the total number of arcs describing the tank cross-section. The coordinates of the intersection points of two adjacent arcs are obtained through simultaneous solution of the equations for arcs s and $(s + 1)$. The solution yields the maximum values for y and z coordinates of the arc s and the minimum values for the arc $(s + 1)$.

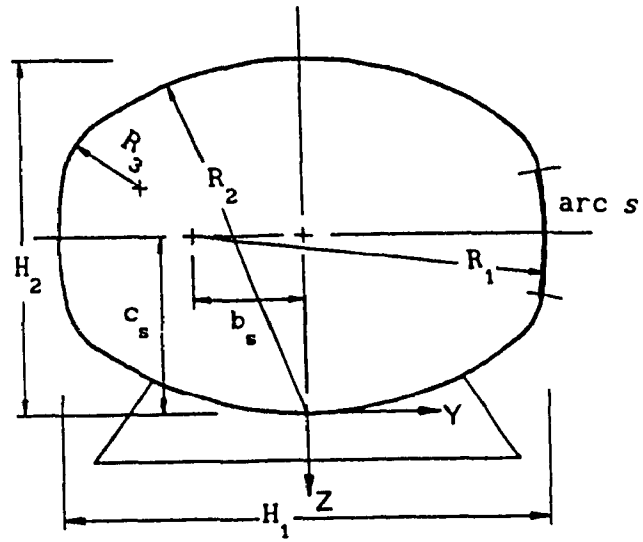
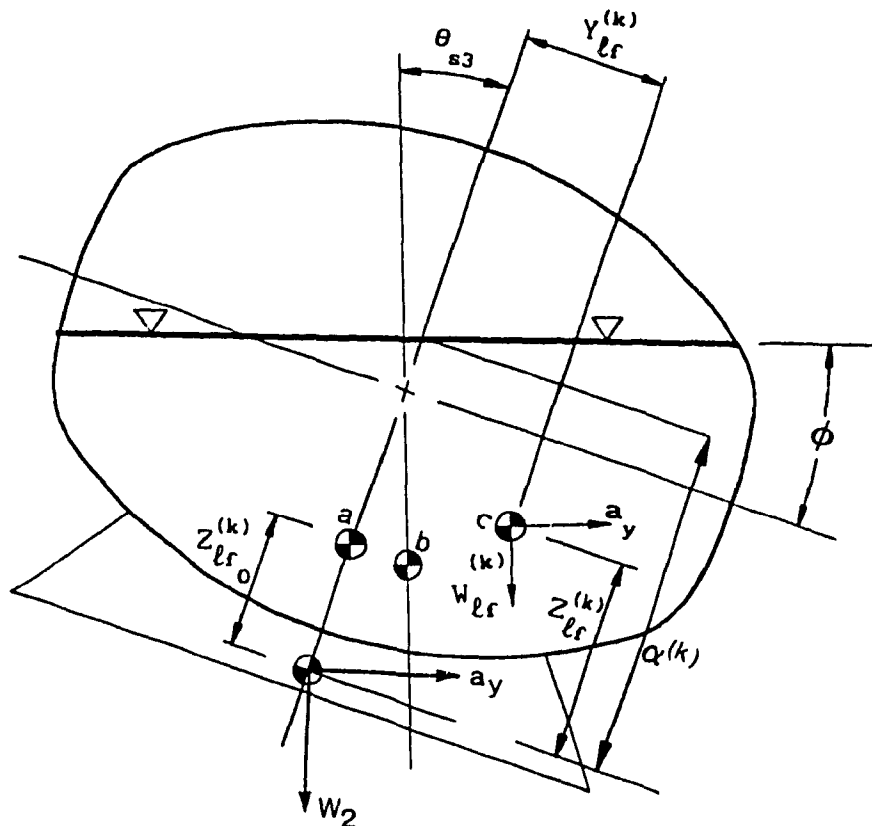


Figure 2.8 Cross-section of a Modified-oval tank



- a - C.G. of solid load
- b - C.G. due to tank tilt alone
- c - C.G. due to tank tilt and lateral acceleration

Figure 2.9 Roll plane steady state fluid model of a partially filled modified oval tank cross-section

Figure 2.9 shows the roll plane steady state fluid model of a partially filled modified oval tank. The free surface of liquid intersects two of the circular arcs describing the tank geometry. The coordinates of these intersection points are determined by solving the equations of the free surface and the arcs. The equation of free surface of liquid in compartment k in the absence of tank tilt and lateral acceleration is determined by the fill level $h_o^{(k)}$:

$$z = -h_o^{(k)} ; \quad k = 1, 2, \dots, n \quad (2.9)$$

The algorithm identifies the two arcs p and q being intersected by the free surface by comparing the height $h_o^{(k)}$ with the minimum and maximum of each arc enclosing the tank cross-section. The intersection points (y_p, z_p) and (y_q, z_q) are computed by simultaneously solving the Eqns. (2.8) and (2.9). The intersection point (y_p, z_p) is a mirror reflection of the intersection point (y_q, z_q) , in the absence of tank tilt and lateral acceleration, due to the symmetry of the tank about the Z -axis. Hence, $y_p = -y_q$ and the fluid volume per unit length of the tank compartment k , $A_o^{(k)}$ can be computed from the area integral:

$$A_o^{(k)} = 2 \int_0^{y_p} \int_{f_1(y)}^{h_o^{(k)}} dz dy \quad (2.10)$$

where $f_1(y)$, derived from the equations of arcs describing the tank geometry (Eqn. 2.8) and $h_o^{(k)}$ define the domains of integration about the Z -axis.

The equation of the inclined free surface of liquid due to tank

tilt and lateral acceleration encountered during steady turning can be expressed in terms of its gradient, evaluated from Eqn. (2.5):

$$z = - \left(\frac{\theta_{s3} - a_y}{(1 + \theta_{s3} a_y)} \right) y + \alpha^{(k)} \quad (2.11)$$

where $\alpha^{(k)}$ is the intercept of the free surface of liquid with the Z-axis in compartment k (Figure 2.9). The total volume per unit length remains constant while neglecting the pitching motion of the tank, the intercept $\alpha^{(k)}$ can be computed using an iterative algorithm. A starting value of $\alpha^{(k)}$ is assumed to be the initial height of the free surface of the liquid $h_0^{(k)}$. Equations (2.8) and (2.11) are solved simultaneously to compute the intersection points of the free surface of liquid and the circular arcs describing the tank geometry, (y_p, z_p) and (y_q, z_q) . The fluid volume per unit length in compartment k is then computed from the area integral :

$$A^{(k)} = \int_{y_p}^{y_q} \int_{f_1^{(k)}(y)}^{f_2^{(k)}(y)} dz dy \quad (2.12)$$

where $f_2^{(k)}(y)$ describes the free surface of liquid, determined from Eqn. (2.11). $f_1^{(k)}(y)$ and $f_2^{(k)}(y)$ define the domains of integration about the Z-axis.

The total fluid volume per unit length $A^{(k)}$ is compared with the initial volume $A_0^{(k)}$, computed for $a_y = \theta_{s3} = 0$. The corresponding magnitude of error is evaluated as:

$$\varepsilon = | A^{(k)} - A_0^{(k)} | \quad (2.13)$$

The iterative process is repeated, for an updated value of $\alpha^{(k)}$, until the error ε is within a specified tolerance. The corresponding coordinates of the centre of mass of the liquid in compartment k , $Y_{\ell f}^{(k)}$ and $Z_{\ell f}^{(k)}$, are then evaluated from the following moment integrals:

$$Z_{\ell f}^{(k)} = \frac{1}{A^{(k)}} \int_{y_p}^{y_q} \int_{f_1(y)}^{f_2^{(k)}(y)} z \, dz \, dy ; k = 1, 2, \dots, n \quad (2.14)$$

and

$$Y_{\ell f}^{(k)} = \frac{1}{A^{(k)}} \int_{y_p}^{y_q} \int_{f_1(y)}^{f_2^{(k)}(y)} y \, dz \, dy ; k = 1, 2, \dots, n \quad (2.15)$$

The $f_2^{(k)}(y)$ reduces to the initial fill level $-h_0^{(k)}$ in the absence of the tank tilt and lateral acceleration. Equations (2.14) and (2.15) then yield the location of the centre of mass of liquid, $Y_{\ell f_0}^{(k)}$ and $Z_{\ell f_0}^{(k)}$, in the compartment k , for $a_y = 0 = \theta_{s3}$.

2.7.3 Modified Square Cross-section

A modified square cross-section, as shown in Figure 2.2 (d), can be realized from a modified oval cross-section, by selecting large values of R_1 and R_2 . The equations which described the circular arcs formed due to radii R_1 and R_2 will now be described by equations of a straight line parallel to the Y- or Z-axis. Hence the algorithm developed for the modified oval cross-section tank can be used to compute the lateral and vertical translation of the centre of mass of liquid within a modified square tank cross-section.

2.7.4 Elliptical Cross-section

In the case of an elliptical tank cross-section, the equation of

the ellipse in the coordinate frame attached to the tank base is given by:

$$\frac{y^2}{a^2} + \frac{(z + b)^2}{b^2} = 1 \quad (2.16)$$

where a and b are the semi-major and semi-minor axes of the ellipse. The roll plane steady state fluid model of an elliptical tank cross-section is presented in Figure 2.10. The roll plane model of the elliptical cross-section tank is developed in the same lines as that of the modified oval tank. The vertical and horizontal translation of the centre of mass of liquid within the elliptical tank cross-section is computed using the moment integral equations (2.14) and (2.15), through suitable substitutions for the domains of integration.

2.8 Kineto-Static Roll Plane Model of an Articulated Tank Vehicle

An articulated vehicle with multiple axles and a compartmented tank of arbitrary cross-section is considered for the simulation of the steady turning rollover threshold of the vehicle. The dynamics of the roll motion are not included in this model. Instead, roll response in a steady turn is computed by solving the static equilibrium equations for small increments in the trailer sprung mass roll angle. The multi-axled vehicle is represented by three composite axles by grouping axles with similar suspension properties. The lumped axles represent the tractor front axle, a single tractor rear axle (by grouping the tandem axle), and a single trailer axle (by grouping all the axles on the trailer), as shown in Figure 2.11. The tandem axle of the tractor, and the tandem- and closely spaced tri-axles of the trailer, can be adequately represented by a single equivalent axle. The single axle representation

-
- The diagram shows a rectangular plate with dimensions $2a$ and $2b$. A horizontal line passes through the center, with two triangles indicating a discontinuity or specific boundary condition. A vertical axis is labeled θ_{e3} . A point $c^{(k)}$ is located at a distance $y^{(k)}$ from the top edge and $z_{\ell f}^{(k)}$ from the right edge. A force $w_{\ell f}^{(k)}$ acts vertically downwards at this point. Another point is shown at a distance a_y from the bottom edge, with a force w_2 acting vertically downwards. The angle between the vertical axis and the line connecting the center to point $c^{(k)}$ is ϕ . Other labels include $Q^{(k)}$, $Z_{\ell f}^{(k)}$, and a_y .

- 39 -

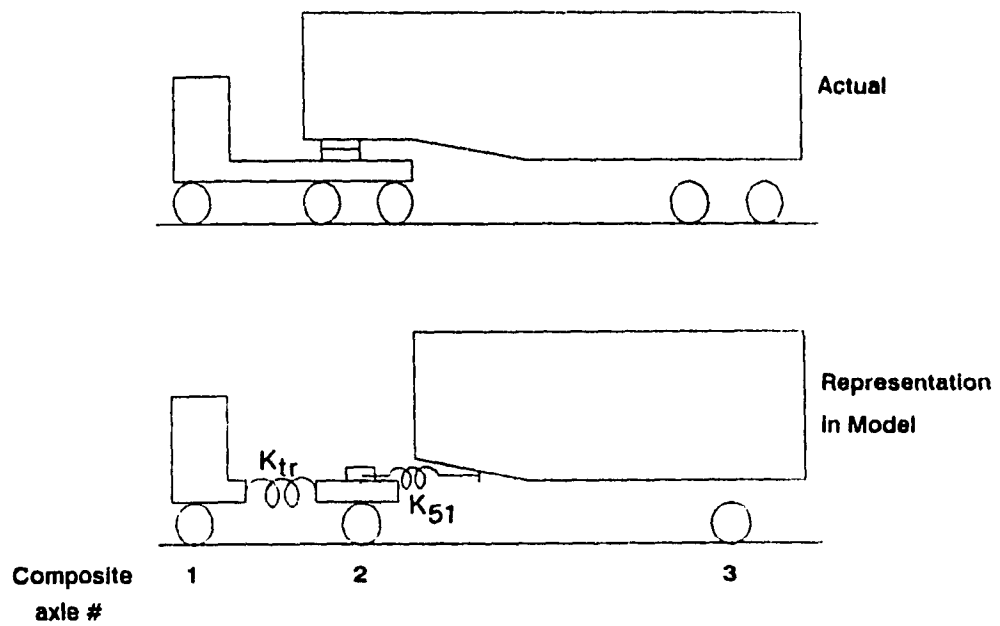


Figure 2.11 Composite axle representation of a tractor-semitrailer

of the wide spread tri- and quad-axle semitrailers, however, may lead to errors. The simplified model with composite axle representation, however, can provide significant insight pertaining to the influence of liquid motion on the steady turning characteristics of the vehicle.

The sprung weight of the tractor is represented by two sprung weights, W_f and W_r , supported by the front and the rear composite axles of the tractor, respectively. The two sprung weights are coupled through the torsional compliance of the tractor frame, as shown in Figure 2.12. The torsional compliance of the tractor frame is represented by a torsional spring element, K_{tr} , and coulomb friction, C_{tr} . The typical torque-deflection characteristics of a tractor chassis are presented in Figure 2.13.

The trailer sprung weight is represented by $(n + 1)$ sprung weights: sprung weight of the tank-semitrailer structure, W_2 and n sprung weights, $W_{lf}^{(k)}$, $k = 1, 2, \dots, n$, due to liquid cargo in n compartments. The sprung weight due to the tank-semitrailer is coupled to the tractor sprung weight, W_r , through the torsional compliance of the fifth wheel and tank-trailer structure, K_{s1} as shown in Figure 2.12. The kineto-static roll plane model of the tank vehicle is developed by integrating the roll plane steady state fluid model of the tank and the roll plane model of the articulated vehicle, as shown in Figure 2.14. It should be noted that the coordinates of the centre of mass of liquid in the compartment k are represented by $(Y_{lf}^{(k)}, Z_{lf}^{(k)})$ with respect to the fixed sprung mass centre of the tank-semitrailer structure.

The following simplifying assumptions are made during the development of the kineto-static roll plane model of the tank vehicle.

- (i) The sprung weights are assumed to rotate about their respective

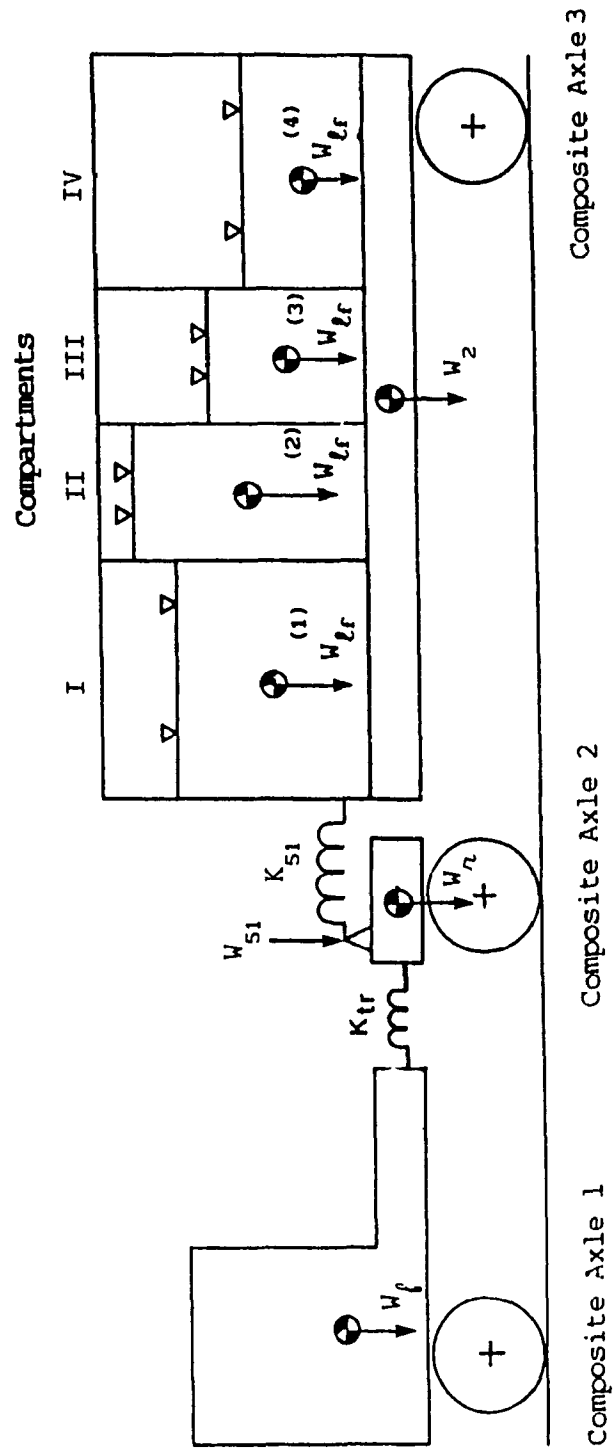


Figure 2.12 Representation of the tractor-tank semitrailer and the axles

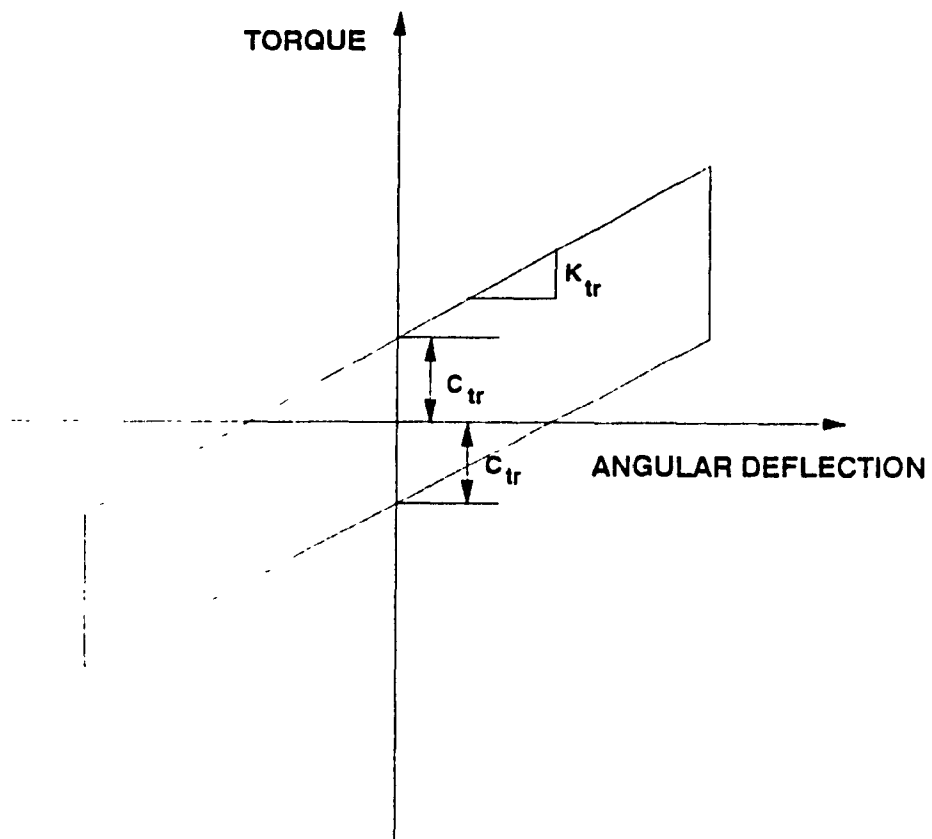


Figure 2.13 Typical torque-deflection characteristics of the tractor frame

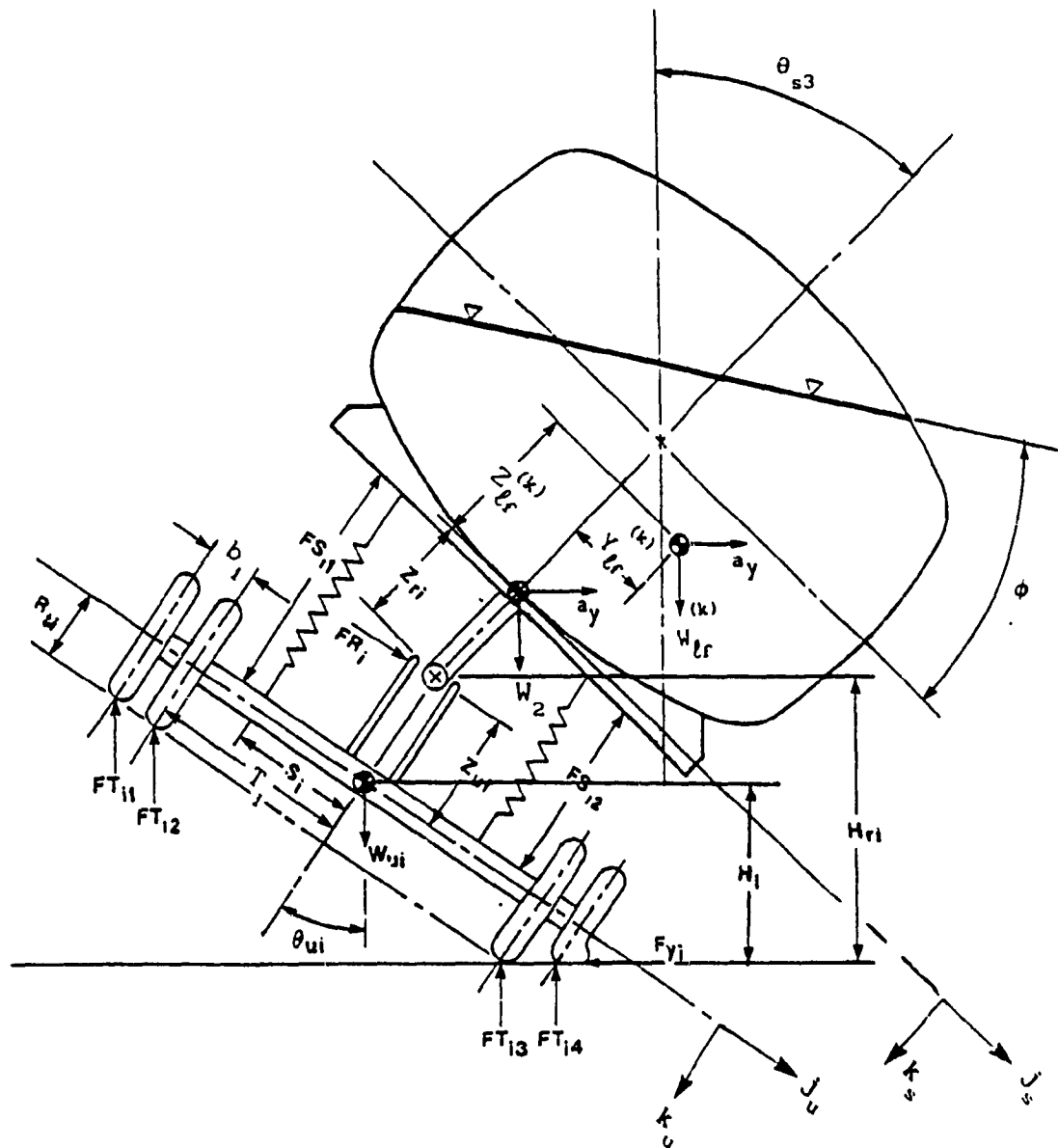


Figure 2.14 Kineto-static roll plane model of a tank vehicle

roll centres, which are located at a fixed distance from their centre of mass.

- (ii) The suspension springs, K_{ui} are considered to deflect along the vertical direction parallel to the vertical axis of the unsprung mass. Hence, the axle forces acting in a direction parallel to K_{ui} axes are balanced by the suspension forces and the axle forces in a direction perpendicular to K_{ui} axes are assumed to act at the roll centres.
- (iii) The suspension non-linearities such as the backlash, interleaf friction and progressively hardening nature of the spring characteristics are incorporated through a tabular input and linearized about the operating point during the simulation. The force-displacement characteristics of typical suspension springs at the three composite axles are presented in Figure 2.15.
- (iv) The lateral and vertical stiffness of the tires (KY_{ij} and KT_{ij} , i represents i th axle and j represents the number of tires on each composite axle, respectively) are assumed to be linear.
- (v) At lateral accelerations close to the rollover limit of the vehicle, the load transfer to the tires located on the outside of the turn is quite significant. Thus the lateral forces developed by the tires on the inside of the turn are assumed to be negligible when compared to those developed by the tires on the outside of the turn. The lateral deflections of the tires are thus computed only for the tires on the outside of the turn. A linear spring of stiffness $(KY_{i3} + KY_{i4})$, oriented along the J_{ui} axis of the axle, represents the compliance of the tires in the lateral direction.

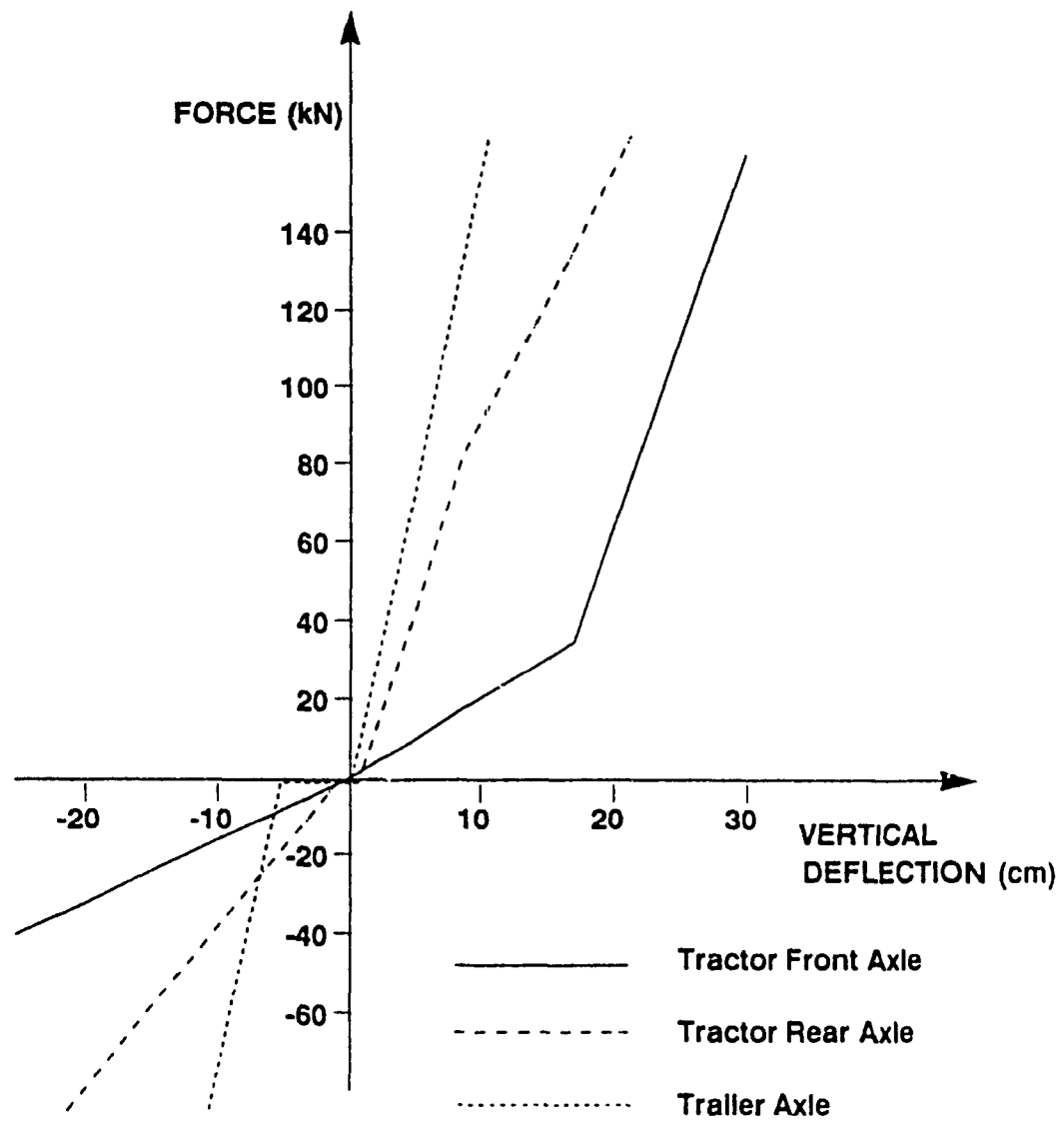


Figure 2.15 Force deflection characteristics of the suspension springs [10]

- (vi) The roll resisting moments developed due to camber are represented through torsional springs, $KOVT_{ij}$ located at the tire/road interface.
- (vii) The relative motion between the sprung and unsprung weight is assumed to occur about the roll centre.
- (viii) Roll angles are assumed to be small for both the sprung and unsprung masses, such that $\sin\theta = \theta$ and $\cos\theta = 1$.
- (ix) The influence of the articulation on the roll response of the tank vehicle is neglected while assuming small articulation angles. The sprung weights at various axles experience different vertical deflections, thus vehicle pitching during rollover can be incorporated in the model. The variation in total axle load due to vehicle pitching, however, are assumed to be negligible.

2.9 Equations of Kineto-Static Roll Equilibrium

A total of 15 algebraic equations along with '2n' equations describing the load shift within n compartments of the tank are required to describe the kineto-static roll equilibrium of the tank vehicle. The 15 algebraic equations are obtained by balancing the roll moments acting on the sprung and unsprung weights; vertical suspension and tire forces; and lateral forces acting on the tires. The roll equilibrium equations of the tank vehicle are presented in terms of small variations of the vehicle response parameters. A detailed derivation of the equations of roll equilibrium of the articulated vehicle are presented in Appendix I.

2.9.1 Roll Moments Acting on Sprung Weights

The roll moments acting on the sprung weights include moments due to suspension forces, torsional compliance of the tractor and tank-trailer structure, lateral forces acting through the roll centre,

lateral components of the sprung weights, and moments due to the translation of liquid load in each compartment:

$$\sum (\text{Moments about sprung weight centre of gravity}) = 0$$

$$\begin{aligned} W_{s1} (\Delta a_y - \Delta \theta_{s1}) Z_{r1} + (FS_{11} + FS_{12}) Z_{r1} (\Delta \theta_{s1} - \Delta \theta_{u1}) + \\ (K_{11} - K_{12}) s_1 \Delta Z_{u1} - (K_{11} + K_{12}) s_1^2 (\Delta \theta_{s1} - \Delta \theta_{u1}) + \\ \Delta \alpha_1 + \Delta \beta_1 + \Delta \gamma_1 + \Delta \delta_1 + \Delta \epsilon_1 = 0 \end{aligned} \quad (2.17)$$

where $i = 1, 2, 3$ denotes the composite axles on the tractor front, tractor rear and trailer respectively. The moments due to the torsional stiffness of the tractor frame, $\Delta \alpha_1$, is given by :

$$\Delta \alpha_1 = \begin{cases} (-1)^{i+1} K_{tr} (\Delta \theta_{s2} - \Delta \theta_{s1}) ; i = 1, 2 \\ 0 ; i = 3 \end{cases} \quad (2.18)$$

The moments due to the shear force W_{fr} acting on the tractor frame, $\Delta \beta_1$, is expressed as,

$$\Delta \beta_1 = \begin{cases} (-1)^{i+1} W_{fr} (\Delta a_y - \Delta \theta_{s1}) Z_{f1} ; i = 1, 2 \\ 0 ; i = 3 \end{cases} \quad (2.19)$$

where Z_{f1} is the vertical height of tractor frame with respect to the centre of gravity of the i th sprung weight. The moment due to the fifth wheel load, W_{s1} , acting on the tractor rear and trailer sprung weights, $\Delta \gamma_1$, is given by:

$$\Delta \gamma_i = \begin{cases} 0 ; i = 1 \\ (-1)^i W_{s1} Z_{s1} (\Delta a_y - \Delta \theta_{s1}) ; i = 2, 3 \end{cases} \quad (2.20)$$

where Z_{s1} is the height of the fifth wheel from the centre of gravity of the i th sprung weight. The moment due to the torsional compliance of the fifth wheel and the trailer structure, $\Delta \delta_i$, is expressed as:

$$\Delta \delta_i = \begin{cases} 0 ; i = 1 \\ (-1)^i K_{s1} (\Delta \theta_{s3} - \Delta \theta_{s2}) ; i = 2, 3 \end{cases} \quad (2.21)$$

and the roll moments acting on the trailer sprung weight, due to the lateral and vertical liquid load shift, $Z_{\ell f}^{(k)}$ and $Y_{\ell f}^{(k)}$, within various compartments of the tank, $\Delta \epsilon_i$, is given by:

$$\Delta \epsilon_i = \begin{cases} 0 ; i = 1, 2 \\ \sum_{k=1}^n W_{\ell f}^{(k)} \left[\Delta Y_{\ell f}^{(k)} (1 + a_y \theta_{s1}) + Y_{\ell f}^{(k)} (a_y \Delta \theta_{s1} + \Delta a_y \theta_{s1}) \right] - \\ \sum_{k=1}^n W_{\ell f}^{(k)} \left[\Delta Z_{\ell f}^{(k)} (\theta_{s1} - a_y) + Z_{\ell f}^{(k)} (\Delta \theta_{s1} - \Delta a_y) \right] ; i = 3 \end{cases} \quad (2.22)$$

2.9.2 Roll Moments Acting on Unsprung Weights

The equation for roll moments of the unsprung weights includes moments arising from suspension and tire forces, lateral forces acting through the roll centre and lateral forces developed at the tires. The equation of roll equilibrium for the i th unsprung mass can be expressed as.

$$\sum (\text{Moments about the unsprung weight centre of gravity}) = 0$$

$$\begin{aligned} & (K_{11} + K_{12})s_1^2 \Delta\theta_{s1} - (W_{s1}H_{r1} + W_{u1}H_1)\Delta a_y + [-(K_{11} - K_{12})s_1 + \\ & W_{s1}(a_y - \theta_{u1})]\Delta Z_{u1} + [(KT_{11} - KT_{14})(T_1 + b_1) + (KT_{12} - KT_{13})T_1 - \\ & (KT_{13} + KT_{14})y_1 + (W_{s1} + W_{u1})a_y]\Delta H_{u1} - [(K_{11} + K_{12})s_1^2 - W_{s1}Z_{u1} - \\ & (W_{s1} + W_{u1})R_{t1} + KOVT_{13} + KOVT_{14} + KT_{11}(T_1 + b_1)^2 + KT_{12}T_1^2 + \\ & KT_{13}(T_1 + y_1)^2 + KT_{14}(T_1 + b_1 + y_1)^2]\Delta\theta_{u1} - [FT_{13} + FT_{14} + \\ & (KT_{13} + KT_{14})(T_1 + y_1) + KT_{14}b_1]\theta_{u1}]\Delta y_1 = 0 ; \quad i = 1, 2, 3 \quad (2.23) \end{aligned}$$

where KT_{1j} is the vertical spring rate of all j tires, located on the i th composite axle and K_{1j} is the spring rate of all j suspensions at the i th composite axle.

2.9.3 Forces Acting through the Suspension Springs

The forces generated by the compression/extension of the suspension springs must satisfy the following equation :

$$\begin{aligned} & (K_{11} + K_{12})\Delta Z_{u1} - (K_{11} + K_{12})s_1 \Delta\theta_{s1} + (K_{11} - K_{12})s_1 \Delta\theta_{u1} = \\ & W_{s1}\theta_{u1}\Delta a_y + W_{s1}a_y\Delta\theta_{u1} ; \quad i = 1, 2, 3 \quad (2.24) \end{aligned}$$

2.9.4 Vertical Forces Generated by the Tires

The vertical load carried by each composite axle is assumed to remain constant, neglecting influence of grade and vehicle pitch. Thus, the following equilibrium equation must be satisfied:

$$\Delta \sum_{j=1}^4 FT_{1j} = 0 ; \quad i = 1, 2, 3 \quad (2.25)$$

$$\begin{aligned} & [(-KT_{11} + KT_{14})(T_1 + b_1) + (-KT_{12} + KT_{14})T_1 \\ & - (KT_{13} + KT_{14})y_1]\Delta\theta_{u1} + (KT_{11} + KT_{12} + KT_{13} + KT_{14})\Delta H_{u1} \\ & + (KT_{13} + KT_{14})\theta_{u1}\Delta y_1 = 0 ; \quad i = 1, 2, 3 \quad (2.26) \end{aligned}$$

2.9.5 Lateral Forces Generated by the Tires

When the lateral acceleration approaches the rollover limit of the tank vehicle, the tires on the outside of the turn carry almost the entire axle load. The inertial forces acting on the i th axle must be balanced by the lateral forces generated by the tires:

$$(KY_{13} + KY_{14})\Delta y_i = (W_{s1} + W_{u1})\Delta a_y ; \quad i = 1,2,3 \quad (2.27)$$

Equations (2.17) thru (2.27) provide a total of 15 equations representing the force and moment equilibrium of the tank vehicle in the roll plane. Equations (2.6) thru (2.16) provide the set of $2n$ equations required to compute the instantaneous centre of mass of the liquid within a tank of arbitrary cross-section. Thus a total of $(15 + 2n)$ equations are developed to describe the kineto-static roll plane model of an n compartmented tank vehicle.

2.10 Summary

A kineto-static roll plane model of a tank vehicle is developed by integrating the roll plane steady state fluid model of a partially filled arbitrarily shaped tank and the roll plane model of an articulated vehicle. The liquid load shift occurring within a partially filled arbitrarily shaped tank cross-section is computed using a numerical iterative algorithm. The equations for kineto-static roll plane model of the tank vehicle are derived in order to compute the rollover threshold acceleration limits of articulated tank vehicles.

REFERENCES FOR CHAPTER 2

1. Nalecz, A.G. and Genin, J., "Dynamic Stability of Heavy Articulated vehicles", Int. J. of Vehicle Design, Vol. 5, No.4, 1984.
2. Bauer, H.F., "Dynamic Behaviour of an Elastic Separating Wall in Vehicle Containers : Part I", Int. J. of Vehicle Design, Vol. 12, No. 1, 1981.
3. Bechtold, James C., "Vehicle Stability and 102 inches", Modern Bulk Transporter, pp. 65-69, 1983.
4. Isermann, H., "Overturning Limits of Articulated Vehicles with Solid and Liquid Loads", Motor Industry Research Assoc., Translation No. 58/70, 1970.
5. Miller, D.W.G. and Barter, N.F., "Rollover of Articulated Vehicles", I. Mech. Engr. Conference on Vehicle Safety Legislation, Paper No. C203/73, 1973.
6. Gillespie, T.D. and Verma, M.K., "Analysis of the Rollover Dynamics of Double-Bottom Tankers", SAE Paper No. 781065, 1978.
7. Mallikarjunarao, C., "Road Tanker Design: Its influence on the risk and economic aspects of transporting gasoline in Michigan", Ph.D. thesis, University of Michigan, 1982.
8. Strandberg, L. "Lateral Stability of Road Tankers", National Road and Traffic Research Institute Report No. 138, Sweden, 1978.
9. Strandberg, L., Nordstrom, O. and Nordmark, S., "Safety Problems in Commercial Vehicle Handling", Symposium on Commercial Vehicle Braking and Handling, Highway Safety Research Institute, University of Michigan, 1975.
10. Ervin, R.D., Guy, Y., "The influence of Weights and Dimensions on the stability and control of heavy-duty trucks in Canada", UMTRI Report No. 86-35, July 1986.
11. Rakheja, S., Sankar, S. and Ranganathan, R., "Study on Liquid Tanker Stability: Steady Turning Stability of Partially Filled Tank Vehicle", CONCAVE Research Report No. 13-87, October 1987.
12. Streeter, V.L. and Benjamin, W.E., "Fluid Mechanics", McGraw Hill Book Co., Sixth Edition, 1975.

CHAPTER 3

ROLLOVER THRESHOLD LIMITS OF LIQUID TANK VEHICLES

3.1 General

The vehicle rollover during steady turning is strongly related to its rollover threshold (overturning limit). The rollover threshold of a vehicle is defined as the maximum lateral acceleration that the vehicle can withstand. The $(15 + 2n)$ equations describing the kineto-static roll equilibrium of a tractor-tank-semitrailer vehicle derived in the previous chapter, are solved simultaneously to evaluate its steady turning response and rollover threshold. In this chapter, the method of solution for solving the kineto-static roll equilibrium equations is presented along with the simulation results. The rollover threshold levels of an articulated vehicle equipped with tanks of various cross-section are compared to that of an equivalent rigid cargo vehicle to establish the influence of liquid motion within a partially filled tank vehicle. The influence of the tank cross-section on the steady turning stability of the vehicle is also investigated along with the rollover threshold limits of compartmented tank vehicles.

3.2 Method of Solution

The equations of static roll equilibrium (2.17) through (2.27), are expressed in terms of variations in roll angles, vertical motion of sprung weights, lateral and vertical motions of unsprung weights, lateral and vertical translations of the centre of mass of liquid load in each compartment, and lateral acceleration. The algebraic equations can be written in matrix notation in the following manner:

$$[P] \{\Delta x\} = \{Q\} \Delta \theta_{s3} \quad (3.1)$$

where $[P]$ is a (15×15) matrix of coefficients, and $\{Q\}$ is a vector of

dimension (15 X 1), and $\{\Delta x\}$ is the vector of vehicle response parameters due to variations in the roll angle of tank trailer sprung weight ($\Delta\theta_{s3}$), expressed as:

$$\{\Delta x\}^T = \{\Delta a_y, \Delta\theta_{s1}, \Delta\theta_{s2}, \Delta\theta_{u1}, \Delta Z_{u1}, \Delta H_{u1}, \Delta y_1\} \quad (3.2)$$

where T indicates transpose, and $i = 1, 2, 3$ represent the three composite axles.

Initially, the vehicle is assumed to be in the upright position ($\theta_{s1} = \theta_{u1} = 0$). Equation (3.1) is solved for a small increment in the roll angle of the tank semitrailer sprung weight ($\Delta\theta_{s3}$). The response vector $\{\Delta x\}$ is computed for a series of increments of $\Delta\theta_{s3}$; the corresponding lateral and vertical translations of liquid within each compartment are evaluated, and the matrix [P] and vector {Q} are updated. The tire deflections and normal loads are computed for each increment of $\Delta\theta_{s3}$. The calculations are terminated when the normal load on inside tire of the tractor rear and trailer composite axles approach zero. The vehicle rollover is thus detected due to the lift off of these tires. The highest lateral acceleration encountered during the computing process determines the rollover threshold acceleration of the tank vehicle.

Computer simulations are carried out for the following tank geometry:

<u>Circular</u> (MC 307, 312)	Diameter, D = 2.03 m		
<u>Modified Oval</u> (MC 306 A1)	$R_1 = 1.78$ m	$R_2 = 1.78$ m	$R_3 = 0.39$ m
	$H_1 = 2.44$ m	$H_2 = 1.65$ m	
<u>Modified Square</u>	$H_1 = 2.44$ m	$H_2 = 1.65$ m	$R = 0.39$ m
<u>Elliptic</u>	$2a = 2.28$ m	$2b = 2.03$ m	

The parameters for the candidate vehicle used in the simulation are listed in Table 3.1. The effect of tank roll and lateral acceleration on the load shift are computed using equations (2.6) thru (2.16), depending upon the tank geometry. The overturning lateral acceleration limit of the tank-vehicle is evaluated for various % fill levels, where the % fill level is defined as the percent ratio of the liquid height in the compartment k , $h_o^{(k)}$, to the total height of the tank:

$$\% \text{ Fill} = \begin{cases} \frac{h_o^{(k)}}{D} * 100 ; \text{Circular tanks} \\ \frac{h_o^{(k)}}{2b} * 100 ; \text{Elliptical tanks} \\ \frac{h_o^{(k)}}{H_2} * 100 ; \text{Modified oval and square tanks} \end{cases} \quad (3.3)$$

3.3 Load Shift during Steady Turning

The motion of the free surface of liquid within a partially filled tank can lead to significant lateral load shift during steady turning. The magnitude of the lateral shift ($Y_{lf}^{(k)}$) of the load depends upon the gradient of the free surface, fill level, and tank cross-section. Figure 3.1 shows the lateral translation of centre of mass of liquid bulk in a cylindrical tank due to tank roll alone. The lateral load shift increases with increase in the tank roll and is quite significant for low fill conditions.

The lateral acceleration imposed on the liquid bulk shifts the centre of mass further. To obtain its qualitative estimate, the gradient of the free surface of liquid is computed using Equation (2.5). The gradient of the free surface increases with increase in steady

TABLE 3.1

SPECIFICATIONS OF THE TANK VEHICLE USED IN SIMULATION

TRACTOR

<u>Type:</u>	<u>Three Axle:</u>
Sprung Weight:	46882 N (10540 lb)
Unsprung Weight (front axle):	9340 N (2100 lb)
Unsprung Weight (rear axle):	22240 N (5000 lb)
Front Axle Suspension Rating:	88960 N (20000 lb)
Rear Axle Suspension Rating:	97856 N (22000 lb)
Wheel Base:	4.37 m (172 in)

TANK and TRAILER

<u>Type:</u>	<u>Triaxle:</u>
Sprung Weight (empty):	87448 N (19660 lb)
Tank Length:	12.19 m (480 in)
Axle Rating:	97856 N (22000 lb)
Weight Density:	0.0068 N/cm ³ (0.025 lb/in ³)
Compartment Length - I, IV:	4.06 m (160 in)
Compartment Length - II, III:	2.03 m (80 in)
Vertical spring rate of tires:	7880 N/cm (4500 lb/in)
Lateral spring rate of tires:	8755 N/cm (5000 lb/in)

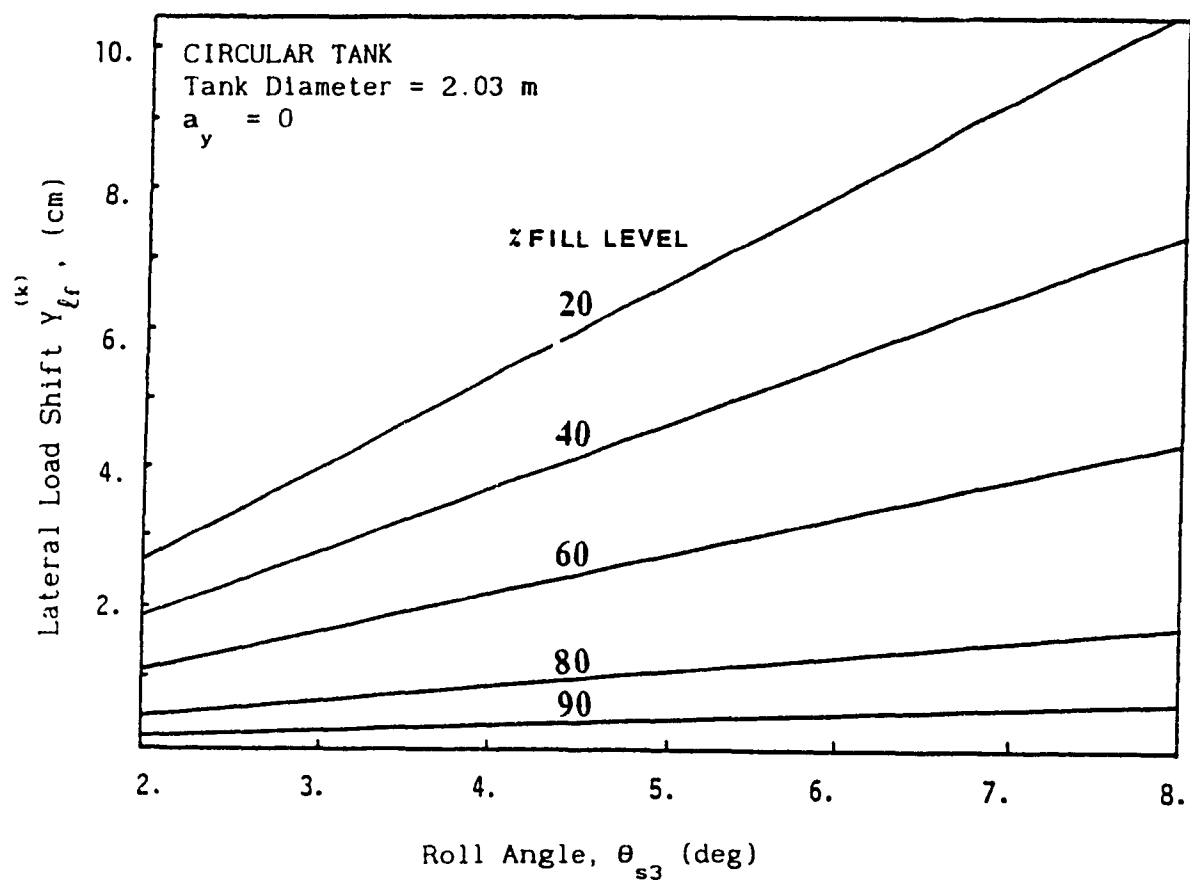


Figure 3.1 Lateral translation of C.G of liquid due to tank roll alone

turning lateral acceleration of the vehicle. Figure 3.2 presents the lateral translation ($Y_{\ell_f}^{(k)}$) of the centre of mass of liquid in circular, modified oval, and modified square tanks for various acceleration levels, while the tank tilt is kept constant (5 degrees).

The magnitude of lateral translation of the centre of mass of liquid and thus the lateral load shift increases significantly with increase in vehicle acceleration, for low fill levels. The magnitude of lateral translation of C.G. of liquid within modified oval and modified square tanks is significantly higher than that in a circular tank, as shown in Figure 3.2. Figure 3.3 presents a comparison of the lateral translation ($Y_{\ell_f}^{(k)}$) of the centre of mass of liquid in circular, modified oval, and modified square tanks with 40% fill for various acceleration levels, while the tank tilt is kept constant ($\theta_{s3} = 5$ degrees). A 40% filled tank, when subjected to lateral acceleration of 0.30g, the lateral shift of the centre of mass in a modified oval tank is 80% greater than that in a circular tank, while the lateral shift in a modified square tank is approximately 33% greater than that in a circular tank.

The corresponding magnitude of the vertical translation of the centre of mass of liquid, ($Z_{\ell_f}^{(k)}$) within various tanks is only marginal, as shown in Figure 3.4. Figure 3.5 presents a comparison of the magnitude of vertical translation of liquid ($Z_{\ell_f}^{(k)}$) in circular, modified oval, and modified square tanks with 60% fill for various acceleration levels, while the tank tilt is kept constant ($\theta_{s3} = 5$ degrees). It can be seen that the vertical translation of centre of mass of liquid within the circular and modified square configurations is significantly larger than that in a modified oval tank.

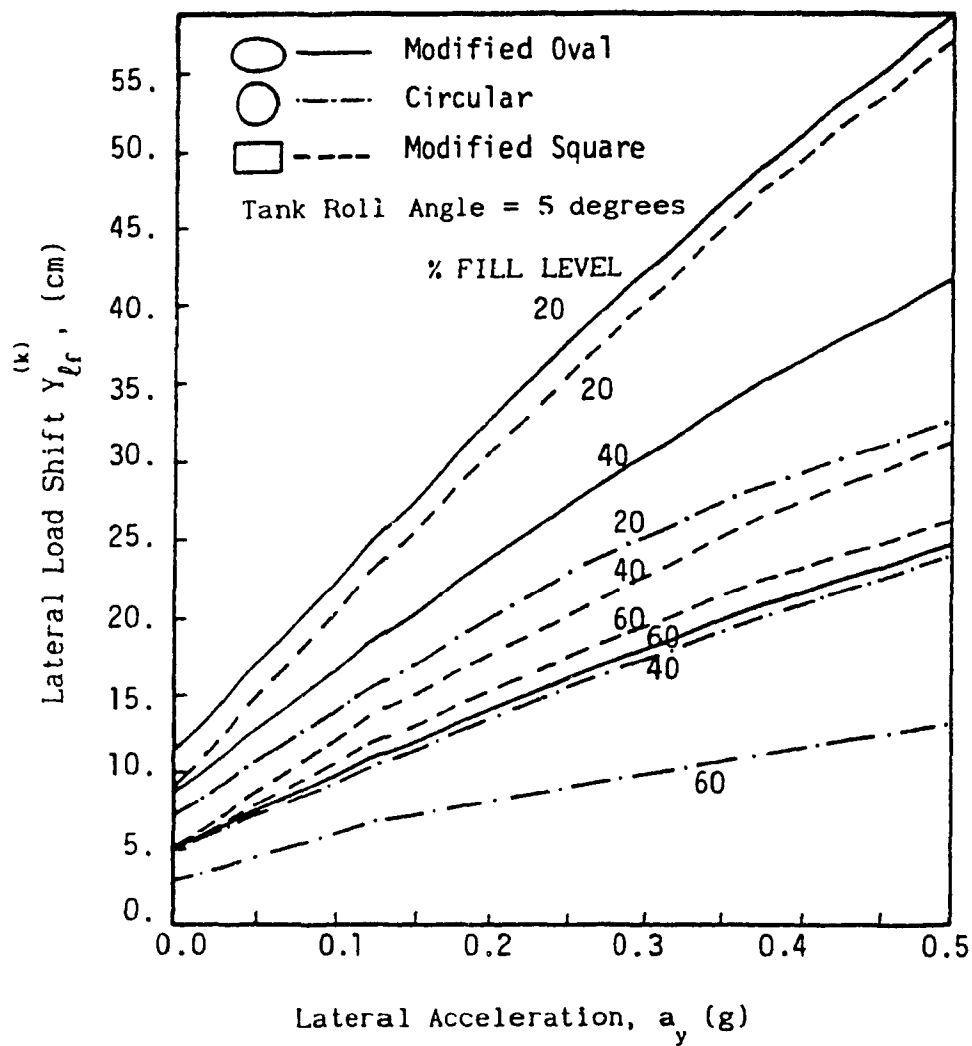


Figure 3 2 Lateral translation of C.G. of liquid due to tank roll and lateral acceleration

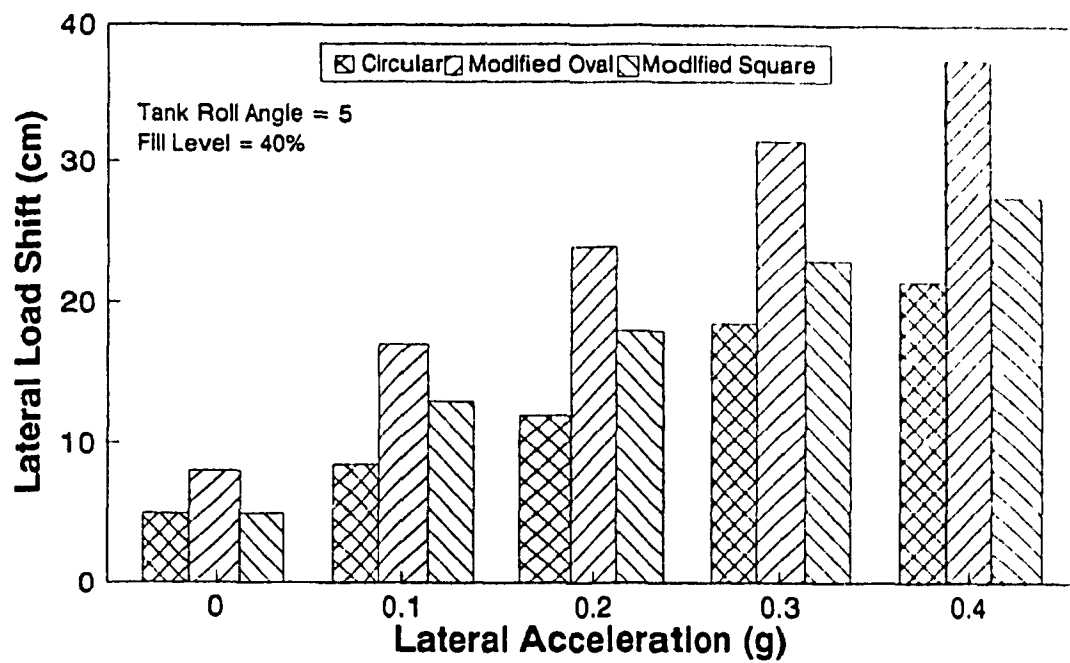


Figure 3.3 Comparison of lateral translation of C.G of liquid in various tanks

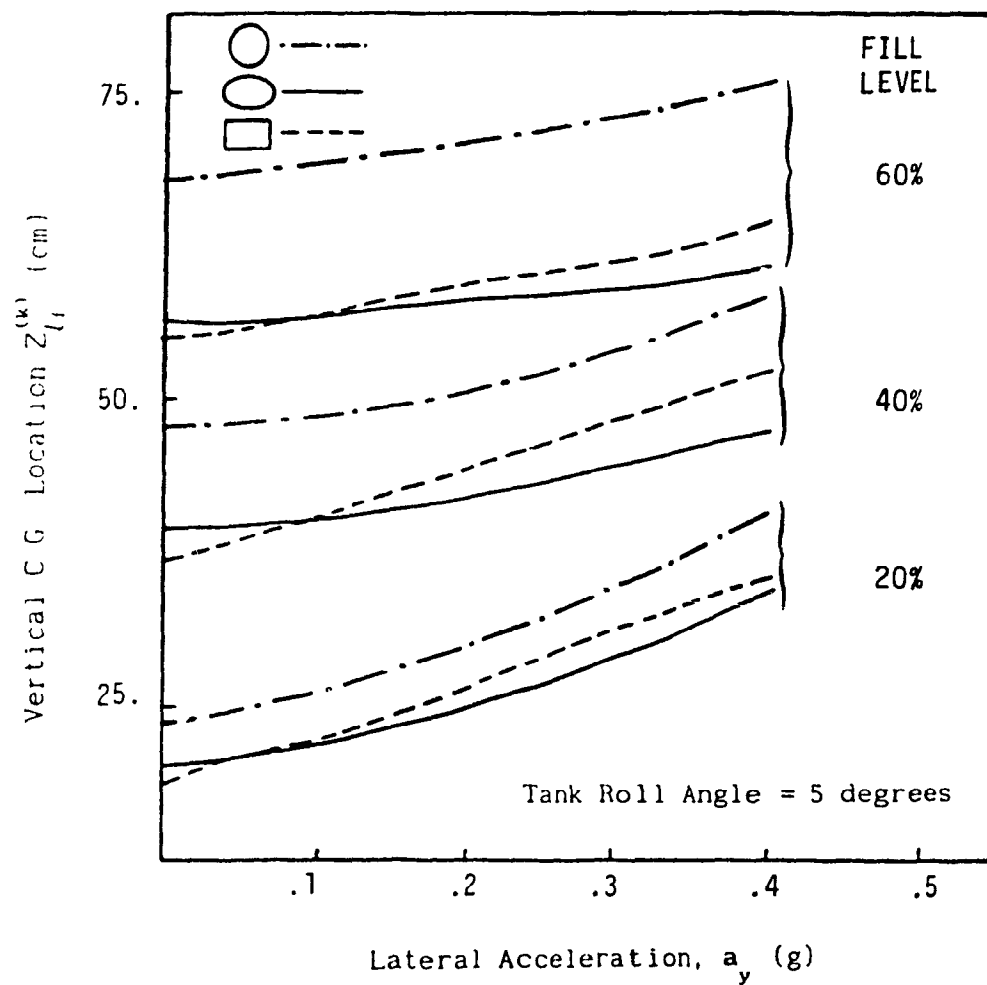


Figure 3.4 Vertical translation of C.G of liquid due to tank roll and lateral acceleration

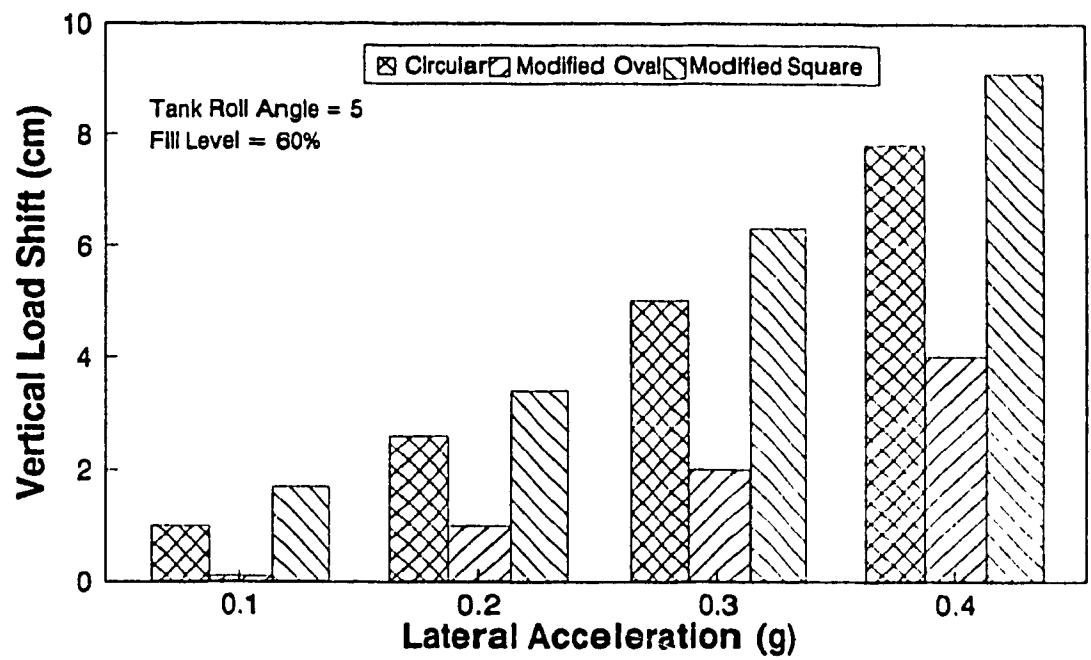


Figure 3.5 Comparison of vertical translation of C.G of liquid in various tanks

3.4 Rollover Acceleration Limits of Tank Vehicles

The rollover threshold of articulated tank vehicles is computed for partial fill conditions arising from two scenarios: (i) Partial fill during local deliveries (variable axle loads), and (ii) partial fill due to increased weight density (constant axle loads). The static equilibrium equation (3.1), is solved simultaneously along with the equations (2.6) thru (2.16) required to compute the liquid load shift, to evaluate the rollover threshold of tank vehicles equipped with partially filled circular, modified oval, elliptical, and modified square tanks.

3.4.1 Rollover Threshold of Tank Vehicles (Variable Axle Loads)

The rollover acceleration limits of tank vehicles, equipped with partially filled tanks of circular, modified-oval, modified square, and elliptic cross-sections are compared to those of a vehicle carrying an equivalent rigid cargo, and are presented in Figures 3.6 thru 3.9. The simulation results of tank vehicles are validated by comparing their response to that of an equivalent rigid cargo vehicle [1] corresponding to 0% and 100% fill conditions. The rollover threshold limit of a vehicle with equivalent rigid cargo decreases as the cargo load is increased. The decrease in the rollover threshold is primarily attributed to the increase in the height of the sprung weight centre of mass. The rollover threshold levels of liquid tank vehicles are significantly lower compared to those of the vehicles carrying equivalent rigid cargo, as shown in the Figures 3.6 thru 3.9. The reduced overturning limits of a partially filled tank vehicle is attributed to the load shift occurring during the steady turning process. The rollover limits of tank vehicles with low fill levels are

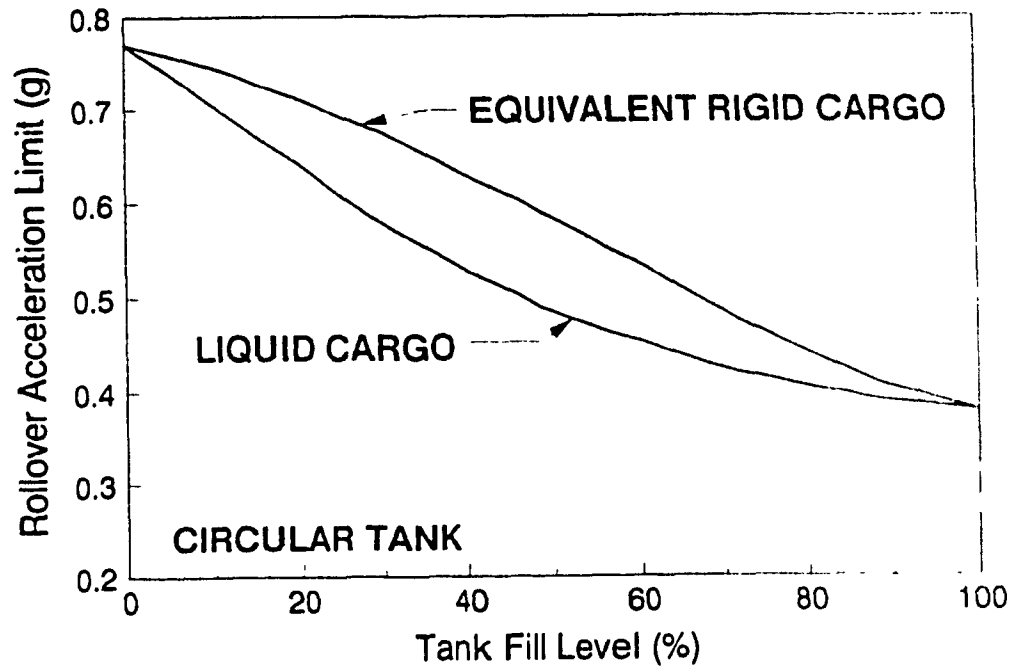


Figure 3.6 Rollover threshold acceleration of equivalent rigid cargo and circular tank vehicles (Variable axle loads)

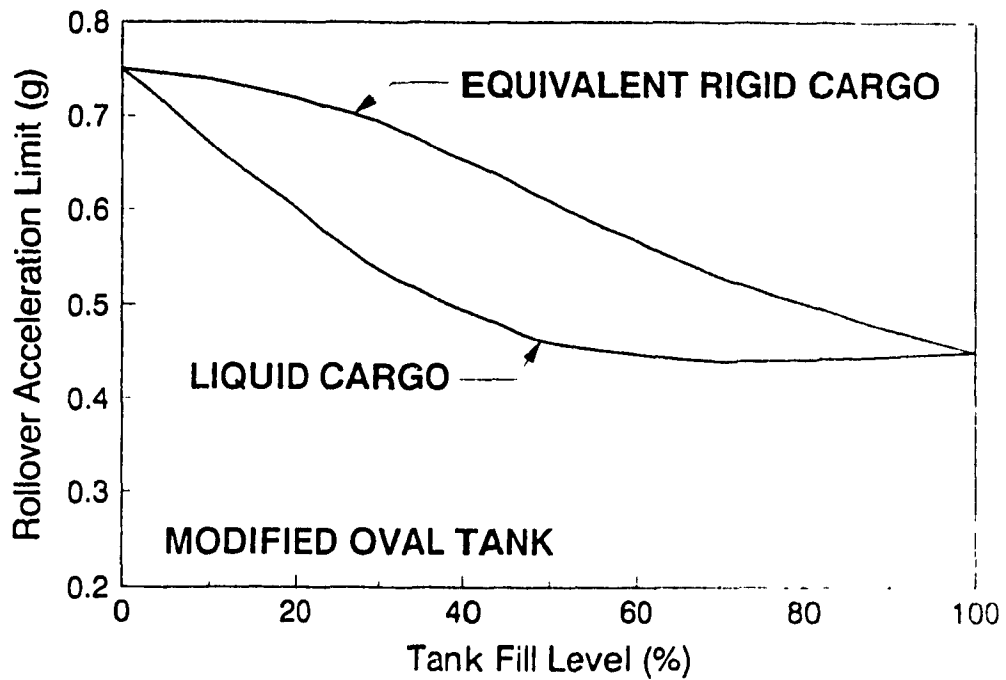


Figure 3.7 Rollover threshold acceleration of equivalent rigid cargo and modified-oval tank vehicles (Variable axle loads)

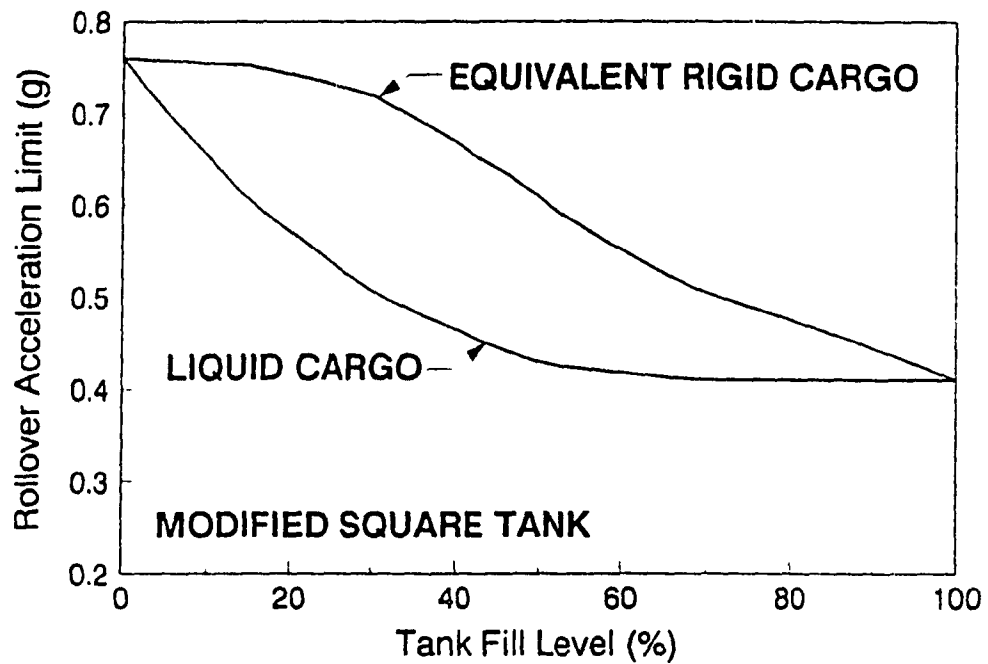


Figure 3.8 Rollover threshold acceleration of equivalent rigid cargo and modified-square tank vehicles (Variable axle loads)

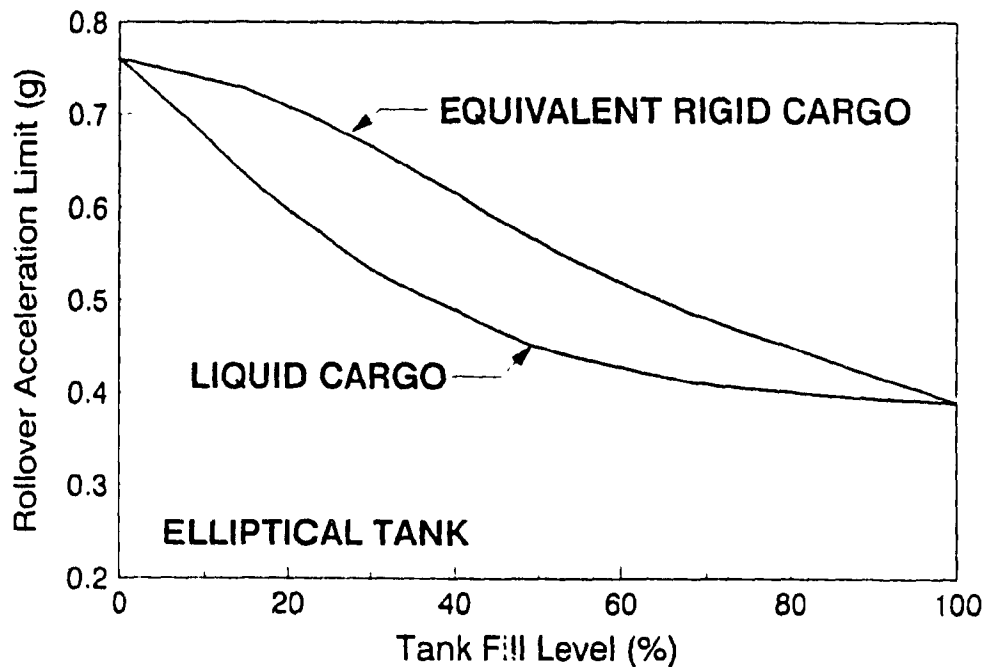


Figure 3.9 Rollover threshold acceleration of equivalent rigid cargo and elliptic tank vehicles (Variable axle loads)

considerably lower than those of the equivalent rigid cargo due to the large lateral load shift.

A comparison of rollover immunity levels of tank vehicles with different tank cross-sections are shown in Figure 3.10. It reveals that vehicles with modified oval and modified square tanks can rollover at lower values of lateral acceleration compared to circular cross-sectional tanks. Under 40% fill condition, lateral load shift due to the motion of free surface reduces the rollover threshold acceleration of a circular tank by 0.11g and that of an elliptic tank by 0.12g, whereas the rollover threshold of modified oval and modified square tank configurations is reduced by 0.17g and 0.20g respectively compared to that of an equivalent rigid cargo vehicle. The rollover limits of tank vehicles approach that of an equivalent rigid cargo vehicle for fill levels greater than 90%.

3.4.2 Rollover Threshold of Tank Vehicles (Constant Axle Loads)

In the case of variable axle loads, the load carried by each composite axle decreases as the liquid fill level is decreased. Tank vehicles used in general purpose chemical fleet, due to variations in weight density of chemicals transported, often carry partial loads, in order to maintain maximum permissible axle loads. The rollover acceleration limits of partially filled tank vehicles are compared to those of the equivalent rigid cargo vehicle, while the loads carried by each composite axle are maintained constant by varying the weight density of the liquid carried. The results are presented in Figures 3.11 to 3.14.

The 100% fill condition and corresponding composite axle loads are based upon fuel oil of weight density 0.0068 N/cm^3 . The rollover

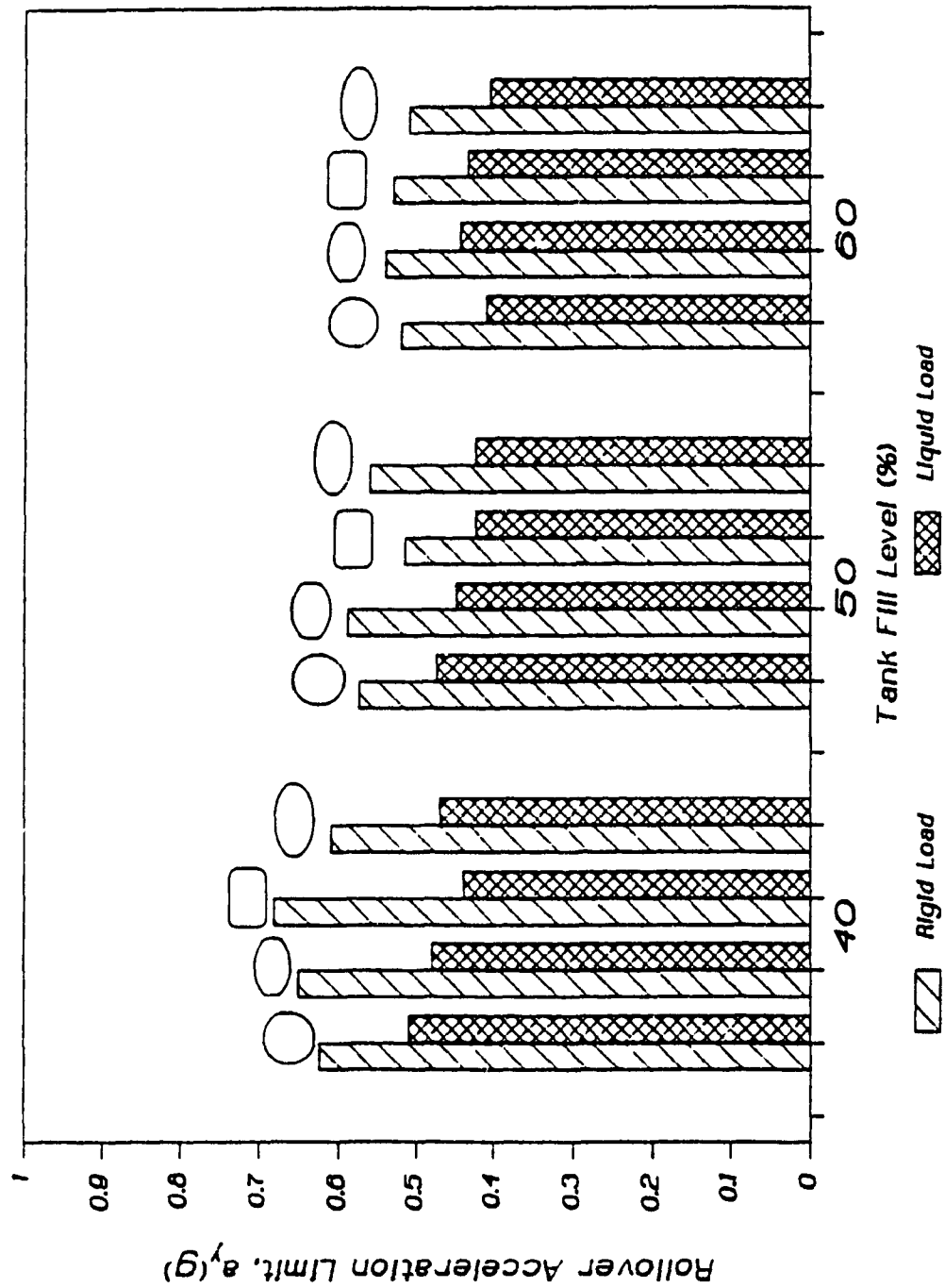


Figure 3.10 Comparison of rollover acceleration limits of tank vehicles with various tank cross-sections (Variable axle loads)

immunity of the vehicle for partial fill conditions is evaluated by varying the weight density, while the composite axle loads are kept constant. The rollover acceleration limit of an equivalent rigid cargo vehicle rapidly increases due to reduced centre of mass height of the sprung weight. In case of liquid tank vehicles, the expected increase in the rollover threshold limits due to reduced centre of mass height is compensated by the load shift occurring during partial filling of the tank, hence the rollover threshold value tends to remain constant (Figure 3.11) in case of circular tanks. The rollover threshold limits of modified oval, modified square, and elliptical tanks, however, exhibit a small decrease, as shown in Figures 3.12 to 3.14, respectively. The reduction in the rollover threshold limits is attributed to larger lateral load shift encountered in modified oval, modified square, and elliptical tanks compared to cylindrical tanks.

The rollover immunity levels of tank vehicles with circular, elliptical, modified oval, and modified square tank configurations carrying various liquids are summarized in Figure 3.15, while the payload and composite axle loads are held constant. The total payload carried by tank vehicles is held constant around 268 kN (60320 lbs). The modified oval and modified square tanks reveal improved threshold limits while carrying lighter liquids, whereas the circular tanks show better stability for denser liquids.

3.5 Rollover Threshold Limits of Compartmented Tank Vehicles

In view of the reduced rollover threshold value of partially filled tank vehicles, compartmented tanks are often used to minimize the occurrence of partial fill conditions. Specifically, vehicles delivering fuel oils within the city employ compartmented tanks, so that

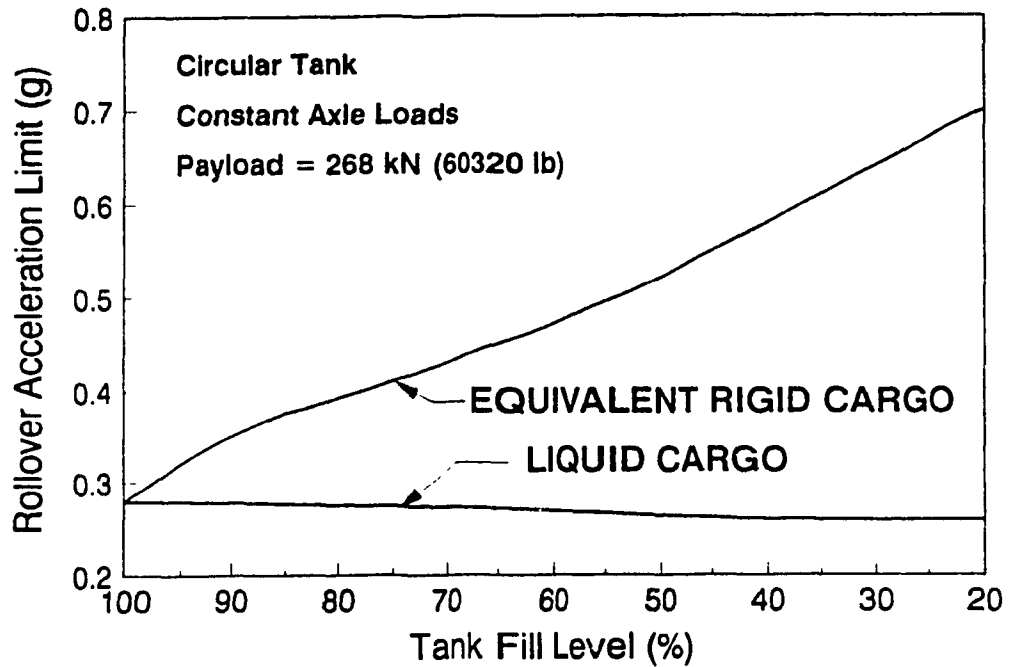


Figure 3.11 Rollover threshold acceleration of equivalent rigid cargo and circular tank vehicles (Constant axle loads)

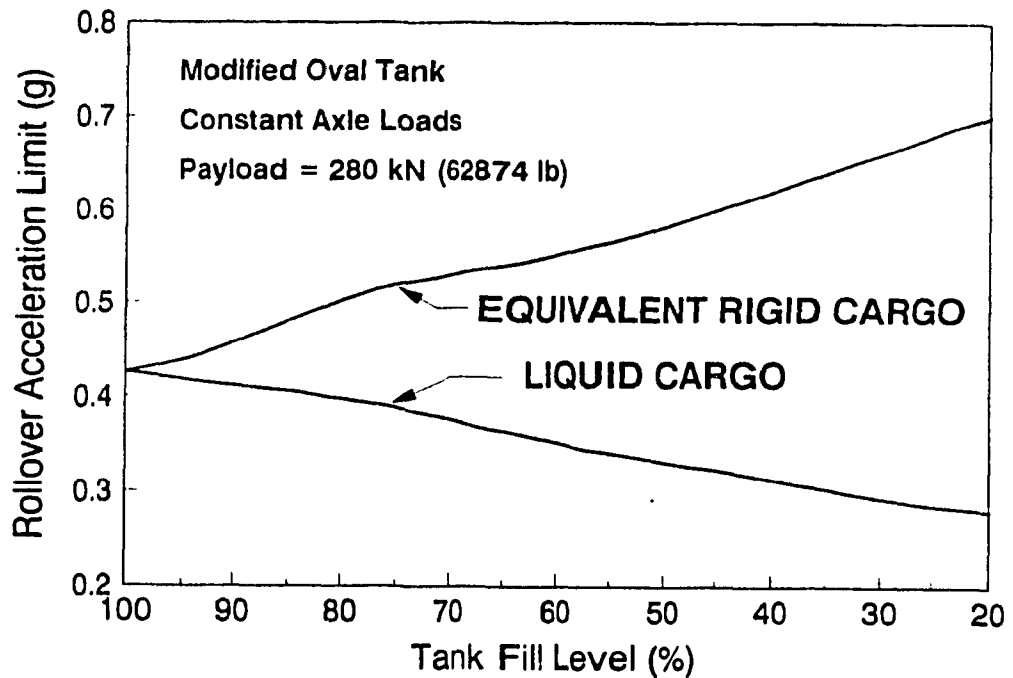


Figure 3.12 Rollover threshold acceleration of equivalent rigid cargo and modified-oval tank vehicles (Constant axle loads)

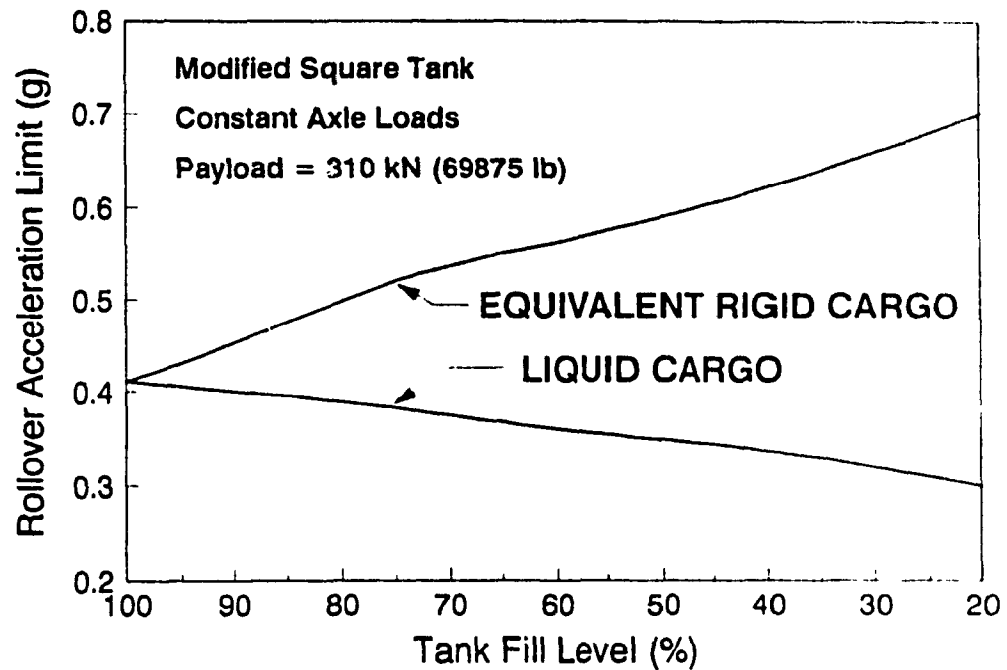


Figure 3.13 Rollover threshold acceleration of equivalent rigid cargo and modified-square tank vehicles (Constant axle loads)

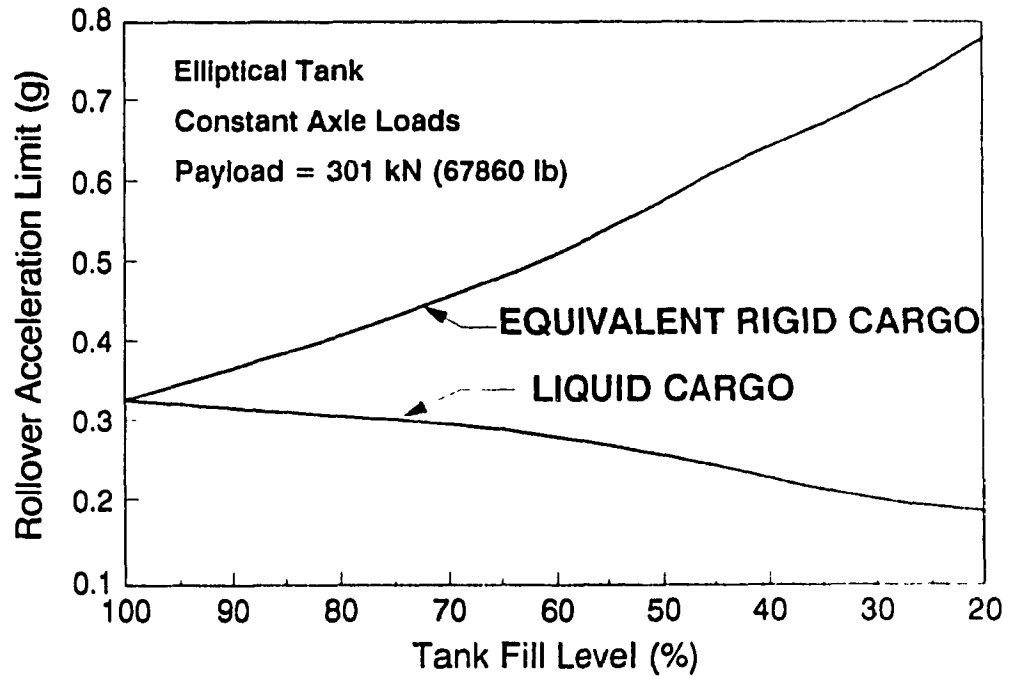
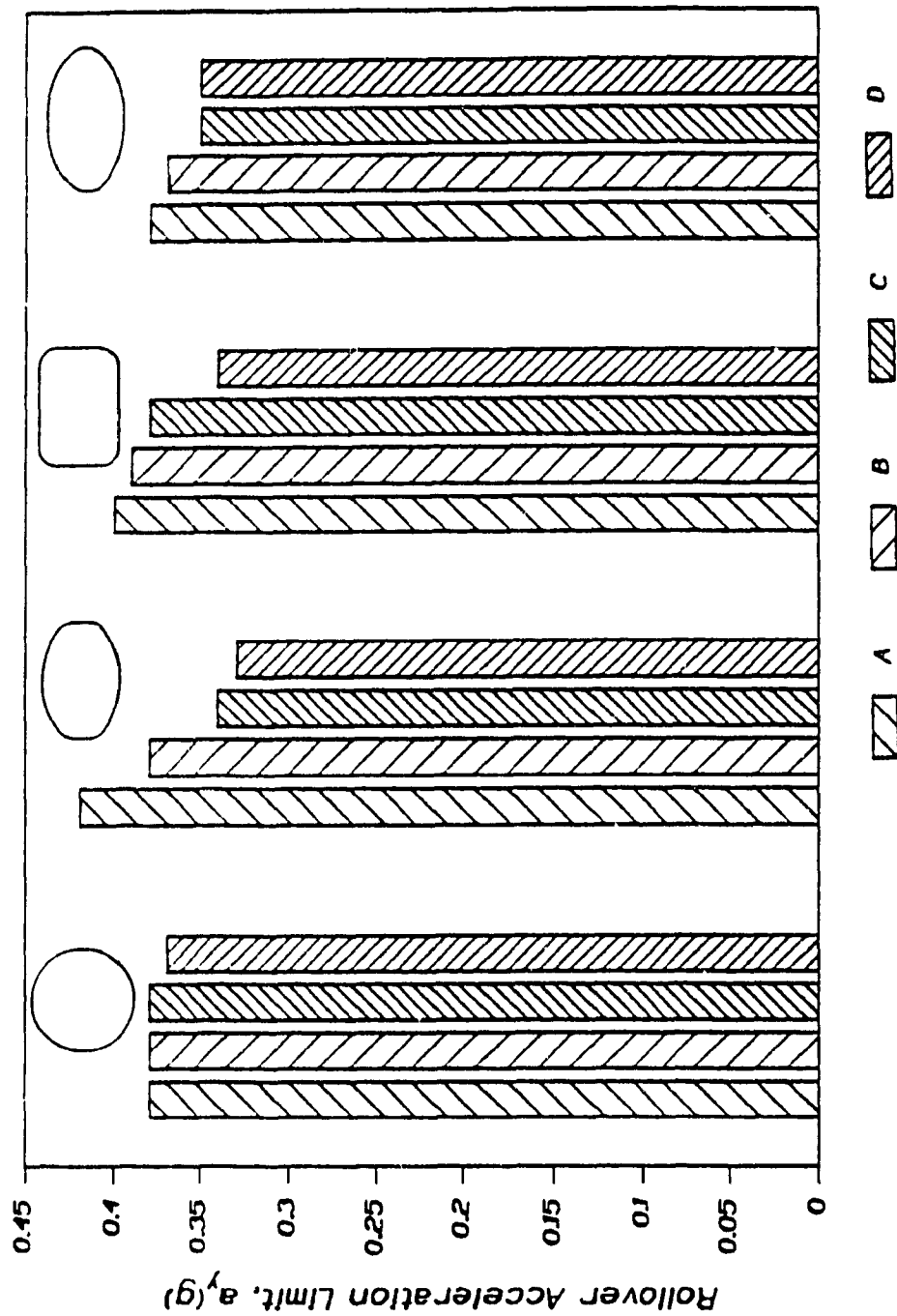


Figure 3.14 Rollover threshold acceleration of equivalent rigid cargo and elliptic tank vehicles (Constant axle loads)



A - Fuel Oil; B - Domestic Oil; C - Diesel; D - Industrial Acid

Cargo Load = 268 kN (60320 lb)

Figure 3.15 Comparison of rollover acceleration limits of tank Vehicles with various tank cross-sections (Constant axle loads)

one or more of the compartments may be emptied completely, while the remaining compartments carry full load. Often semitrailer vehicles carry tanks with 4 or 5 compartments. The rollover limits of such vehicles depend upon the load distribution among the various compartments. The tanks employed in general purpose chemical fleets are often cleanbore to facilitate cleaning.

The rollover threshold of a tank vehicle, equipped with a four compartmented tank of cylindrical cross-section, as shown in Figure 3.16 is investigated. The rollover acceleration limits of the four compartmented cylindrical tank vehicle with one of the compartments carrying partial load and the other compartments fully loaded is presented in Figure 3.17. The tank vehicle exhibits highest rollover limit when compartment II is partially filled, for fill levels below 50%. For fill levels greater than 50%, partial fill in compartments II or III reveals the same overturning limit. Partial filling of compartment IV yields minimum value of rollover acceleration limit due to reduction in load carried by the trailer composite axle. Thus under partial fill conditions, the compartment II must be emptied first in order to achieve highest value of rollover limit of the vehicle.

The rollover threshold values of the tank vehicle with an empty compartment (II) and a partially filled compartment are presented in Figure 3.18. A partial load in compartment III reveals a higher value of rollover acceleration limit, when compared to that of partially filled compartments I and IV. In the event that two of the compartments are required to be empty and another compartment is to carry partial load, it is appropriate to keep the mid-compartments of the tank (II and III) empty, while the fill level in compartments I and IV may be varied.

COMPARTMENTS

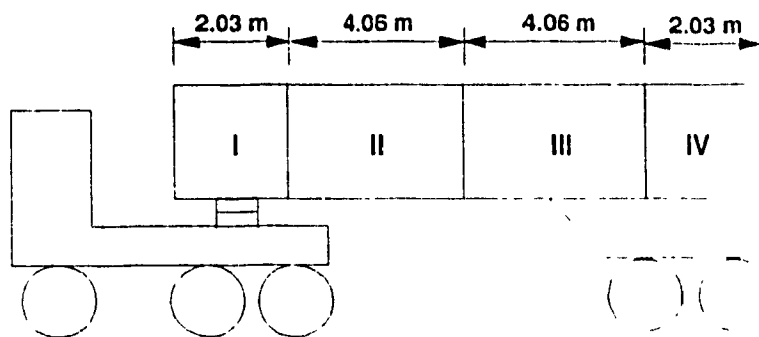


Figure 3.16 Schematic of a compartmented tank vehicle

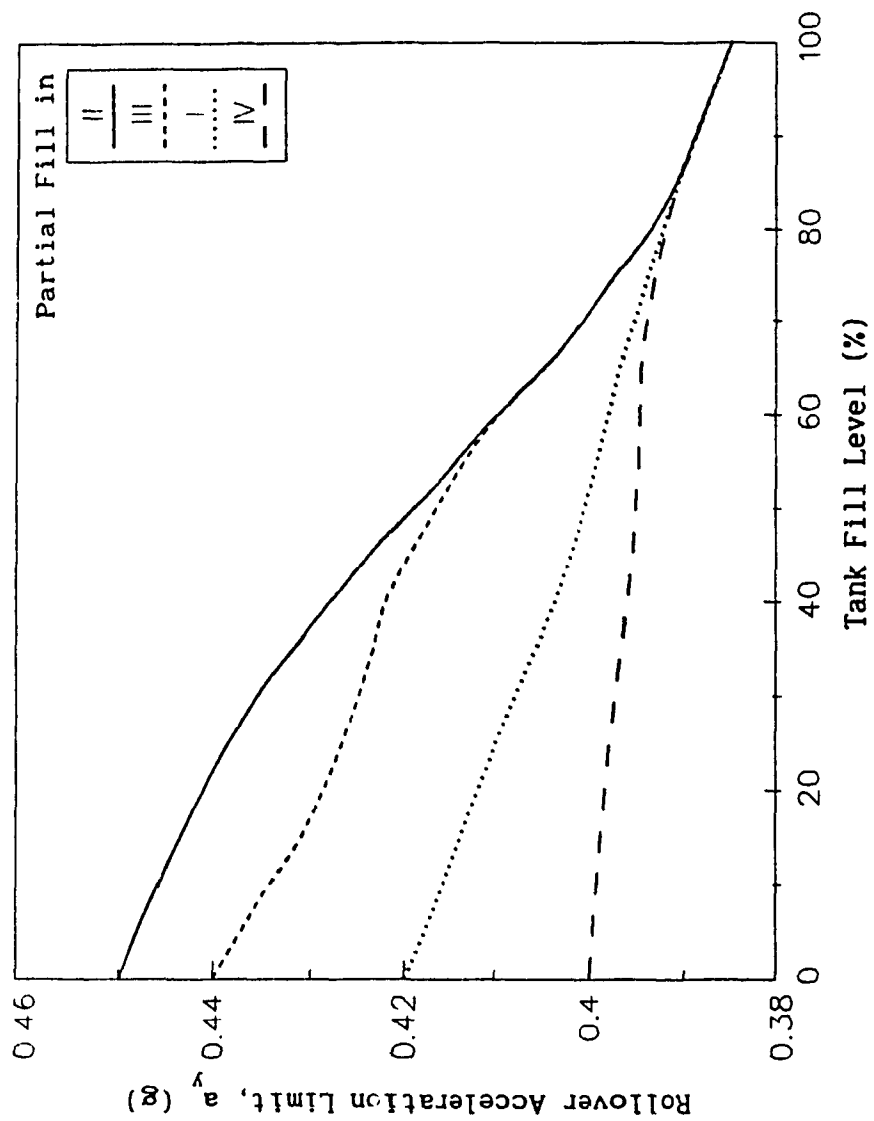


Figure 3.17 Rollover acceleration limits of a compartmented tank vehicle with partial load in one of the compartments

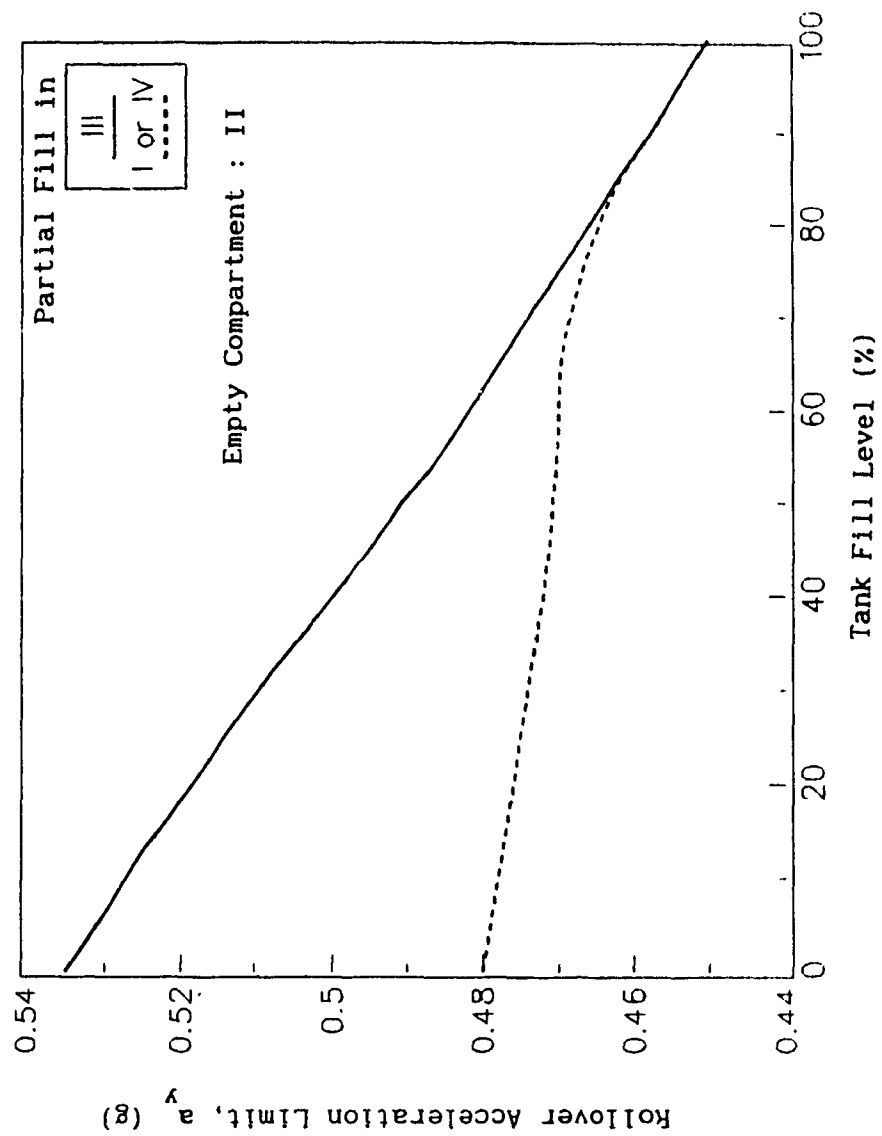


Figure 3.18 Rollover acceleration limits of a compartmented tank vehicle with an empty compartment and partial load in one of the other compartments

The rollover acceleration limits for such a tank vehicle is presented in Figure 3.19, for various fill levels in either compartment I or IV, while the mid-compartments are empty. It can be observed that for fill levels less than 70%, the partial load in compartment I yields higher values of the overturning acceleration limits of the vehicle. Thus the order of unloading the various compartments can be proposed to achieve the best values for vehicle rollover acceleration limits.

From Figures 3.17 to 3.19, it can be concluded that the order of unloading a four-compartment tank vehicle shown in Figure 3.16, is II, III, I and IV. In general, the order of unloading the various compartments, however, is dependent on a number of vehicle design factors, such as the compartment location, the capacity of various compartments, and the location of the trailer's composite axle.

3.6 Summary

In this chapter, the rollover threshold limits of a tank vehicle equipped with partially filled arbitrarily shaped tanks is computed using a kineto-static roll plane model. The simulation results reveal that during steady turning, the translation of the centre of mass of liquid within the moving tank vehicle, is considerably influenced by the tank geometry, fill level, and lateral acceleration levels. The lateral translation of the centre of mass of liquid, computed for various tank cross-sections, is observed to be significant and has a direct influence on the rollover limits. The additional roll moments arising due to the load shift lowers the rollover limits of the tank vehicle considerably, compared to those of an equivalent rigid cargo vehicle. The influence of tank geometry on the rollover limits of the tank vehicle are also discussed by comparing the rollover threshold values of circular,

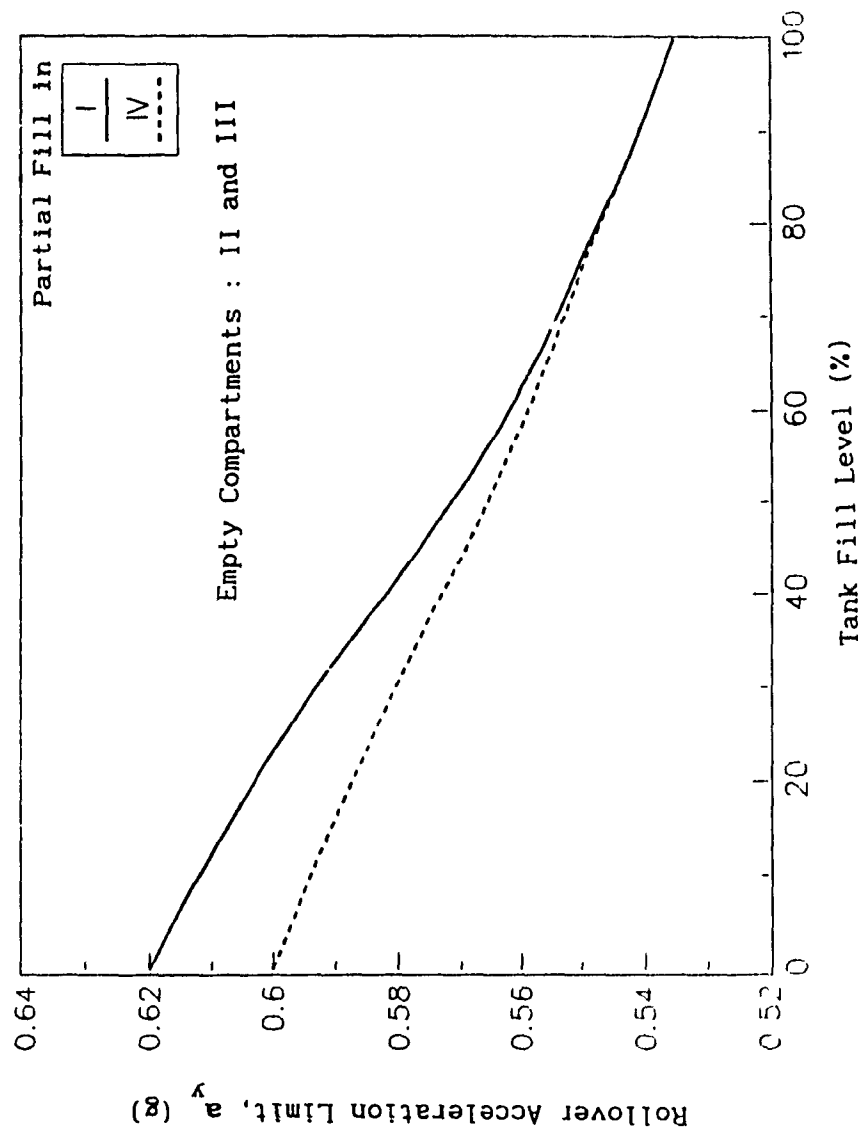


Figure 3.19 Rollover acceleration limits of a compartmented tank vehicle with two empty compartments and partial load in one of the other compartments

elliptical, modified oval, and modified square tank vehicles carrying identical payload. Computer simulation of steady turning characteristics of a four compartment tank of arbitrary geometry is carried out. The effect of compartmenting on the rollover limits is established. The order of unloading the various compartments to achieve highest value of rollover acceleration limit is also presented.

REFERENCES FOR CHAPTER 3

1. Wong, J.Y., "Vehicle Weights and Dimensions Study - Users Guide to UMTRI Models", Interim Technical Report, Road and Transport Association of Canada, 1985.
2. Ervin, Robert D., "The Influence of Size and Weight Variables on the Roll Stability of Heavy Duty Trucks", SAE Paper No. 831163, 1983.
3. Mallikarjunarao, C., "Road Tanker Design: Its Influence on the Risk and Economic Aspects of Transporting Gasoline in Michigan", Ph.D., Thesis, 1982.
4. Rakheja, S., Sankar, S. and Ranganathan, R., "Roll Plane Analysis of Articulated Tank Vehicles with Circular Tank Cross-section During Steady Turning", CONCAVE Research Report, No. 01-87, Concordia University, 1987.

CHAPTER 4

QUASI-DYNAMIC DIRECTIONAL RESPONSE MODEL OF A PARTIALLY FILLED TANK VEHICLE

4.1 General

Analysis of kineto-static roll plane model, presented in Chapters 2 and 3, provides the rollover threshold limits of tank vehicles during steady turning. In case of high speed vehicle manoeuvres, such as lane change and evasive manoeuvres, the rollover threshold limits of partially filled tank vehicles are further deteriorated. The rearmost trailer of a multiple articulated vehicle combination exhibits amplified lateral forces and moments during dynamic highway manoeuvres [1]. Experiments conducted on double bottom tanker configuration transporting gasoline in Michigan [2] have shown that the rearmost trailer had a tendency to rollover during an evasive or accident avoidance type of manoeuvre. Heavy vehicles exhibit unstable behaviour at lateral acceleration levels considerably lower than the rollover threshold, when executing high speed directional manoeuvres. Thus, it is vital to examine the stability of tank vehicles for various highway manoeuvres.

In this chapter, previous investigations on dynamic stability analysis of heavy vehicle combinations are briefly reviewed. A quasi-dynamic tank vehicle model capable of predicting the directional response of tank vehicle combinations subjected to transient steering manoeuvres is developed, assuming inviscid fluid flow conditions. The model is capable of evaluating the directional response of tank vehicles equipped with tanks of circular or modified oval cross-sections for both open-loop steer and closed-loop path follower manoeuvres. The steering input for the closed-loop path follower model is computed using an

optimal preview control method.

4.2 Review of Previous Investigations

The directional dynamics of heavy vehicles carrying rigid cargo have been extensively investigated by Jindra [3], Pacejka [4], Bernard [5], and Mallikarjunarao [6]. The yaw plane dynamics of articulated vehicles was first presented by a set of differential equations by Jindra [3]. The coupled linear differential equations were solved for eigenvalues, using a digital computer, to evaluate vehicle stability. Pacejka [4] investigated the handling characteristics of articulated vehicles during steady turning using a linearized yaw plane model of the vehicle, while neglecting the roll dynamics. Bernard [5] developed a comprehensive three-dimensional model to study the transient directional response of rigid cargo tractor-trailer combinations.

The rigid cargo is often attached to the trailer bed and thus the cargo interactions with the directional dynamics of the vehicle are neglected. Mallikarjunarao [6] investigated the directional response of liquid tank vehicles, transporting gasoline in Michigan using a yaw-roll model of the vehicle. The yaw-roll model, however, does not account for the influence of liquid motion within the partially filled tank vehicle.

The liquid slosh forces encountered within a partially filled tank vehicle affect the directional behaviour of the tank vehicle considerably. The longitudinal and lateral forces due to liquid slosh within a tank can lead to decreased controllability/manoeuvrability and increased stresses on the tank structure [7]. The use of lateral baffles and compartmenting of the tank can reduce the longitudinal slosh forces to a great extent. The load shift caused by the lateral liquid slosh increases the magnitude of the roll moments leading to

roll/lateral instability of the vehicle.

An analytical model, capable of simulating dynamic response of tractor-semitrailers and double trailers to various types of steer inputs, was developed by Strandberg *et al* [8]. The model has been used to evaluate the vehicle response to standardized directional manoeuvres and to establish performance standards in Sweden. The assumption of small roll angles, however, did not permit the simulation of vehicle rollovers.

The study of sloshing behaviour of liquids within a moving container involves complex modeling and analysis. Slibar and Troger [9] developed an equivalent single-degree-of-freedom mechanical oscillator to simulate the liquid slosh forces within a tank vehicle. The dynamic liquid slosh is represented by an oscillating mass elastically coupled to another fixed mass. The derivation of the equivalent mass and spring for the oscillating liquid was derived from the field test data. Abramson [10] developed a pendulum analogy model to study liquid slosh forces in a fuel tank of a spacecraft.

Strandberg [11] investigated the influence of sloshing forces due to liquid within road tankers on the vehicle skidding and overturning, using a simplified vehicle model developed assuming negligible yaw and roll motion. The investigations were based upon measured liquid forces in laterally oscillated scale model tanks having dynamic similarity with actual tanks. The fundamental slosh frequency of liquid motion within the partially filled tank was determined using a scale model. Budiansky [12] estimated the fundamental sloshing frequency within circular canals and spherical tanks using a linear hydrodynamic theory. The sloshing frequency (0.6 Hz) of a partially (50%) filled tank vehicle may coincide

with the steering frequency during an emergency type of manoeuvre leading to resonant forces from the sloshing fluid [11].

The analytical computation of the slosh frequency of a partially filled tank involves complex fluid modeling involving fluid density, viscosity, and flow numbers. The governing equations are solved by applying the Finite Difference Methodology with respect to non-dimensional primitive variables, such as the pressure and velocity [13]. The fundamental slosh frequencies of liquid within a cylindrical tank for various fill conditions were computed from the nonlinear fluid equations.

The references cited above indicate that analytical models for directional dynamics of articulated tank vehicles either lack comprehensive modeling of liquid slosh behaviour or model representing the vehicle roll and lateral behaviour. A comprehensive model of a tank vehicle that integrates a detailed comprehensive fluid slosh model requires complex modeling and analysis. In this chapter, a quasi-dynamic model of a tank vehicle is developed by incorporating a steady state fluid slosh model with a three-dimensional vehicle dynamics model to investigate the directional response of the tank vehicle subject to various dynamic manoeuvres.

4.3 Development of a Quasi-Dynamic Tank Vehicle Model

A partially filled tank vehicle is modeled to study the influence of liquid load shift on the directional dynamics. The tank vehicle model is formulated by integrating a steady state roll plane model of the fluid motion to the three-dimensional vehicle dynamics model, assuming constant vehicle speed. The partially loaded liquid tank vehicle negotiating the various highway manoeuvres at a constant vehicle

speed is assumed to behave independent of the slosh frequency of the liquid load within the tank. Hence, the motion of the free surface of liquid is computed assuming inviscid fluid flow conditions. The steady state roll plane model of fluid motion within a partially filled circular and modified oval tanks are developed and integrated to the three-dimensional model of the tank vehicle.

4.3.1 Steady State Roll Plane Model of Fluid Motion in a Partially Filled Circular Tank

An articulated tank vehicle, in general is subjected to roll and lateral acceleration during a constant speed directional manoeuvre. The entire fluid bulk within the tank is assumed to move as a rigid body, due to the roll and lateral acceleration imposed by the vehicle, as shown in Figure 4.1. The motion of the free surface of liquid shifts the centre of mass of the liquid and alters its inertial properties. The load shift and the corresponding change in the inertia due to the steering manoeuvre can be computed assuming steady state fluid motion. The shift in the centre of mass of the fluid and the variations in mass moment of inertia are dependent on the tank cross-section, fill level, and the gradient of the free surface.

The gradient of the free surface of the liquid within a semitrailer, (ϕ_f) can be estimated from the roll angle of the semitrailer sprung mass (θ_{sf}) , expressed in radians and the lateral acceleration imposed on the liquid bulk (a_{lf}) , expressed in g units. As shown in Chapter 2, by assuming inviscid fluid flow conditions, the equation for the gradient of the free surface is expressed by:

$$\tan \phi_f = \left(\frac{\theta_{sf} + a_{lf}}{1 - a_{lf} \theta_{sf}} \right) \quad (4.1)$$

- a - C.G. of solid load
- b - C.G. due to tank tilt alone
- c - C.G. due to tank tilt and lateral acceleration

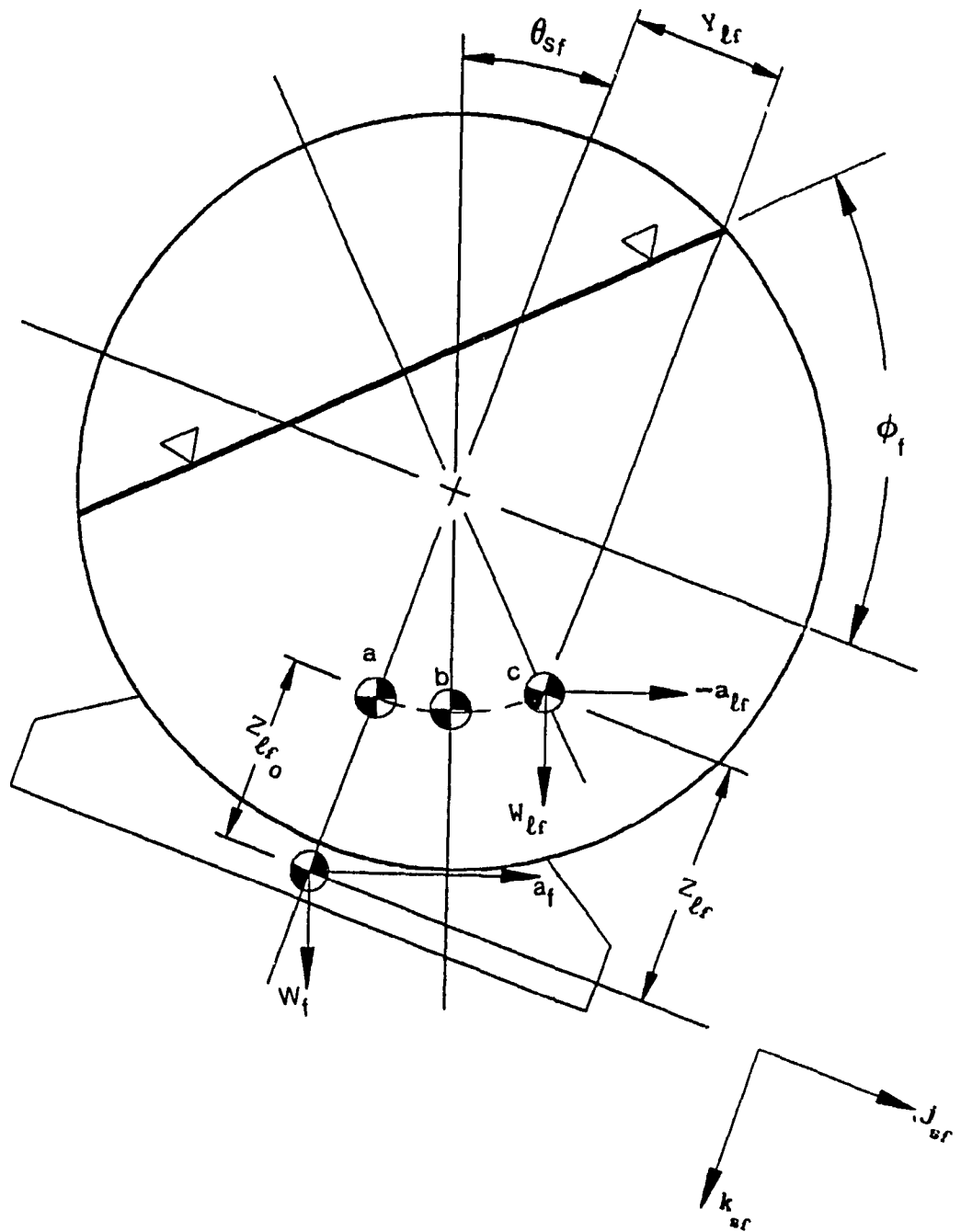


Figure 4.1 Roll plane model of a circular tank cross-section

where the subscript $f = 2$ for the semitrailer of a tractor semitrailer and $f = 2$ for the first semitrailer and $f = 3$ for the second semitrailer of a B-train.

The vertical and lateral translation of the centre of mass of liquid bulk in a partially filled cylindrical tank is given by the following expressions as derived from the geometry of the tank in Chapter 2:

$$\begin{aligned} Z_{\ell f} &= R_f - \left(R_f - Z_{\ell f 0} \right) \cos \phi_f \\ Y_{\ell f} &= \left(R_f - Z_{\ell f 0} \right) \sin \phi_f \end{aligned} \quad (4.2)$$

where R_f is the radius of the tank, $Z_{\ell f 0}$ is the height of the centre of mass of liquid in the absence of tank roll and lateral acceleration ($\theta_{sf} = a_{\ell f} = 0$), and $Y_{\ell f}$ and $Z_{\ell f}$ are the lateral and vertical locations of the instantaneous centre of mass of liquid respectively, measured with respect to the centre of mass of the tank trailer structure, as shown in Figure 4.1.

The computation of moments of inertia of the liquid cargo about the coordinate system (i_ℓ, j_ℓ, k_ℓ) attached to its C.G is performed by splitting the liquid bulk into a number of thin sections and summing up the inertia about its C.G. The roll and the lateral acceleration encountered during a highway manoeuvre cause the motion of the free surface of liquid creating a displaced shape of the liquid bulk within the circular tank. Due to the symmetric tank shape, the moments of inertia of the displaced shape remain same about the axis of symmetry. The moments of inertia values of the displaced liquid are then computed

using the gradient of the free surface of liquid, expressed by the following equations:

$$\begin{aligned}
 I_{x\ell_f} &= I_{x\ell_0} \\
 I_{y\ell_f} &= I_{y\ell_0} \cos^2(\phi_f) + I_{z\ell_0} \sin^2(\phi_f) \\
 I_{z\ell_f} &= I_{z\ell_0} \cos^2(\phi_f) + I_{y\ell_0} \sin^2(\phi_f)
 \end{aligned} \tag{4.3}$$

where $I_{x\ell_0}$, $I_{y\ell_0}$, $I_{z\ell_0}$ are the moments of inertia of the liquid mass when the liquid free surface gradient is zero.

4.3.2 Steady State Roll Plane Model of Fluid Motion in a Partially Filled Modified Oval Tank

The computation of the vertical and lateral translation of the centre of mass of liquid and the change in the moments of inertia within a partially filled modified oval tank during a highway manoeuvre is quite complex. The periphery of a modified oval tank, shown in Figure 2.8 can be observed as a combination of 8 circular arcs and is symmetric about the vertical axis. The numerical algorithm developed to compute the centre of mass of liquid within the modified oval tank has been presented in Chapter 2. The moments of inertia of the liquid mass as well as the displaced shape of liquid due to the tank tilt and lateral acceleration are computed by discretizing the entire fluid into a number of thin sections, as shown in Figure 4.2. The moments of inertia are then summed up about the overall centre of gravity of the fluid. The moments of inertia of the liquid cargo about the rotated sprung mass coordinates are then obtained by the transformation of the inertia vector using the transformation matrix obtained from the roll angle of

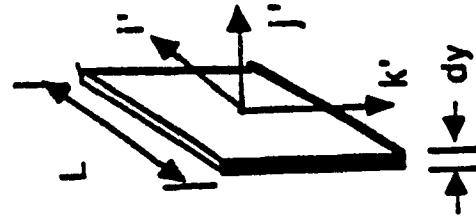
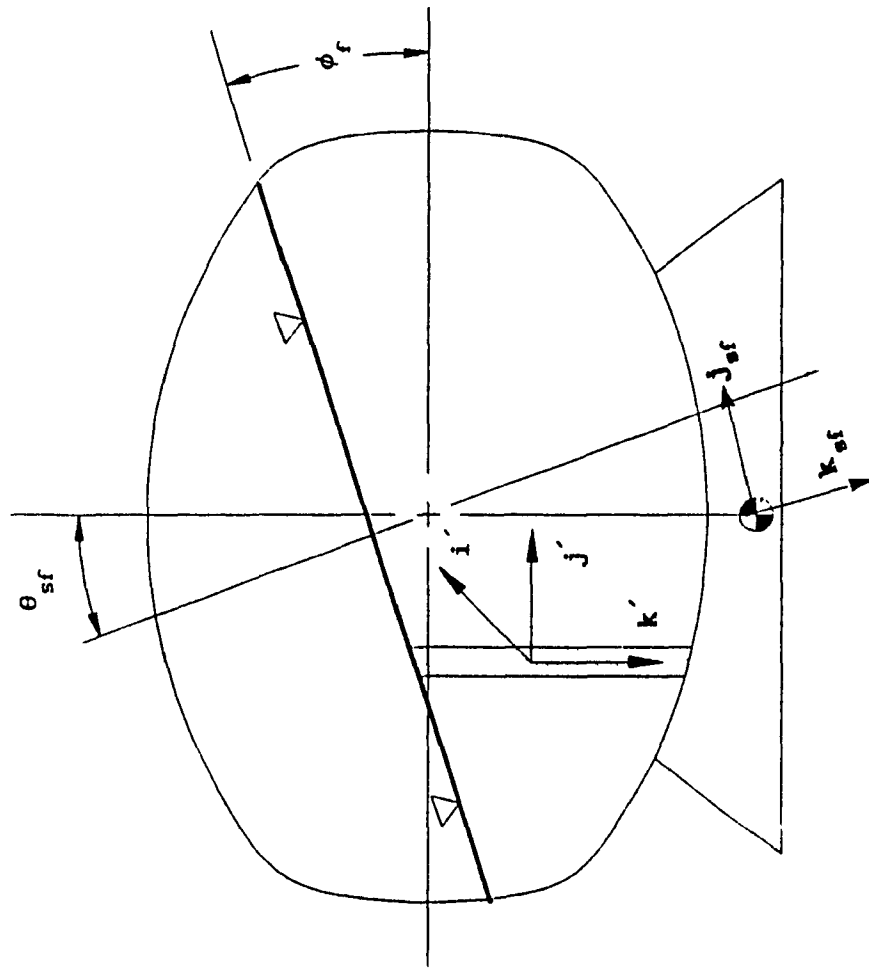


Figure 4.2 Computation of the moment of inertias of the liquid mass

the sprung unit.

$$\begin{aligned}
 I_{xlf} &= I'_{xl} \\
 I_{ylf} &= I'_{yl} \cos^2(\theta_{sf}) + I'_{zl} \sin^2(\theta_{sf}) \\
 I_{zlf} &= I'_{zl} \cos^2(\theta_{sf}) + I'_{yl} \sin^2(\theta_{sf})
 \end{aligned} \tag{4.4}$$

where I'_{xl} , I'_{yl} , I'_{zl} are the moments of inertia of the displaced shape of the liquid.

4.4 Modeling of a Tractor-Semitrailer Tank Vehicle

A tractor-semitrailer tank vehicle is modeled as two sprung masses: the sprung mass of the tractor, m_1 ; and the tare mass of the semitrailer structure and empty tank, m_2 . The liquid mass m_{lf} ($f=2$) is considered as a floating mass with respect to the C.G of the semitrailer sprung mass. The axles are modeled as independent unsprung masses, m_{ui} ($i=1, \dots, 5$; for five-axle vehicle and $i=1, \dots, 6$; for six-axle vehicle). The sprung weights of the vehicle are treated as rigid bodies with five degrees of freedom: lateral, vertical, yaw, roll, and pitch. The unsprung weights are free to roll and bounce with respect to the sprung weights to which they are attached. The roll plane of a three-dimensional model of the tractor-semitrailer tank vehicle is shown in Figure 4.3. The pitch plane of the tractor-semitrailer tank vehicle model and the various coordinate systems attached to the sprung and unsprung masses are shown in Figure 4.4. The constraint forces at the coupling are evaluated from kinematic expressions, relating the acceleration of the two sprung weights. The constraint moments are evaluated from the relative angular displacement between the tractor and semitrailer sprung weights.

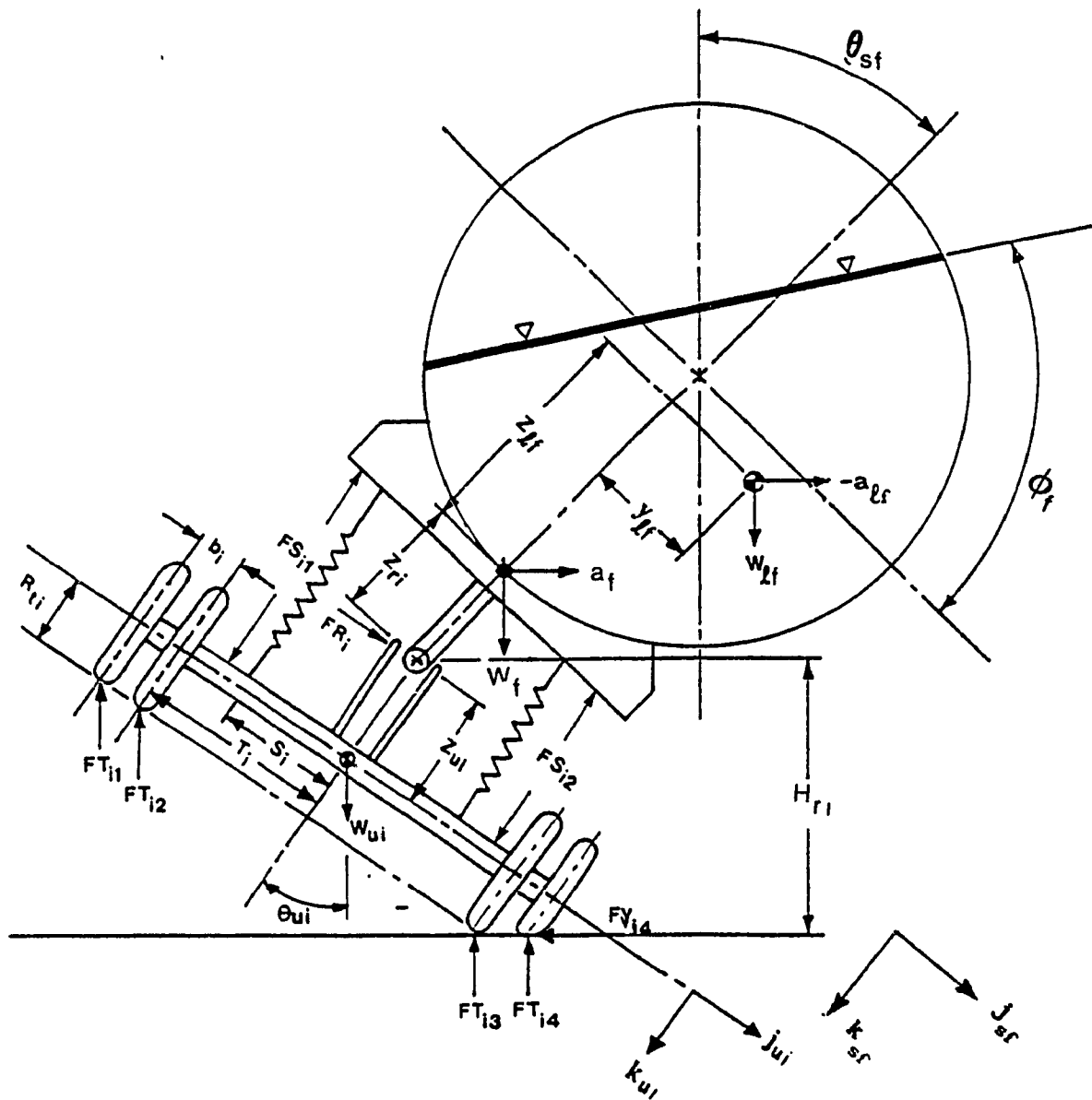


Figure 4.3 Roll plane model of the tank vehicle
 (f = 2, for tractor-tank semitrailer;
 f = 2 and 3, for B-train tank vehicle)

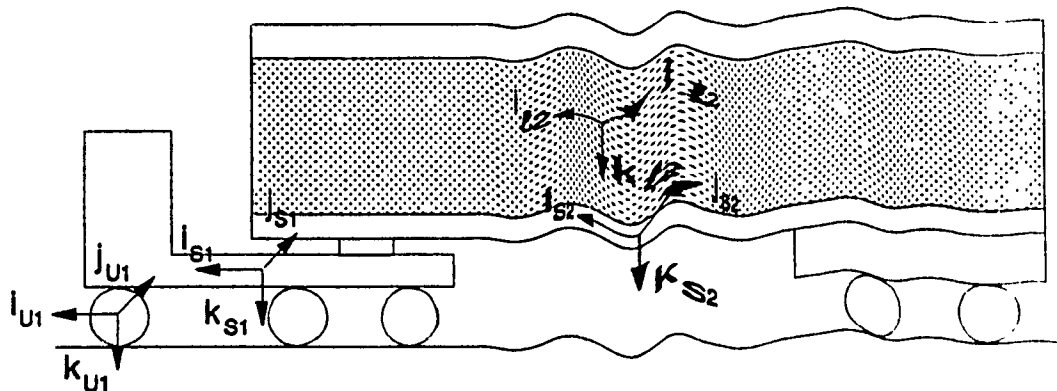


Figure 4.4 Pitch plane of the tractor-semitrailer tank vehicle and the various coordinate systems

4.5 Modeling of a B-Train Tank Vehicle

A 7-axle B-Train is modeled as three sprung masses: the sprung mass of the tractor m_1 ; the tare mass of the semitrailer A and the empty tank, m_2 ; the tare mass of the semitrailer B and the empty tank, m_3 . The liquid in the two semitrailers is modeled as two sprung masses, m_{lf} ($f = 2,3$), and each axle is modeled as an unsprung mass m_{ui} ($i = 1,2,\dots,7$). The roll plane of the semitrailer and the pitch plane of the 3-dimensional tank vehicle model are shown in Figures 4.3 and 4.5, respectively. The fifth wheel couplings are modeled to be rigid with respect to the translation but relatively compliant with respect to the rotation. The constraint forces and moments at the couplings are evaluated from kinematic expressions, relating the acceleration and the relative angular displacements of the sprung weights.

4.6 Model Assumptions

The equations of motion for an articulated tank vehicle are developed subject to a number of simplifying assumptions [1]. The vehicle is assumed to move on a horizontal surface, possessing even frictional properties, at a constant speed. The pitch rotation (α_{sf}) of the sprung weights are assumed to be small such that $\sin\alpha_{sf} = \alpha_{sf}$ and $\cos\alpha_{sf} = 1$. The relative roll between the sprung and unsprung weights are also considered to be small and the sprung units are assumed to roll about the roll center located at a fixed distance below the sprung weight C.G.

The suspension forces are assumed to act along the vertical axis of the unsprung mass, with only compression and tensile forces being transmitted to the sprung mass. The roll centre is free to move along the vertical axis of the unsprung mass, such that the lateral forces

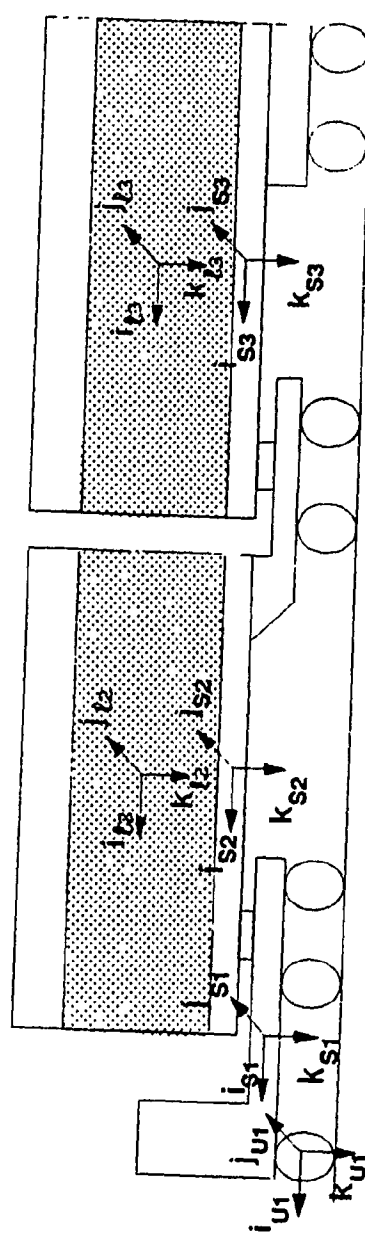


Figure 4.5 Pitch plane of the B-train tank vehicle and the various coordinate systems

acting on the roll centre remain parallel to the horizontal axis of the unsprung mass. In case of suspension consisting of leaf springs, the swaying in the springs resulting in the roll-resisting moment is represented through an auxiliary roll stiffness, KRS_1 , as shown in Figure 4.6. Each primary vehicle suspension is represented by a nonlinear spring, coulomb friction, and viscous damper. The typical force-displacement characteristics of the suspension springs at the tractor front, rear, and trailer axles are shown in Figure 2.15. The nonlinear spring characteristics are linearized about the operating point, using a look-up table. Inter axle load transfers are neglected hence the axle loads are held constant throughout the simulation. The principal axes of inertia of the sprung masses and the unsprung masses are assumed to coincide with their respective body-fixed coordinate systems.

The cornering forces and aligning moments due to tires are determined as nonlinear functions of side slip angle and normal loads. The vertical load on each tire is computed from the instantaneous tire deflection and the vertical tire stiffness. The cornering force and the aligning moment characteristics of a typical radial truck tire are nonlinear functions of the slip angle and vertical load, as shown in Figure 4.7 [14]. The cornering forces and the aligning moments arising at the tire-road interface are computed using the look-up table depending on the dynamic vertical load and the tire slip angle.

4.7 Equations of Motion of an Articulated Tank Vehicle

The equations of motion of the yaw/roll model of an articulated partially filled tank vehicle are derived by integrating the equations of steady state fluid motion to the equations of motion for an

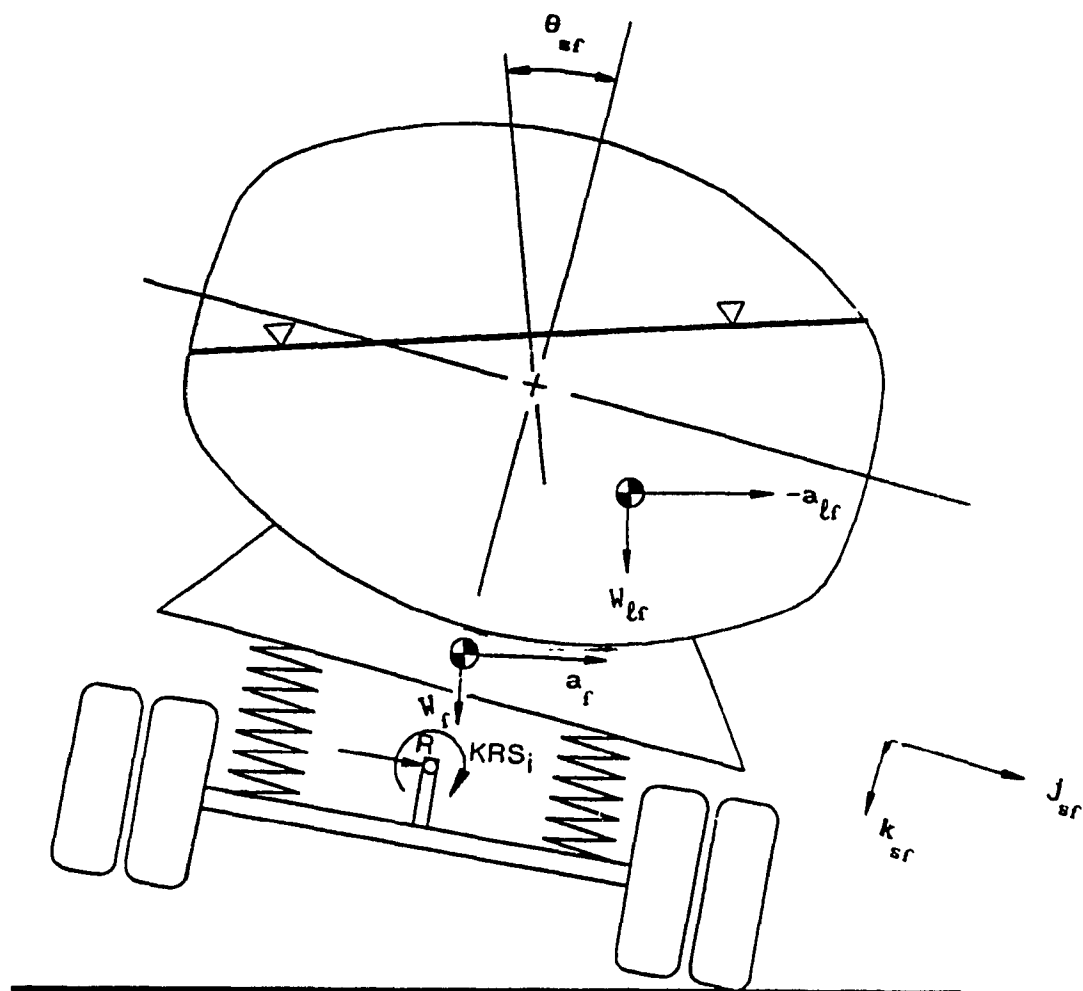


Figure 4.6 Idealized representation of the axles and suspension in the roll plane of the tank vehicle

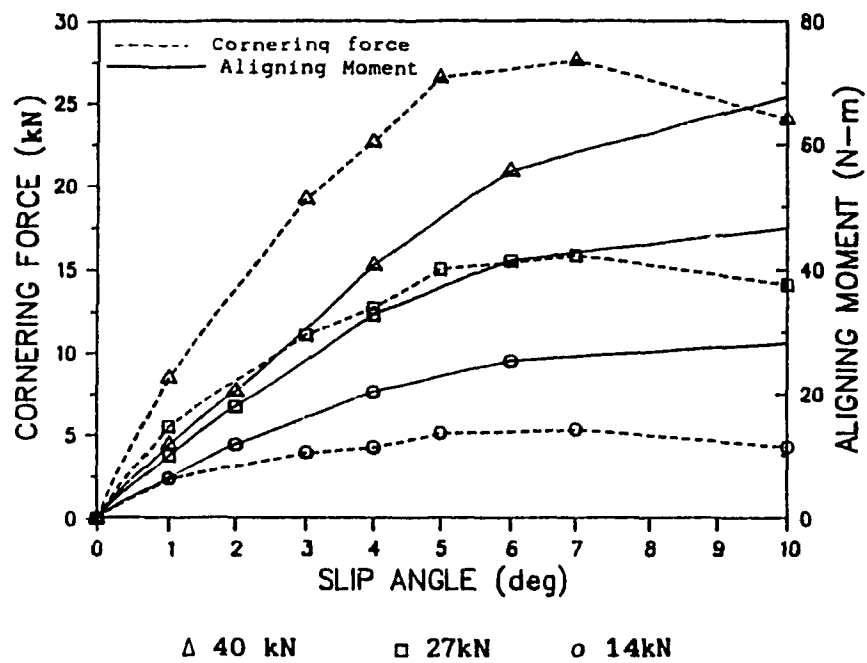


Figure 4.7 Cornering force and aligning moment characteristics of the tires under various normal loads [14]

articulated rigid cargo vehicle [1]. The rigid cargo vehicle model completely neglects the dynamics associated with steady state fluid motion and hence the cargo and semitrailer are represented by one single sprung mass. In case of liquid cargo, however, the semitrailer sprung mass comprises of two masses: the tare tank-semitrailer mass and the floating mass due to the liquid cargo. Thus an additional floating axis system is required to describe the motion of the liquid within the tank. The change in the C.G. and the inertial properties of the liquid cargo due to the motion of free surface of liquid within the tank are computed using equations (4.1) to (4.4). A complete derivation of the equations of motion is presented in Appendix II. The equations of motion of an articulated tank vehicle incorporating the forces and moments arising from the floating liquid cargo are presented in the following sections.

4.7.1. Axis System

The equations of motion of the tank vehicle are derived using the following coordinate system, as shown in Figures 4.4 and 4.5:

1. An inertial axis system fixed in space
2. An axis system fixed to each of the sprung weights
3. An axis system fixed to each of the unsprung weights
4. An axis system fixed to the floating C.G of liquid

Euler angles are used to define the orientation of the sprung and unsprung weights with respect to the inertial axis system. The transformation matrix relating the sprung and unsprung masses to the inertial axis system are derived in Appendix II.

4.7.2. Equations of Motion

The motion of each sprung mass is described by five second order differential equations and the motion of each unsprung mass is described

by two differential equations. The number of equations required to describe the directional behaviour of the multiple-articulated tank vehicle is given by:

$$k = 5 \eta_s + 2 \eta_a \quad (4.5)$$

where η_s and η_a are the number of sprung and unsprung units of the articulated tank vehicle. The complete derivation of the equations of motion is presented in Appendix II. The equations of motion incorporating the liquid forces and moments are presented in the following section along with the equations for computation of acceleration of the liquid C.G:

Lateral Force Equations

$$\begin{aligned} m_f a_{f sf} \vec{j}_{sf} + m_{lf} a_{lf sf} \vec{j}_{sf} &= (\text{Lateral component of the Constraint Forces}) \\ &+ (\text{Lateral component of the Suspension Forces}) \\ &+ (m_f + m_{lf}) g \theta_{sf} \end{aligned} \quad (4.6)$$

Vertical Force Equations

$$\begin{aligned} m_f a_{f sf} \vec{k}_{sf} + m_{lf} a_{lf sf} \vec{k}_{sf} &= (\text{Vertical component of the Constraint Forces}) \\ &+ (\text{Vertical component of the Suspension Forces}) \\ &+ (m_f + m_{lf}) g \end{aligned} \quad (4.7)$$

Roll Moment Equations

$$\begin{aligned} (I_{xf} + I_{xlf}) \dot{p}_f - (I_{yf} + I_{ylf} - I_{zf} - I_{zlf}) q_f r_f &= \\ (\text{Roll Moments from the Constraints}) + \\ (\text{Roll Moments from the Suspensions}) \\ + m_{lf} a_{lf sf} \vec{j}_{sf} Z_{lf} + m_{lf} a_{lf sf} \vec{k}_{sf} Y_{lf} + m_{lf} g (\theta_{sf} Z_{lf} + Y_{lf}) \end{aligned} \quad (4.8)$$

Pitch Moment Equations

$$\begin{aligned}
 & (I_{yf} + I_{y_{lf}}) \dot{q}_f - (I_{zf} + I_{z_{lf}} - I_{x_f} - I_{x_{lf}}) p_f r_f = \\
 & \quad \text{(Pitch Moments from the Constraints) +} \\
 & \quad \text{(Pitch Moments from the Suspensions)} \\
 & - m_{lf} a_{lf} \vec{k}_{sf} X_{lf} - m_{lf} a_{lf} \vec{i}_{sf} Z_{lf} - m_{lf} g (X_{lf} + \alpha_{sf} Z_{lf}) \quad (4.9)
 \end{aligned}$$

Yaw Moment Equations

$$\begin{aligned}
 & (I_{zf} + \sum_{i=N_1}^{N_2} I_{z_{ui}} + I_{z_{lf}}) \dot{r}_f - (I_{x_f} + I_{x_{lf}} - I_{y_f} - I_{y_{lf}}) p_f q_f = \\
 & \quad \text{(Yaw Moments from the Constraints) +} \\
 & \quad \text{(Yaw Moments from the Suspensions)} \\
 & + m_{lf} a_{lf} \vec{i}_{sf} Y_{lf} + m_{lf} a_{lf} \vec{j}_{sf} X_{lf} \quad (4.10)
 \end{aligned}$$

Unsprung Mass Roll Moment Equations

$$\begin{aligned}
 I_{x_{ui}} \dot{p}_{ui} &= \quad \text{(Roll Moment produced by the suspension forces)} \\
 &+ \quad \text{(Roll Moments produced by the tire forces)} \quad (4.11)
 \end{aligned}$$

Unsprung Mass Vertical Force Equations

$$\begin{aligned}
 m_{ui} a_{ui} \vec{k}_{ui} &= \quad \text{(Vertical component of suspension forces) +} \\
 & \quad \text{(Vertical component of tire forces)} \\
 &+ m_{ui} g \quad (4.12)
 \end{aligned}$$

where a_f and a_{ui} are the acceleration vectors of the sprung mass f and unsprung mass i respectively. (p_f, q_f, r_f) are the rotational velocities of the sprung mass f and p_{ui} is the roll velocity of the axle i .

The procedure for evaluating the acceleration of the fluid bulk within the tank-trailer is presented in the following section. Also, in order to evaluate the right hand side of the equations (4.6) through (4.12), the forces produced by the suspension, constraint mechanism and

the tires need to be determined. The derivation of the suspension and tire forces are presented in Appendix II. The unknown constraint forces are evaluated from the kinematic expressions relating the accelerations at the constraint point, while the constraint moments are computed from the relative angular displacement of the sprung masses.

4.7.3. Computation of the Liquid Mass Acceleration

The entire fluid bulk is assumed to move as a rigid body, due to the tank roll and lateral acceleration imposed by the vehicle. The roll, pitch and yaw velocities of the liquid bulk is assumed to be equal to that of the trailer sprung weight. The acceleration of the liquid bulk a_{lf} , is computed from the acceleration of the trailer sprung weight a_f and the instantaneous centre of gravity of the liquid bulk with respect to the trailer C.G. Hence, the acceleration of the liquid bulk in the unit f is expressed by:

$$a_{lf} = a_f + a_{lf/f} ; f = 2, \dots, \eta_l \quad (4.13)$$

where $a_{lf/f}$ is the acceleration of liquid C.G. with respect to the C.G. of the tank trailer f , given by:

$$\begin{aligned} a_{lf/f} = & (\dot{q}_f Z_{lf} - \dot{r}_f Y_{lf} - q_f^2 X_{lf} + p_f q_f Y_{lf} + r_f p_f Z_{lf} - r_f^2 X_{lf}) \vec{i}_{sf} \\ & + (-\dot{p}_f Z_{lf} + \dot{r}_f X_{lf} - p_f^2 Y_{lf} + p_f q_f X_{lf} + r_f q_f Z_{lf} - r_f^2 Y_{lf}) \vec{j}_{sf} \\ & + (\dot{p}_f Y_{lf} - \dot{q}_f X_{lf} - p_f^2 Z_{lf} + p_f r_f X_{lf} - r_f q_f Y_{lf} + q_f^2 Z_{lf}) \vec{k}_{sf} \end{aligned} \quad (4.14)$$

where (u_f, v_f, w_f) are the linear velocities of the sprung mass f along the sprung mass coordinates and (X_{lf}, Y_{lf}, Z_{lf}) are the coordinates of the instantaneous centre of mass of liquid with respect to the tank trailer C.G.

4.7.4. Constraint Equations

The differential equations (4.6) through (4.10), describing the

motion of the sprung masses of the tank vehicle combinations, include the forces and the moments arising from the fifth wheel couplings. The constraint forces are evaluated from the kinematic expressions that relate the accelerations at the constraint point due to the sprung masses attached to it. The constraint moments are calculated as a function of the relative angular displacement of the sprung masses, as shown in Appendix II. The set of second order differential equations describing the motion of the tank vehicle combination can be expressed as:

$$M \ddot{x} = f_c + N y \quad (4.15)$$

where M is the inertia matrix, \ddot{x} is the acceleration vector, f_c is the vector comprising of gravitational, suspension, roll centre, and the liquid slosh forces and moments, N is a transformation matrix containing vehicle dimensions and velocities, and y is the vector of unknown constraint forces to be evaluated from the constraint relationships. The inertia matrix M which comprises of the sprung, unsprung and liquid masses and the their moments of inertia is updated during the simulation with the new values of the moments of inertia of the displaced liquid cargo. Also the vector f_c , which contains the liquid slosh forces and moments, is updated in order to account for the new C.G location of the floating liquid cargo. The kinematic constraint equation that relates the acceleration at the constraint point, when transferred to a common sprung mass axis system, can be expressed as:

$$C \ddot{x} = d \quad (4.16)$$

where C is a matrix of the vehicle dimensions, and d is a vector, containing displacements x , velocities \dot{x} , and vehicle dimensions. The final equation describing the acceleration vector in terms of the

vehicle parameters can be derived from (4.15) and (4.16), as shown in Appendix II, and is expressed as:

$$\ddot{\mathbf{x}} = \mathbf{M}^{-1}\mathbf{f}_c + \mathbf{M}^{-1}\mathbf{N} [\mathbf{CM}^{-1}\mathbf{N}]^{-1} \{\mathbf{d} - \mathbf{CM}^{-1}\mathbf{f}_c\} \quad (4.17)$$

Equation (4.17) represent the equations of motion of tank vehicle combination, incorporating the forces and moments arising from the liquid motion. The model is capable of simulating both closed-loop and open-loop steering manoeuvres. In the open-loop model, the time history of the steer input to the front wheels of the vehicle is provided as the input. In the closed-loop model, the trajectory of the vehicle to be followed by the vehicle is specified and the corresponding steering angle necessary to follow the path specified is computed using the driver model. The closed-loop model is described in detail in Appendix II. The forces due to tires and suspension are evaluated as a function of the steer angle along with the constraint moments. Equation (4.17) is solved via numerical integration to yield directional response characteristics of the vehicle combination for a given vehicle manoeuvre.

4.8 Summary

A comprehensive three-dimensional tank vehicle model is developed to investigate the influence of the motion of free surface of liquid on the directional response characteristics of tank vehicle combinations. Quasi-dynamic roll plane models of the partially filled tanks of circular and modified oval cross-sections are developed and integrated to the three-dimensional model of the tank vehicle combination, assuming constant forward speed. The model is capable of simulating both open- and closed-loop steering manoeuvres.

REFERENCES FOR CHAPTER 4

1. Mallikarjunarao, C., Road tanker design: its influence on the risk and economic aspects of transporting gasoline in Michigan, Ph. D. Thesis, 1982.
2. Ervin, R.D., "Ad Hoc Study of Certain Safety-Related Aspects of Double-Bottom Tankers", Final Report, Highway Safety Research Institute, The University of Michigan, Report No. UM-HSRI-78-18, May 1978.
3. Jindra, F., Handling Characteristics of Tractor-Trailer Combinations, SAE paper No. 650720, 1965.
4. Pacejka, H.B., Simplified Analysis of Steady-state Turning Behaviour of Motor Vehicles, Vehicle System Dynamics, Vol. 2, pp. 161-172, 1973.
5. Bernard, J.E., Winkler, C.B. and Fancher, P.S., A Computer-Based Mathematical Method for predicting the Directional Response of Trucks and Tractor Trailers: Phase II Technical Report, Highway Safety Research Institute, Univ. of Michigan, 1973.
6. Mallikarjunarao, C. and Fancher, P., Analysis of the Directional Response Characteristics of Double Tankers, SAE paper No. 781064, 1978.
7. Bauer, H.F., Dynamic behaviour of an elastic separating wall in vehicle containers: Part I, Int. J. of Vehicle Design, Vol. 2, no. 1, pp. 44-77, 1981.
8. Strandberg, L., Nordstrom, O. and Nordmark, S., Safety Problems in Commercial Vehicle Handling, Proceedings, Symposium on Commercial Vehicle Braking and Handling, University of Michigan, 1975.
9. Slibar, A. and Troger, H., The steady state behaviour of tank trailer system carrying rigid or liquid cargo, VSD-IUTAM Symposium on Dynamics of Vehicles on Roads and Tracks, Vienna, 1977.
10. Abramson, H.N., The dynamic behaviour of liquid in moving containers, NASA Report No. SP-106, 1966.
11. Strandberg, L., Lateral stability of Road Tankers, VTI Rapport No. 138A, Sweden, Vol. 1, 1978.
12. Budiansky, B., "Sloshing of Liquids in Circular Canals and Spherical Tanks", J. of Aerospace Sci., Vol. 27, No. 3, March 1960.
13. Popov, G., Vatistas, G.H., Sankar, S. and Sankar, T.S., "Liquid Sloshing in a Horizontal Cylindrical Container", 1989 ASME Computers in Engineering Conference.
14. Ervin, R.D., Guy, Y., "The influence of Weights and Dimensions on the stability and control of heavy-duty trucks in Canada", UMTRI Report No. 86-35, July 1986.

CHAPTER 5

DIRECTIONAL RESPONSE OF TANK VEHICLE COMBINATIONS

5.1 General

The potential safety hazards posed by the tank vehicle combinations are directly related to their directional stability limits. The three-dimensional vehicle model incorporating the steady state roll plane fluid model of the tank, is solved for various directional manoeuvres to determine the transient directional response and thus the dynamic stability of candidate tank vehicle combinations, discussed in Chapter 2. The directional stability limits of tank vehicle combinations are investigated for various directional manoeuvres, such as constant or steady steer, lane change, and evasive manoeuvres. The directional analyses are carried out for tractor-tank semitrailer (five- and six-axles) and B-train combination (seven-axles). The directional dynamics of tank vehicles is further investigated in view of various vehicle design and operational parameters. The influence of fill level, vehicle speed, tank shape, compartments, and severity of the directional manoeuvre on the directional stability of tank vehicle combinations are extensively investigated and discussed.

5.2 Method of Solution

The directional dynamic model of the tank vehicle is capable of analyzing the directional response for both open- and closed-loop directional manoeuvres. In an open-loop manoeuvre, the time history of the steer input is provided while the target trajectory to be followed by the vehicle is considered in a closed-loop manoeuvre. The front wheel steer angles required to execute the required manoeuvre are computed using a driver model, presented in Appendix II. The final

equation describing the acceleration vector in terms of various vehicle parameters is expressed as:

$$\ddot{\mathbf{x}} = \mathbf{M}^{-1}\mathbf{f}_c + \mathbf{M}^{-1}\mathbf{N} [\mathbf{C}\mathbf{M}^{-1}\mathbf{N}]^{-1} \{\mathbf{d} - \mathbf{C}\mathbf{M}^{-1}\mathbf{f}_c\} \quad (5.1)$$

where \mathbf{M} is the inertia matrix, \mathbf{f}_c is the force vector comprising of fluid slosh, gravitational, suspension and roll centre forces, \mathbf{N} is the transformation matrix containing vehicle dimensions and velocities, \mathbf{C} is a matrix of vehicle dimensions, and \mathbf{d} is a vector containing displacements \mathbf{x} , velocities $\dot{\mathbf{x}}$, and vehicle dimensions.

A numerical integration algorithm, based on Adam's predictor-corrector method is employed to solve the equations of motion, (5.1) in order to compute the vehicle velocities and displacements. The inertia vector of the liquid mass due to the tank roll and lateral acceleration and the corresponding coordinates of the C.G of the liquid bulk are updated using the equations (4.2) to (4.4). The matrix \mathbf{C} and the vector \mathbf{d} representing the constraint forces are updated with the present values of vehicle velocities and displacements along with the transformation matrix \mathbf{N} , depending on the sprung and unsprung Euler angles. The tire forces and aligning moment arising due to the side slip angle are computed depending on the steer input and the sprung mass velocities, as shown in Appendix II. The time step of integration is automatically computed by the integration scheme in order to minimize the truncation errors. The directional response simulations are terminated when the simulation time reaches the maximum simulation time specified by the user or when the vehicle reaches an instability, with roll angle of one of the units exceeding 0.5 radians.

5.3 Directional Response of Tractor SemiTrailer Tank Vehicle

The dynamic response of a tank vehicle is a function of various design and operational parameters of the tank and the vehicle. The transient directional and thus the directional stability response of the tank vehicle is compared to that of an equivalent rigid cargo vehicle in order to study the influence of the liquid motion within the partially filled tank. The influence of the fill level, tank geometry, vehicle speed, and fluid density on the dynamic response of the tank vehicle are investigated for specified steer as well as path inputs.

5.3.1 Open-Loop Constant Steer Manoeuvre

The directional response of five- and six-axle tractor-tank semitrailers, equipped with a partially filled cylindrical cleanbore tank and a compartmented modified oval tank, are evaluated for steady steer inputs via computer simulation. A steady or constant steer is defined as a modified step steer where the steer angle initially increases as a ramp function until it reaches a specified value, the steer angle is then held constant during the simulation. The vehicle response parameters, such as lateral acceleration, roll angle, roll rate and the vehicle path, are obtained for both liquid cargo and the equivalent rigid cargo vehicles. The directional response characteristics of the liquid and rigid cargo vehicles are compared to demonstrate the influence of liquid load shift on the directional behaviour.

5.3.1.1 Directional Response of Five-Axle Tractor-Semitrailer Combination (Variable Axle Loads)

The directional response of the five-axle cylindrical tank vehicle with various fill levels is computed for constant steer inputs (1° and

4°) and constant forward speed of 60 km/h. Figures 5.1 and 5.2 present a comparison of the roll angle and lateral acceleration response, respectively, of a partially filled tank semitrailer to that of a semitrailer with equivalent rigid cargo. The percent fill level is defined as the ratio of liquid height to the tank diameter expressed as a percentage. Figures 5.1 and 5.2 illustrate that the roll angle and lateral acceleration response of the 40% and 70% filled tank semitrailers do not deviate significantly from that of the equivalent rigid cargo vehicle for 1° steer input. The roll angle as well as the lateral acceleration response of the partially filled tank semitrailer, however, is considerably larger than that of the rigid cargo vehicle, when the steer angle is increased to 4°. The destabilizing effects of the liquid load shift become quite apparent, when the fill level is increased to 70%, due to excessive load shift from the inner to the outer track. A 70% filled tank vehicle, subjected to 4° constant steer input, exhibits unstable behaviour leading to vehicle rollover, as shown in the Figures 5.1 and 5.2. The equivalent rigid cargo vehicle also experiences an increase in the roll and lateral acceleration, and lift-off of the rearmost trailer axle.

The onset of directional instability of heavy vehicles can be related to the dynamic vertical load factor, defined as the ratio of the instantaneous vertical load on the inner or outer track of a given axle to the static vertical load on that track. During a vehicle manoeuvre, the dynamic load factor describes the impending wheel lift-off and the magnitude of load shift caused by the motion of the free surface of liquid within a partially filled tank. The dynamic load factor has an initial value of unity and becomes zero when the tires on the inner

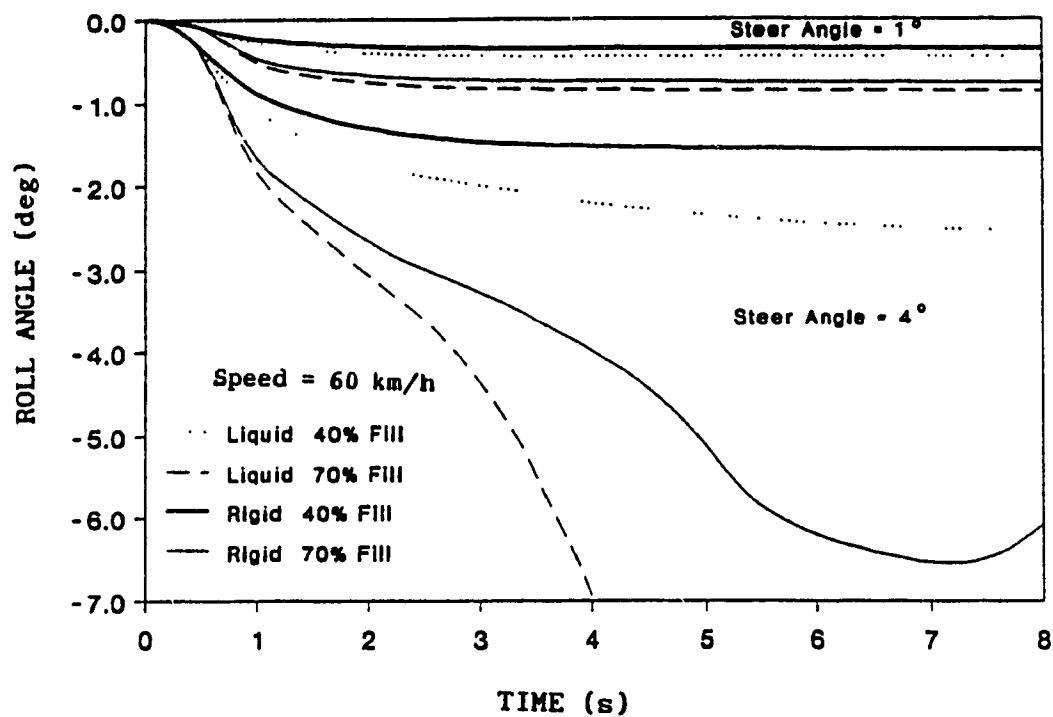


Figure 5.1 Roll response of a two-axle semitrailer with liquid and equivalent rigid cargo loads

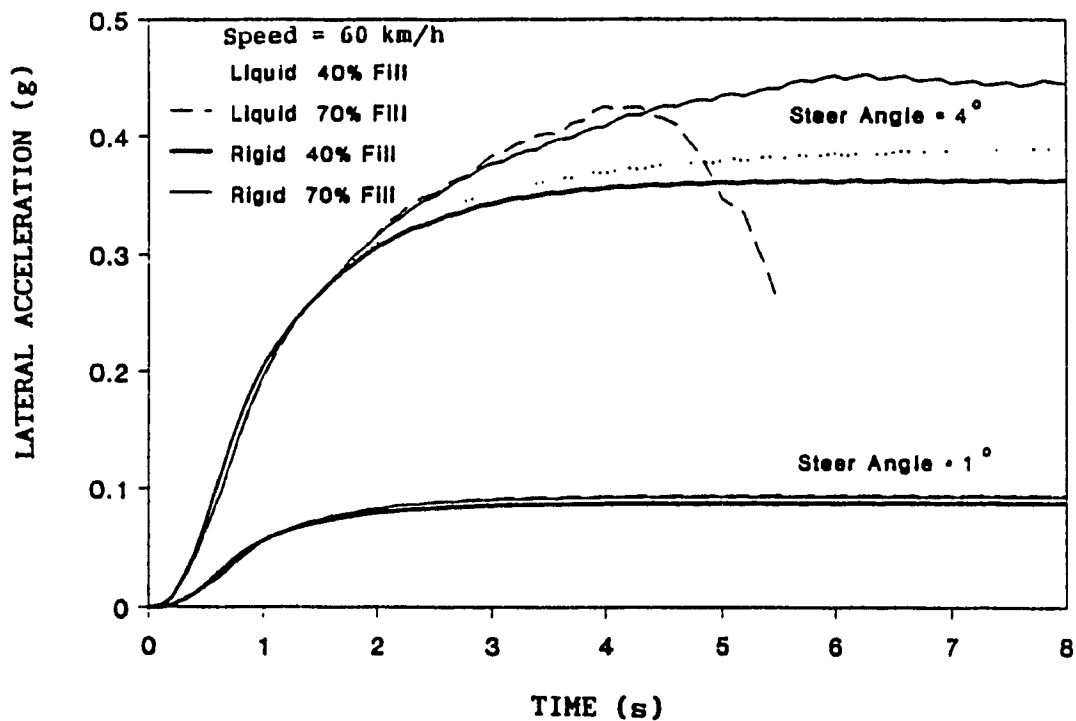


Figure 5.2 Lateral acceleration response of a two-axle semitrailer with liquid and equivalent rigid cargo loads

track lose contact with the road, while the dynamic vertical load factor for the outer track approaches the maximum value of two. Figure 5.3 shows the dynamic vertical load factor of the inner track of the rearmost axle for various steer angles and fill levels.

The load transfer, from the inner to the outer track of the vehicle, occurring during a steady steer manoeuvre is influenced by the fill level, vehicle speed and the steer input. In case of 40% filled liquid tank vehicle, the dynamic vertical load factor reaches a steady state value for both the steer inputs (1° and 4°). For larger steer inputs, however, the dynamic load factor reduces by 0.15 when compared to that of the equivalent rigid cargo vehicle, leading to approximately 15% more load on the outer track of the rearmost axle. In case of 70% filled liquid tank vehicle and the equivalent rigid cargo vehicle, the dynamic load factor reaches a steady state value in case of 1° steer input, however, the destabilizing liquid slosh forces at higher steer input (4°) lead to complete transfer of load from the inner track to the outer track causing the wheel lift-off, as shown in Figure 5.3. The wheels on the rearmost axle of the 70% filled tank semitrailer lift-off the ground after 3.6 seconds of steady steer input, while the rigid cargo vehicle exhibits wheel lift-off after 5.6 seconds of the steady steer input. The wheel lift-off in the rearmost axle of the five-axle tractor semitrailer leads to rapid increase in the roll angle of the semitrailer and drop in the lateral acceleration response, as shown in the Figures 5.1 and 5.2.

Vehicle Path During a Constant Steer Manoeuvre

The load shift occurring during the constant steer manoeuvre increases the cornering forces at the outer track of the vehicle leading

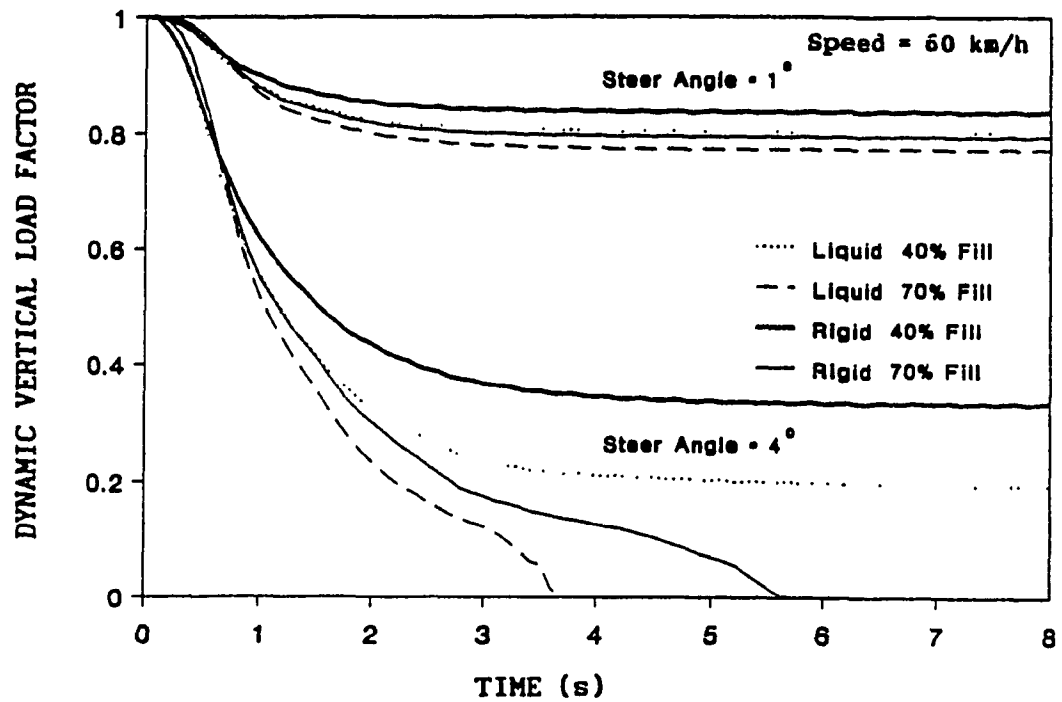


Figure 5.3 Dynamic vertical load factor on the left track of the last axle of the five-axle tractor semitrailer

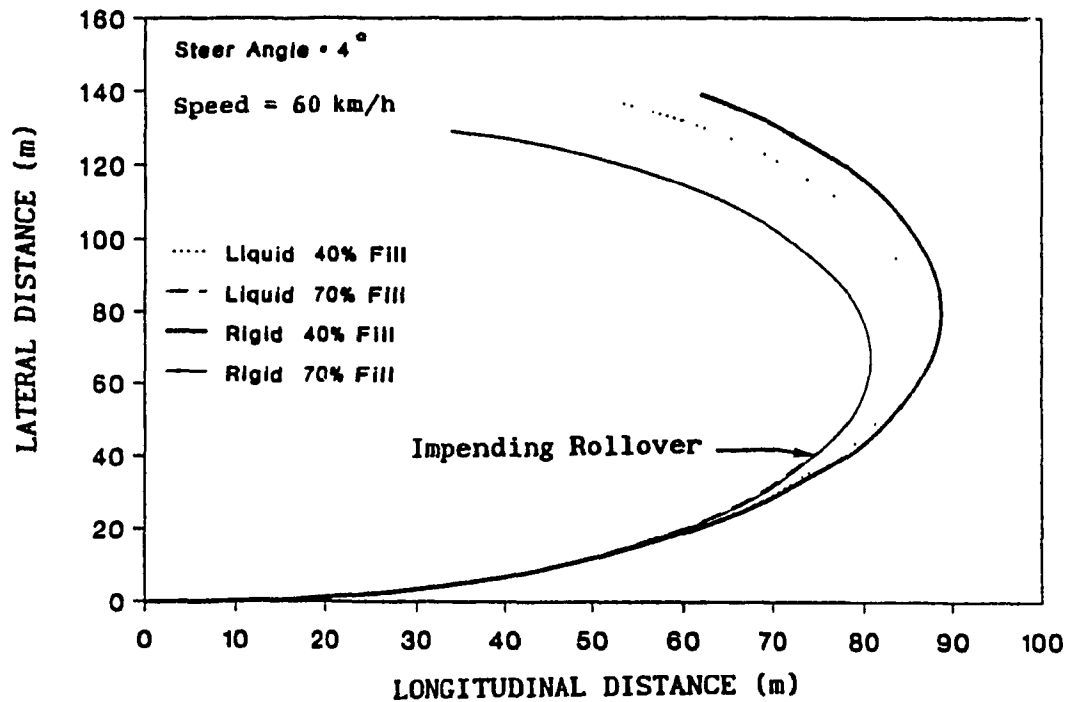


Figure 5.4 Comparison of path followed by a partially filled tank and equivalent rigid cargo five-axle tractor semitrailer vehicle

to considerable deviation in the path followed by the liquid tank vehicle. The path followed by the rigid cargo and partially filled tank vehicles due to steady steer input of 4° at a speed of 60 km/h, are presented in Figure 5.4. A comparison of the path followed by the rigid cargo and liquid tank vehicles reveals that 40% filled tank vehicle deviates considerably from the path followed by the equivalent rigid cargo vehicle. A 40% filled tank vehicle exhibits a lateral path deviation of approximately 10 meters than that of the rigid cargo vehicle. The excessive load shift encountered in a 70% filled tank vehicle, however, leads to vehicle rollover, as shown in Figure 5.3.

Influence of Vehicle Speed on the Directional Response

The directional response of a vehicle combination is strongly influenced by the vehicle speed. Figures 5.5 and 5.6 present the roll angle and lateral acceleration response of the sprung mass of the partially filled liquid and rigid cargo semitrailers, respectively, subjected to steady steer input (1° and 2°) at a speed of 90 km/h. Figures 5.5 and 5.6 reveal that the roll angle and the lateral acceleration response increases considerably with speed. A comparison of the roll angle response of the rigid and liquid cargo vehicles subjected to 1° steer angle reveals that the tank trailer sprung mass experiences larger roll than the sprung mass of the rigid cargo trailer, as shown in Figure 5.5. As the steer angle, however, is increased to 2° , the roll angle response of 40% filled tank vehicle increases considerably and the lateral acceleration response of the vehicle continues to increase, as shown in Figures 5.5 and 5.6 respectively. The 40% filled tank vehicle subjected to 2° steer input at a speed of 90 km/h, approaches unstable behaviour asymptotically. The equivalent

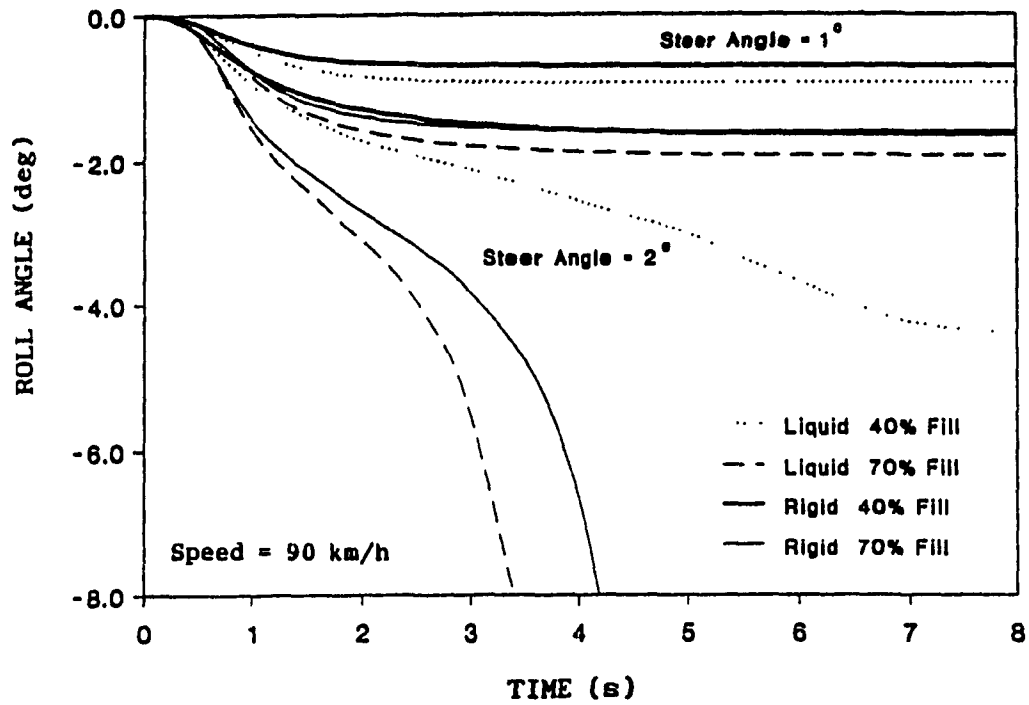


Figure 5.5 Roll response of a two-axle semitrailer with liquid and equivalent rigid cargo loads

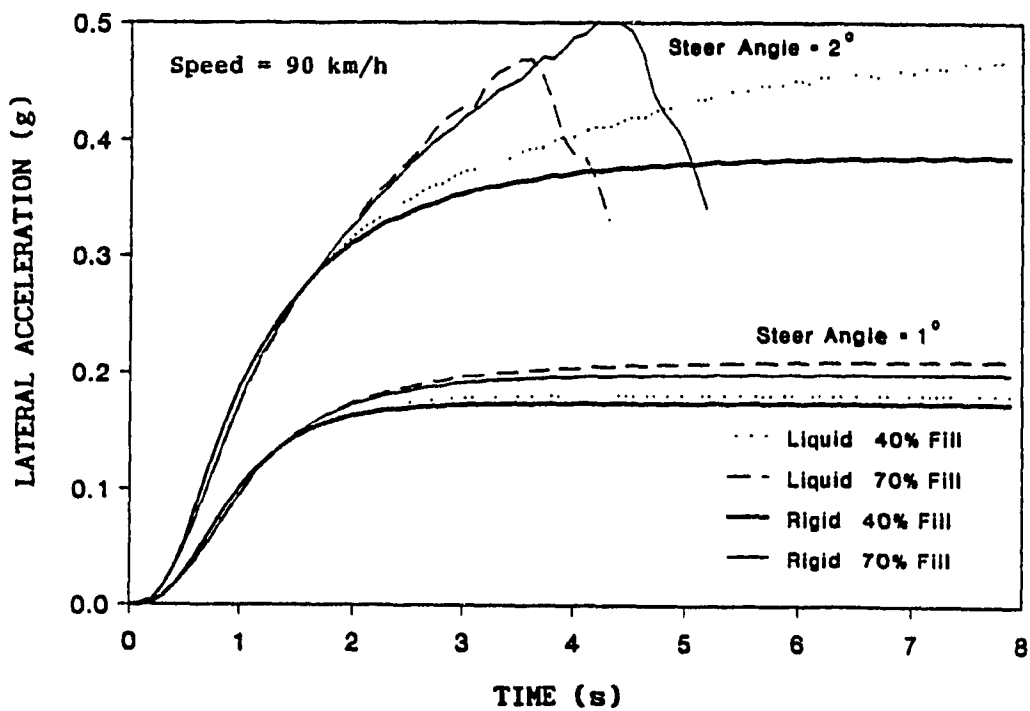


Figure 5.6 Lateral acceleration response of a two-axle semitrailer with liquid and equivalent rigid cargo loads

rigid cargo vehicle exhibits a stable directional response. The 70% filled tank and equivalent rigid cargo vehicles exhibit vehicle rollover when subjected to 2° steer input at a speed of 90 km/h. The liquid tank vehicle, however, rolls over much quicker as compared to the rigid cargo vehicle.

A comparison of the dynamic response of the vehicles corresponding to 60 km/h (Figures 5.1 and 5.2) and 90 km/h (Figures 5.5 and 5.6) speeds for a constant steer input of 1° indicates that the increase in the vehicle speed increases the difference in the dynamic response characteristics between the rigid and liquid cargo semitrailers. The steady state lateral acceleration value of the rigid and liquid cargo trailers nearly doubles from 0.1g to 0.2g when the speed of the vehicle is increased from 60 to 90 km/h. Also, the difference in the steady state lateral acceleration values between the rigid and liquid cargo which was negligible at 60 km/h increases to approximately 0.02g at 90 km/h. At higher vehicle speeds, the vehicle attains instability at lower steer inputs, as observed from the response plots.

5.3.1.2 Directional Response of Five-Axle Tractor-Semitrailer Combination (Constant Axle Loads)

Figures 5.1 to 5.6 present the directional response of the partially filled five-axle tractor-semitrailer tank vehicle, where the axle loads vary with the fill level. Cleanbore cylindrical tanks, used in general purpose chemical fleet, are often partially filled due to variations in the weight density of various chemicals, however the load carried by each axle is maintained around the maximum permissible value (55 kN for the tractor front, and 170 kN for the tractor rear and the trailer axles). Computer simulation are performed to investigate the

directional response of 40% filled tank vehicle carrying an industrial acid of density 0.0186 N/cm^3 (0.0673 lb/in^3) and 70% filled tank vehicle carrying diesel oil of density $= 0.0092 \text{ N/cm}^3$ (0.034 lb/in^3) such that the axle loads remain constant around the maximum permissible values.

Figures 5.7 and 5.8 present the directional response of the 40% and 70% filled tank and the equivalent rigid cargo vehicles under constant axle loads, for a steady steer input of 3° . The 40% and 70% filled tank semitrailers experience similar roll angle and lateral acceleration response, for a constant steer input at a speed of 60 km/h. The 40% and 70% filled liquid tank vehicles approach unstable behaviour asymptotically, as observed from the rapid increase in the lateral acceleration and the roll angle of the trailer. The equivalent rigid cargo vehicles exhibit stable behaviour under identical conditions of fill level, vehicle speed and steer angle, while the axle loads are held constant. A comparison of the roll and lateral acceleration response of the rigid cargo vehicles indicates improved directional stability of the 40% filled vehicle compared to the 70% filled vehicle, under constant axle loading conditions. This is attributed to the low overall centre of gravity of the 40% filled rigid cargo vehicle. In case of the liquid load, however, the 40% fill condition yields reduced directional stability due to excessive sloshing.

Figure 5.9 shows the dynamic vertical load factor of the inner track of the rearmost axle on the tank semitrailer for various fill and steady steer inputs, under constant axle loading conditions. In case of the rigid cargo vehicles, the dynamic load factor reaches a steady state value for both the steer inputs. In case of the liquid tank vehicles, however, they exhibit stable behaviour at small steer input and the

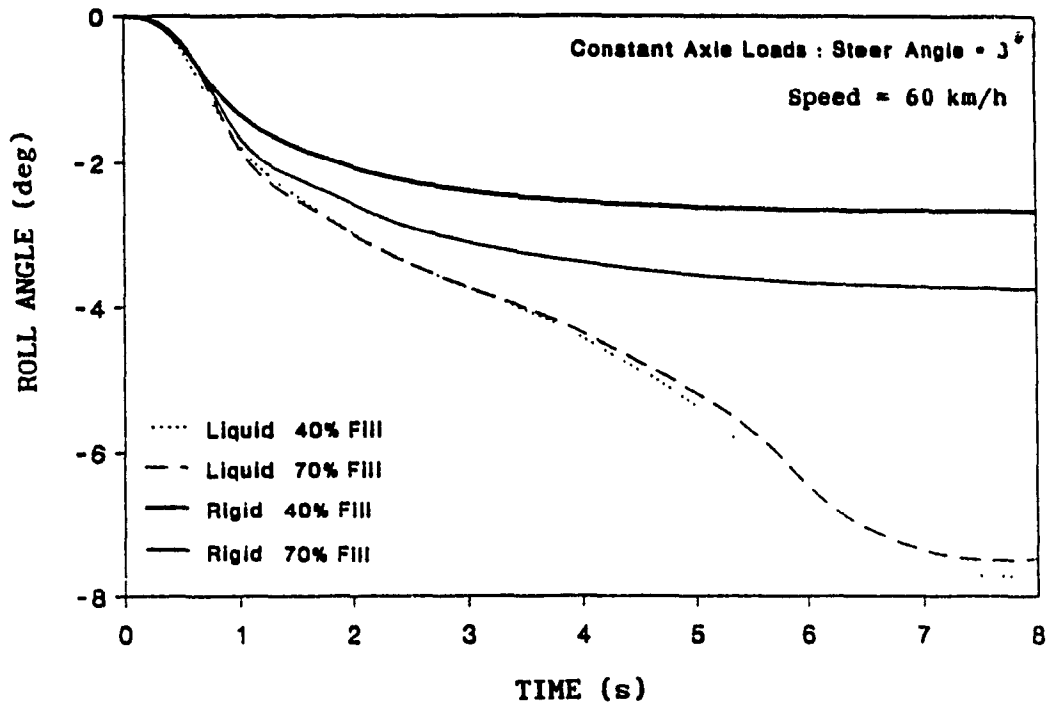


Figure 5.7 Roll response of a two-axle semitrailer with liquid and equivalent rigid cargo loads

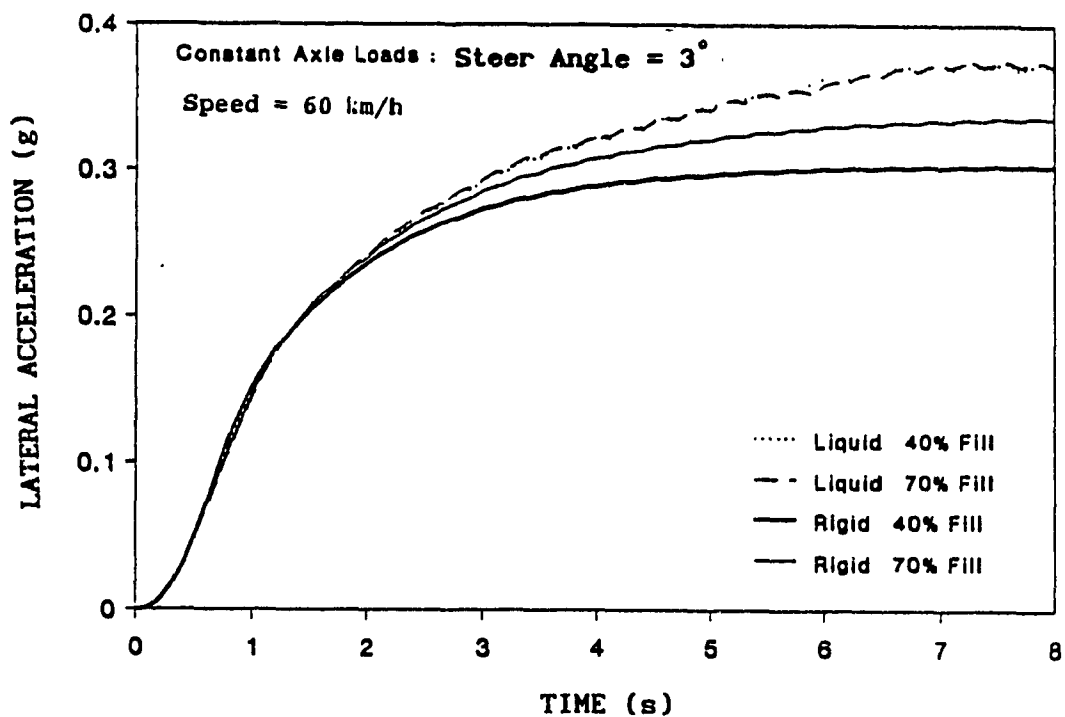


Figure 5.8 Lateral acceleration response of a two-axle semitrailer with liquid and equivalent rigid cargo loads

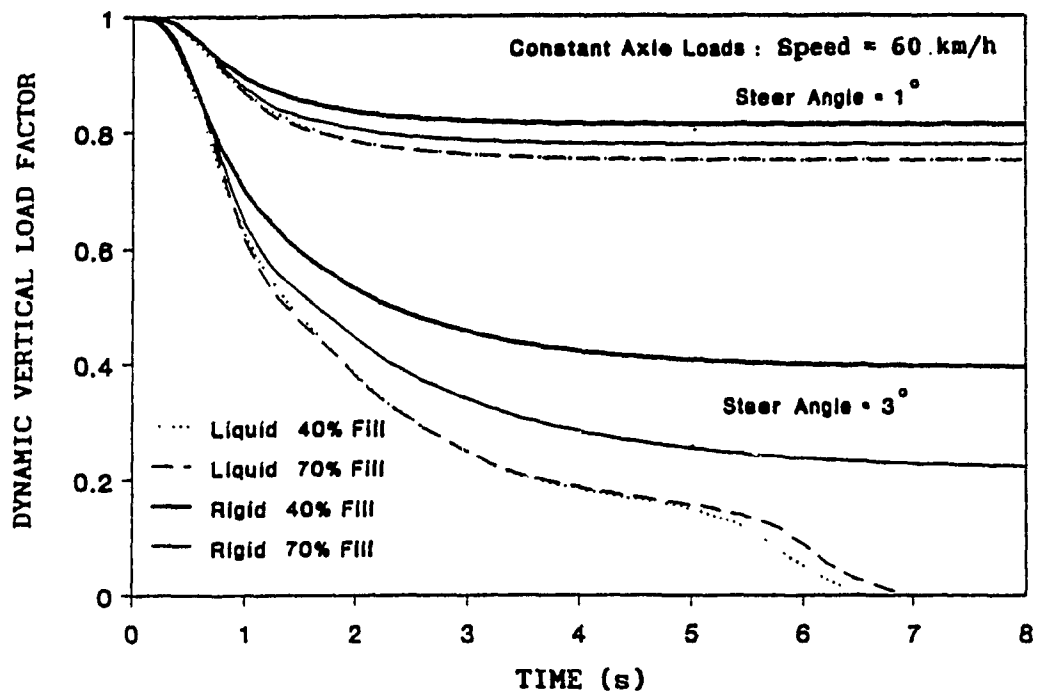


Figure 5.9 Dynamic vertical load factor on the left track of the last axle of the five-axle tractor semitrailer

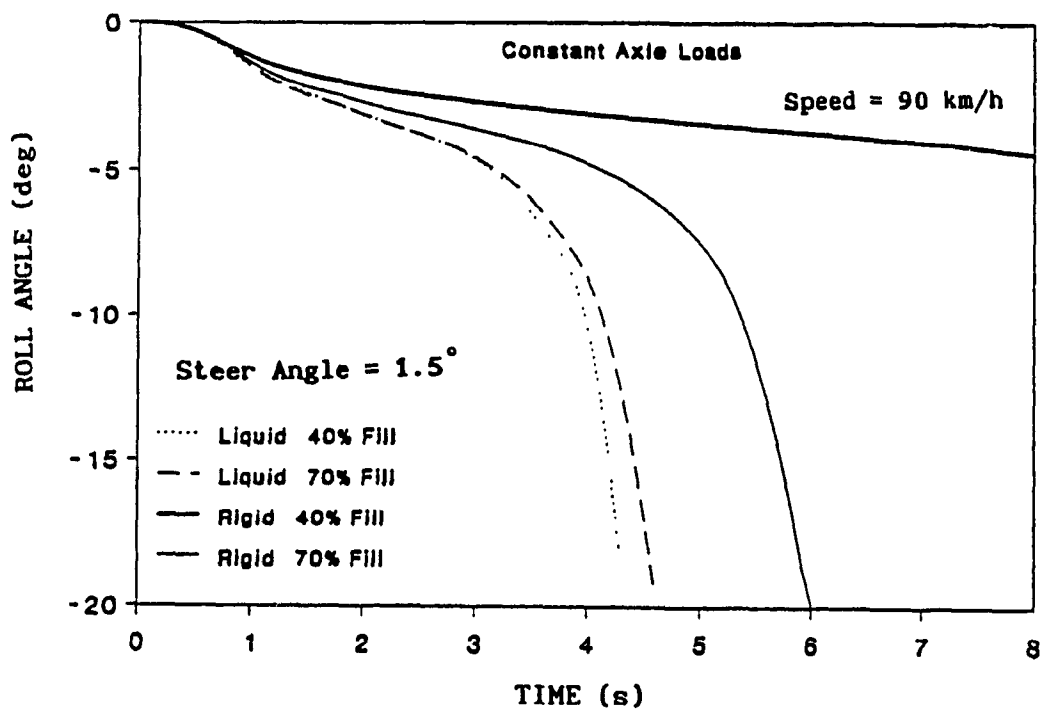


Figure 5.10 Roll response of a two-axle semitrailer with liquid and equivalent rigid cargo loads

dynamic load factor reaches a steady state value. At larger steer inputs, the dynamic load factor approaches zero, indicating wheel lift-off, as shown in Figure 5.9. The 40% filled tank vehicle experiences a wheel lift-off around 6.5 seconds while a 70% filled tank vehicle experiences lift off around 7 seconds. This is attributed to larger load shift at low fill conditions.

Figure 5.10 presents the roll angle response of the sprung mass of the partially filled liquid and rigid cargo trailers, for a steady steer input at a speed of 90 km/h while the axle loads are held constant. An increase in the vehicle speed adversely affects the vehicle dynamic response, leading to sharp increase in the roll angle, as shown in Figure 5.10. The 40% and 70% filled tank vehicles with constant axle loads, subjected to a steady steer of 1.5° , experience large roll angle leading to rollover. A 40% filled rigid cargo vehicle exhibits a stable behaviour compared to a 70% filled rigid cargo vehicle which experiences rollover. This is attributed to the low overall C.G of the 40% filled vehicle compared to a 70% filled vehicle.

5.3:1.3 Directional Response of Six-Axle Tractor-Semitrailer Combination (Constant Axle Loads)

Computer simulations are carried out to investigate the directional response of partially filled six-axle tractor semitrailer tank vehicle subjected to steady steer inputs. The axle loads are held constant around the maximum permissible values (55 kN for the tractor front, 170 kN for the tractor rear and 240 kN for the trailer axles). Figures 5.11 and 5.12 present the directional response of 40% and 70% filled liquid and equivalent rigid cargo vehicles under constant axle loading conditions, for a steady steer input of 3° . The 40% and 70% filled tank semitrailers approach identical steady state response, as shown in

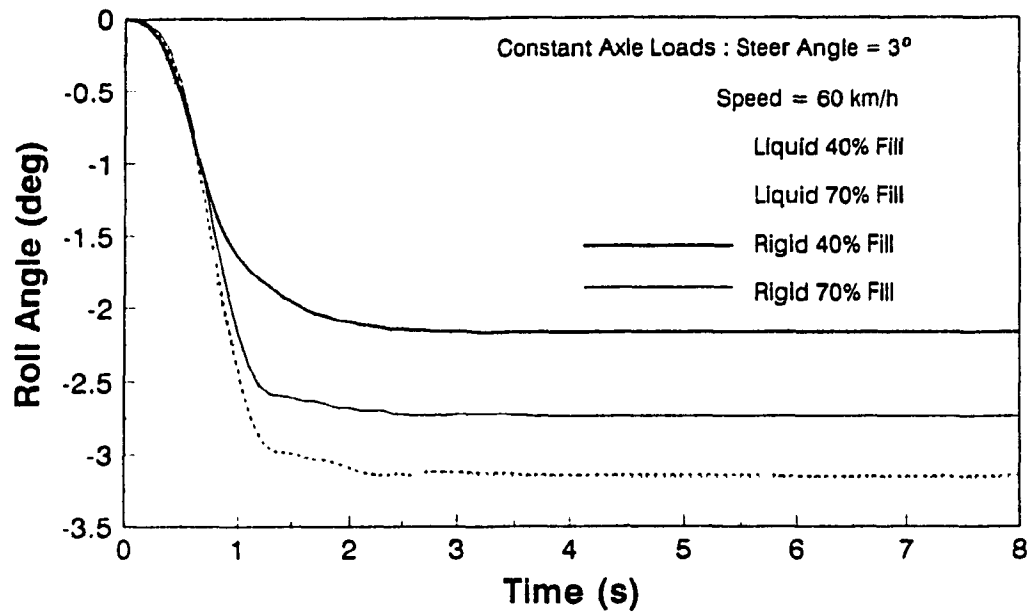


Figure 5.11 Roll response of a three-axle semitrailer with liquid and equivalent rigid cargo loads

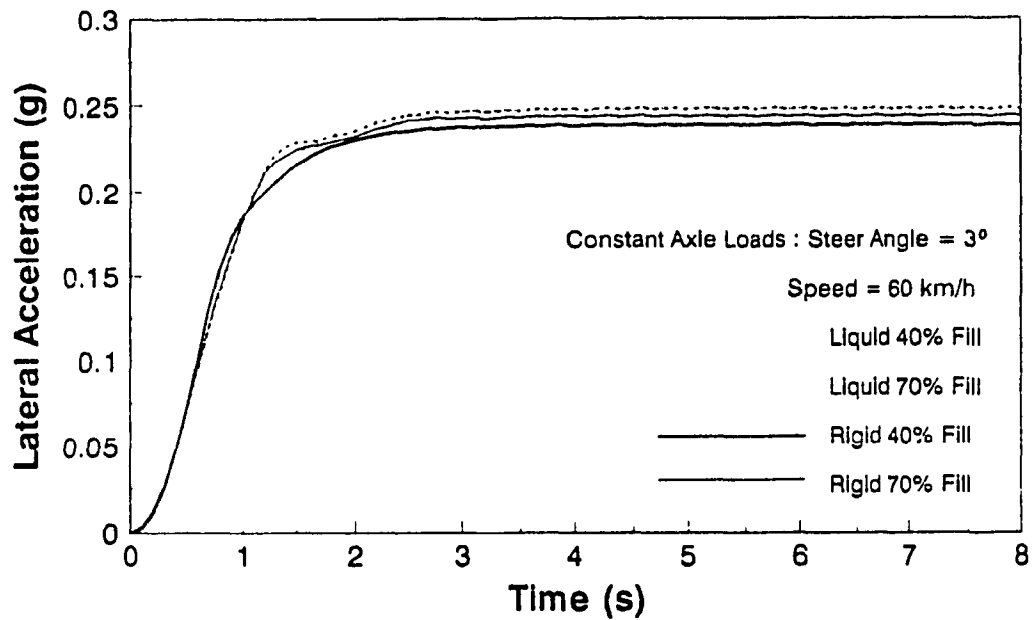


Figure 5.12 Lateral acceleration response of a three-axle semitrailer with liquid and equivalent rigid cargo loads

Figures 5.11 and 5.12. The roll and lateral acceleration response of the 40% filled equivalent rigid cargo semitrailer are found to be lowest due to the low overall C.G. height, under identical conditions of fill level, vehicle speed and steer angle. Table 5.1 presents a comparison of the directional response characteristics of partially filled five- and six-axle tractor semitrailer tank vehicles, subjected to 1° steady steer input. The comparison reveals that a six-axle vehicle is considerably more stable than the five-axle vehicle.

5.3.2. Closed-Loop Transient Steer Manoeuvre

5.3.2.1 Directional Response of Five-Axle Tractor-Semitrailer Combination (Variable Axle Loads)

The directional response of a partially filled five-axle tractor-semitrailer vehicle is investigated for typical lane-change and evasive manoeuvres as shown in Figure 5.13, using a closed-loop driver model [1]. The front wheel steer angles, required to follow the prescribed path are computed using the closed-loop driver model, and are presented in Figure 5.14. Figure 5.15 shows the lateral load shift within the 40% and 70% filled tank vehicles, negotiating a 30m lane change manoeuvre at a speed of 90 km/h. It can be seen that load shift in a 40% filled tank is considerably larger than that in a 70% filled tank. The lateral load shift in the liquid trailers, leads to larger vehicle roll as compared to that of the equivalent rigid cargo trailers, as shown in Figure 5.16. The roll angle response of 70% filled trailers are considerably larger than that of a 40% filled trailers, independent of the cargo, due to high C.G. location.

The lateral load shift encountered in a 70% filled tank semitrailer, subjected to an evasive manoeuvre at a constant forward

TABLE 5.1

COMPARISON OF THE DIRECTIONAL CHARACTERISTICS OF
5-AXLE AND 6-AXLE TRACTOR SEMITRAILER TANK VEHICLE

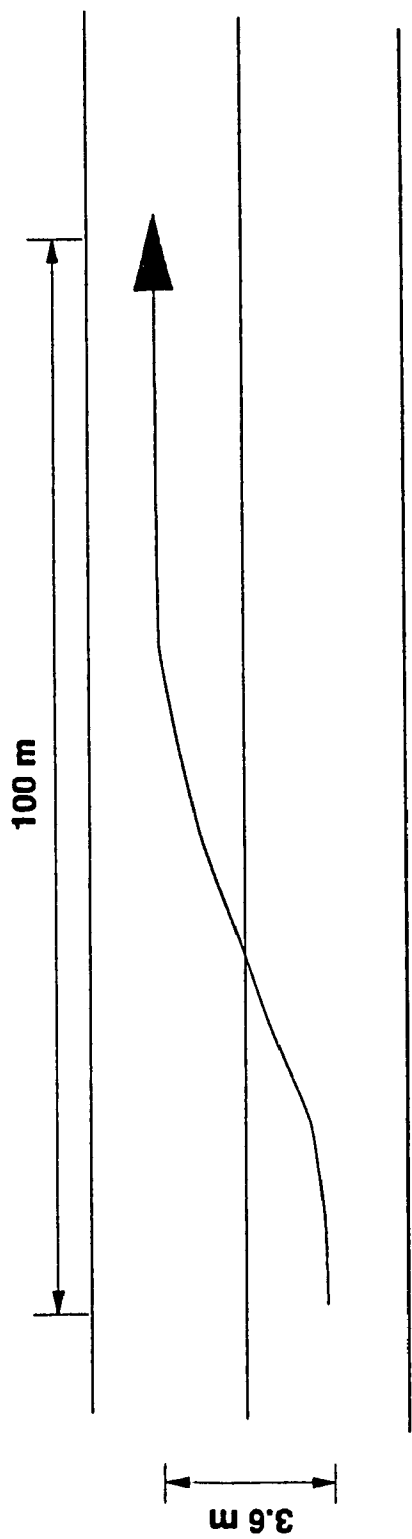
Constant Steer Input : Steer Angle = 1° - Right Turn

Constant Axle Loads

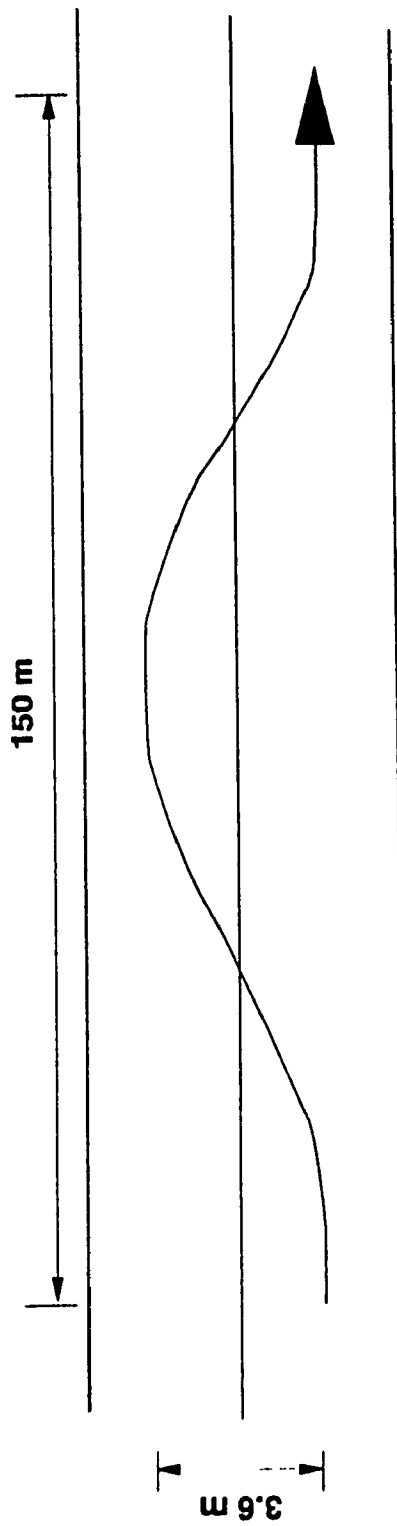
Cargo Load : 5-Axle Tractor Semitrailer : 213 kN (47930 lb)

6-Axle Tractor Semitrailer : 242 kN (54440 lb)

Response Parameter	Vehicle Configuration	
	Five-Axle	Six-Axle
Load Shift		
Y_{l2}	-15 cm; unstable	-9.2 cm
Z_{l2}	5 cm; unstable	0.81 cm
Roll Angle		
Rigid	-2.4°	-1.26°
Liquid	-14.0° ; unstable	-1.88°
Lateral Acceleration		
Rigid	0.24g	0.14g
Liquid	0.40g; unstable	0.15g
Yaw Rate		
Rigid	5.2 deg/s (peak)	3.1 deg/s
Liquid	9.3 deg/s; unstable	3.3 deg/s
Roll Rate		
Rigid	-1.8 deg/s (peak)	-1.54 deg/s
Liquid	-2.1 deg/s; unstable	-2.18 deg/s



LANE CHANGE MANOEUVRE



EVASIVE MANOEUVRE

Figure 5.13 Vehicle path during typical lane change and evasive manoeuvres

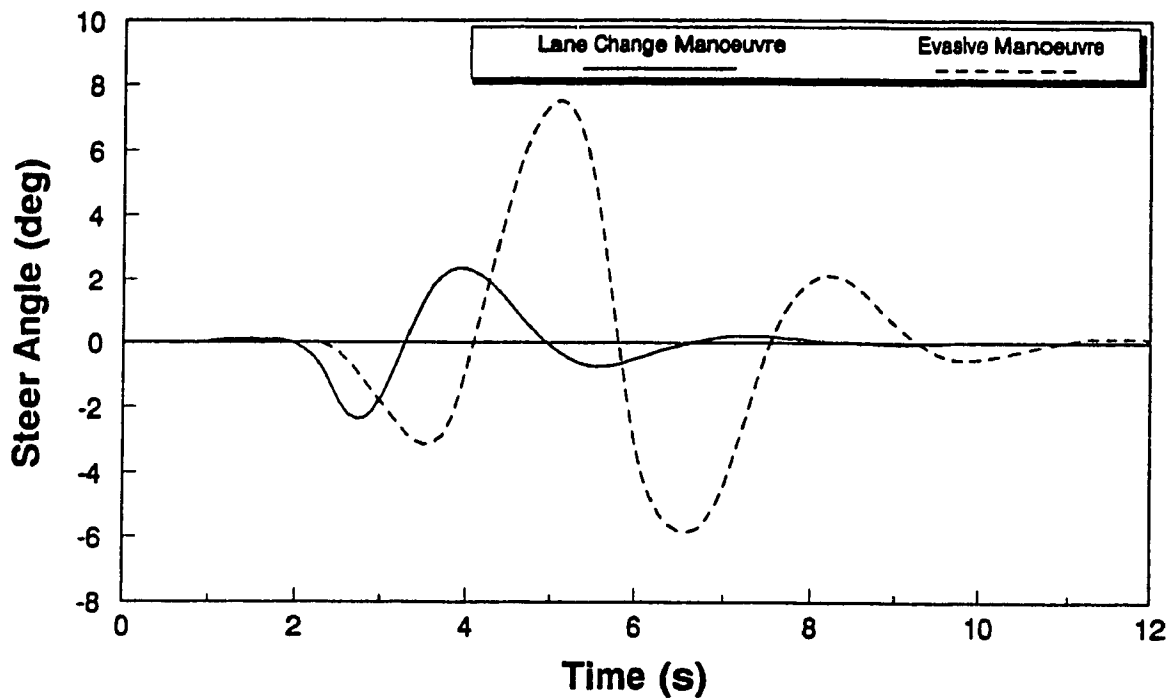


Figure 5.14 Front wheel steer angles required to perform a typical lane change and an evasive manoeuvre

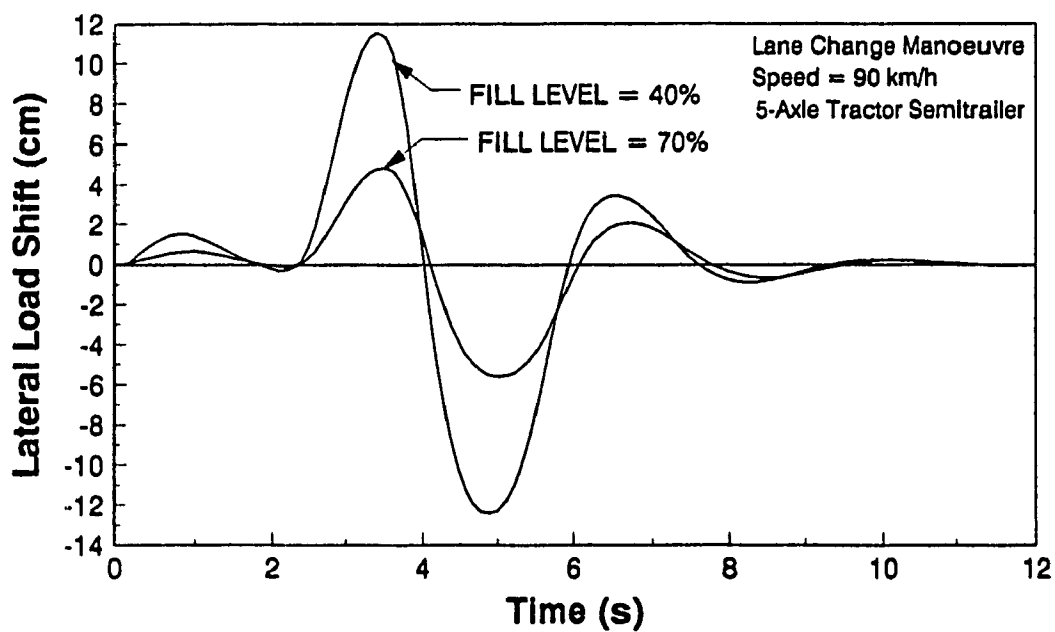


Figure 5.15 Lateral load shift in a partially filled two-axle tank trailer during a lane change manoeuvre

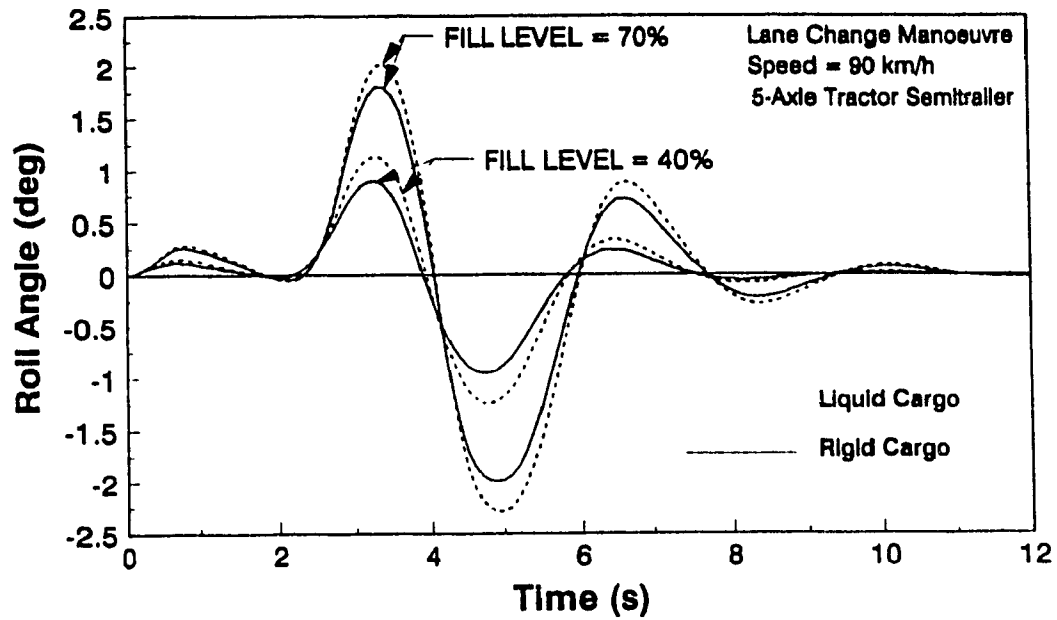


Figure 5.16 Roll angle response of a partially filled liquid and equivalent rigid cargo two-axle semitrailers during a lane change manoeuvre

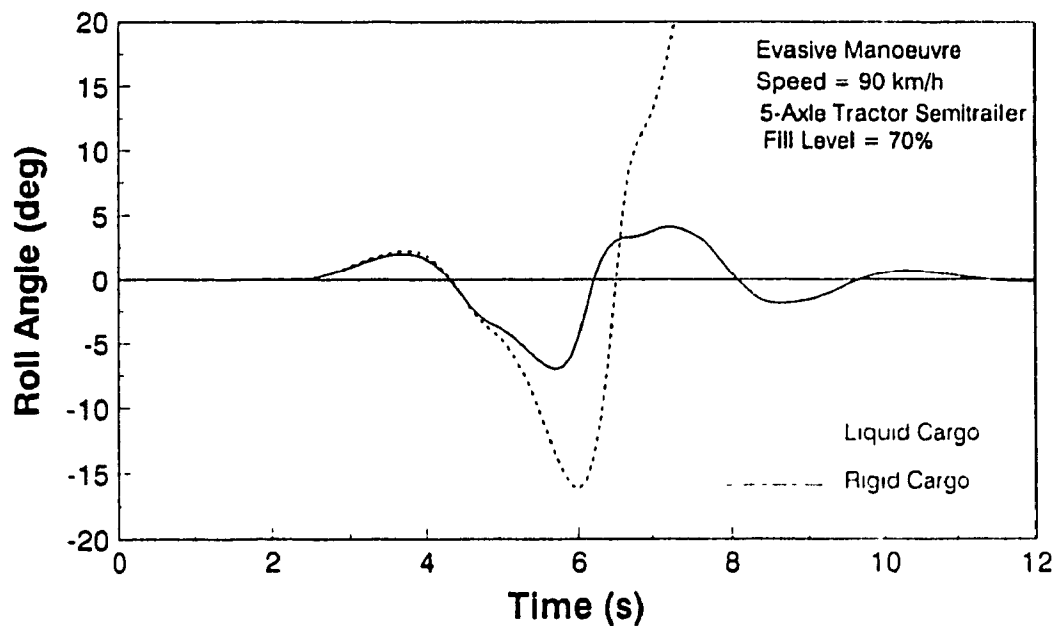


Figure 5.17 Roll angle response of a partially filled liquid and equivalent rigid cargo two-axle semitrailers during an evasive manoeuvre

speed of 90 km/h, results in excessive roll angle leading to vehicle rollover, as shown in Figure 5.17. The roll angle response of the corresponding equivalent cargo vehicle, however, is considerably smaller and thus the equivalent rigid cargo vehicle remains stable under identical steering manoeuvre.

5.3.2.2 Directional Response of Five-Axle Tractor-Semitrailer Combination (Constant Axle Loads)

Transportation of denser chemicals often leads to partial fill conditions in order to conform with the maximum permissible axle loads. The directional response of an articulated five-axle tank vehicle is investigated for 70% fill condition, while the axle loads are held around the maximum permissible values. The roll angle response of 70% filled tank vehicle is compared to that of an equivalent rigid cargo vehicle, when both the vehicles are subjected to the evasive manoeuvre, as shown in Figure 5.18. It can be seen that the partially filled five-axle tank semitrailer vehicle, with axle loads around the maximum permissible values, rolls over immediately after the steering input is applied, while the equivalent rigid cargo vehicle does not exhibit any roll instabilities. Figure 5.19 presents the vertical load on the left track of the rearmost axle of the 70% filled tank vehicle, subjected to the evasive manoeuvre, when axle loads are held constant. The right track load of the equivalent rigid cargo vehicle approaches 0, around 5.4.s, indicating the wheel lift-off. The wheel-road contact, however, is regained when steer direction is reversed, as shown in Figure 5.19. The liquid cargo vehicle, exhibits the wheel lift-off around 5.2 s after the steer input is applied and eventually the vehicle rolls over. The corresponding vertical load on the right track of the rearmost axle is presented in Figure 5.20.

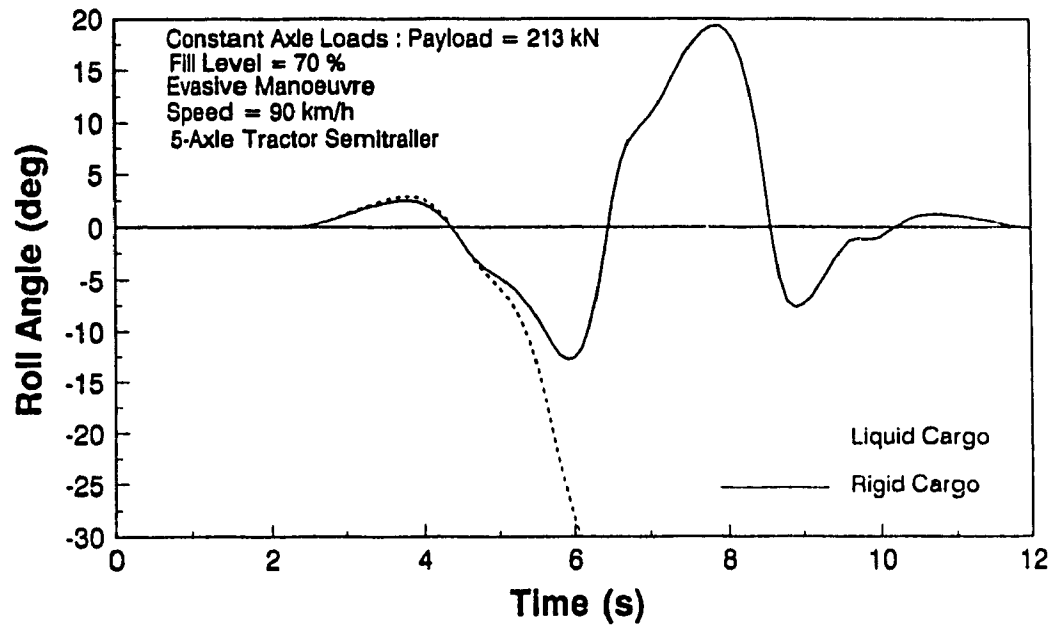


Figure 5.18 Roll angle response of a partially filled liquid and equivalent rigid cargo two-axle semitrailers during an evasive manoeuvre

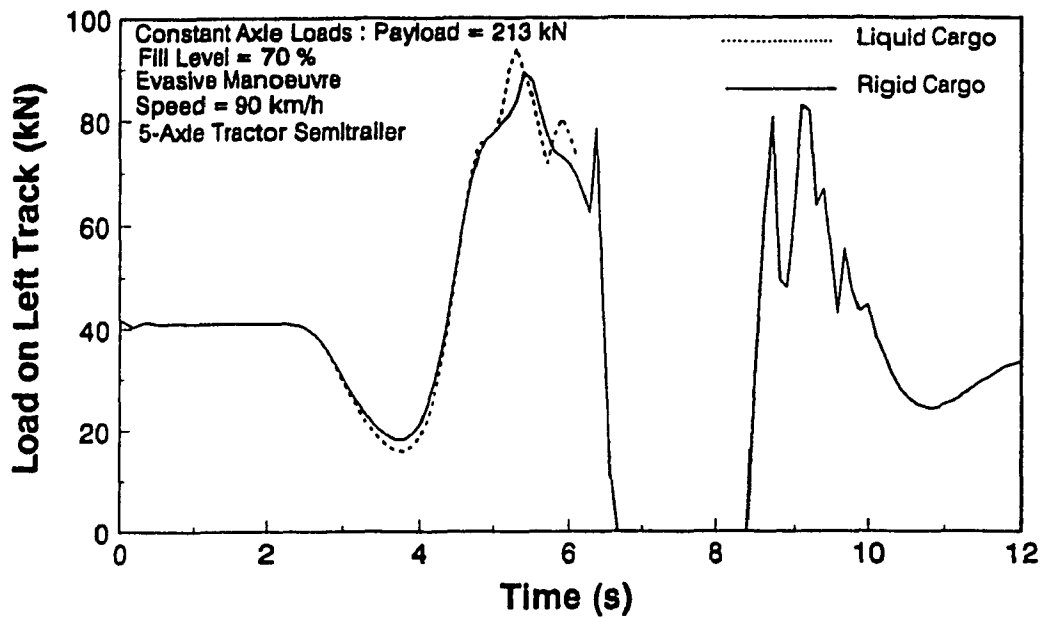


Figure 5.19 Vertical load on the left track of the rearmost axle of a five-axle tractor semitrailer carrying liquid and equivalent rigid cargo, during an evasive manoeuvre

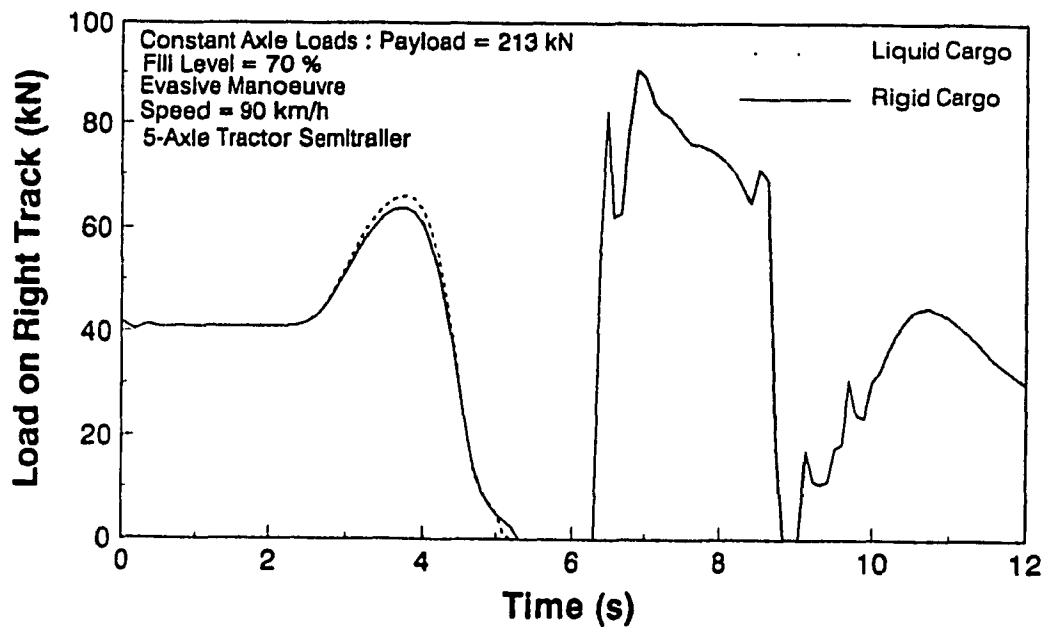


Figure 5.20 Vertical load on the right track of the rearmost axle of a five-axle tractor semitrailer carrying liquid and equivalent rigid cargo, during an evasive manoeuvre

5.3.2.3 Directional Response of Six-Axle Tractor-Semitrailer Combination (Constant Axle Loads)

The directional response of a partially filled six-axle tractor semitrailer tank vehicle, under constant axle loading conditions, is investigated for lane-change and evasive manoeuvres, using the closed-loop path follower model. Figures 5.21 and 5.22 present a comparison of the roll angle and lateral acceleration response of the 70% filled tank trailer and the equivalent rigid cargo trailer, when both the vehicles are subjected to a lane change manoeuvre at a speed of 90 km/h. The lateral load shift within the partially filled tank trailer leads to larger roll of the trailer compared to the equivalent rigid cargo trailer, as shown in Figure 5.21. The lateral acceleration response, however, shows very little deviation between the liquid and rigid cargo trailers, as shown in Figure 5.22.

The roll response of 70% filled six-axle tank vehicle is compared to that of an equivalent rigid cargo vehicle, when both the vehicles are subjected to the evasive manoeuvre, as shown in Figure 5.23. The liquid tank trailer experiences approximately 2 degrees more roll than that of the equivalent rigid cargo trailer, under identical vehicle speed and axle loading conditions. The six-axle tractor semitrailer, however, is more stable compared to the five-axle tractor semitrailer, when both the vehicles carry maximum loads, as seen from Figures 5.18 and 5.23. Table 5.2 presents a comparison of the directional response characteristics of five- and six-axle tractor semitrailer tank vehicles, subjected to an evasive manoeuvre, under constant axle loading conditions.

5.3.3 Directional Response of a Compartmented Tank Vehicle

The magnitude of lateral load shift in a cleanbore tank vehicle can

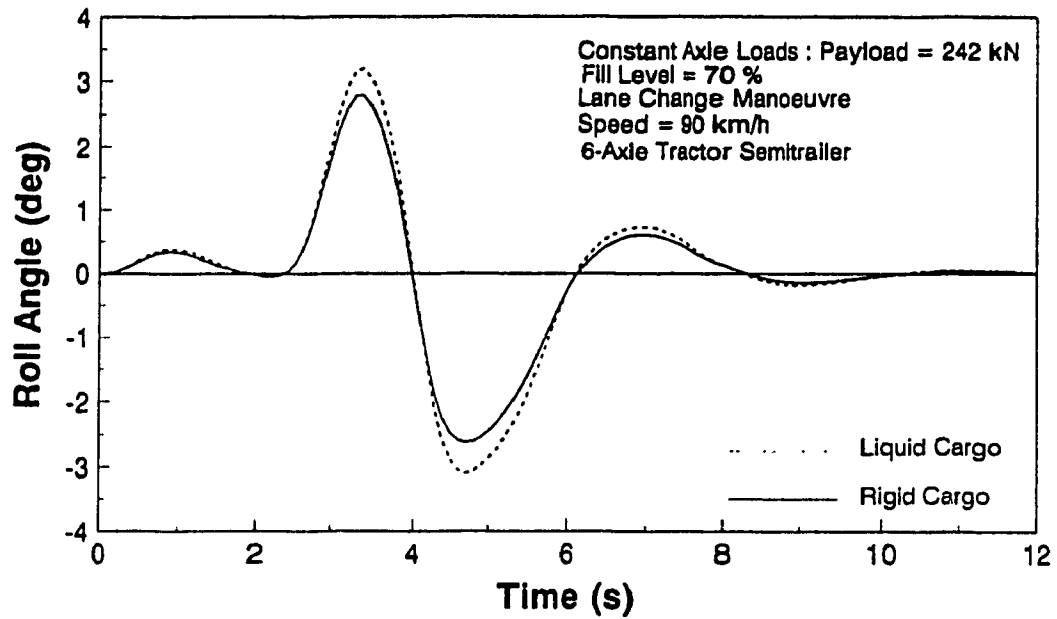


Figure 5.21 Roll response of a partially filled liquid and equivalent rigid cargo three-axle semitrailers, during a lane change manoeuvre

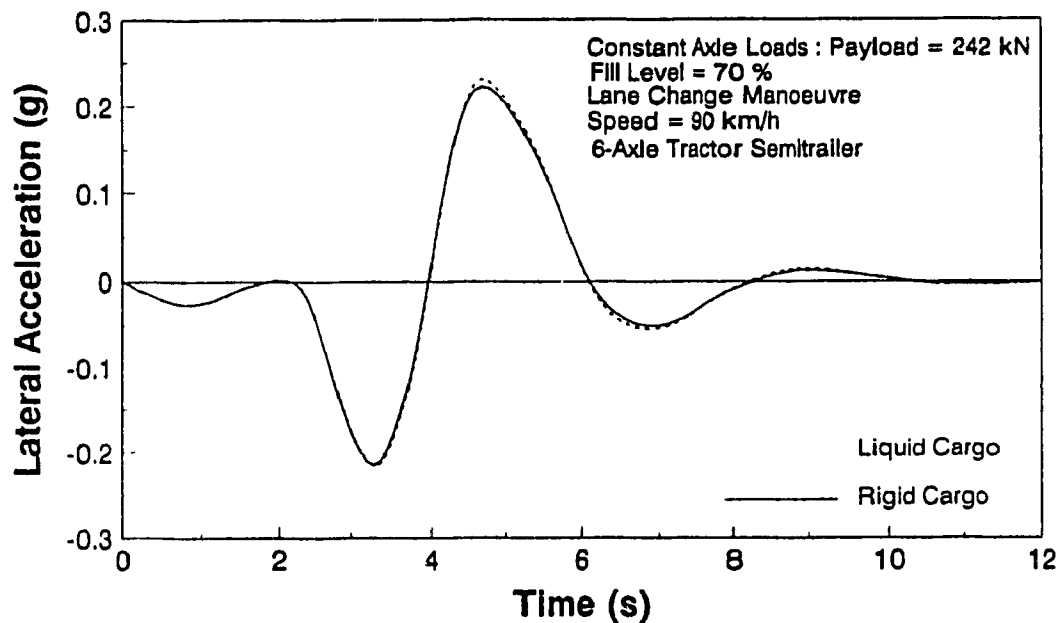


Figure 5.22 Lateral acceleration response of a partially filled liquid and equivalent rigid cargo three-axle semitrailers, during a lane change manoeuvre

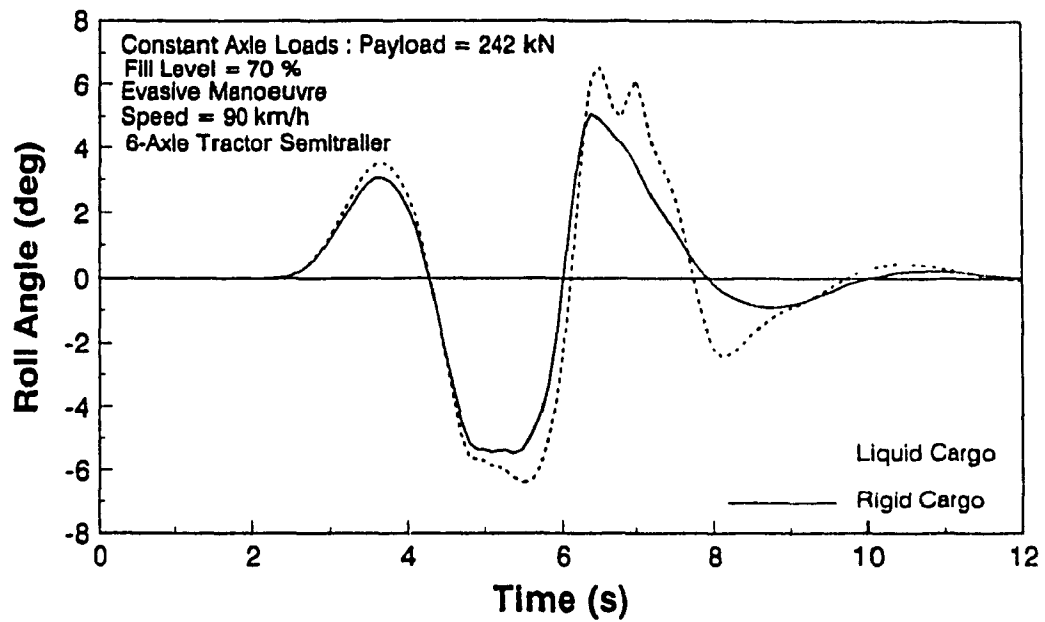


Figure 5.23 Roll response of a partially filled liquid and equivalent rigid cargo three-axle semitrailers, during an evasive manoeuvre

TABLE 5.2

**COMPARISON OF THE DIRECTIONAL CHARACTERISTICS OF
5-AXLE AND 6-AXLE TRACTOR SEMITRAILER TANK VEHICLES**

Evasive Manoeuvre : Path Follower Model

Constant Axle Loads

Cargo Load : 5-Axle Tractor Semitrailer : 213 kN (47930 lb)

 6-Axle Tractor Semitrailer : 242 kN (54440 lb)

Response Parameter (peak)	Vehicle Configuration	
	Five-Axle	Six-Axle
Load Shift		
Y_{l2}	-18 cm; unstable	-16.3 cm
Z_{l2}	7.5 cm; unstable	7.2 cm
Roll Angle		
Rigid	10.0°	5.2°
Liquid	30.0°; unstable	7.2°
Lateral Acceleration		
Rigid	-0.48g	0.62g
Liquid	-0.51g; unstable	0.73g
Roll Rate		
Rigid	-38.0 deg/s (peak)	18.6 deg/s
Liquid	33.0 deg/s; unstable	24.8 deg/s

be reduced considerably by introducing number of compartments within the tank. The directional stability of the tank vehicle can be thus improved due to reduced slosh and load transfer. Circular tanks used in general purpose chemical transportation are generally cleanbore while the modified-oval tanks (MC 306 A1) are often compartmented [2]. The directional response of a 5-axle tractor-semitrailer equipped with a four-compartmented modified oval tank, presented in Figure 5.24, subjected to constant steer input, is investigated through computer simulation. The axle loads are assumed to be held constant around the maximum permissible values.

The roll and the lateral acceleration response characteristics of the modified-oval tank vehicle are evaluated with varying fills in the different compartments and compared to those of an equivalent cleanbore tank vehicle. The total payload is held constant around 209 kN (47,045 lb). The vehicle is subjected to a constant steer input of 2.5 degrees at a speed of 60 km/h. The constant loading in the equivalent cleanbore tank is achieved by partially filling the tank to 80%, while the loading distribution in the four compartmented tank vehicle can be realized many ways. The loading sequences considered for the study, are presented in Table 5.3. The roll response of the cleanbore tank vehicle increases rapidly as shown in Figure 5.25. The roll response of the compartmented tank vehicles, however, approach a steady state value expect for the loading sequence (a) where the last compartment is empty. The response characteristics of the tank vehicle with empty mid-compartments and partially filled end compartments, (sequence c or d) indicate a very stable behaviour. The lateral acceleration response of the tank vehicle reveals a very similar trend, as shown in Figure 5.25. This is

COMPARTMENTS

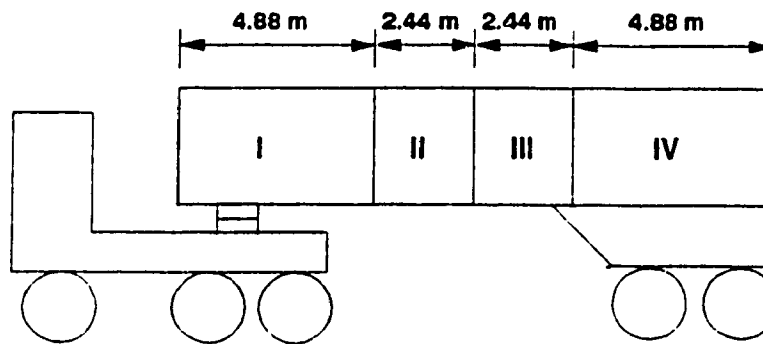


Figure 5.24 Four compartmented modified oval tank

TABLE 5.3

LOAD DISTRIBUTION SEQUENCE IN A FOUR COMPARTMENTED MODIFIED OVAL TANK VEHICLE

Total Payload 209 kN (47045 lb)

sequence	% Fill in Compartment			
	I	II	III	IV
(a)	80	100	100	0
(b)	0	100	100	80
(c)	100	0	0	80
(d)	80	0	0	100
(e)	60	60	60	60

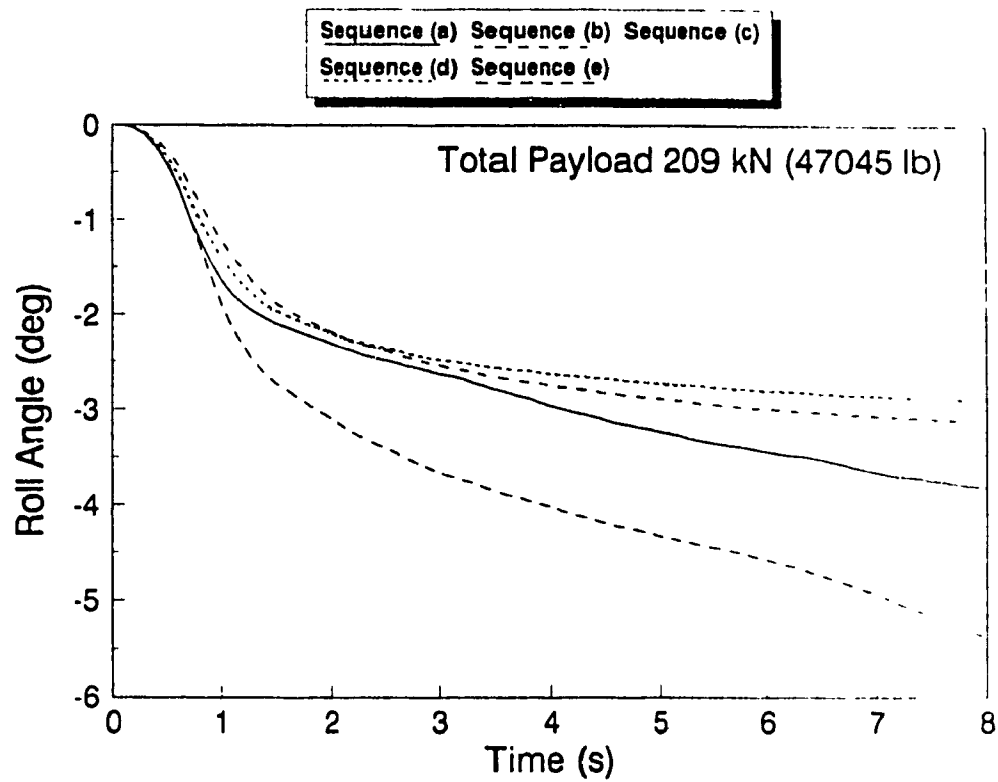


Figure 5.25 Comparison of roll response of a compartmented and cleanbore modified oval tank vehicle

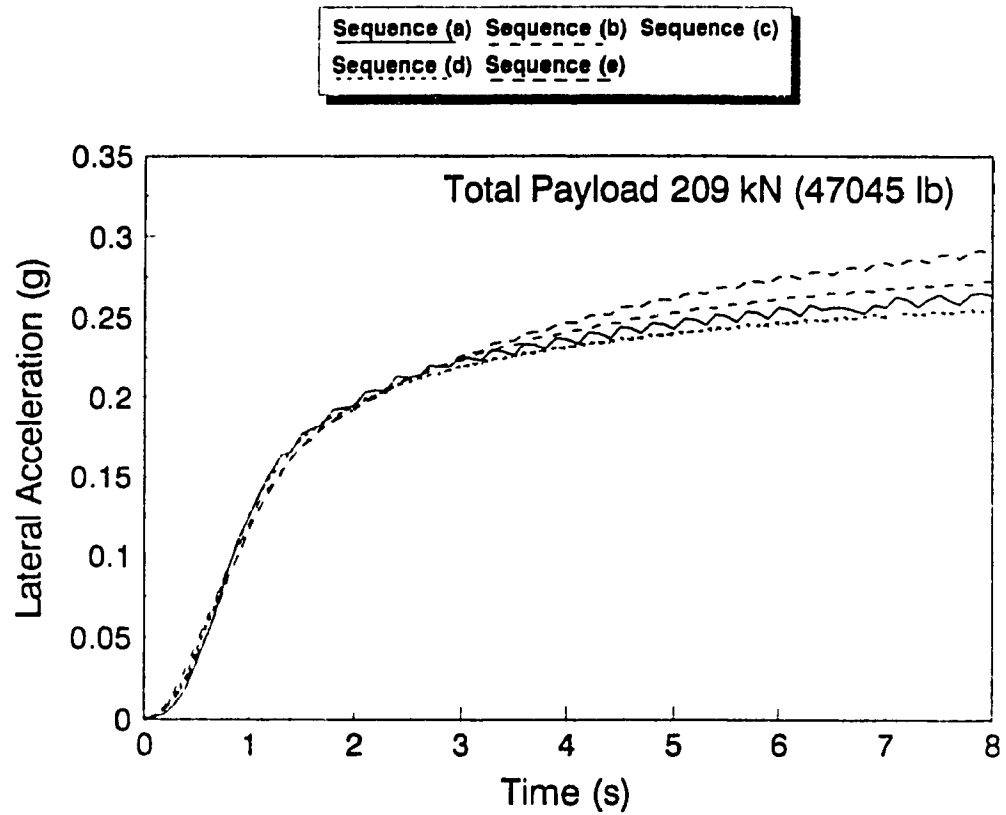


Figure 5.26 Comparison of lateral acceleration response of a compartmented and cleanbore modified oval tank vehicle

attributed to the fact that emptying of either the front or the rear compartments directly influences the load on the tractor rear and the trailer axles. The directional response characteristics of the compartmented tank vehicle indicate that the mid-compartments must be emptied first in order to obtain better directional stability.

5.4 Directional Response of a B-Train Tank Vehicle

5.4.1. Open-Loop Constant Steer Manoeuvre (Constant Axle Loads)

The directional dynamics of a 7-axle B-Train equipped with a circular cross-section tank subjected to steady steer input is investigated through computer simulation. Cleanbore cylindrical tanks, used in general purpose chemical fleet are often partially filled due to variations in the weight density of the various chemicals transported. The load carried by each axle, however, is maintained around the maximum permissible value. The payload carried by the semitrailers are held constant at the value corresponding to the fully loaded tanks carrying fuel oil of weight density = 0.0068 N/cm^3 (0.025 lb/in^3) in order to obtain maximum permissible axle loads. The fill conditions vary with the type of liquid being transported, due to change in the weight density. Computer simulations are carried out to investigate the directional response characteristics of the B-Train tank vehicle combination carrying the following types of cargo:

Industrial Acids : Weight Density = 0.0136 N/cm^3 (0.05 lb/in^3)
Fill Level = 50%

Diesel Oils : Weight Density = 0.0084 N/cm^3 (0.031 lb/in^3)
Fill Level = 75%

The dynamic response parameters of the liquid tank vehicle, such as the roll angle, lateral acceleration and roll rate are obtained, assuming steady state inviscid fluid motion. The dynamic response of

the rearmost tank trailer of the B-Train tank vehicle is compared to that of an equivalent rigid cargo vehicle. The effect of vehicle speed and steer angle on the dynamic response of the tank vehicle is also investigated. Table 5.4 summarizes the specifications of the tank vehicle used in the simulation.

The directional response of the rearmost semitrailer is computed for constant steer input of 2 degrees and vehicle speed of 50 km/h. The roll angle, lateral acceleration and roll rate response characteristics of the 100% and 50% filled tank trailers are compared to those of the equivalent rigid cargo trailers, as shown in Figures 5.27, 5.28 and 5.29 respectively. The overall sprung mass C.G. height of the equivalent rigid cargo semitrailer decreases when the fill level is reduced, consequently the magnitude of the roll angle, lateral acceleration and roll rate response decreases. The liquid load shift encountered due to partial fill in the tank, however, adversely influences the directional characteristics of the liquid cargo vehicle, as shown in Figures 5.27 thru 5.29. The vehicle combination carrying rigid cargo equivalent to 50% fill exhibits the lowest sprung mass roll and lateral acceleration while the 100% filled trailer exhibits the highest vehicle roll and lateral acceleration response. The 50% filled liquid cargo trailer, however, experiences dynamic response almost similar to that of a completely full trailer, due to the associated slosh forces arising from the liquid load shift. The 100% filled and the 50% filled rearmost trailer of the B-Train experience a steady state roll of approximately 1.65 degrees, while the trailer with rigid cargo equivalent to 50% fill reaches a steady state roll angle of approximately 1.2 degrees, as shown in Figure 5.27.

TABLE 5.4**SPECIFICATIONS OF THE B-TRAIN TANK VEHICLE USED IN THE SIMULATION**

<u>Tractor</u>	
Type:	Three Axle
Sprung Weight:	52486N (11800 lb)
Unsprung Weight (front axle):	5338N (1200 lb)
Unsprung Weight (rear axle):	11120N (2500 lb)
Front Axle Suspension Rating:	88960N (20000 lb)
Rear Axle Suspension Rating:	97856N (22000 lb)
Wheel Base:	4.42m (174 in)
Tare Centre of Gravity Height:	1.12m (44 in)
Roll Moment of Inertia:	2938 N.m.s ² (26000 lb.in.s ²)
Yaw Moment of Inertia:	19207 N.m.s ² (170000 lb.in.s ²)
Pitch Moment of Inertia:	19207 N.m.s ² (170000 lb.in.s ²)
<u>Semitrailer A</u>	
Type:	Tandem Axle
Sprung Weight (Empty):	51828N (11652 lb)
Unsprung Weight:	13344N (3000 lb)
Tank Length:	7.85m (309 in)
Tank Diameter:	2.03m (80 in)
Axle Rating:	97856N (22000 lb)
Weight Density (Fuel Oil):	0.0068N/cm ³ (0.0251lb/in ³)
Tare Centre of Gravity Height:	1.54m (60.79 in)
Roll Moment of Inertia:	9039 N.m.s ² (80000 lb.in.s ²)
Yaw Moment of Inertia:	11298 N.m.s ² (100000 lb.in.s ²)
Pitch Moment of Inertia:	11298 N.m.s ² (100000 lb.in.s ²)
<u>Semitrailer B (rear-most semitrailer)</u>	
Type:	Tandem Axle
Sprung Weight (Empty):	38813N (8726 lb)
Unsprung Weight:	13344N (3000 lb)
Tank Length:	7.60m (299 in)
Tank Diameter:	2.03m (80 in)
Axle Rating:	97856N (22000 lb)
Tare Centre of Gravity Height:	1.54m (60.79 in)
Roll Moment of Inertia:	9039 N.m.s ² (80000 lb.in.s ²)
Yaw Moment of Inertia:	11298 N.m.s ² (100000 lb.in.s ²)
Pitch Moment of Inertia:	11298 N.m.s ² (100000 lb.in.s ²)

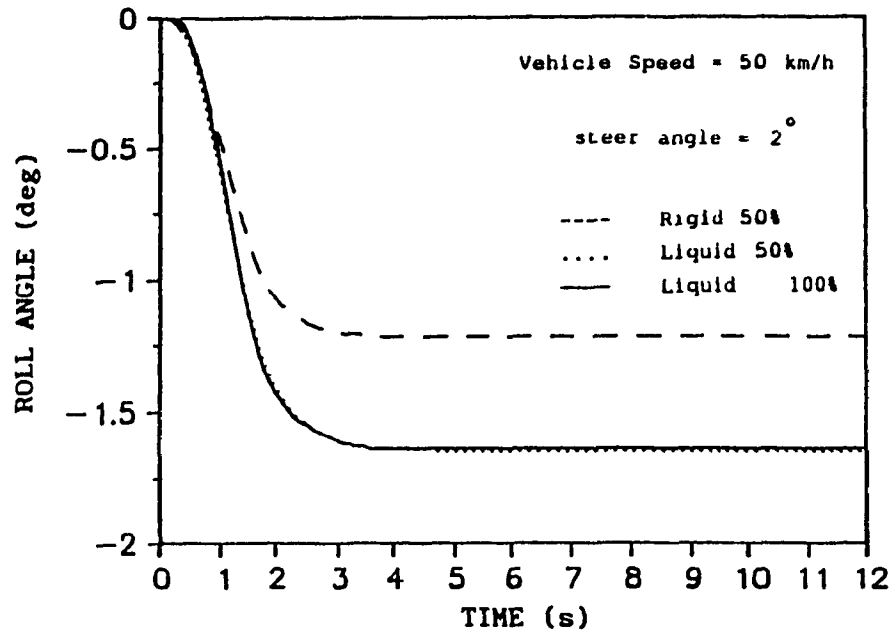


Figure 5.27 Roll response of semitrailer B of a 7-axle B-train with liquid and equivalent rigid cargo loads

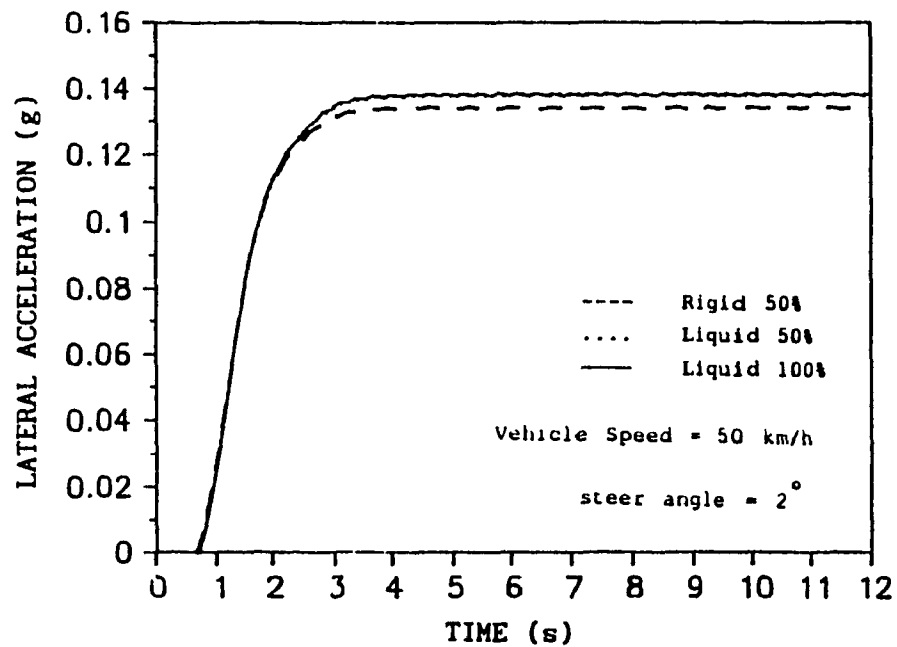


Figure 5.28 Lateral acceleration response of semitrailer B of a 7-axle B-train with liquid and equivalent rigid cargo loads

The steady state lateral acceleration response of the 50% fill equivalent rigid cargo is approximately 0.005g less than that of the 100% and 50% filled liquid cargo vehicles, as shown in Figure 5.28. The lateral acceleration response of the 50% filled liquid trailer is almost identical to that of the completely full trailer, under constant axle loading conditions. The peak roll rate corresponding to the completely full vehicle is approximately 1.28 deg/s compared to 1.18 deg/s in case of the 50% filled liquid tank vehicle and 0.8 deg/s in case of the equivalent rigid cargo vehicle, as shown in Figure 5.29.

Influence of Fill Level

The liquid load shift encountered within a partially filled tank is a function of the fill level. Thus, the dynamic response of the tank vehicle is strongly influenced by the fill level. The roll response characteristics of the rearmost semitrailer carrying industrial acid (fill level = 50%) and diesel oil (fill level = 75%), are compared in Figure 5.30 for a 2 degree constant steer input. The total payload is held constant for both the cargo. In case of rigid cargo vehicles, the rigid cargo equivalent to 75% fill yields considerably larger roll than that equivalent to 50% fill due to increased C.G. height. Although the C.G. height of the 50% filled tank vehicle is considerably lower than that of the 75% filled tank vehicle, the roll response of the two vehicles is identical. This is attributed to the increased lateral load shift within a 50% filled tank.

Influence of Front Wheel Steer Angle

The roll angle response of the semitrailer B with 50% filled liquid and equivalent rigid cargo is presented in Figure 5.31 for 2 and 4 degrees constant steer input. The roll angle of the trailer increases

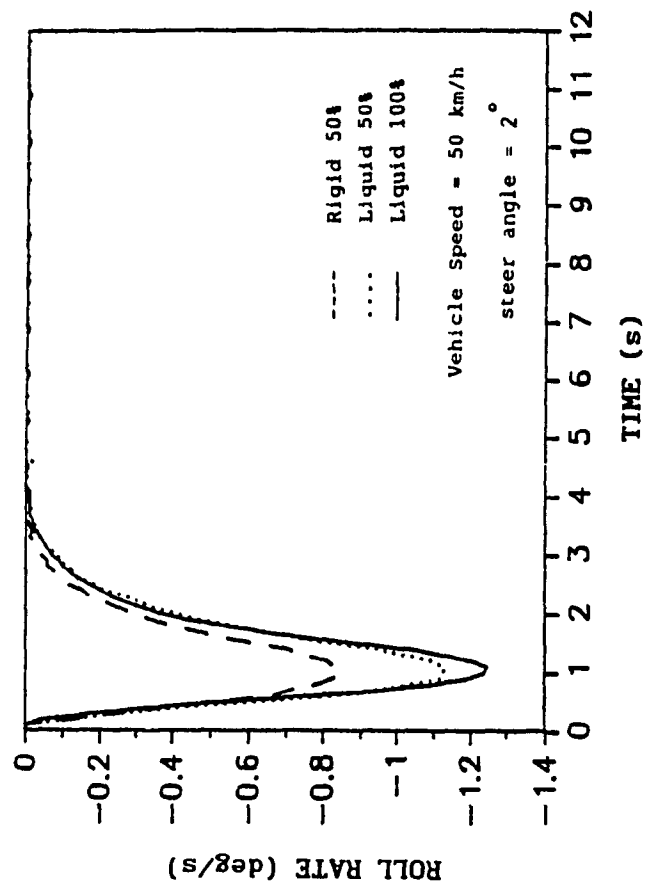


Figure 5.29 Roll rate response of semitrailer B of a 7-axle B-train with liquid and equivalent rigid cargo loads

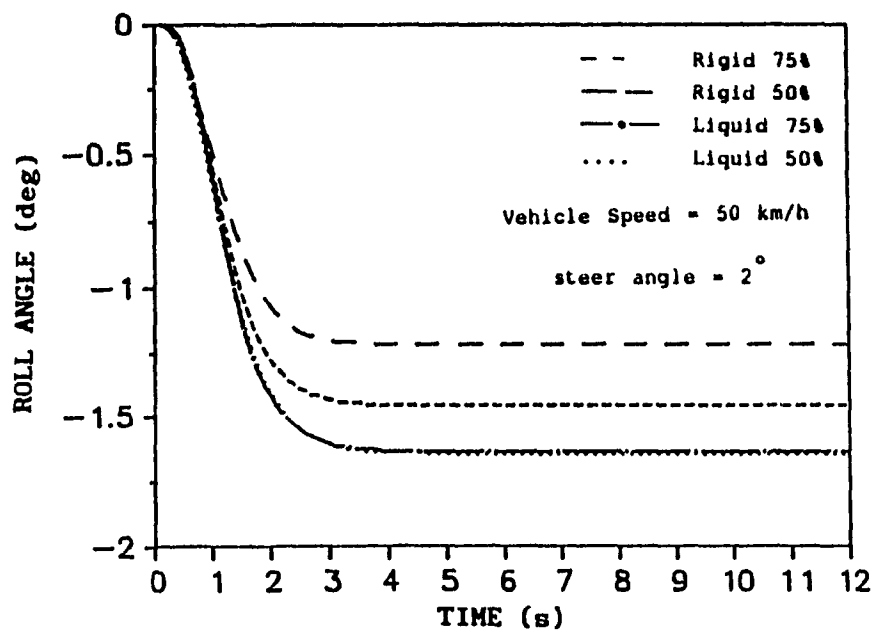


Figure 5.30 Roll response of semitrailer B of a 7-axle B-train with liquid and equivalent rigid cargo loads

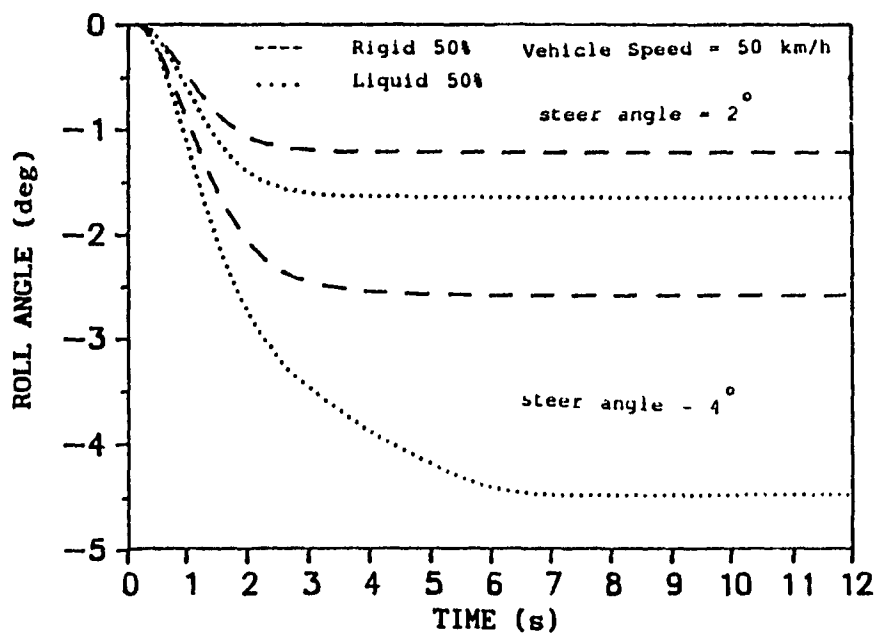


Figure 5.31 Roll response of semitrailer B of a 7-axle B-train with liquid and equivalent rigid cargo loads

with increase in the steer angle. A comparison of the roll angle response of the liquid and rigid cargo vehicle subjected to 2° constant steer input reveals that the liquid tank vehicle experiences approximately 0.5 degrees more roll while the difference in the roll response is approximately 2 degrees when the vehicle is subjected to a constant steer of 4° . The increased roll as well as the lateral acceleration response due to increased front wheel steer increases the centrifugal forces and hence the liquid load shift encountered during the constant steer manoeuvre.

Vehicle Path During a Constant Steer Manoeuvre

The unequal distribution of the vertical load on the tracks, arising from the lateral load shift, increases the cornering forces at the outer track of the vehicle leading to considerable deviation in the path of the tank vehicle, as shown in the Figure 5.32. Figure 5.32 presents the trajectories of the path followed by the 50% filled liquid and rigid cargo vehicles subjected to 4° constant steer at 50 km/h. A comparison of the paths followed by the liquid and rigid cargo vehicles reveals that the magnitude of path deviation diverges with time. The path followed by the tank vehicle deviates approximately 10 meters from that of the rigid cargo vehicle at the end of 12 seconds.

Influence of Vehicle Speed

The influence of the vehicle speed on the roll response characteristics of the tank vehicle combination is investigated for a steady steer input of 4 degrees. Figure 5.33 presents the roll response of 50% filled semitrailer B for different vehicle speeds. A comparison of the roll response of the 50% filled tank and an equivalent rigid cargo vehicle at a vehicle speed of 50 km/h subject to 4° steer input

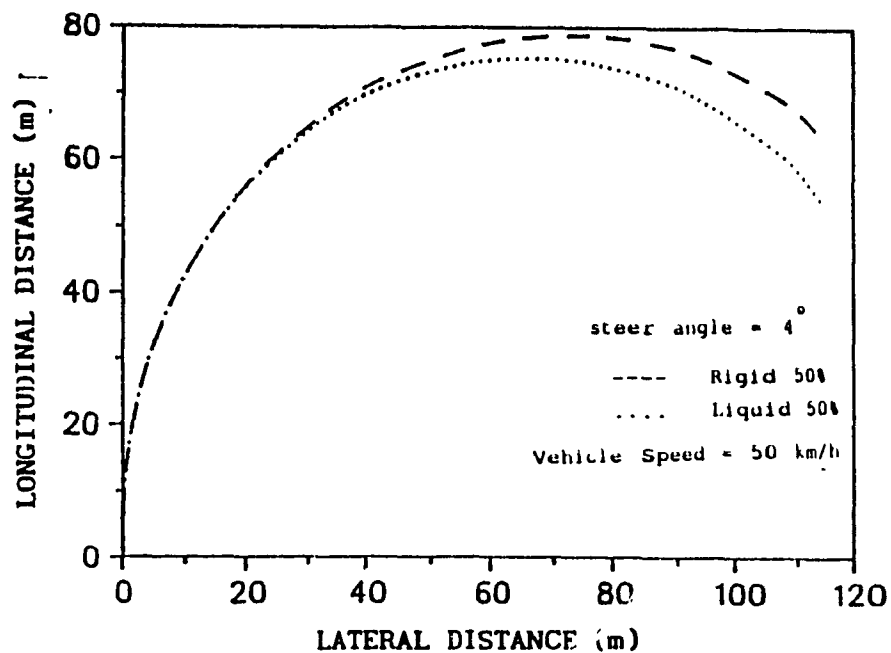


Figure 5.32 Comparison of vehicle path followed by a partially filled and an equivalent rigid cargo B-train tank vehicles

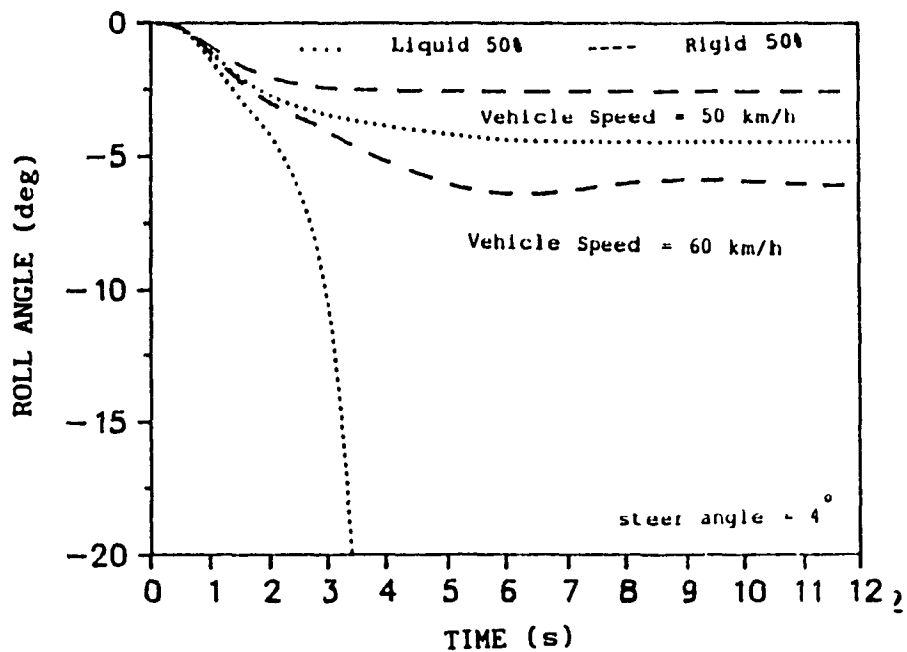


Figure 5.33 Roll response of semitrailer B of a 7-axle B-train with liquid and equivalent rigid cargo loads

shows that the liquid tank vehicle experiences approximately 2 degrees higher roll. The speed of the vehicle, however, when increased to 60 km/h, the partially filled tank vehicle approaches rollover, while the rigid cargo vehicle exhibits a stable roll response.

5.4.2 Closed-Loop Transient Steer Manoeuvre (Constant Axle Loads)

The directional response of the B-Train tank vehicle equipped with cleanbore circular tanks is investigated for typical highway manoeuvres, shown in Figure 5.13 using a "Driver Model" [1]. The front wheel steer angle required to follow the desired path is computed using the driver model. The directional response characteristics of the B-train tank vehicle are determined for typical highway manoeuvres and compared to those of an equivalent rigid cargo vehicle, while the axle loads are held constant.

5.4.2.1 Lane Change Manoeuvre

The directional response characteristics of the B-train tank vehicle are evaluated for a 3.6m (12 feet) lane change manoeuvre executed at a constant speed of 80 km/h. The roll angle and the lateral acceleration response characteristics of the rearmost semitrailer are presented in Figures 5.34 and 5.35 respectively. The fill level in the cleanbore tanks is varied by changing the weight density of the liquid cargo such that the axle loads are held constant. The roll angle and the lateral acceleration response characteristics of the 50% filled rearmost liquid trailer are compared to those of an equivalent rigid cargo and completely filled trailers, as shown in Figure 5.34 and 5.35. The peak roll angle response of the 50% equivalent rigid cargo vehicle is considerable smaller than that of the 100% filled tank trailer, due to low centre of gravity height of the cargo. The peak roll response of

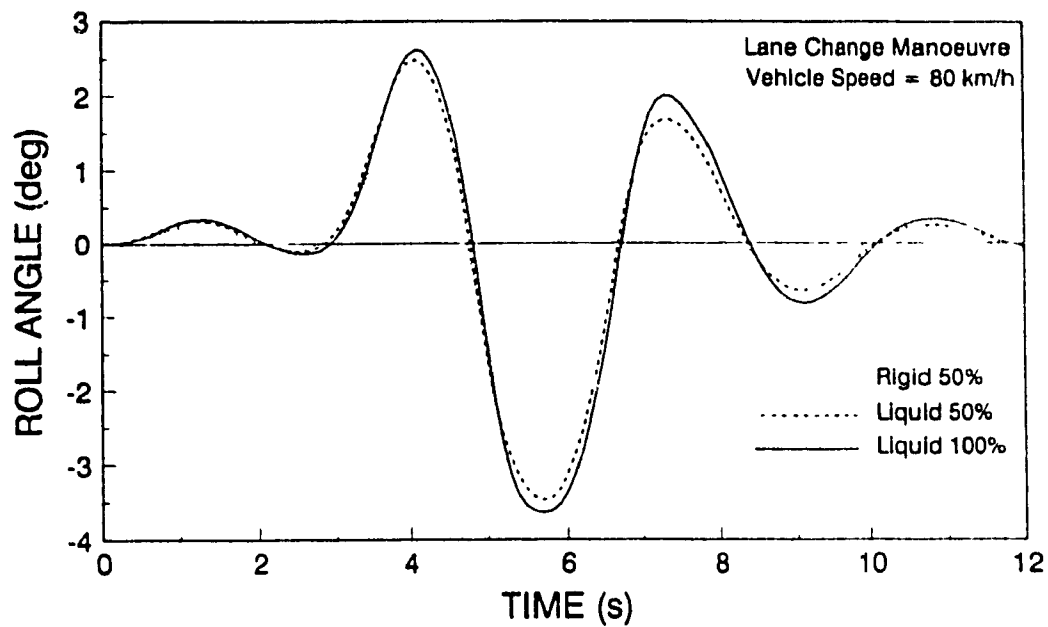


Figure 5.34 Roll response of semitrailer B of a 7-axle B-train with liquid and equivalent rigid cargo loads, during a lane change manoeuvre

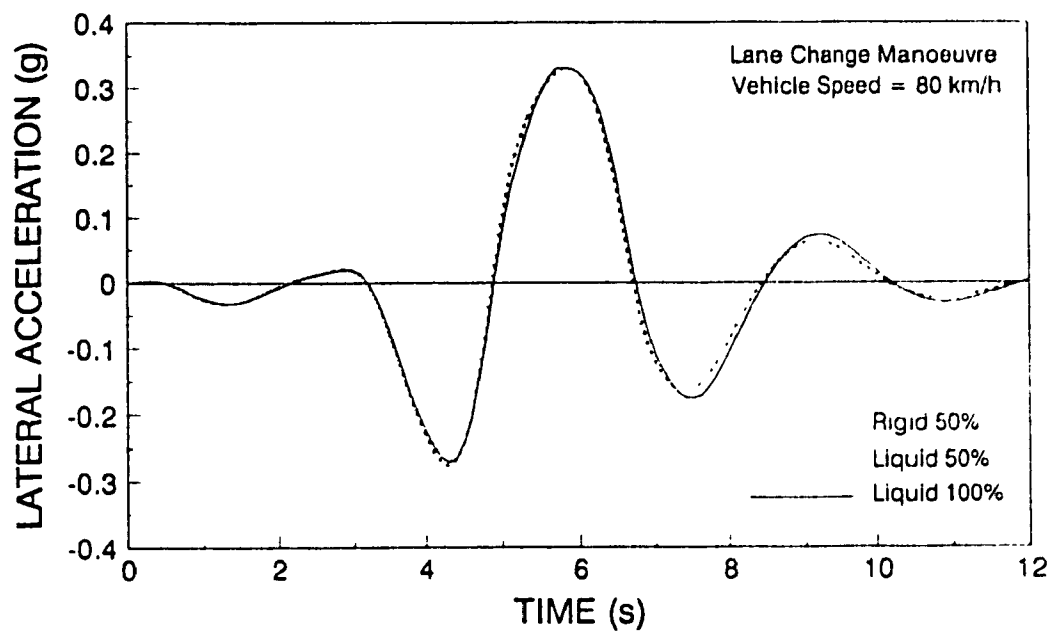


Figure 5.35 Lateral acceleration response of semitrailer B of a 7-axle B-train with liquid and equivalent rigid cargo loads, during a lane change manoeuvre

the 50% filled liquid trailer, however, approaches that of the 100% filled trailer due to the associated liquid load shift, as shown in Figure 5.34. The peak lateral acceleration response of all the trailers are observed to be identical during the lane change manoeuvre. The lateral acceleration response of the 50% filled liquid tank trailer, during the correction phase of the lane change manoeuvre, however, is approximately 0.03g higher than that of the equivalent rigid cargo trailer, and is comparable to that of fully loaded tank trailer, as shown in Figure 5.35.

Influence of Vehicle Speed

The directional response of B-train combination is computed for different vehicle speeds to investigate the influence of vehicle speed on the performance of the liquid tank vehicle. Figure 5.36 presents the roll response of 50% filled rearmost trailer when the vehicle is negotiating a lane change manoeuvre at 70 and 80 km/h. Figure 5.36 reveals that the peak roll response of the liquid tank vehicle increases from the 2.5 degrees to 3.5 degrees when the speed is increased from 70 to 80 km/h. The difference in the roll response between the rigid and liquid cargo vehicles also increases with the increase in the speed. The peak roll angle increases by approximately 0.5 degrees in case of the rigid cargo trailer while in case of the liquid tank trailer the increase is approximately 1.0 degree when the vehicle speed is increased from 70 to 80 km/h.

5.4.2.2 Evasive Manoeuvre

The directional performance of the B-train tank vehicle combination is investigated for an evasive or double lane change manoeuvre, as a function of fill level and vehicle speed. The variations in fill level

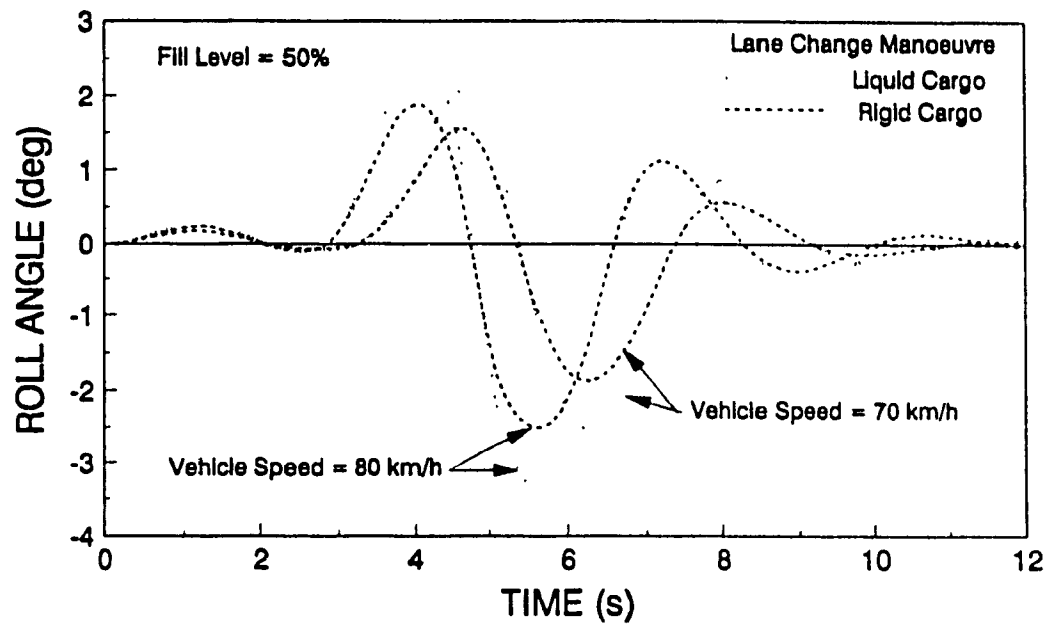


Figure 5.36 Roll response of semitrailer B of a 7-axle B-train with liquid and equivalent rigid cargo loads, during a lane change manoeuvre

are realized by varying weight density of the liquid cargo in order to retain constant axle loads. The roll angle and lateral acceleration response characteristics of a partially filled (50%) tank vehicle are compared to those of an equivalent rigid cargo vehicle. The dynamic response parameters of the partially filled tank vehicle are also compared to those of a completely full vehicle, under same axle loading conditions, as shown in Figures 5.37 and 5.38. The peak roll angle response of the rearmost trailer of the partially filled liquid tank vehicle is observed to be twice as large when compared to that of the equivalent rigid cargo vehicle as the vehicle makes the first lane change. The peak roll angle response of the rearmost trailer of completely full vehicle is identical to that of the partially filled liquid trailer. During the return to the original lane, the completely full vehicle experiences higher roll response on the rearmost trailer compared to the partially filled rearmost trailer of the liquid tank vehicle.

The lateral acceleration response of the rearmost trailer of the partially and completely filled liquid tank are compared to that of an equivalent rigid cargo in Figure 5.38. The lateral acceleration response of the tank vehicle and the completely full rigid cargo vehicle shows a large number of fluctuations while the 50% fill rigid cargo vehicle exhibits a smooth response during the evasive manoeuvre. The fluctuations in the lateral acceleration response are attributed to the wheel lift off encountered during the manoeuvre.

The relatively high lateral acceleration and roll angle encountered during the evasive manoeuvre increases the liquid load shift in case of the partially filled tank vehicle leading to wheel lift off. Figure

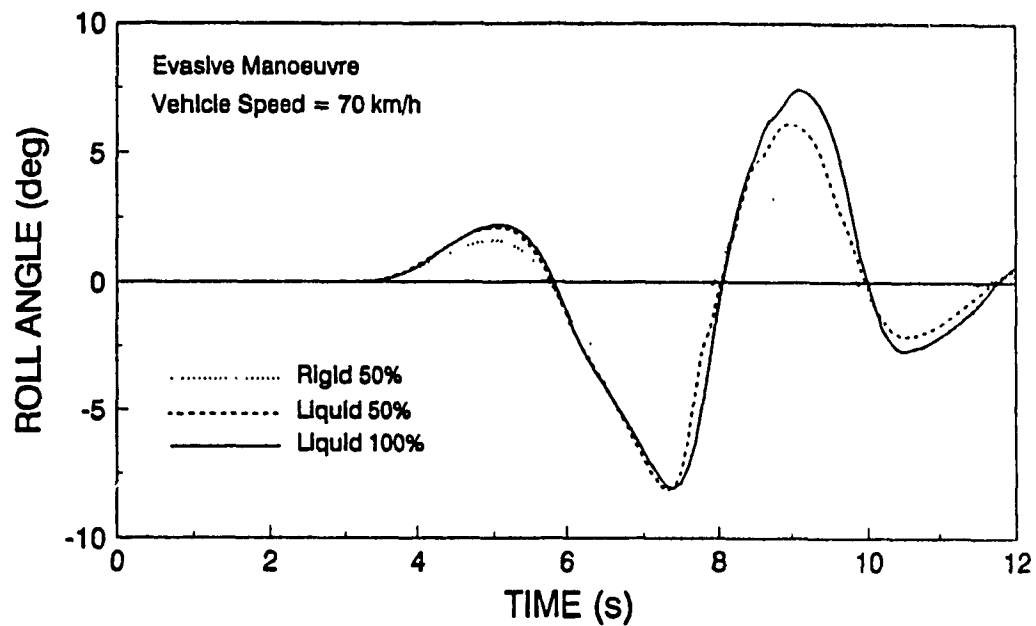


Figure 5.37 Roll response of semitrailer B of a 7-axle B-train with liquid and equivalent rigid cargo loads, during an evasive manoeuvre

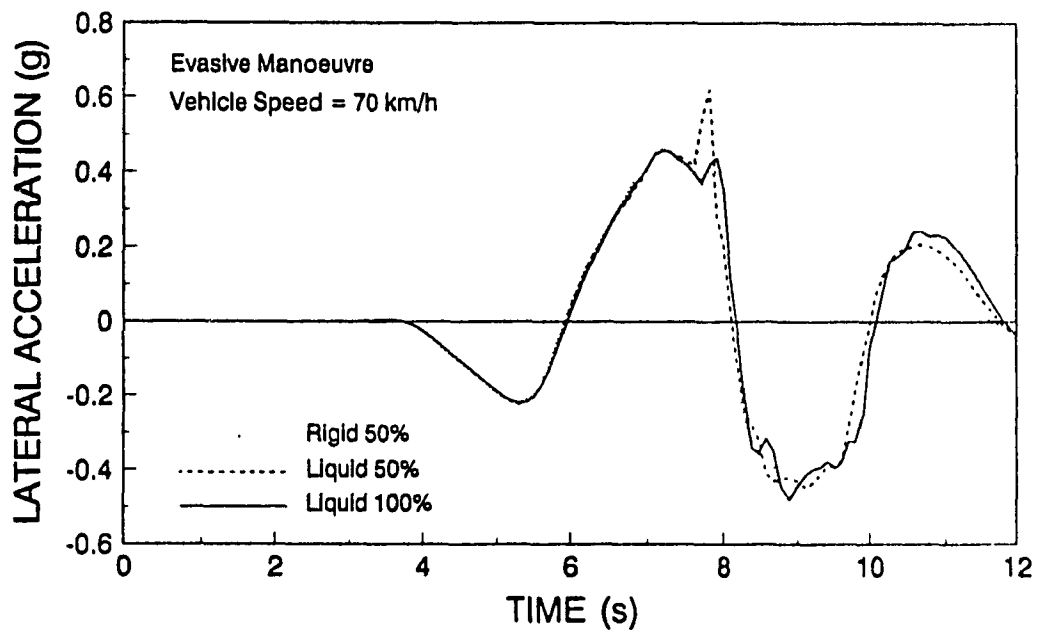


Figure 5.38 Lateral acceleration response of semitrailer B of a 7-axle B-train with liquid and equivalent rigid cargo loads, during an evasive manoeuvre

5.39 presents the dynamic vertical load ratio on the left track of the rearmost axle of the 50% full liquid and equivalent rigid cargo vehicles. The dynamic load on the left track of the rearmost axle for the rigid cargo vehicle reaches a low value of approximately 1.85 times the static load, while the liquid tank vehicle exhibits the wheel lift off on the right track for the duration 7.1 to 8.2 seconds. The left track of the last axle of the tank vehicle combination experiences wheel lift off for a brief period between 8.8 to 9 seconds, as shown in Figure 5.39. The entire axle load is transferred to the left track indicating that the wheels on the right track have lifted off. The rigid cargo vehicle never encounters the wheel lift off through out the manoeuvre and is quite stable compared to the liquid tank vehicle.

Influence of Vehicle Speed

The influence of the vehicle speed on the roll response of the tank vehicle during an evasive manoeuvre is shown in Figure 5.40. Figure 5.40 compares the roll response of 50% filled liquid and rigid cargo vehicles while negotiating the evasive manoeuvre at speeds of 70 and 80 km/h. The rigid cargo vehicle is stable at both the vehicle speeds though the peak roll angle response of the rearmost trailer increases from 4 to 7.5 degrees when the speed is increased from 70 to 80 km/h. The rearmost trailer of the liquid tank vehicle at 70 km/h experiences twice as much roll as compared to that of the rigid cargo vehicle. The speed, however, when increased to 80 km/h the liquid tank vehicle experiences large roll leading to rollover, as shown in Figure 5.40.

5.4.3 Roll and Lateral Acceleration Amplification

The impending rollover caused by the directional instabilities originating at the rearmost trailer is often not felt by the driver [3].

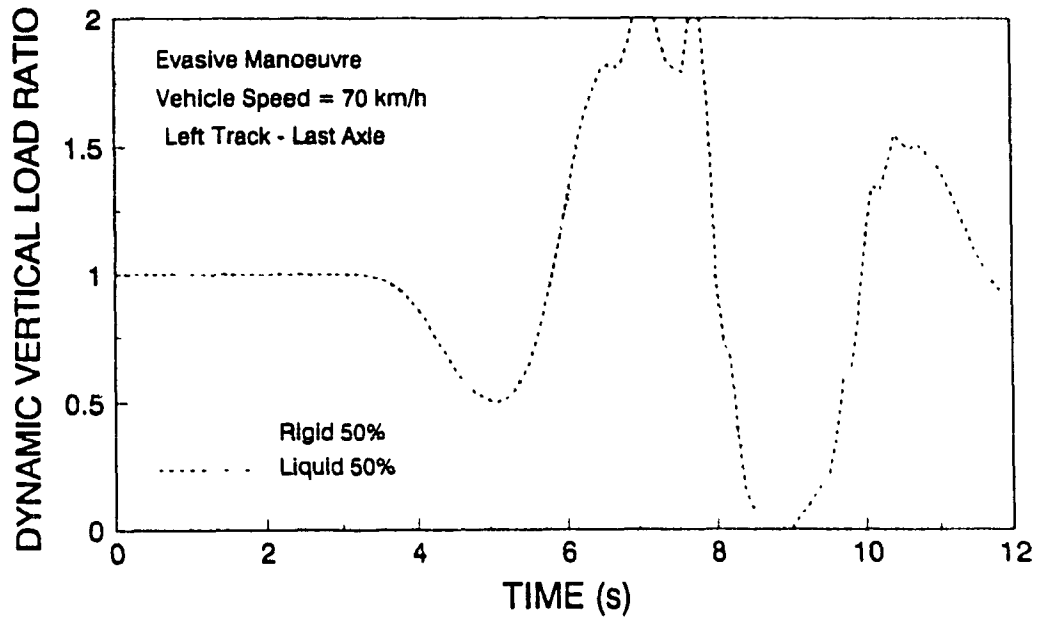


Figure 5.39 Dynamic vertical load ratio on the left track of the rearmost axle of a B-train tank vehicle, during an evasive manoeuvre

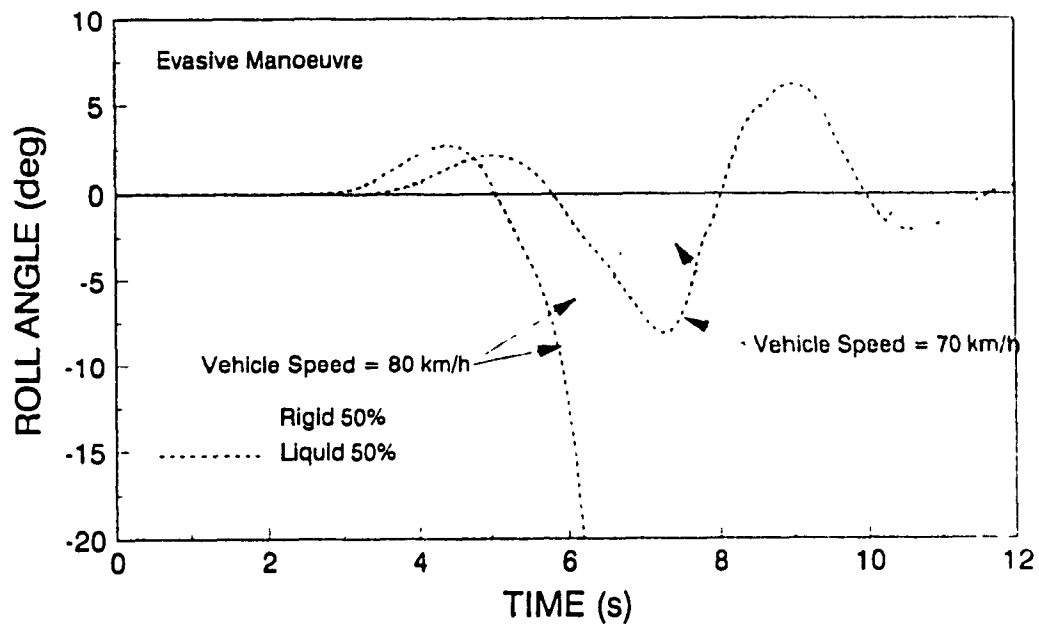


Figure 5.40 Roll response of semitrailer B of a 7-axle B-train with liquid and equivalent rigid cargo loads, during an evasive manoeuvre

Generally, the last trailer's response could change markedly without any detectable change in the directional response of the tractor [4]. The ratio of the directional response parameters of the rearmost trailer to those of the tractor are defined as the amplification factors. The roll and lateral acceleration amplification factors define the severity of impending rollover of the trailers.

Roll Amplification A_{θ} is defined by:

$$A_{\theta} = \frac{\text{peak roll angle response of the rearmost trailer } \theta_{sf}}{\text{peak roll angle response of the tractor } \theta_{s1}} \quad (5.2)$$

and lateral acceleration amplification A_a is given by:

$$A_a = \frac{\text{peak lateral acceleration response of the rearmost trailer } a_f}{\text{peak lateral acceleration response of the tractor } a_1} \quad (5.3)$$

Table 5.5 summarizes the roll and lateral acceleration amplification of the B-Train during lane change and evasive manoeuvres at various vehicle speeds. The roll and the acceleration amplification factors for the 50% rigid cargo vehicle are observed to be low while the liquid tank vehicle experiences higher amplification of the dynamic response parameters. During a lane change manoeuvre, the partially filled liquid tank vehicle exhibits amplification factors very close to the 100% fill vehicle due to the motion of the free surface of liquid leading to liquid load shift and increased roll moments. The high roll and lateral acceleration response of the tank vehicle leads to vehicle rollover, during an emergency type of manoeuvre.

5.5 Summary

The directional response characteristics of various candidate tank vehicle combinations, such as the five- and six-axle tractor semitrailer, and seven-axle B-train, are computed for constant and

TABLE 5.5

**ROLL AND LATERAL ACCELERATION AMPLIFICATION FACTORS FOR THE
B-TRAIN SUBJECTED TO LANE CHANGE AND EVASIVE MANOEUVRES AT VARIOUS
VEHICLE SPEEDS**

Manoeuvre	speed km/h	Amp. Factor	Fill Condition				
			Full 100%	Liquid 50%	Rigid 50%	Liquid 75%	Rigid 75%
EVASIVE MANOEUVRE	70	A_{θ}	1.27	1.23	1.21	1.27	1.27
		A_a	1.96	1.87	1.64	1.94	1.83
	80	A_{θ}	*	*	1.31	*	*
		A_a	*	*	1.57	*	*
LANE CHANGE	70	A_{θ}	1.21	1.22	1.17	1.21	1.19
		A_a	1.44	1.41	1.35	1.44	1.42
	80	A_{θ}	1.23	1.23	1.20	1.23	1.21
		A_a	1.64	1.62	1.56	1.64	1.62

* Indicates Vehicle Rollover

transient steer inputs. The directional response characteristics of the partially filled tank vehicles, are compared to those of the equivalent rigid cargo vehicles to demonstrate the adverse influence of liquid load shift.

Parametric sensitivity analyses are carried out to study the influence of tank cross-section, fill level, axle loads, and vehicle speed on the directional response of tank vehicle combinations. The magnitude of the load shift within a partially filled tank and hence the dynamic response of the tank vehicle strongly depends on the tank cross-section, fill level, vehicle speed, and steer input. The increase in vertical load on the outer track develops uneven cornering forces at the two tracks, leading to considerable deviation in the path of the liquid tank vehicle combination compared to that of the equivalent rigid cargo vehicle. The directional dynamic response of a tank vehicle equipped with a compartmented modified-oval tank is investigated as a function of the longitudinal load distribution.

The roll stability limits of partially filled tank vehicle combinations during an emergency or an obstacle avoidance type of manoeuvres at highway speeds are observed to be considerably lower than those of the rigid cargo vehicles. The excessive load shift occurring within the partially filled tank vehicle combinations yields wheel lift off and possible vehicle rollover, at typical highway speeds.

REFERENCES FOR CHAPTER 5

1. MacAdam, C.C., Application of an Optimal Preview Control for Simulation of Closed-Loop Automobile Driving, *IEEE Trans. on Systems, Man and Cybernetics*, Vol. 11, No. 6, pp 393-399, 1981.
2. Canadian Standards Association, "Highway Tanks and Portable Tanks for the Transportation of Dangerous Goods", CSA preliminary Standard B338-1982, March 1982.
3. Billing, A.M., Rollover Tests of Double Trailer Combinations, Ontario Ministry of Transportation and Communications Report No. TVS-CV-82-114, 1982.
4. Strandberg, L., Lateral stability of Road Tankers, VTI Rapport No. 138A, Sweden, Vol. 1, 1978.

CHAPTER 6

DYNAMIC STABILITY ANALYSIS OF LIQUID TANK VEHICLES SUBJECTED TO LIQUID SLOSH FORCES

6.1 General

The directional dynamic model of the tank vehicle, developed in Chapter 4, integrates a kineto-static fluid motion model of the partially filled tank, where the slosh forces are estimated assuming inviscid fluid motion and negligible fluid-vehicle interactions. The influence of the fundamental slosh frequency on the directional performance of vehicle is neglected by assuming the fundamental slosh frequency to be quite high in relation to the steer frequency. Such a tank vehicle model can provide considerable insight to the directional stability and performance in view of the lateral liquid load transfer, caused by the liquid slosh forces.

Research investigation on the dynamics of liquid tank vehicles indicate that the directional stability of partially filled tank vehicles are strongly related to the dynamic slosh loads and fluid-vehicle interactions [1]. It is further speculated that the directional dynamics of the tank vehicle is also influenced by the fundamental slosh frequency. Thus, it is essential to develop the directional dynamic model of the vehicle incorporating a dynamic fluid slosh model in order to gain an understanding of the vehicle's stability and directional response behaviour in view of the fundamental slosh frequency, dynamic slosh loads, and fluid-vehicle interactions.

In this chapter, a brief review of past investigations on the subject of fluid slosh and tank vehicle stability is presented. A comprehensive directional dynamic model of the tank vehicle is

formulated by integrating a two-dimensional non-linear fluid slosh model of a partially filled cylindrical tank [2] to the three dimensional vehicle model. The two-dimensional fluid slosh model formulates the non-linear equations of motion of the liquid within the tank, subjected to the acceleration input from the vehicle. The equations are solved in an Eulerian mesh in terms of the non-dimensional variables. The fundamental slosh frequency, and dynamic slosh forces and moments are computed for various fill levels. The dynamic forces and moments at every instant in time are then incorporated into the vehicle model to study the dynamic stability and the directional performance of the tank vehicle.

The directional performance characteristics of the tank vehicle, incorporating the dynamic liquid slosh model are compared to those of the vehicle incorporating the steady state liquid model, in order to demonstrate the influence of dynamic slosh forces on the vehicle stability.

6.2 Survey of Past Investigations on Dynamic Behaviour of Liquid within a Moving Vehicle

The liquid slosh within a tank is quantified primarily by the slosh frequencies and the magnitude of slosh forces. The fundamental or natural slosh frequency of the liquid within a container is a function of a number of tank parameters and liquid properties. Lamb [3] was the first to analytically obtain the fundamental transverse natural frequency of a 50% filled horizontal cylindrical tank, expressed by:

$$\omega_n = 1.169 \sqrt{g/D} \quad (6.1)$$

where ω_n is the fundamental slosh frequency, g is the acceleration due to gravity and D is the diameter of the tank. The fundamental slosh

frequency of the liquid, however, varies with the fill level. The analytical model, proposed by Lamb [3], is unable to compute the fundamental frequencies for fill levels other than 50%.

The relationship between the liquid fill and the fundamental natural frequency of the liquid was established by Budiansky [4]. The study concluded that the fundamental natural frequency of the liquid increases slowly and monotonically with increase in fill level for fill levels less than 60%, while it increases progressively faster for higher fills. The natural frequency associated with the second mode of oscillation has been observed to be at the minimum for 50% fill and increases when the fill level is either increased or decreased. The natural frequencies associated with first and second modes of oscillation are presented in Figure 6.1, for varying fill levels in a partially filled horizontal cylinder subjected to transverse disturbances [4]. The computation of the natural frequencies assumed linear theory of sloshing. The normalized frequency, K presented in Budiansky's plot is related to the slosh frequency by the relationship:

$$\omega_n = K \sqrt{g/R}$$

where g is the acceleration due to gravity and R is the tank radius.

Hutton [5] developed the fluid slosh frequencies assuming linear velocity potential and non-viscous flow. Therefore, the results may be sufficiently accurate for small amplitude oscillations, as confirmed by the experiments conducted by McCarty and Stephens [6].

The linear fluid theory, however, fails to predict the frequencies and the amplitude of sloshing, during an intense fluid oscillation. The study of sloshing behaviour of liquids within moving containers requires complex modelling and analysis. Abramson [7] investigated the dynamic

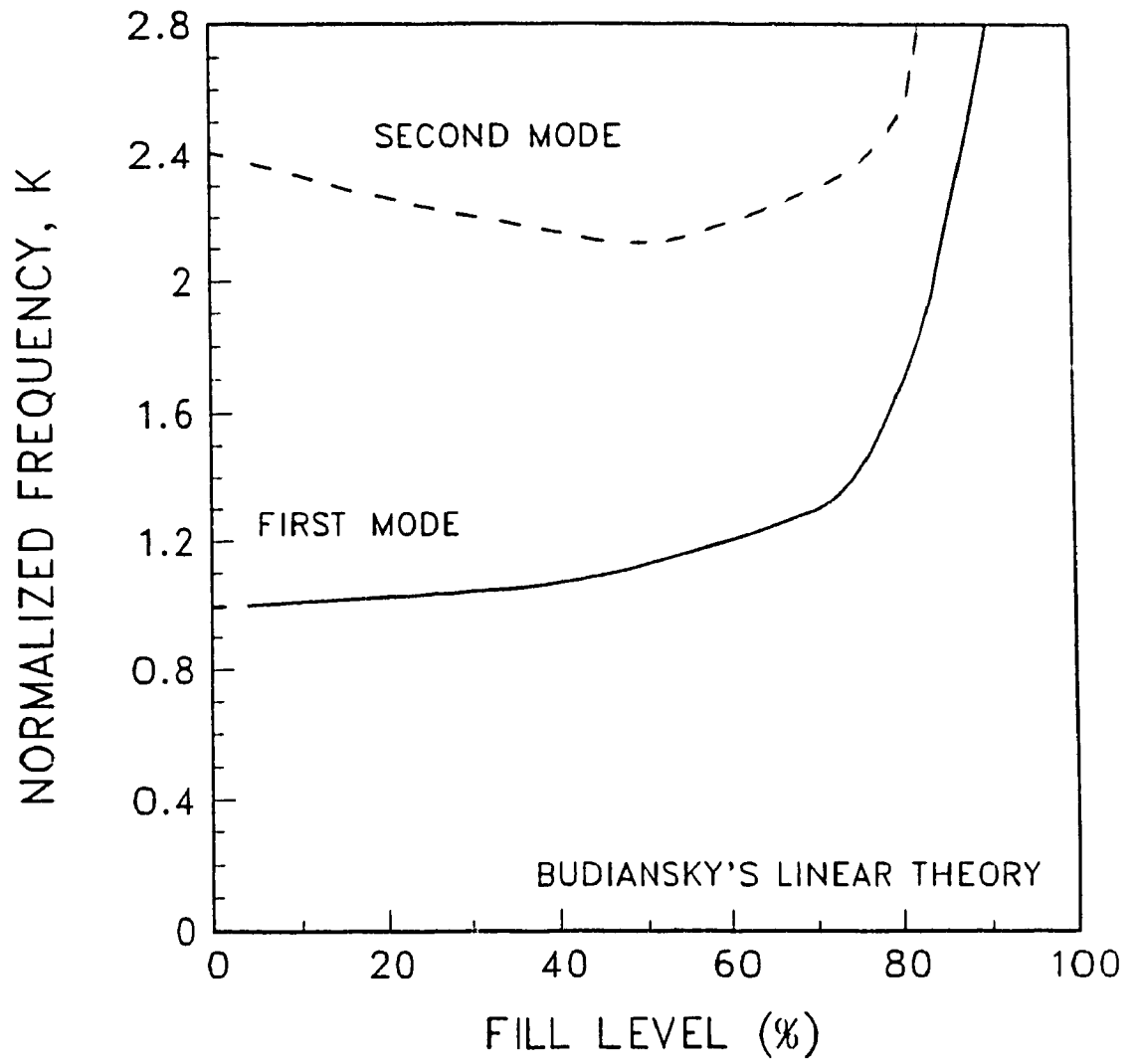


Figure 6.1 Natural frequency of liquid as a function of fill condition within a cylindrical tank cross-section

liquid slosh within the tanks of spacecrafts and established the slosh frequencies, mode shapes, and forced response characteristics, for various tank configurations. The model uses a linear theory in order to represent the slosh forces through an equivalent mechanical model. The liquid forces along various directions within the tank are computed by integrating the pressure distribution at the container walls. Bauer [1] investigated the longitudinal and lateral forces due to the liquid slosh within the tank and concluded that these forces can lead to decreased stability of the vehicle and increased stresses on the tank structure.

Slibar and Troger [8] studied the dynamics of the liquid tank vehicle using an equivalent single degree of freedom mechanical oscillator to simulate the liquid slosh forces. A simplified tank vehicle model was developed neglecting roll and yaw motion by Strandberg [9]. The simplified tank vehicle model was used to investigate the influence of liquid slosh behaviour on the skidding and overturning tendency of the vehicle [9]. The investigations were based on experimentally measured slosh forces on laterally oscillated scale model tanks having dynamic similarity with actual tanks.

The effects of sloshing liquid cargo on the dynamic performance of the liquid tank vehicle was investigated assuming small amplitude oscillations of the liquid within an elliptical tank [10]. The equations of motion for sloshing fluid were derived using Lagrange's equation assuming irrotational fluid flow conditions. The directional performance of the tank vehicle may deteriorate considerably when the slosh frequency is in the vicinity of the steer frequency. The steer frequency, corresponding to a rapid lane change or an obstacle avoidance manoeuvre lie below 0.2 Hz. The fundamental slosh frequency of the

liquid in tanks with extremely low fill levels may coincide with the steering frequency during an emergency type of manoeuvre leading to resonant slosh forces and thus possible loss of vehicle's directional stability.

A numerical solution procedure of the non-linear liquid motion in a horizontal cylindrical container excited by the lateral acceleration has been developed by Popov et al [11]. The 2-dimensional governing equations are discretized in an Eulerian mesh and solved with respect to non-dimensional primitive parameters. The model is capable of generating dynamic slosh forces and moments, velocity and pressure distributions within the tank, and the gradient of the fluid free surface, for a given acceleration input.

The references cited above either lacked in complete representation of the slosh forces within the partially filled tank or a comprehensive integration of the vehicle dynamics and liquid slosh. A comprehensive tank vehicle model is realized by integrating the fluid slosh model to the three-dimensional vehicle model developed in chapter 4. The methodologies associated with model development and simulation are discussed in the following sections.

6.3 Development of the Tank Vehicle Model

An articulated tank vehicle, equipped with a cleanbore cylindrical tank cross-section is modeled in order to simulate the directional response of the vehicle subjected to liquid slosh forces and moments. The 2-dimensional liquid slosh model of circular tank cross-section is integrated to the yaw/roll model of the tank vehicle, assuming constant vehicle speed. Although the computer model is capable of simulating any vehicle combinations with a maximum of 4 units and 11 axles, simulations

have been carried out only for a 5-axle tractor tank semitrailer vehicle equipped with a cleanbore cylindrical tank. The yaw/roll model, developed in Chapter 4, is modified in order to integrate it with the liquid slosh model.

6.3.1 Development of the Liquid Slosh Model [11]

The non-linear sloshing problem is solved by using the finite difference method. The slosh model is developed using a modified Marker and Cell method [11]. The modifications to the conventional Marker and Cell method concern a special treatment of the boundary conditions, which are computed from the extrapolation along the directions normal to the boundaries. The free surface heights are corrected in accordance with the initial volume of liquid. The tank is discretized in an Eulerian mesh and the system of coordinates and the mesh arrangements are presented in Figure 6.2. The Navier-Stokes equations describing the fluid flow within the tank along with the free-surface equations and the boundary conditions are given by [11]:

$$St \frac{\partial v}{\partial T} + \frac{\partial v^2}{\partial Y} + \frac{\partial vw}{\partial Z} = \frac{G_y}{Fr} - Eu \frac{\partial P}{\partial Y} + \frac{1}{Re} \left[\frac{\partial^2 v}{\partial Y^2} + \frac{\partial^2 v}{\partial Z^2} \right] \quad (6.2)$$

$$St \frac{\partial w}{\partial T} + \frac{\partial w^2}{\partial Z} + \frac{\partial vw}{\partial Y} = \frac{G_z}{Fr} - Eu \frac{\partial P}{\partial Z} + \frac{1}{Re} \left[\frac{\partial^2 w}{\partial Y^2} + \frac{\partial^2 w}{\partial Z^2} \right] \quad (6.3)$$

$$\frac{\partial v}{\partial Y} + \frac{\partial w}{\partial Z} = 0 \quad (6.4)$$

$$\left. \begin{array}{l} St \frac{\partial H}{\partial T} = v - w \frac{\partial H}{\partial Y} \\ P = P_0 \end{array} \right\} \text{on the free surface} \quad (6.5)$$

where v and w are the non-dimensional lateral and vertical velocities, G_y and G_z are the non-dimensional accelerations along the Y and Z axes

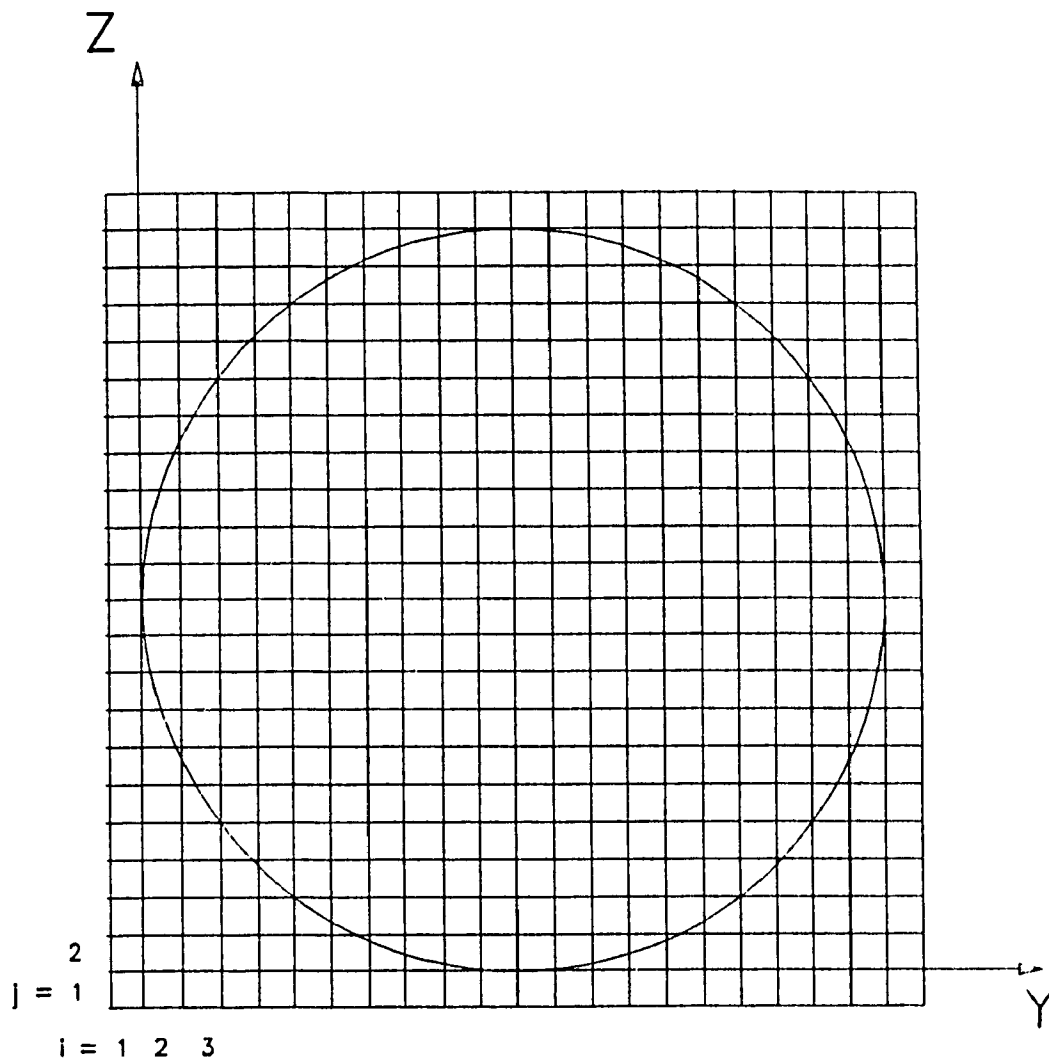


Figure 6.2 Coordinate system and mesh arrangement of a circular tank cross-section

respectively. P is the fluid pressure, P_0 is the pressure on the free surface or the atmospheric pressure, and H is the height of liquid. The various fluid flow numbers are given by the following equations:

$$\text{St, the Strouhal number} = \frac{L_0}{T_0 W_0}$$

$$\text{Fr, the Froude number} = \frac{W_0^2}{g L_0}$$

$$\text{Eu, the Euler number} = \frac{P_0}{\rho W_0^2}$$

$$\text{Re, the Reynolds number} = \frac{L_0 W_0}{\nu}$$

and

$$G_y = \frac{a_y}{g}, \quad G_z = \frac{a_z}{g}, \quad v = \frac{\bar{v}}{W_0}, \quad w = \frac{\bar{w}}{W_0}, \quad X = \frac{\bar{X}}{L_0}, \quad Y = \frac{\bar{Y}}{L_0}$$

$$H = \frac{\bar{H}}{L_0}, \quad P = \frac{\bar{P}}{P_0}, \quad T = \frac{\bar{T}}{T_0}$$

where a_y , a_z are the vehicle accelerations along the Y and Z axes and all the quantities with bar correspond to the dimensional form of the various position, velocity, pressure, and time parameters and

L_0 = characteristic length or the length of the tank;

$$T_0 = \sqrt{L_0 / g}, \text{ the characteristic time;}$$

$$W_0 = \sqrt{g_z / L_0}, \text{ the characteristic velocity;}$$

ρ = mass density of the liquid;

ν = kinematic viscosity of the liquid

The entire circular cross-section is subdivided in the Y-Z plane into a number of equi-spaced, and equal sized cells. The differential equations are solved using a finite difference method in order to obtain the non-dimensional parameters. The boundary conditions on the wetted wall are defined either from the free-slip or no-slip conditions:

- (i) The normal velocities are zero on the the wetted wall for free-slip condition. There exists a finite velocity at the wall along the tangential direction for free-slip condition; and,
- (ii) the normal and the tangential velocities are zero on the wetted wall, for no-slip condition.

The Navier-Stokes equation can be solved under both no-slip and free-slip conditions, the transition between the no-slip to free-slip condition depends on the Reynold's number. Since the differential equations are solved in the non-dimensional region, the obtained results are true to all geometrically similar class of problems for which the Strouhal, Froude, Euler and Reynold's numbers remain identical. The differential equations are then solved using discretization by forward differences in time and by central differences in space, the upstream differencing was used to neutralize the computational instability and the over-relaxation to increase the convergence of the iterative procedure. The region of flow of liquid is subdivided into three groups of cells: completely filled, partially filled and the empty cells. The upper layer of full cells and the lower layer of the bottom cells bound the flow domain from top to bottom. The cell (i,j) is considered to be interior or a full one, if its velocities v_{ij} and w_{ij} are lying in the flow domain. If at least one of the velocities is outside the flow domain then the cell is considered exterior. The equations of motion are solved only over the interior cells domain. The fluid forces are computed by integrating the pressure distribution along the wetted wall, separately in the horizontal and vertical directions. The overturning moment about the tank base is computed from the force components and their location. The complete solution procedure along with the boundary

conditions are presented in the reference [11].

The fluid tank when accelerated, the velocities, pressure, fluid height and forces undergo an oscillatory motion with certain frequency dictated by the geometry of the tank, properties of the fluid and the excitation. The solution of the fluid equations provide the instantaneous slosh forces and moments which is then integrated to the vehicle model in order to compute the dynamic response of the tank vehicle.

6.3.2 Dynamic Model of the Tank Vehicle

A five-axle articulated tank vehicle is modeled to compute the dynamic response of the vehicle subjected to the liquid slosh forces and moments. The yaw/roll model developed in Chapter 4 is modified in order to use it in conjunction with the fluid slosh model. The tractor-semitrailer tank vehicle is modeled as two sprung masses: the sprung mass of the tractor, m_1 ; the tare mass of the semitrailer tank structure and the empty tank, m_2 . The liquid mass m_{lf} ($f = 2$) is modeled as a floating mass with respect to the semitrailer sprung weight. The axles are modeled as independent unsprung masses m_{ui} ($i = 1, \dots, 5$). The sprung weights are treated as rigid bodies with five degrees of freedom: lateral, vertical, yaw, roll and pitch. The unsprung weights are free to roll and bounce with respect to the sprung weights to which they are attached. The slosh forces and moments from the liquid mass are computed from the slosh model in the roll plane of the tank vehicle. The inertias of the liquid mass in the pitch and the yaw planes are assumed to remain constant during the simulation. The roll moment due to the liquid motion is computed from the new C.G. of liquid mass, while the inertial components in the roll plane are

evaluated from the fluid slosh model. The set of differential equations representing the equations of motion of the sprung mass, derived in Chapter 4 (Equations 4.6 to 4.10) are modified in order to account for the slosh forces and moments, evaluated from fluid slosh model.

6.4 Equations of Motion

Lateral Force Equations:

$$m_f \vec{a}_f \vec{j}_{sf} = (\text{Lateral component of Constraint Forces}) + \\ (\text{Lateral component of Suspension Forces}) + (m_f + m_{lf})g\theta_{sf} + F_{yf} \quad (6.6)$$

Vertical Force Equations:

$$m_f \vec{a}_f \vec{k}_{sf} = (\text{Vertical component of Constraint Forces}) + \\ (\text{Vertical component of Suspension Forces}) + m_f g + F_{zf} \quad (6.7)$$

Roll Moment Equations:

$$(I_{xf} + I_{xlf}) \dot{p}_f - (I_{yf} + I_{ylf} - I_{zf} - I_{zlf}) q_f r_f = \\ (\text{Roll Moments from Constraints}) + (\text{Roll Moments from Suspensions}) \\ + OM_f + m_{lf} g (\theta_{sf} Z_{lf} + Y_{lf}) \quad (6.8)$$

Pitch Moment Equations:

$$(I_{yf} + I_{ylf}) \dot{q}_f - (I_{zf} + I_{zlf} - I_{xf} - I_{xlf}) p_f r_f = \\ (\text{Pitch Moments from Constraints}) + (\text{Pitch Moments from Suspensions}) \\ - F_{zf} X_{lf} - m_{lf} g (X_{lf} + \alpha_{sf} Z_{lf}) \quad (6.9)$$

Yaw Moment Equations:

$$(I_{zf} + \sum_{i=N}^{N_2} I_{zui} + I_{zlf}) \dot{r}_f - (I_{xf} + I_{xlf} - I_{yf} - I_{ylf}) p_f q_f =$$

(Yaw Moments from Constraints) + (Yaw Moments from Suspensions)

$$- F_{yf} X_{lf} \quad (6.10)$$

where $f = 1, 2$ and

$$N_1 = \begin{cases} 1 \\ 4 \end{cases}; \quad N_2 = \begin{cases} 3 \\ 5 \end{cases}; \quad \text{for } f = \begin{cases} 1 \\ 2 \end{cases} \quad (6.11)$$

F_{yf} and F_{zf} are the horizontal and vertical slosh forces, respectively and OM_f is the overturning slosh moment about the trailer sprung weight C.G. The slosh forces and the moments vanish for the tractor unit ($f = 1$) due to the absence of the liquid cargo. The derivation of the suspension forces, roll centre forces, tire forces, and the constraint forces are presented in detail in Appendix II. The mass matrix is modified in order to account for the slosh forces and moments based on equations (6.6) to (6.10). Equations of motion are solved using a numerical integration method to yield the directional response characteristics of the 5-axle tractor semitrailer vehicle for a dynamic manoeuvre of the vehicle.

6.5 Method of Solution

The solution procedure is initiated by solving the differential equations of motion describing the yaw/roll dynamics of the vehicle via numerical integration. Equation (4.36) is solved for a small increment in time for a given steer input, say from $t = 0.0$ to $t = \Delta t$ to compute the tank roll and the lateral acceleration at the end of the time period. The lateral and vertical acceleration of the tank along the

sprung mass coordinates are transformed to non-dimensional accelerations g_y and g_z along the tank axes. The accelerations are then incorporated to the fluid slosh model to compute the slosh forces and moments. The acceleration of each cell in the dynamic fluid slosh tank model is computed from the coordinates of the cell in the tank axis system and the roll velocity of the semitrailer. Equations (6.2) to (6.5) are then solved using the finite difference scheme for the time interval, $0 < t < \Delta t$, and the corresponding slosh forces and moments at the end of the time period are evaluated. The non-dimensional force and moment quantities are then transformed to obtain the magnitude of actual slosh forces and moments. The slosh forces and moments are then incorporated into the vehicle model in order to compute the directional response of the tank vehicle for the following time step. The free surface of the liquid in the slosh model is kept frozen while the vehicle response calculations are performed. The directional response quantities of the vehicle model are then transmitted to the slosh model in order to march on to the next time step. Thus the vehicle response for a given dynamic manoeuvre is obtained using a sequential procedure incorporating the slosh forces and moments, as shown in Figure 6.3.

6.6 Directional Response of the Tank Vehicle

The directional response of a five-axle tractor semitrailer liquid tank vehicle equipped with a cleanbore cylindrical tank is investigated for typical highway manoeuvres. The simulation results are then compared to those obtained using the steady state fluid model, derived in Chapter 4. The response simulations are carried out for both steady and transient steer inputs under constant axle loading conditions. The influence of the tank fill on the slosh behaviour of the liquid within

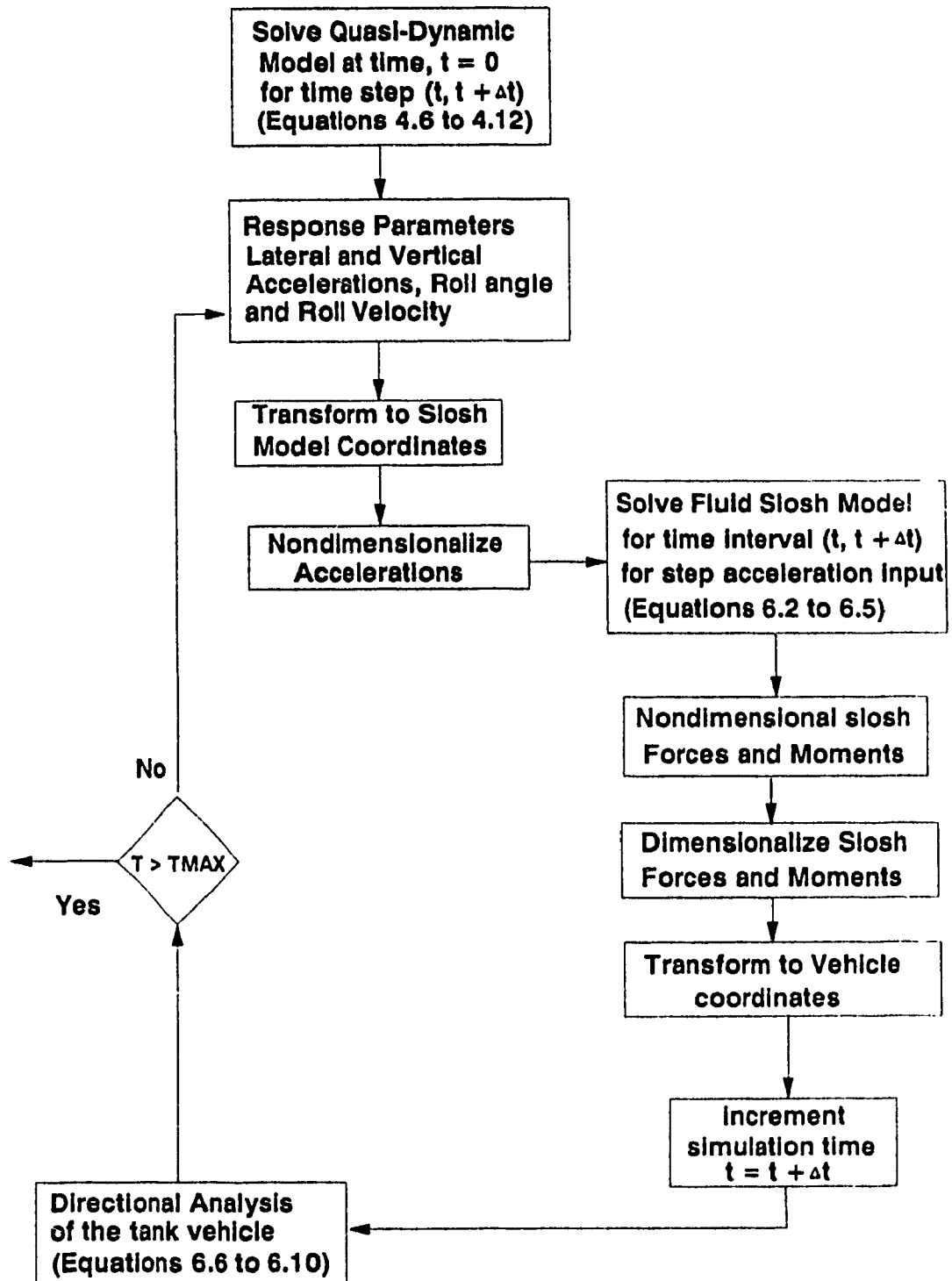


Figure 6 3 Computation of the directional response of a tank vehicle

the partially filled tank vehicle is investigated keeping the axle loads constant.

6.6.1 Constant Steer Manoeuvre

The directional response characteristics of the tank vehicle equipped with a cleanbore cylindrical tank, is investigated for constant steer input. The dynamic slosh forces and moments arising within the partially filled tank is computed using the dynamic fluid slosh model. The slosh behaviour of the liquid within the tank is influenced by the fill level, liquid properties, tank cross-section and the lateral acceleration imposed on the liquid. The cylindrical tank is partially filled with fuel oil of weight density = 0.0068 N/cm^3 (0.025 lb/in^3). The fill levels within the tank are altered by changing the weight density of the fluid carried such that the payload remains constant.

Computer simulations are carried out to determine the directional response of the tank vehicle subject to 2 degrees constant steer input at a constant vehicle speed of 60 km/h. The roll response of the 70% filled tank vehicle subjected to the liquid slosh forces is compared to that of the tank vehicle model employing the quasi-dynamic model, as shown in Figure 6.4. The roll response of the quasi-dynamic model reaches a steady state value of 1.71 degrees. The roll response of the sprung mass incorporating dynamic fluid slosh model, however, exhibits damped oscillation due to the oscillations of the fluid within the partially filled tank. The fluid oscillates at its fundamental mode of vibration around a mean value of 1.52 degrees. The frequency of oscillation of the roll response of liquid tank vehicle is approximately 0.67 Hz. The oscillation frequency lies close to the value derived using the linear approximation theory (Figure 6.1) [4]. The amplitude

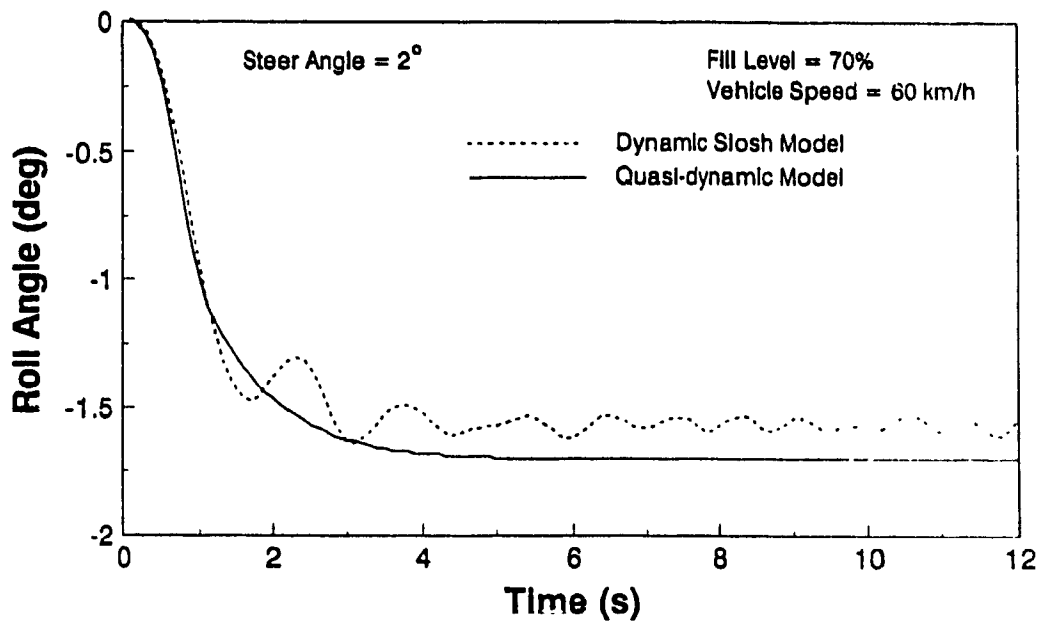


Figure 6.4 Comparison of roll response of dynamic slosh and quasi-dynamic tank vehicle models

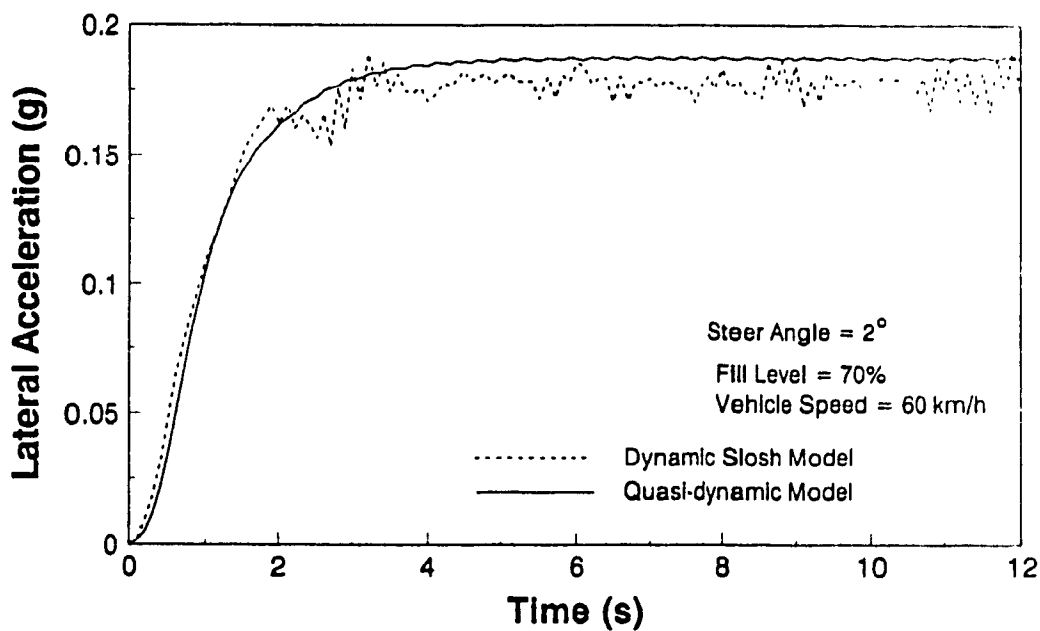


Figure 6.5 Comparison of lateral acceleration response of dynamic slosh and quasi-dynamic tank vehicle models

of roll oscillation decreases gradually with the simulation time. Figure 6.4 also reveals that there is an overestimation of the roll response of the tank vehicle when a quasi-dynamic model is utilized. This can be attributed to the fact that the vehicle employing quasi-dynamic model computes the acceleration of the liquid C.G. and the corresponding translation of liquid C.G using the three-dimensional vehicle model while a two-dimensional roll plane model is employed in case of the fluid slosh model.

The lateral acceleration response of the tank vehicle incorporating the dynamic fluid slosh model is compared to that of the tank vehicle incorporating the quasi-dynamic model, as shown in Figure 6.5. The steady state lateral acceleration response of the vehicle employing quasi-dynamic fluid model approaches 0.184g, while the lateral acceleration response of vehicle employing dynamic fluid slosh model oscillates around 0.175g. The lateral acceleration response of the liquid tank vehicle exhibits oscillations arising from fluid slosh, as shown in Figure 6.5. Figure 6.6 presents a comparison of roll rate response of the tank trailer of the vehicles employing fluid slosh and quasi-dynamic models. The roll rate response of the vehicle employing a quasi-dynamic fluid model quickly approaches the steady state value of zero. while the roll rate response of vehicle employing fluid slosh oscillates around the zero mean. The oscillation occur around the fundamental slosh frequency and the amplitude of oscillations decays with time.

Influence of Tank Fill Level

The fill level within the tank is altered by changing the weight density of the liquid such that the payload is held constant. The roll

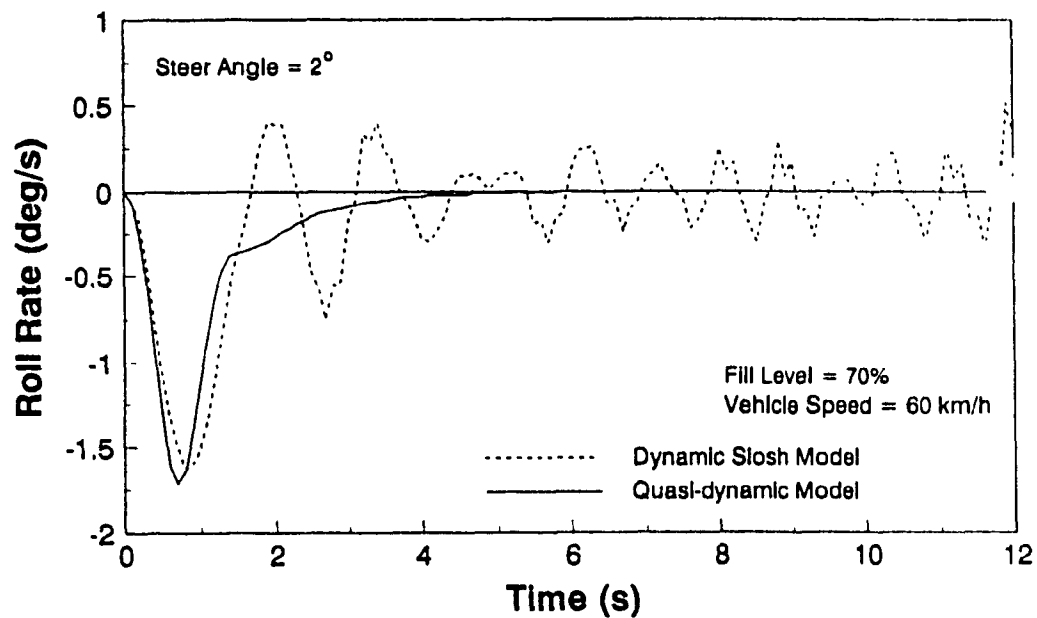


Figure 6.6 Comparison of roll rate response of dynamic slosh and quasi-dynamic tank vehicle models

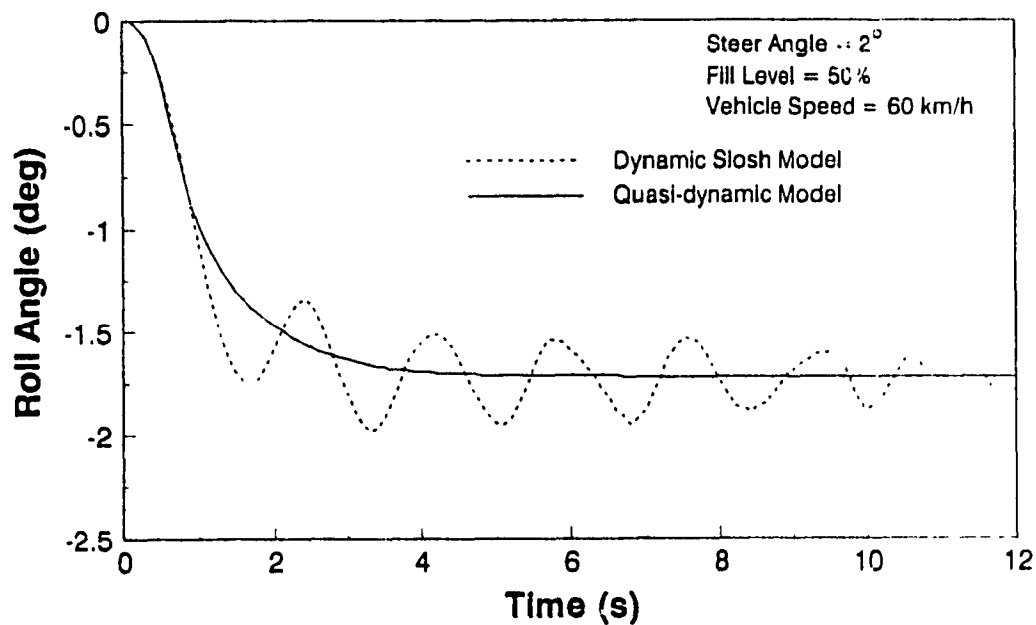


Figure 6.7 Comparison of roll response of dynamic slosh and quasi-dynamic tank vehicle models

response of a 50% filled tank vehicle subjected to a constant steer manoeuvre (2 degrees) at 60 km/h is presented in Figure 6.7. A comparison of Figures 6.4 and 6.7 reveals that frequency of oscillation decreases when the fill level is reduced, while the amplitude of oscillations grows with low fill level. The frequency of oscillation is approximately 0.59 Hz. The roll response of the vehicle employing quasi-dynamic fluid model reaches a steady state value of 1.71 degrees, similar to that for a 70% filled tank vehicle shown in Figure 6.4. With the total payload held constant, the decrease in fill level yields lower overall centre of mass height, the magnitude of liquid load shift, however, increases due to increased sloshing. Thus the steady state roll response characteristics for both 50% and 70% filled tank vehicles are quite similar. The dynamic roll response of the 50% filled tank vehicle employing fluid slosh model reveals oscillations about a mean value of approximately 1.72 degrees. The amplitude of roll oscillations decreases gradually after the steer angle approaches a constant value. The increase in the mean value of the roll response of the vehicle employing the fluid slosh model can be attributed to the increase in the dynamic slosh forces during low fill conditions, computed from the dynamic slosh model.

Figure 6.8 presents the roll angle response of the tank vehicle with various fill levels, while the axle loads are held constant by changing the density of the liquid carried. The vehicle is subjected to a constant steer input of 2 degrees at a speed of 60 km/h. The dynamic slosh frequency as well as the amplitude of oscillations are dependent on the fill level within the tank. The roll response of the tank trailer is observed to oscillate around a mean value depending on the

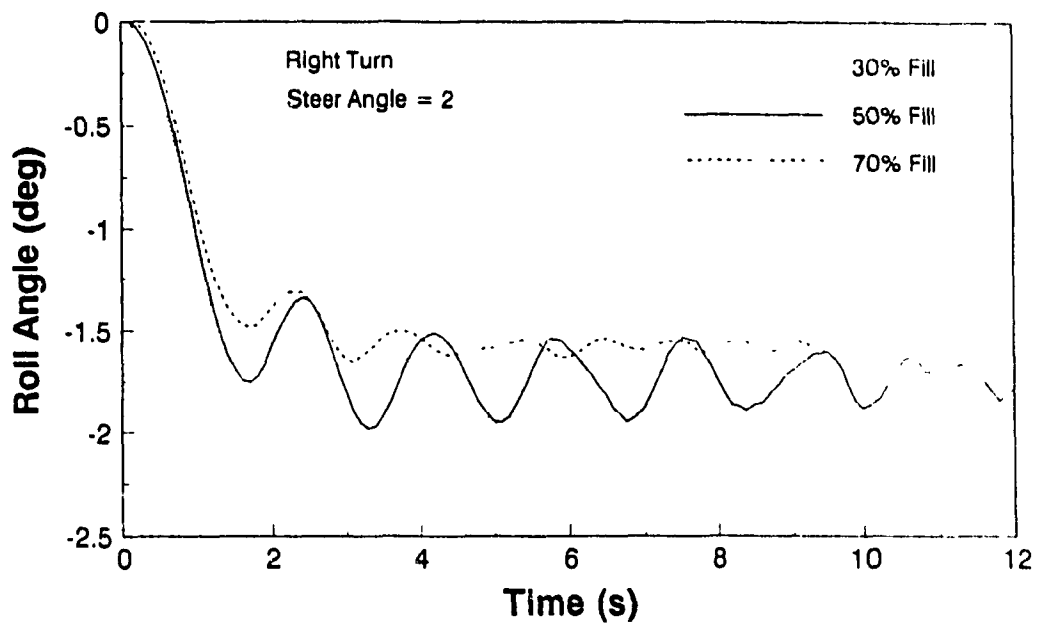


Figure 6.8 Comparison of roll response of dynamic slosh model, under various fill conditions

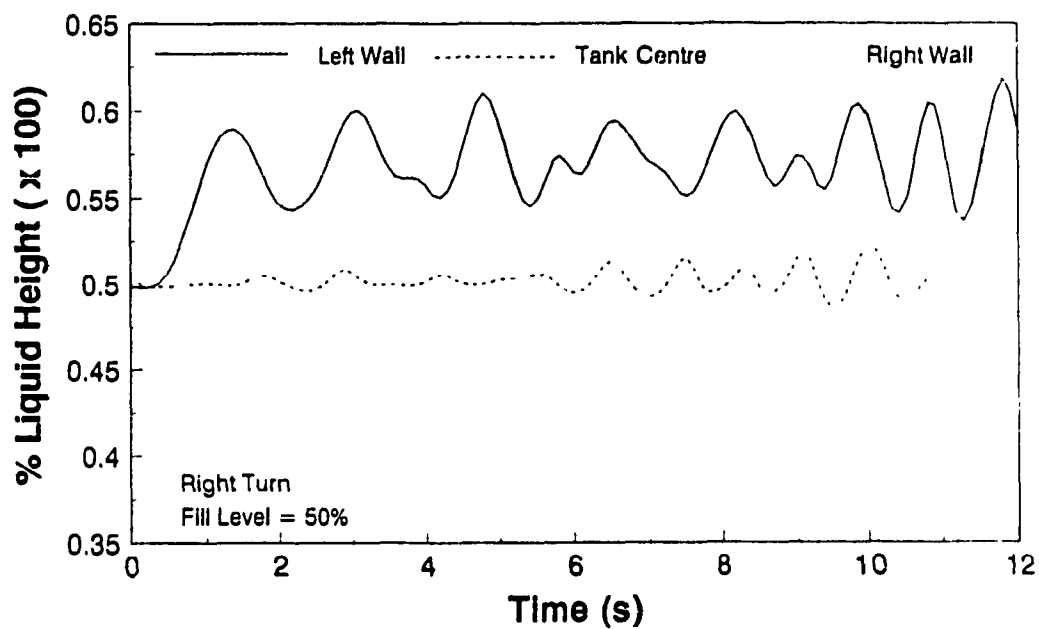


Figure 6.9 Height of the liquid free surface at the centre, right and left walls of the tank, during a constant steer manoeuvre

fill level, as shown in Figure 6.8. Although the overall centre of mass of liquid decreases with reduced fill height, the increase in the dynamic slosh forces at low fill levels increases the roll response of the trailer at low fill conditions. The peak value of roll response for 30% fill is the highest while it is the lowest for a 70% filled tank, as shown in Figure 6.8. The frequency of oscillation, however, increases with the increase in fill level.

Figure 6.9 presents the instantaneous fluid free surface height at centre of the lateral axis of the tank, at the left and right walls of the tank during a constant steer manoeuvre. The fluid height near the left and right walls approach maximum and minimum values respectively, as the steer input is applied. The free surface height is observed to oscillate about a mean value when the steer angle is held constant. The free surface height at the centre of the tank, however, initially remains almost constant during the steering manoeuvre. The free surface near the left and right walls oscillates about the mean steady state values, as shown in Figure 6.9. The amplitude of oscillations of free surface tend to die down until a reflected wave is encountered to induce further oscillations. The oscillations in the fluid free surface at the centre of tank are primarily attributed to the reflected wave.

6.6.2. Transient Steer Manoeuvre

The directional response characteristics of a 50% filled tank vehicle are investigated for typical lane change and evasive manoeuvres at highway speeds using the dynamic slosh model of the tank. The response characteristics of the vehicle are compared to those computed using a quasi-dynamic model. Figure 6.10 presents a comparison of the roll response of a 50% filled tank vehicle during a lane change

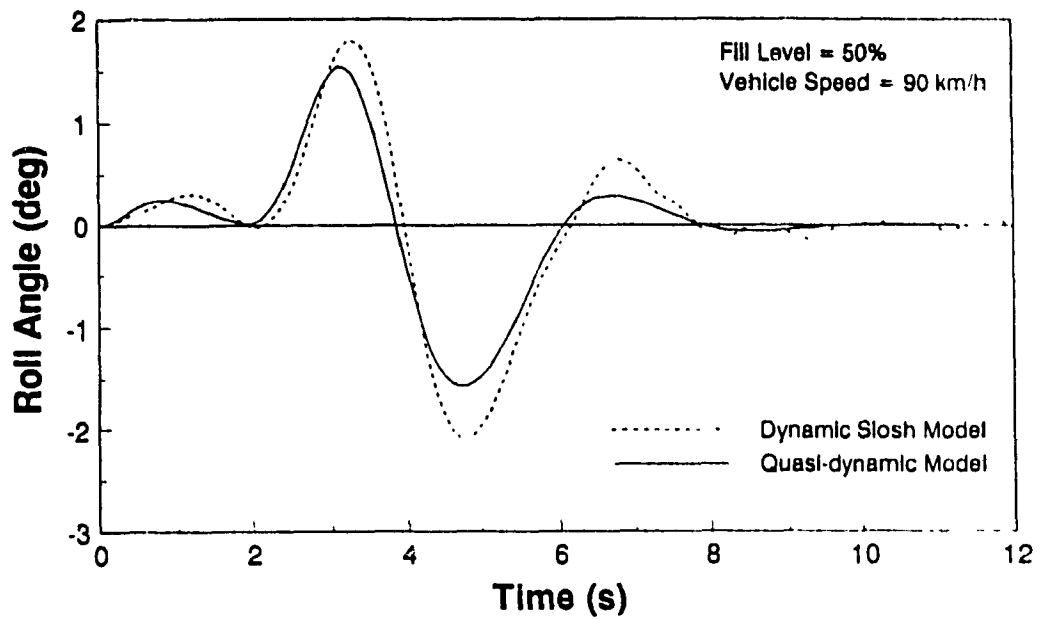


Figure 6.10 Comparison of roll response of dynamic slosh and quasi-dynamic tank vehicle models, during a lane change manoeuvre

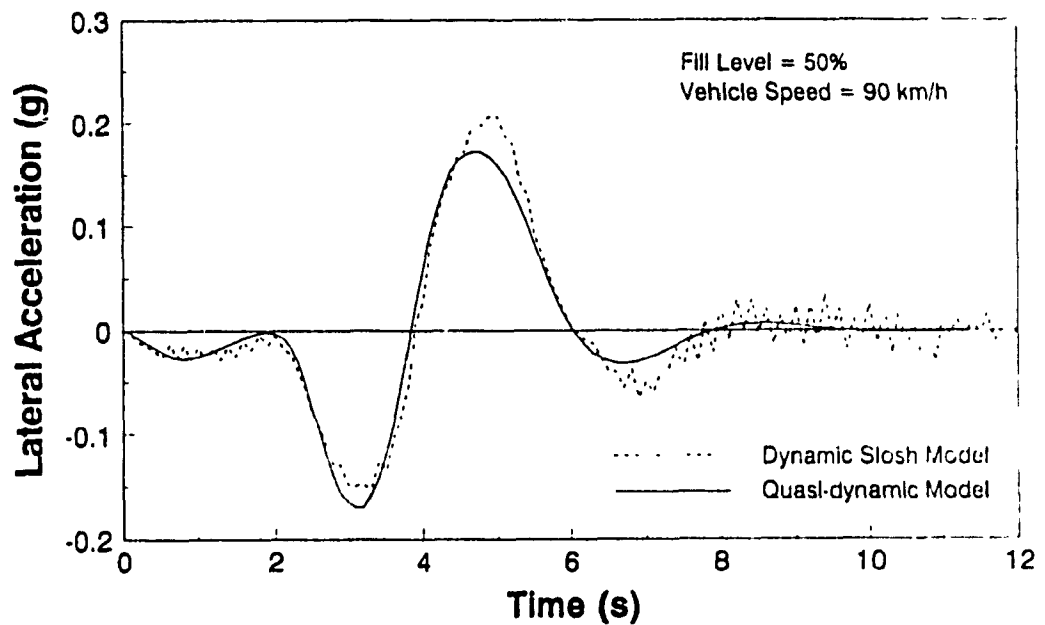


Figure 6.11 Comparison of lateral acceleration response of dynamic slosh and quasi-dynamic tank vehicle models, during a lane change manoeuvre

manoeuvre at a vehicle speed of 90 km/h. Figure 6.10 reveals that the quasi-dynamic model can predict the vehicle roll response quite close to the dynamic fluid slosh model. The dynamics of fluid slosh within the partially filled tank, however, increases the peak roll response of the trailer, as shown in Figure 6.10. The fluid slosh within the partially filled tank vehicle also yields oscillatory roll response of the vehicle after completion of the manoeuvre. These oscillations occur around zero mean, while the quasi-dynamic model reaches zero at the end of the manoeuvre. The steer frequency for the lane change manoeuvre is around 0.25 Hz, which is well below the fundamental slosh frequency for a 50% filled tank (≈ 0.6 Hz).

The comparison of the lateral acceleration response characteristics of tank vehicles employing quasi-dynamic and dynamic slosh models are presented in Figure 6.11. The lateral acceleration response evaluated using the quasi-dynamic model is quite close to that evaluated from the dynamic slosh model. The peak acceleration response of the vehicle employing the dynamic slosh model, however, is slightly higher than that employing the quasi-dynamic model during the correction phase of the manoeuvre, as shown in Figure 6.11. Figure 6.12 presents the roll rate response of the tank vehicle during the lane change manoeuvre. The fluctuations in the roll rate about zero mean arise from the dynamics of fluid oscillation within the tank. The high frequency oscillations in the lateral acceleration and roll rate response arise from the sequential procedure used to compute the vehicle response in the dynamic slosh model.

The influence of the tank fill height on the dynamic response of the tank vehicle during a lane change manoeuvre is presented in Figure

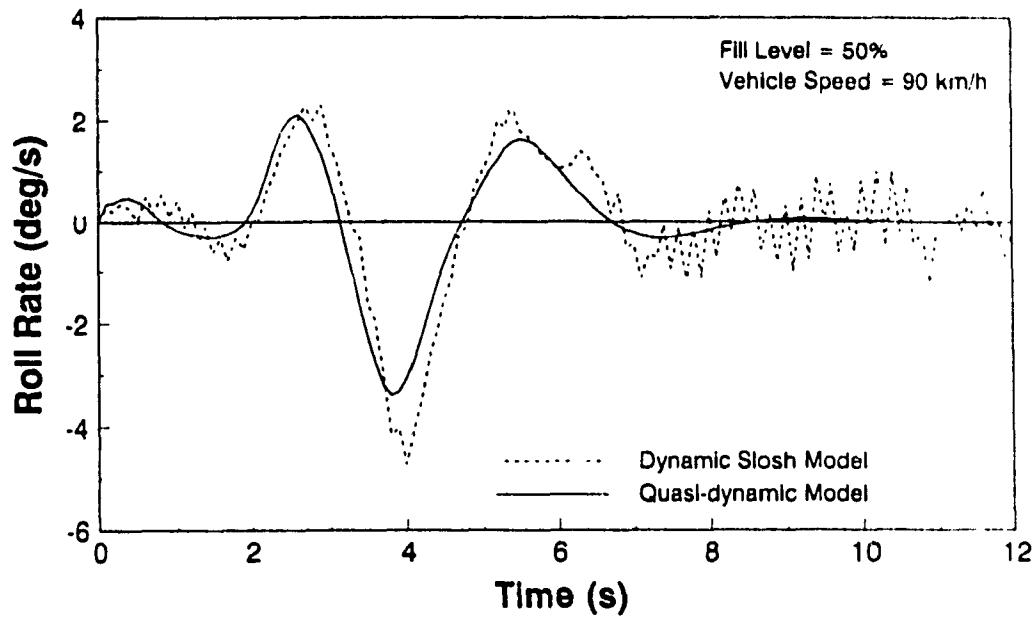


Figure 6.12 Comparison of roll rate response of dynamic slosh and quasi-dynamic tank vehicle models, during a lane change manoeuvre

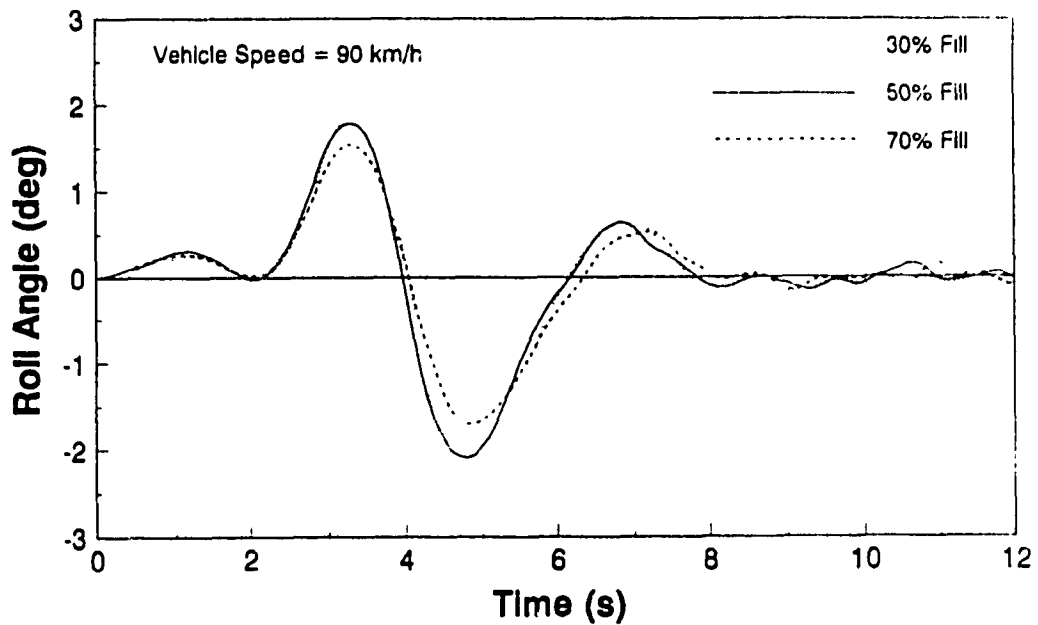


Figure 6.13 Comparison of roll response of dynamic slosh model under various fill conditions, during a lane change manoeuvre

6.13. The 30% filled tank vehicle experiences the highest roll angle while the 70% filled tank experiences the least roll angle, as shown in Figure 6.13. The roll response of the tank vehicle experiences first mode oscillations after the manoeuvre is completed.

Figure 6.14 presents the roll angle response of a 50% filled tank vehicle negotiating a double-lane change (evasive) manoeuvre at a vehicle speed of 70 km/h. The roll angle response of the tank vehicle integrated with the dynamic slosh model is very close to that of vehicle employing a quasi-dynamic model during the first lane change of the manoeuvre. The peak roll angle response of the vehicle incorporating dynamic slosh reaches 2 degrees while the vehicle employing the quasi-dynamic model experiences approximately 1.4 degrees roll, during the second lane change of the manoeuvre. This can be attributed to the different steer frequencies for the first and second lane change. The frequencies of the first and second lane change manoeuvres are approximately 0.24 Hz and 0.33 Hz respectively. Hence, the roll angle response of the tank vehicle increases during the second lane change. Figure 6.14 also indicates that the roll angle of the tank vehicle experiences oscillations about the zero value due to the continued fluid motion within the tank even after the manoeuvre is completed. The lateral acceleration response of the vehicle employing dynamic slosh model indicates identical response behaviour as the vehicle employing the quasi-dynamic model, as shown in Figure 6.15. The response plots seem to indicate that the quasi-dynamic fluid model can predict the vehicle response characteristics quite close to that employing the fluid slosh model, during various highway manoeuvres.

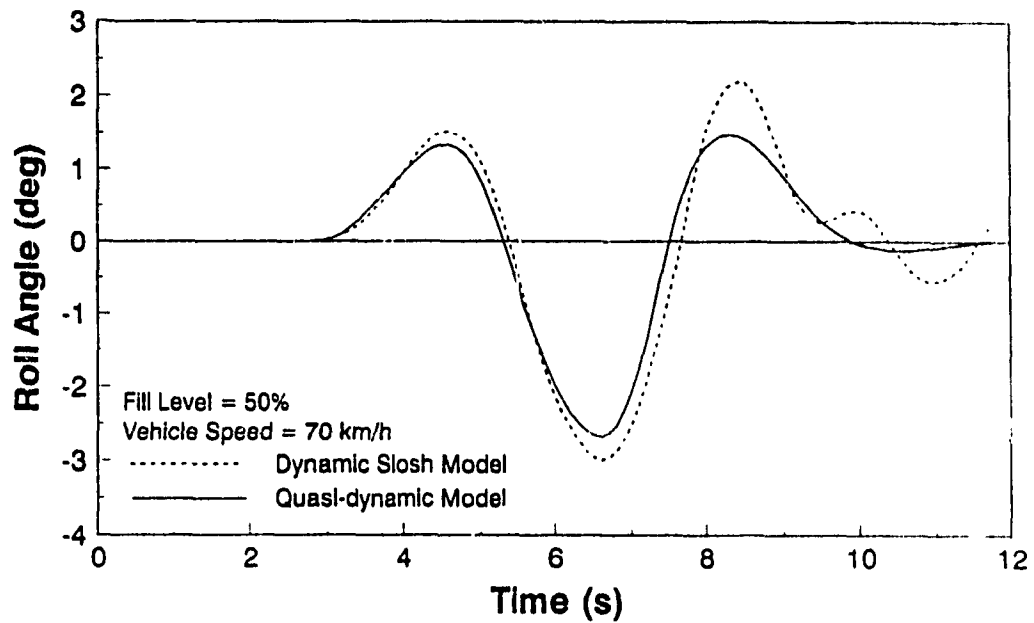


Figure 6.14 Comparison of roll response of dynamic slosh and quasi-dynamic tank vehicle models, during an evasive manoeuvre

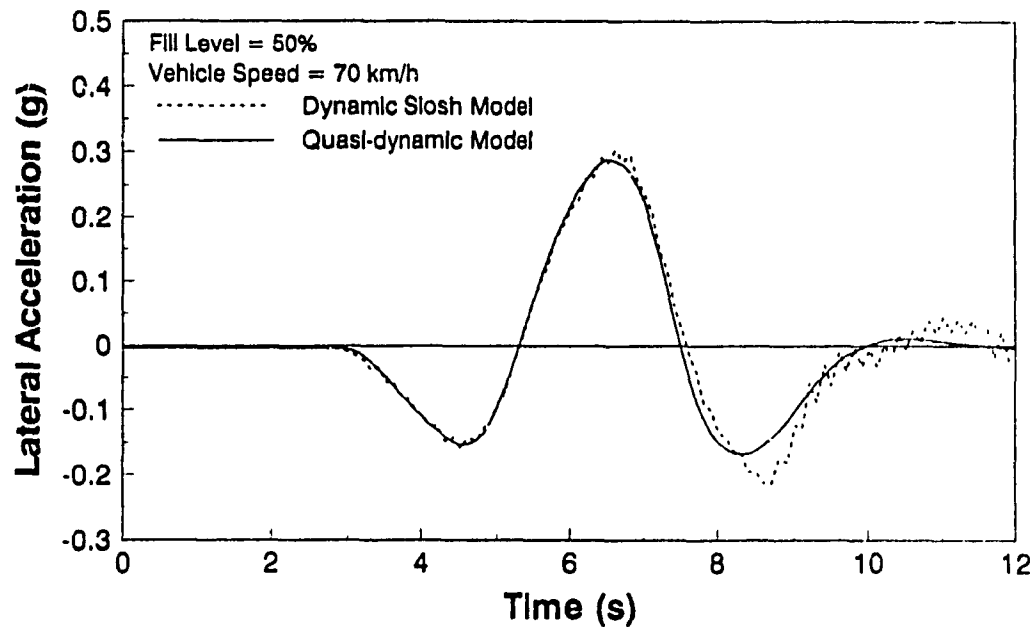


Figure 6.15 Comparison of lateral acceleration response of dynamic slosh and quasi-dynamic tank vehicle models, during an evasive manoeuvre

6.7 Summary

A comprehensive directional dynamics model of a tractor-tank trailer is developed by integrating the non-linear dynamic fluid slosh model to the 3-dimensional vehicle model. The dynamic slosh forces and moments caused by the directional motion of the vehicle are evaluated in the Eulerian mesh in terms of non-dimensional parameters. The slosh forces and moments are then transformed and integrated to the vehicle model to determine the directional response characteristics for various steer manoeuvres. The directional response characteristics of the partially filled tank vehicle are compared to those of the vehicle employing the quasi-dynamic model. The simulation results reveal that the quasi-dynamic model can predict the directional response quite close to that evaluated from the comprehensive fluid slosh model. The quasi-dynamic model over estimates the response characteristics in case of low frequency steer inputs and high fill conditions, while a high degree of correlation is obtained for steer frequencies corresponding to typical highway manoeuvres under various fill conditions. The simulations results indicate that the vehicle model employing the quasi-dynamic model is quite capable of predicting the vehicle dynamic response characteristics under various highway manoeuvres.

REFERENCES FOR CHAPTER 6

1. Bauer, H.F., "Dynamic Behaviour of an Elastic Separating Wall in Vehicle Containers", Part 1, Int. J. of Veh. Design, Vol. 2, No. 1, 1981.
2. Popov, G., Vatistas, G.H., Sankar, S. and Sankar, T.S., "Liquid Sloshing in a Horizontal Cylindrical Container", 1989 ASME Computers in Engineering Conference.
3. Lamb, M., "Hydrodynamics", Section 259, Dover Publications, N.Y., 1945.
4. Budiansky, B., "Sloshing of Liquids in Circular Canals and Spherical Tanks", J. of Aerospace Sci., Vol. 27, No. 3, March 1960.
5. Hutton, R.E., "An Investigation of Resonant, Nonlinear, Nonplanar Free Surface Oscillations of a Liquid", NASA-TND-1870, May 1963.
6. Mccarty, J. and Stephens, D., "Investigation of the Natural Frequencies of Fluids in Spherical and Cylindrical Tanks", NASA-TND-252, 1960.
7. Abramson, H.N., "The Dynamic Behaviour of Liquids in Moving Containers", NASA-SP-106, 1966.
8. Slibar, A. and Troger, H., "The Steady State Behaviour of Tank Trailer System carrying Rigid or Liquid Cargo", VSD-IUTAM Symposium on Dynamics of Vehicles on Roads and Tracks, Vienna, 1977.
9. Strandberg, L., "Lateral Stability of Road Tankers", VTI Rapport No. 138A, Sweden, Vol. 1, 1978.
10. Bohn, P.F., Butler, M.C., Dunkle, H.D. and Eshleman, R.L., "Computer Simulation of the Effect of Cargo Shifting on Articulated Vehicles Performing Braking and Cornering Manoeuvres", Vol. 2, Technical Report, The John Hopkins University, May 1981.
11. Popov, G., Vatistas, G.H., Sankar, S. and Sankar, T.S., "Liquid Sloshing in a Horizontal Cylindrical Container", CONCAVE Research Report, Concordia University, 1988.

CHAPTER 7

FIELD TESTING OF A TANK VEHICLE

7.1 General

The analytical models and simulation results of the tank vehicle combinations are presented in the previous chapters. In order to gain confidence in the analytical investigation for estimating the stability limits of tank vehicle combinations, some form of validation is needed. A validated quasi-dynamic modeling of a partially filled articulated tank vehicle can be used for further studies related to anti-slosh devices and determination of optimal tank shapes. A comprehensive field test program was jointly carried out by the Ontario Ministry of Transportation (MTO) and CONCAVE Research Centre. Test data collected and analyzed are presented here for the purpose of validation.

Due to the high costs involved in performing tests on a real size tank vehicle combination, field tests were performed on a two-axle tractor equipped with a translucent cylindrical tank. The vehicle testing is intended to validate the analytical models developed to investigate the influence of liquid motion within a partially filled tank on the directional response of the vehicle. The results obtained from computer simulation of the quasi-dynamic tank vehicle model are compared to those established from the field tests. The test procedures were designed to represent various directional manoeuvres normally encountered on a highway. A brief description of the test vehicle (assembled by MTO) and the instrumentation used to measure the response of the vehicle is presented along with the detailed description of the test procedure.

7.2 Description of the Test Vehicle

The test vehicle is a 1976 Ford L9000 Model K907 2-axle tractor,

equipped with multi-leaf suspension springs and 11 R 22.5 Michelin radial tires on both the front and rear axles. The wheel base of the truck is 4.13 m(162.5 in). The front and rear axles are rated at 53.4 kN (12,000 lb) and 93.45 kN (21,000 lb) respectively. The force-deflection characteristics of the front and rear suspension springs were determined through laboratory testing conducted by the University of Michigan Transportation Research Institute. The specifications of the front and rear axles and the force-deflection characteristics of the suspension spring are presented in Table 7.1 [1]. The mechanical properties of the tires were obtained from the experimental studies performed on the various types of tires [2].

The vehicle is equipped with a cylindrical tank made of a translucent material so that the motion of the liquid within the tank can be visualized. The tank is equipped with an inlet port on the top and an outlet manifold at the bottom for loading and unloading the tank, as shown in Figure 7.1. The specifications of the tank are listed in Table 7.2. The tank was filled with water during the field testing, however, a coloring agent was added to facilitate the flow visualization.

The tank is mounted on the truck through a mounting assembly, which comprises of a main frame, a subframe, and a saddle adapter. The main frame is rigidly fixed to the chassis frame, while the subframe is linked through force transducers to the main frame. A total of three force transducers are mounted vertically between the subframe and the mainframe, to measure the dynamic forces caused by the vehicle motion and the load shift occurring due to the liquid motion within the tank. The tank is mounted on the tank saddle which in turn is welded to the

TABLE 7.1

SPECIFICATIONS OF FRONT AND REAR AXLES AND FORCE-DEFLECTION
CHARACTERISTICS OF THE SUSPENSION SPRINGS [1]

Suspension File

1976 Ford L9000

Single Axle tractor front suspension: GAWR = 53.4 kN (12000 lb)

Front Suspension	
Roll Moment of Inertia	418 N.m.s ² (3700 in.lb.s ²)
Unsprung Mass	6.675 kN (1500 lb)
Centre of Gravity Height	0.508 m (20 in)
Roll Center Height	0.473 m (18.63 in)
Track Width	2.051 m (80.75 in)
Dual Tire Separation	0 m (0 in)
Spring Spread	0.870 m (34.25 in)
Auxiliary Roll Stiffness	1017 N.m/deg(9000 in.lb/deg)
Rollsteer Coefficient	0.186
Left Hand Viscous Damping	4.91 kN.s/m (28 lb.s/in)
Right Hand Viscous Damping	4.91 kN.s/m (28 lb.s/in)

Spring File

Linear Rate = 196.22 kN/m (1120.0 lb/in)

Coulomb Friction = 1290 N (290.0 lb)

Force (kN)	Deflection (m)
5.32	0.026
8.62	0.069
17.85	0.095
23.32	0.124
30.83	0.161
38.12	0.190
43.14	0.208
45.41	0.214
50.19	0.221
62.05	0.232

TABLE 7.1 (Contd.,)

SPECIFICATIONS OF FRONT AND REAR AXLES AND FORCE-DEFLECTION
CHARACTERISTICS OF THE SUSPENSION SPRINGS [1]

Suspension File

1976 Ford L9000

Single Axle tractor rear suspension: GAWR = 92.56 kN (20800 lb)

Single Rear Suspension	
Roll Moment of Inertia	576 N.m.s ² (5100 in.lbs.s ²)
Unsprung Mass	11.125 kN (2500 lbs)
Centre of Gravity Height	0.508 m (20 in)
Roll Center Height	0.719 m (28.3 in)
Track Width	1.829 m (72 in)
Dual Tire Separation	0.330 m (13 in)
Spring Spread	1.022 m (40.25 in)
Auxiliary Roll Stiffness	2260 N.m/deg (20000 in.lb/deg)
Rollsteer Coefficient	0.024

Spring File

Linear Rate = 4292 kN/m (24500.0 lb/in)

Coulomb Friction = 4183 N (940.0 lb)

Force (kN)	Deflection (m)
- 3.74	0.022
0.82	0.046
3.25	0.065
5.37	0.076
10.53	0.098
20.86	0.131
27.85	0.147
34.23	0.159
53.67	0.180
94.02	0.195

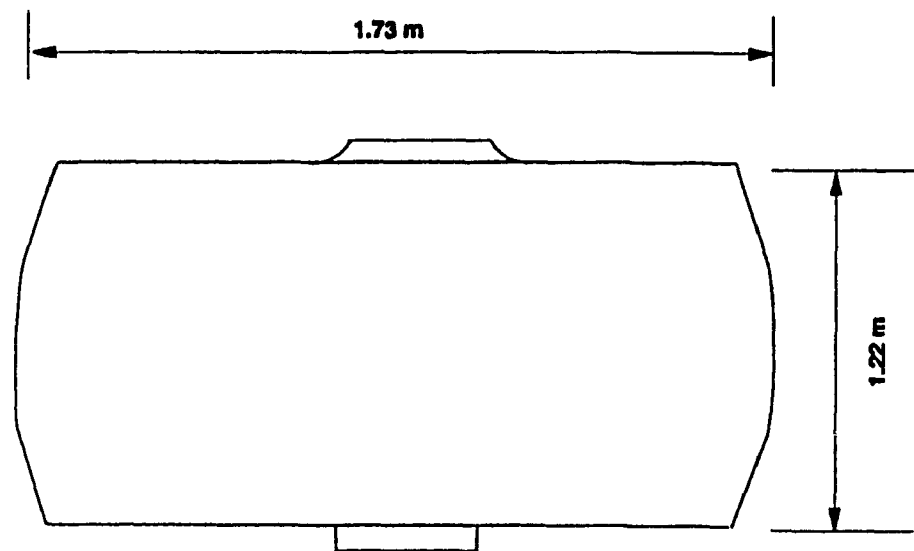


Figure 7.1 Schematic of the test vehicle tank

TABLE 7.2

SPECIFICATIONS OF THE TANK USED IN FIELD TEST

Weight	614 N (138 lb)
Volume	1.89 m ³ (500 Gallons)
Diameter	1.22 m (48 in)
Length	1.73 m (68 in)

saddle adapter and firmly bolted to the subframe. Figure 7.2 presents the tank mounting frame assembly. The complete assembly of the tank and the mounting frame is installed on the tractor such that the geometric centre of the tank lies directly above the center of the rear axle of the vehicle in the roll plane. Figures 7.3 and 7.4 present the rear and side views of the tank vehicle, respectively.

The field tests were conducted for various fill conditions and steering manoeuvres. The liquid load and the fill height, measured corresponding to various fill conditions, are listed in Table 7.3. The corresponding axle loads are listed in Table 7.4.

7.3 Description of the Test Program

Acquisition of meaningful test results is strongly dependent upon the instrumentation, test course, driver's performance and vehicle characteristics. Field testing of vehicle requires appropriate consideration of the following [3]:

1. A single experienced driver must be used throughout the test program to minimize the degree of inconsistencies;
2. Test manoeuvres should be designed to reflect the true highway manoeuvres while avoiding unnecessary risks to the vehicle and the driver;
3. Repeatability of the test data must be examined;
4. The measuring and recording instruments must be carefully calibrated and a routine calibration must be performed during the tests; and
5. The test course must be sufficiently long to perform the steering manoeuvres at appropriate speeds.

The tests were conducted at the Ontario Ministry of Transportation

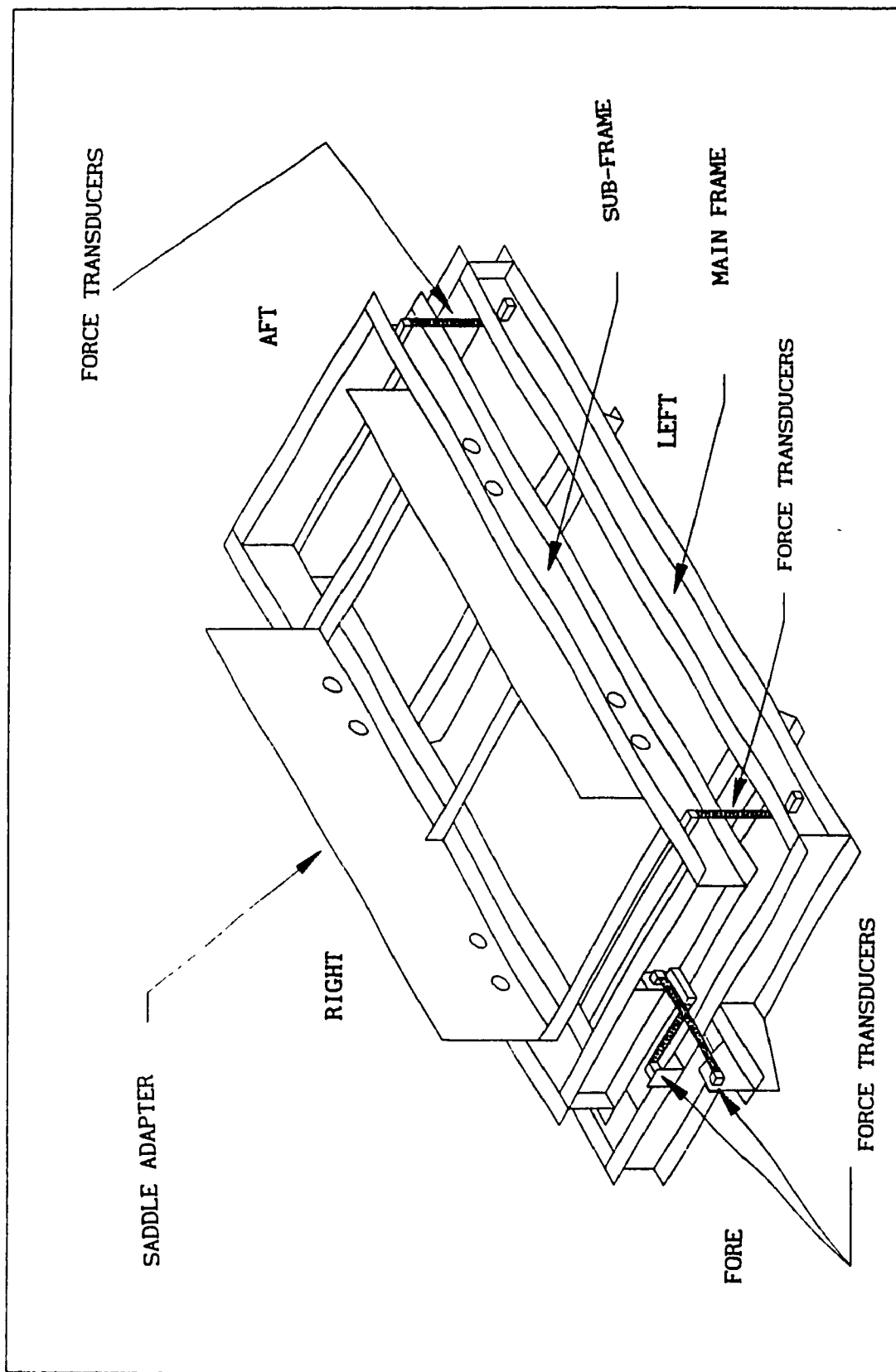


Figure 7.2 Tank mounting frame assembly

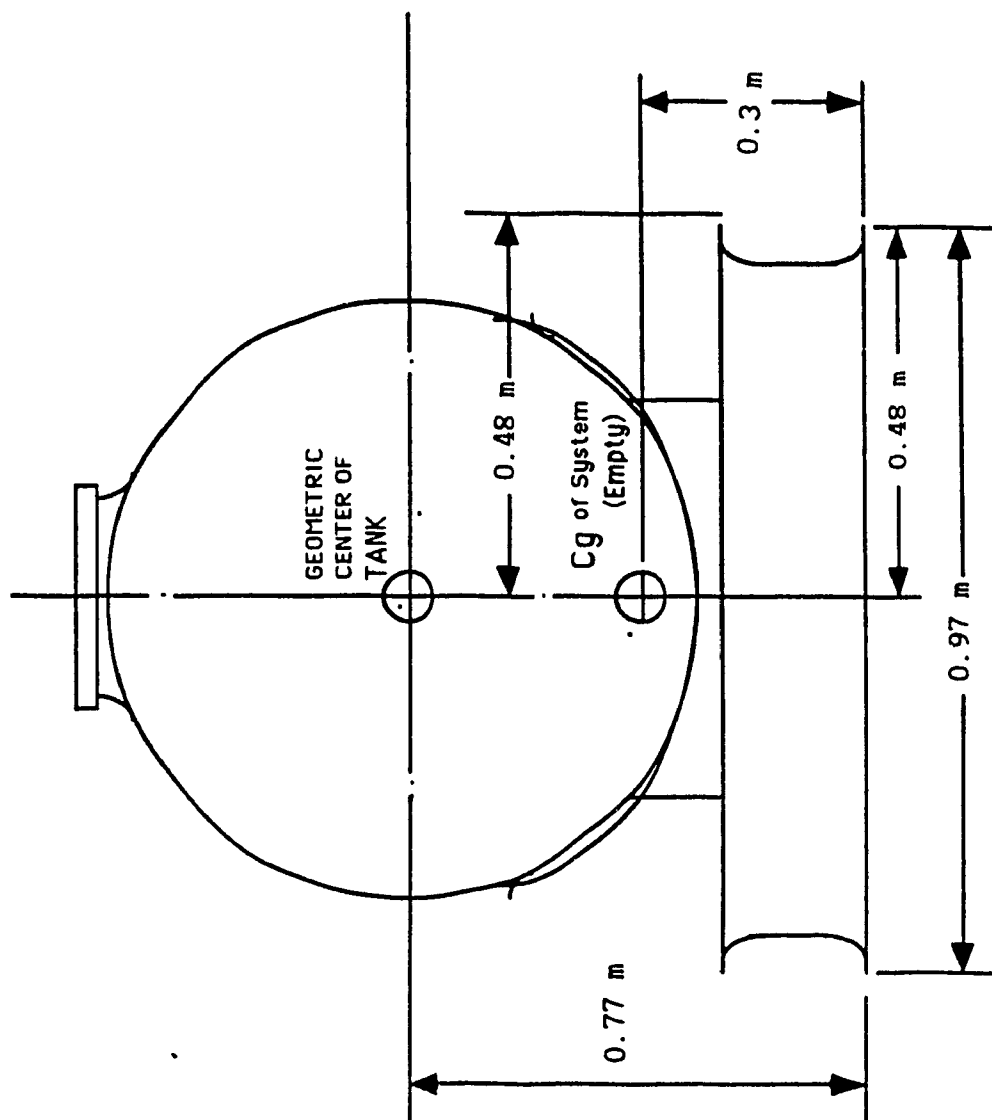


Figure 7.3 Rear view of the tank assembly

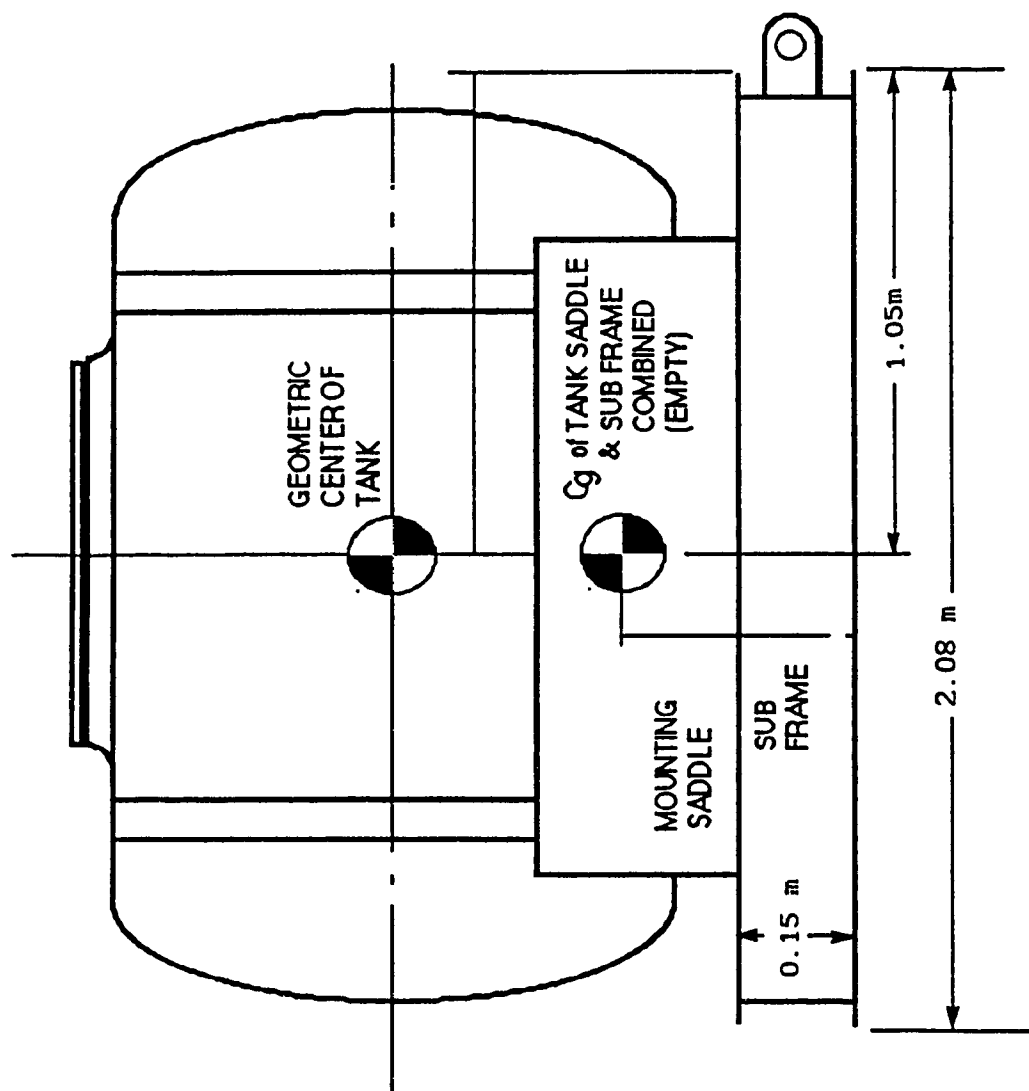


Figure 7.4 Side view of the tank assembly

TABLE 7.3

LIQUID LOAD DATA CORRESPONDING TO VARIOUS FILL CONDITIONS

Load (kN)	% Fill	Ht. above Tank Base (m)
0	0	0.0
5.51	30	0.41
7.36	40	0.51
9.25	50	0.59
11.14	60	0.69
13.03	70	0.78
18.63	100	1.22

TABLE 7.4

AXLE LOADS UNDER VARIOUS FILL CONDITIONS

Liquid Load (kN)	% Fill	Load on the Front Axle (kN)	Load on the Rear Axle (kN)
0	0	35.956	28.658
5.51	30	35.912	34.443
7.36	40	35.912	36.490
9.25	50	35.867	38.315
11.14	60	35.867	40.139
13.03	70	35.867	41.786
18.63	100	35.867	47.386

Vehicle Test Centre, Centralia. A long test track was used in order to achieve desired test speeds. All tests were conducted on uniform and dry pavements. The test course revealed a cross slope of approximately 0.3 to 0.5 degrees in one of its test track leading to a roll angle response under static conditions.

7.3.1 Test Manoeuvres

The field tests were conducted for the following test manoeuvres:

- * 30m Constant radius turn
- * Lane change manoeuvre

30m Constant Radius Turn

Commercial vehicles often exhibit roll instabilities during cornering or while negotiating a tight interchange ramp. During this manoeuvre, the lateral acceleration increases gradually as the vehicle negotiates the corner and then remains at a more-or-less steady value (assuming a constant speed and turn radius) until the turn is completed. The vehicle exits from the turn, tangential to the turn radius, after completing a turn of 90 degrees. The 30 m turn radius test is conducted at three different vehicle speeds: 29 km/h; 35 km/h; and 39 km/h. The vehicle speeds were chosen such that the driver is able to attain the specified speed before entering the manoeuvre and is able to maintain the same throughout the manoeuvre. The test vehicle approaches the turn radius at a specified speed and negotiates the turning manoeuvre, as shown in Figure 7.5, by tracking the cones with the inner (left) front wheel before exiting from the turn.

Lane Change Manoeuvre

Multiple articulated vehicle combinations experience high rearward amplification of the roll and lateral acceleration response during a

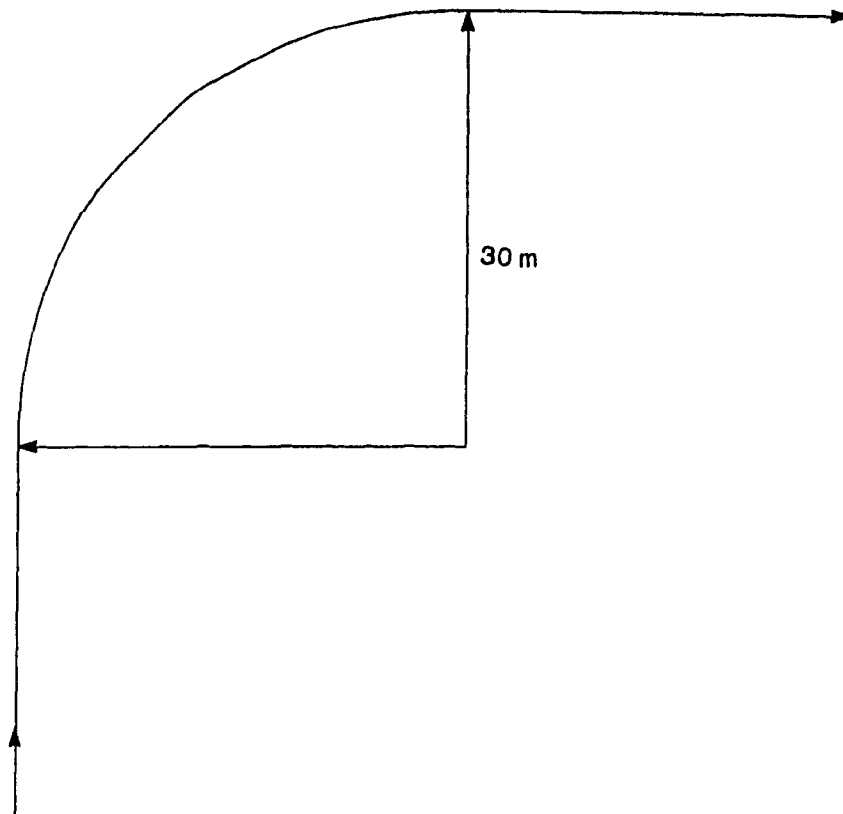


Figure 7.5 Typical 30m radius turn manoeuvre path

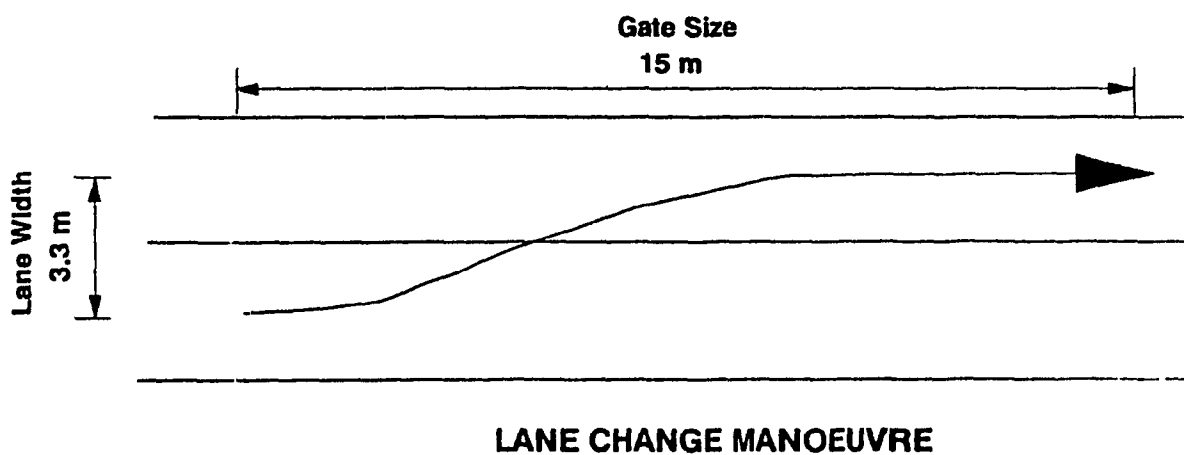


Figure 7.6 Typical 15m lane change manoeuvre path

lane change manoeuvre. This can lead to large sway of the rearmost trailer, increased side-slip, lateral accelerations and possible overturning of the rearmost trailer. The influence of liquid motion within the tank-trailers could worsen the directional dynamics of the partially filled tank vehicles. Though the test vehicle used for our study was a straight truck, the influence of liquid motion within the tank could possibly increase the side-slip on the tractor axles leading to overshoot in the vehicle path and increased roll and lateral acceleration response. In order to examine this tendency, the single lane change manoeuvre was chosen. Three vehicle speeds (35, 39 and 45 km/h) were chosen along with three different gate sizes (15.0, 18.0, and 21.0 m) for the lane change manoeuvre, as shown in Figure 7.6. The driver was instructed to enter the approach lane at its centre at a specified speed and attempt to complete the lane change, to the left, within the distance allowed by the "gate".

7.3.2 Instrumentation

The test vehicle is instrumented to provide a wide range of dynamic variables related to liquid slosh and directional dynamics of the vehicle. The tank is supported on three vertically mounted force transducers: two on the left side and one on the right side of the tank. A force transducer is mounted laterally between the sub-frame and the main frame to measure the lateral forces at the tank mount-vehicle interface. A gyro is installed at the tractor's chassis to measure the roll angle, yaw angle, roll rate and the yaw rate of the sprung mass. The lateral acceleration of the vehicle's sprung mass is measured using a piezo-resistive accelerometer. The relative roll angle of the unsprung mass with respect to the sprung mass is measured using a

potentiometer and the vehicle speed is monitored using a fifth wheel tachometer.

The measured signals were recorded on a tape recorder. Upto 42 variables could be recorded on an analog tape using a Metraplex Model 300 FM multiplexing unit. The recorded data of interest were digitized for post-processing and analyses. The procedure involved in data collection and processing are fully described in the reference [3]. The vehicle is equipped with two video cameras: one at the rear and other on the side of the vehicle to record the liquid motion within the tank, during the test manoeuvres. The measured variables and the associated instrumentation are summarized in Table 7.5. The acquired raw data is then imported into work sheets in Lotus format and the necessary response plots are obtained. The test vehicle with its instrumentation package is pictorially shown in Figure 7.7.

7.4 Comparison of Simulation and Field Test Results

The test vehicle is modeled to characterize the yaw/roll dynamics of the vehicle, using the methodology presented in Chapter 4. Computer simulations are performed to determine the directional dynamics of the test vehicle subjected to selected test manoeuvres and speeds. The directional response characteristics established from the simulation are compared to those obtained from the field tests.

7.4.1 30m Constant Radius Turn

The field test data is analyzed to yield the steer angle, roll angle, yaw angle and lateral acceleration response characteristics of the vehicle negotiating the 30m radius turn. The repeatability of the test data is first examined by performing the right turn test four times. These tests were conducted with a 50% full tank and vehicle

TABLE 7.5

TEST VEHICLE INSTRUMENTATION LIST

Variable	Instrumentation
Front Wheel Steer Angle	Potentiometer
Yaw angle and yaw rate	Humphrey gyro
Lateral Acceleration	Piezoresistive Accelerometer
Roll angle and roll rate	Humphrey gyro
Vehicle Speed	Kingpin Tachometer
Vertical Loads	Force Transducers (3) [†]
Lateral Force	Force Transducer (1) [†]
Liquid Motion	Video Cameras (2) [‡]

† Indicate the number of transducers

‡ Indicate the number of cameras

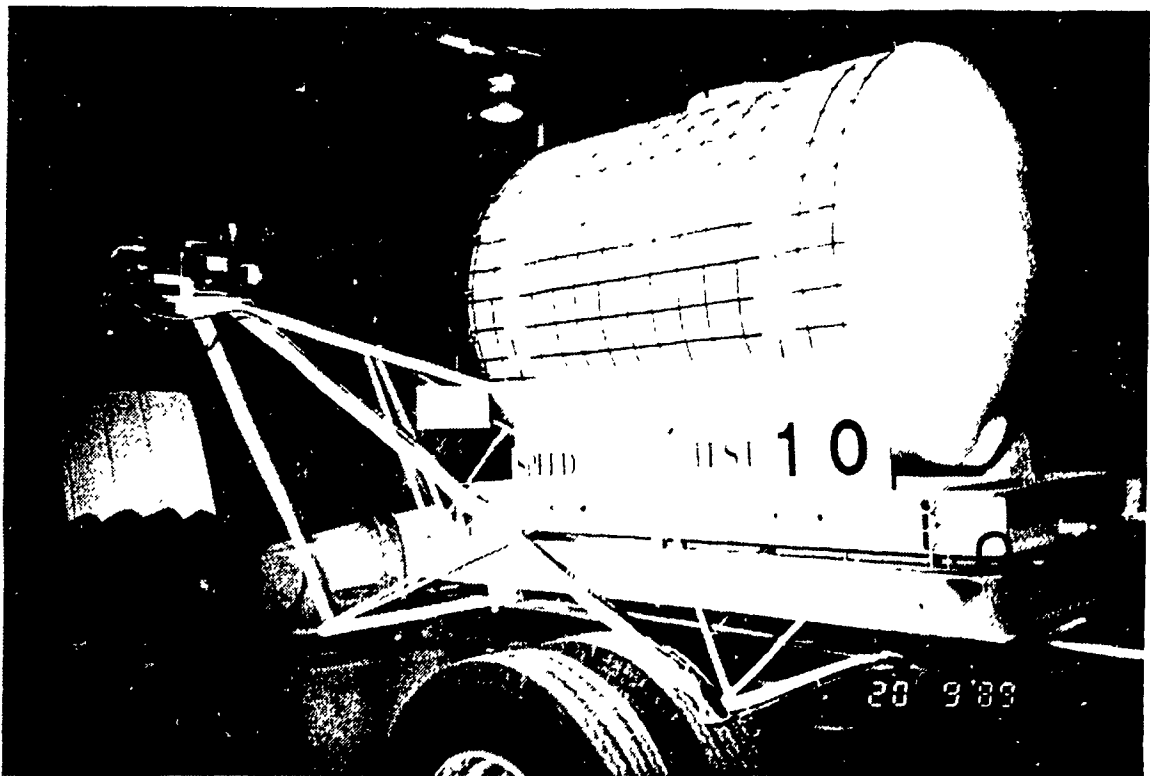
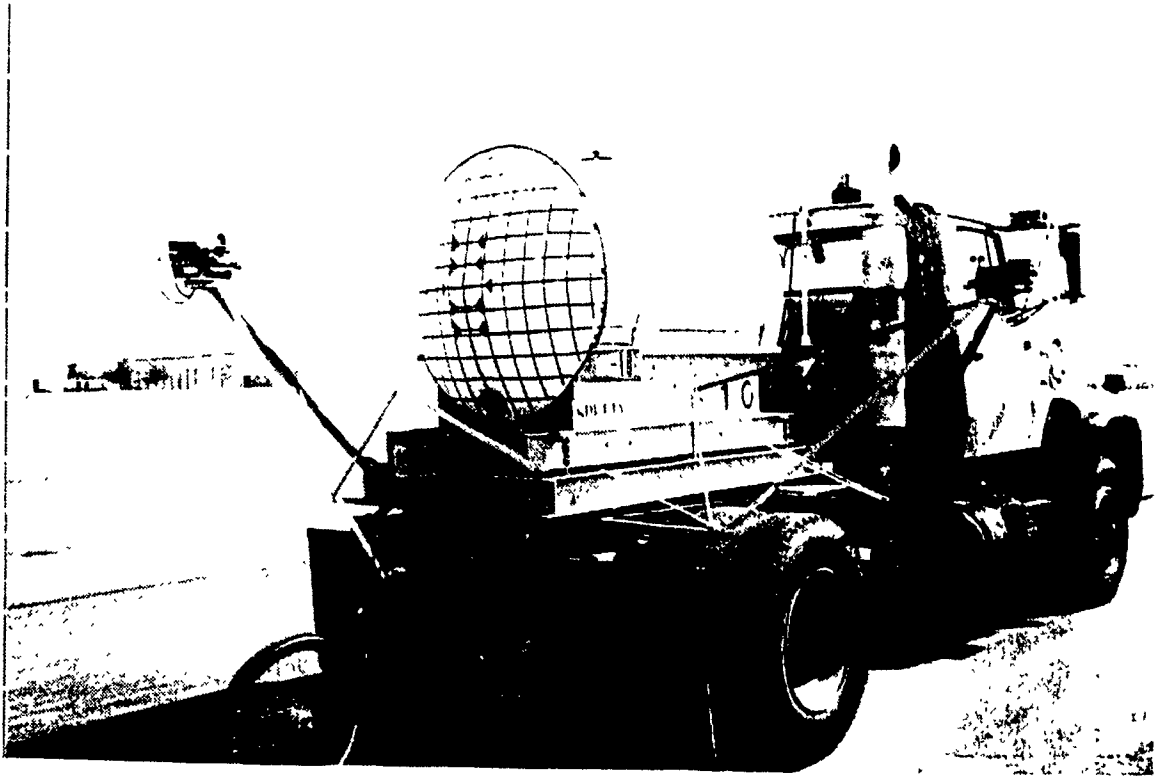


Figure 7.7 Pictorial views of the tank truck used in the field test

speed of 39 km/h. The test data, obtained from the these four tests, is presented in terms of the front wheel steer angle, roll angle, lateral acceleration and yaw angle, as shown in Figure 7.8. The test results demonstrate a high degree of repeatability.

Computer simulations are conducted to evaluate the response characteristics of the 50% filled tank vehicle negotiating a right turn of 30m radius at a constant vehicle speed of 39 km/h. The directional response characteristics of the tank vehicle are compared to those obtained from the field tests, as shown in Figure 7.9. The steer input to the simulation vehicle is derived from the field measured front wheel steer angle, as shown in Figure 7.9. The front wheel steer angle reaches a maximum value of 10 degrees and the total time taken for the manoeuvre is approximately 12 seconds. The field measured roll angle response of the test vehicle correlates reasonably well with the roll angle response obtained via computer simulation. The small discrepancies in the magnitude, however, arise due to the cross-slope of the ground and the ground roughness. The maximum roll angle of the test vehicle reaches approximately 3 degrees while the simulation results indicate a maximum of approximately 2.8 degrees. The lateral acceleration response of the simulation and test vehicle correlate very well, with the exception of the high frequency oscillations. The high frequency oscillations in the lateral acceleration response arise due to the road roughness but the mean response can be observed to follow the simulation data, as shown in Figure 7.9. The maximum value of the lateral acceleration encountered during the manoeuvre is approximately 0.45g. The yaw angle response increases gradually and reaches a maximum value of 90 degrees for both the test and simulation vehicles, as shown in Figure 7.9.

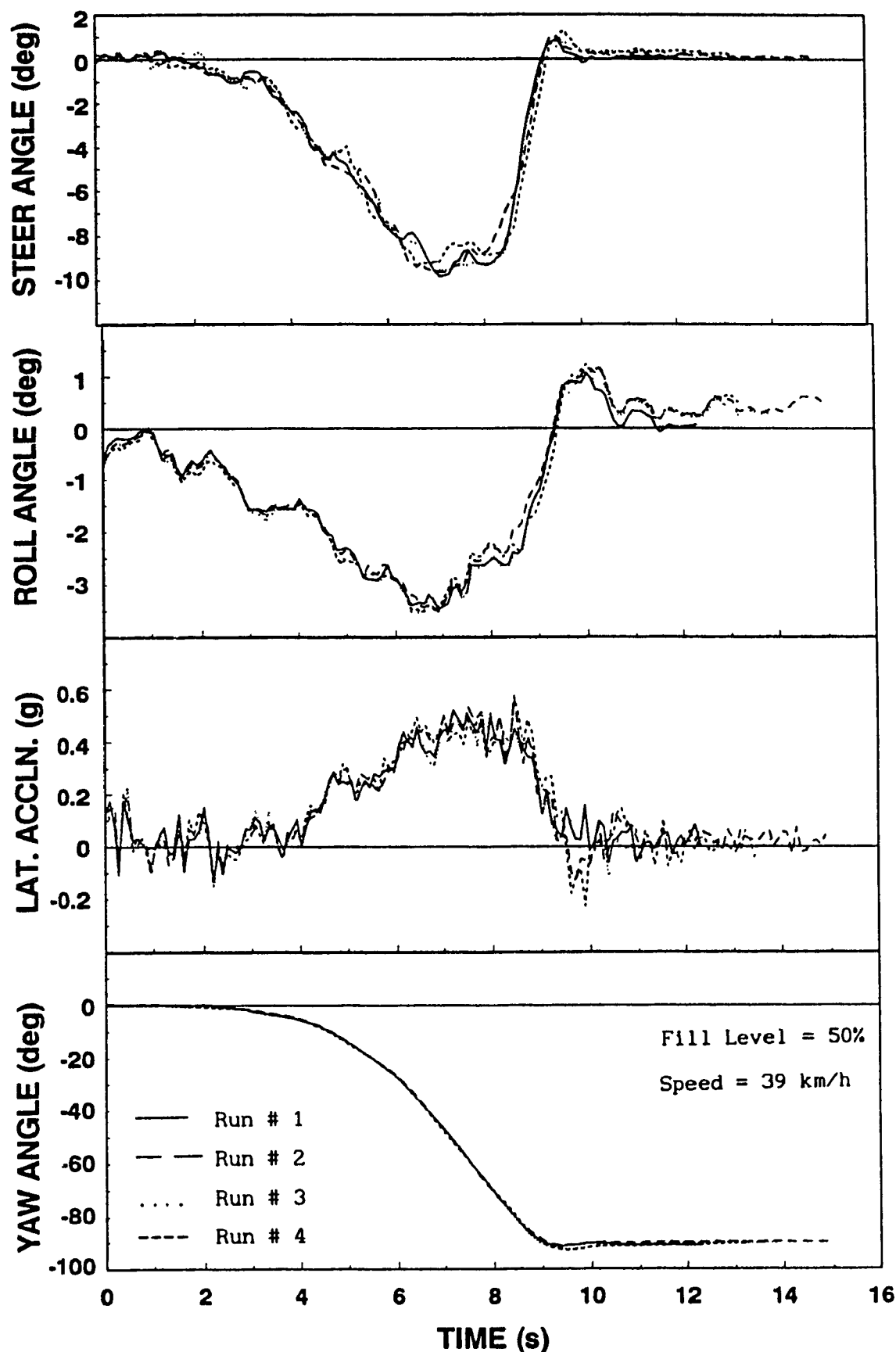


Figure 7.8 Repeatability of the test runs

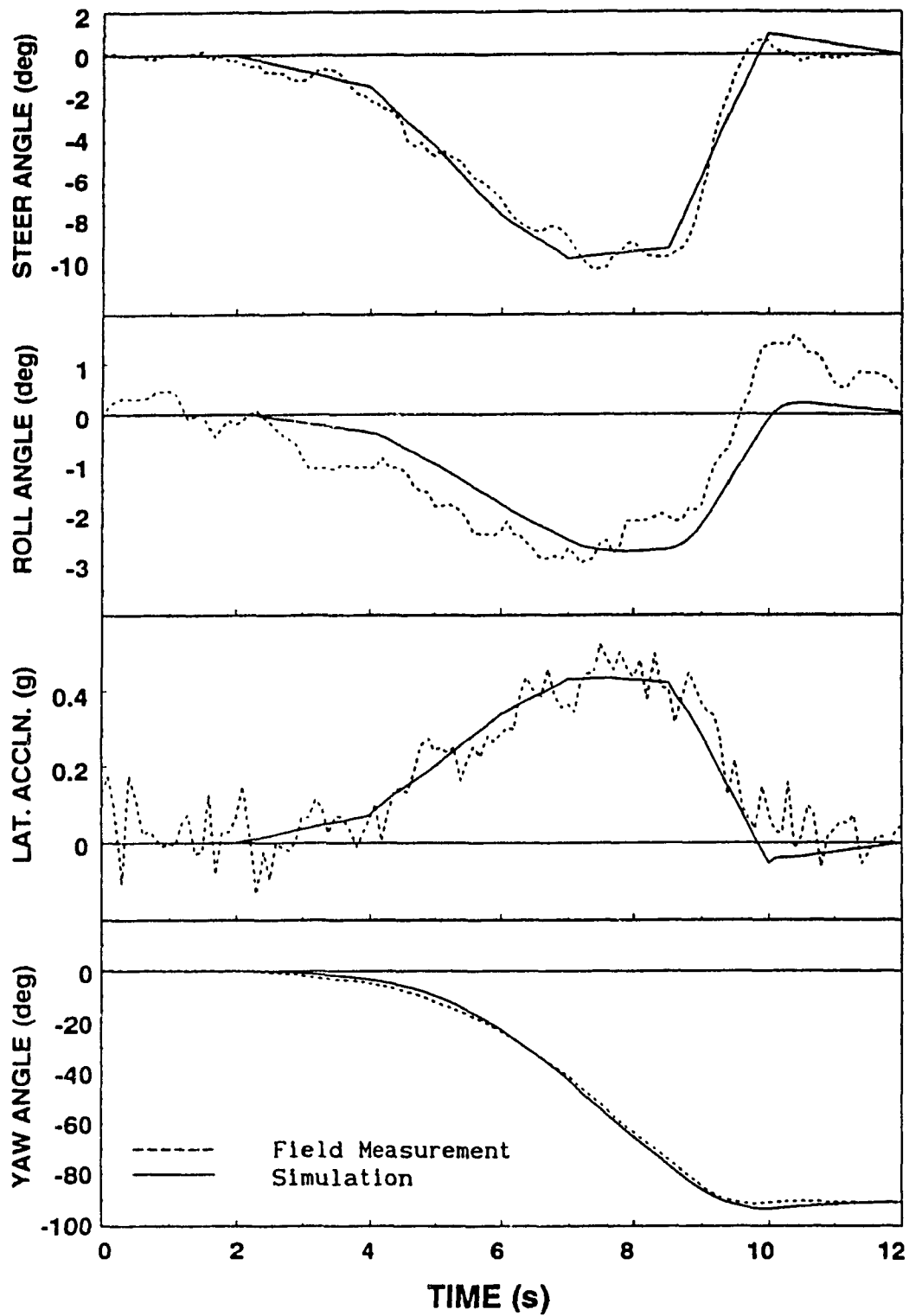


Figure 7.9 Comparison of experimental and simulation response of the 50% filled tank vehicle at a vehicle speed of 39 km/h, during a 30m radius turn

The change in the vehicle speed influences the dynamic response of the tank truck. The lateral and vertical load shifts within the partially filled tank depend on the lateral acceleration and thus the vehicle speed. The analytical model of the tank truck is further validated for different vehicle speed. The road test was conducted at a vehicle speed of 29 km/h for the same fill condition (50%). The simulation and the field results are compared as shown in Figure 7.10. As in the previous case, the computer simulation results show a good correlation with the field measured data. The peak values of the roll angle and lateral acceleration are considerably lower in this case due to the reduced vehicle speed. The vehicle experiences peak roll angles around 2 degrees (experimental) and 1.5 degrees (simulation), while the lateral acceleration peaks occur around 0.25g for both testing and simulation when steer angle reaches the peak value of 9 degrees. The total time taken to complete the manoeuvre is approximately 16 seconds.

In Chapter 5, it was pointed out that the increase in fill height leads to a decrease in roll and lateral stability of the vehicle due to increased centre of mass height from the ground. To corroborate the analytical findings, field tests were conducted for a 70% filled tank and the test results compared with simulation results are presented in Figure 7.11. The vehicle speed was held constant around 39 km/h. The simulation and the field results correlate very well, except for the small deviation in the roll angle arising from the cross-slope in the ground surface. The peak roll angle response of the test vehicle is around 4 degrees and is higher than what resulted for a 50% loaded vehicle (Figures 7.9). The vehicle's lateral acceleration response

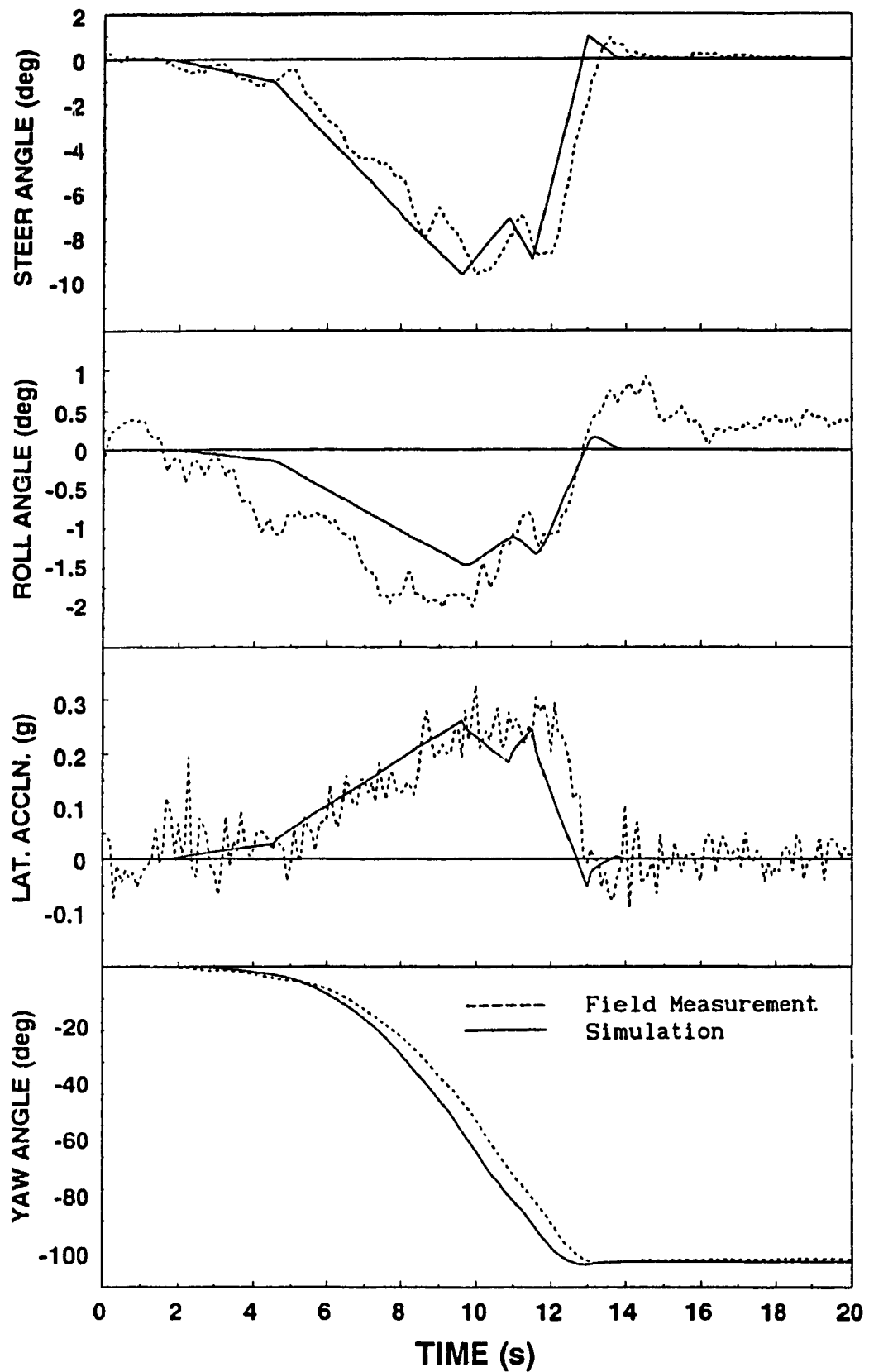


Figure 7.10 Comparison of experimental and simulation response of the 50% filled tank vehicle at a vehicle speed of 29 km/h, during a 30m radius turn

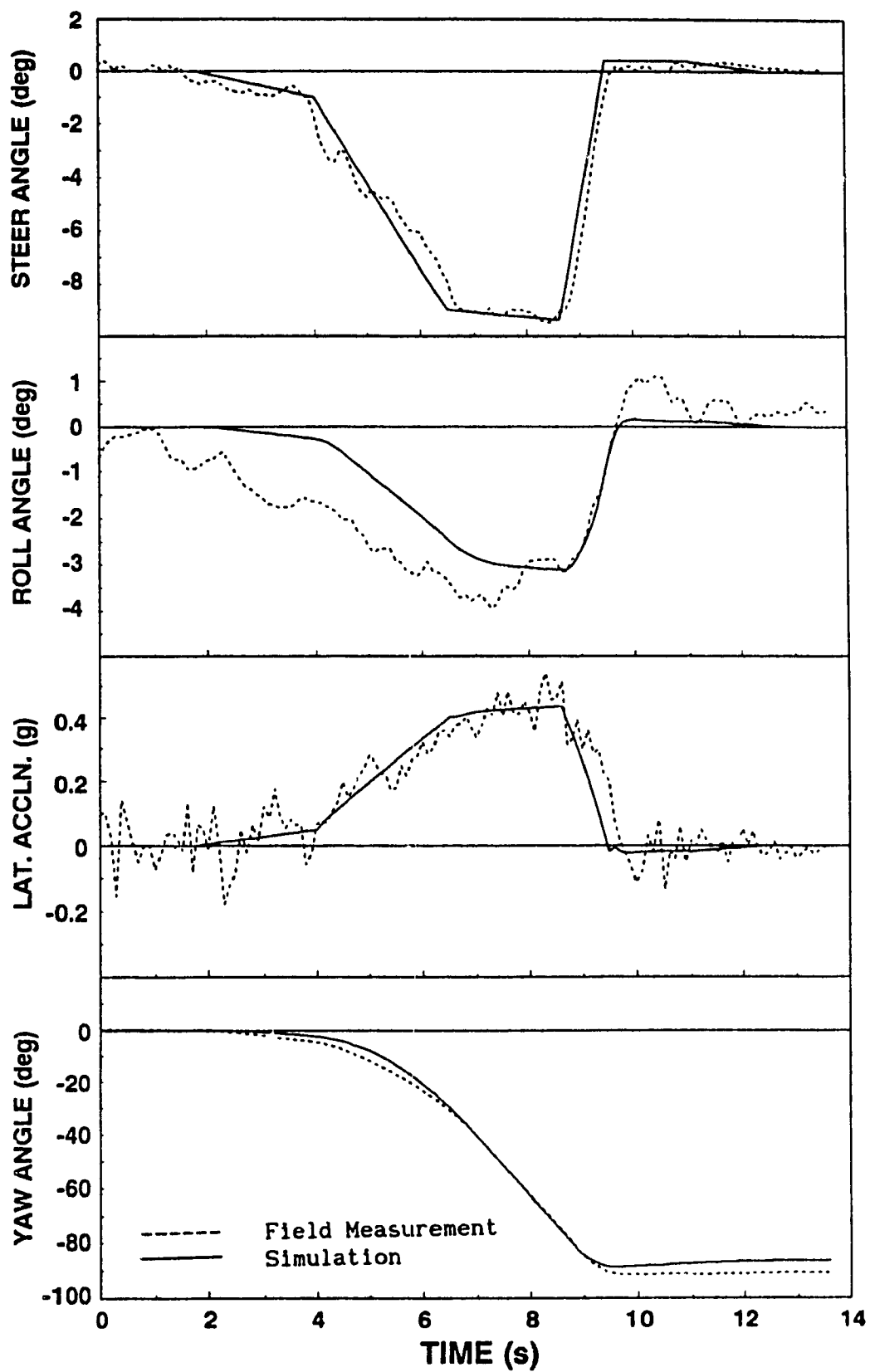


Figure 7.11 Comparison of experimental and simulation response of the 70% filled tank vehicle at a vehicle speed of 39 km/h, during a 30m radius turn

correlates very well with the field measured response and the peak value of the lateral acceleration is quite close to that obtained for a 50% filled tank vehicle. A comparison of Figures 7.9 and 7.11 reveals that there is only a small change in vehicle's response characteristics due to fill level variation from 50% to 70%. This is attributed to the fact that an increase in the fill level yields only a small increase in the payload carried by the vehicle due to the small tank dimensions.

7.4.2 Lane Change Manoeuvre

The directional response of the test vehicle is investigated for a typical lane change manoeuvre in order to further validate the analytical model. The computer simulations are carried out for the steer input derived from the field measurements. The tests are carried out for various values of fill level, vehicle speed, and gate width. Figure 7.12 presents a comparison of the experimental and simulation results for the 50% filled tank truck, negotiating 3.0 m (10 feet) lane change at a vehicle speed of 45 km/h. The gate width for the manoeuvre is selected as 15.0 m (50 feet). The roll angle, lateral acceleration and yaw angle response characteristics obtained via computer simulation and field tests are presented in Figure 7.12. Although, the computer simulation results exhibit a high degree of correlation with the field measured response characteristics, the peak values of roll, lateral acceleration and yaw response of the test vehicle differ from those of the simulation vehicle. The peak roll response of the tank vehicle is approximately 0.6 degrees larger than that established from the simulation results. Similarly, the yaw response is found to be larger by approximately 2 degrees. Moreover, the vehicle response characteristics do not reach the steady state zero position at the end

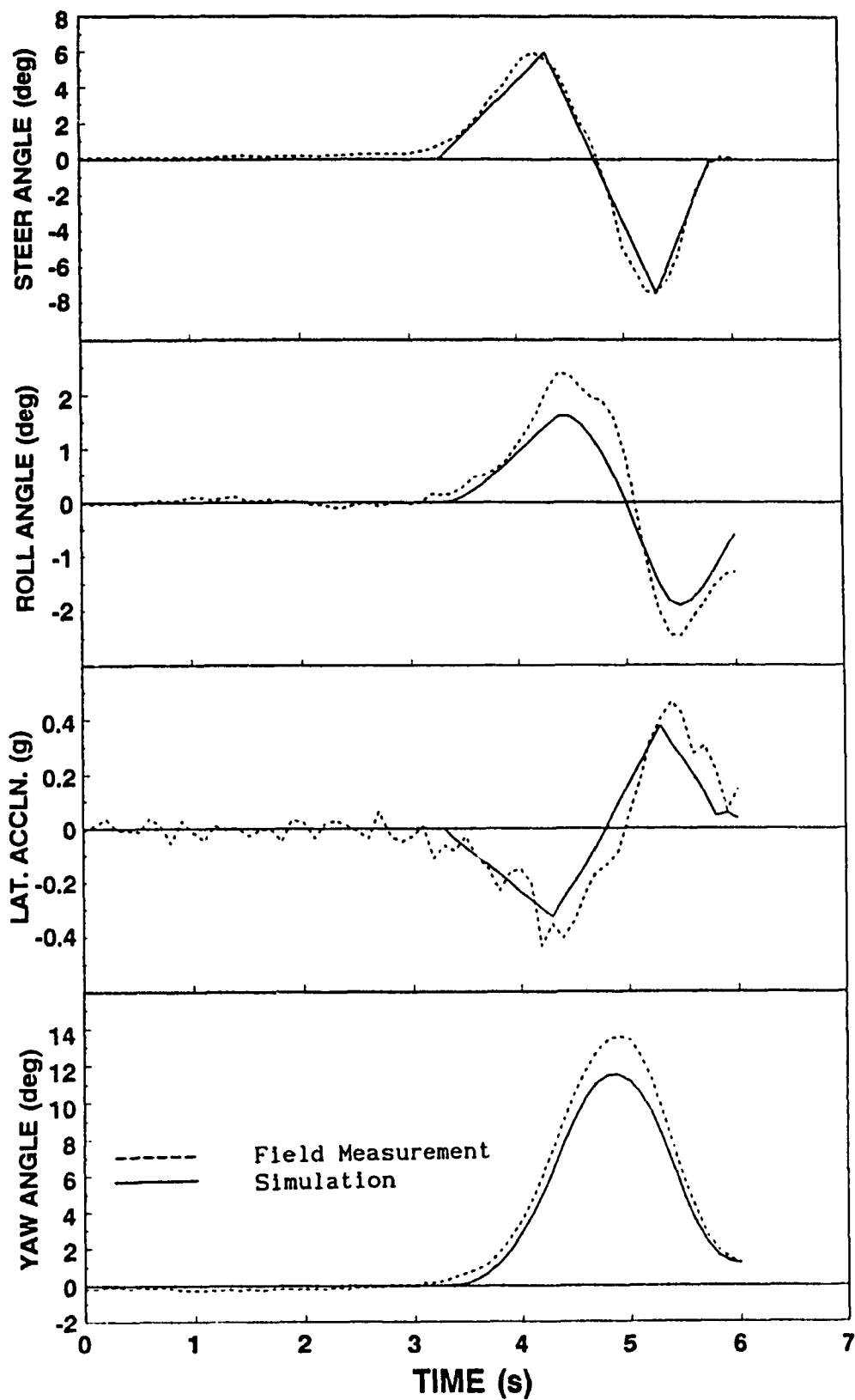


Figure 7.12 Comparison of experimental and simulation response of the 50% filled tank vehicle at a vehicle speed of 45 km/h, during a 15m lane change manoeuvre

of the test run, since the data acquisition was stopped prior to the completion of the corrective steering action.

The influence of the vehicle speed on the roll and lateral response of the tank vehicle is analyzed by reducing the vehicle speed to 35 km/h under identical conditions of fill and the desired vehicle path. Figure 7.13 presents the comparison of the test and simulation results for the lane change manoeuvre conducted at a vehicle speed of 35 km/h. The drop in the vehicle speed increases the simulation time to approximately 10 seconds. The data acquisition was stopped prior to the completion of the corrective action of the steering, thus the response characteristics did not attain the steady state zero response at the end of 10 seconds. The peak roll angle and the lateral acceleration response of the test vehicle are observed to be approximately 1.5 degrees and 0.25g respectively.

Figure 7.14 presents the response characteristics of a 50% filled tank vehicle for a 21.0 m (70 feet) lane change manoeuvre, at a vehicle speed of 45 km/h. The increase in the gate width from 15.0 m (50 feet) to 21.0 m (70 feet) reduces the maximum steer value required to negotiate the turn from 6 degrees to approximately 2.5 degrees, as shown in Figure 7.14. The corresponding peak value of the yaw angle reduces from 14 degrees to 9 degrees, along with the roll angle and lateral acceleration from 2 degrees to 1 degree, and 0.2g to 0.15g respectively. The reduction in the vehicle speed to 35 km/h reduces the roll and lateral acceleration response further, as shown in Figure 7.15. The experimental and the simulation results seem to compare very well except for the roll angle response which again is attributed to the cross-slope of the road surface.

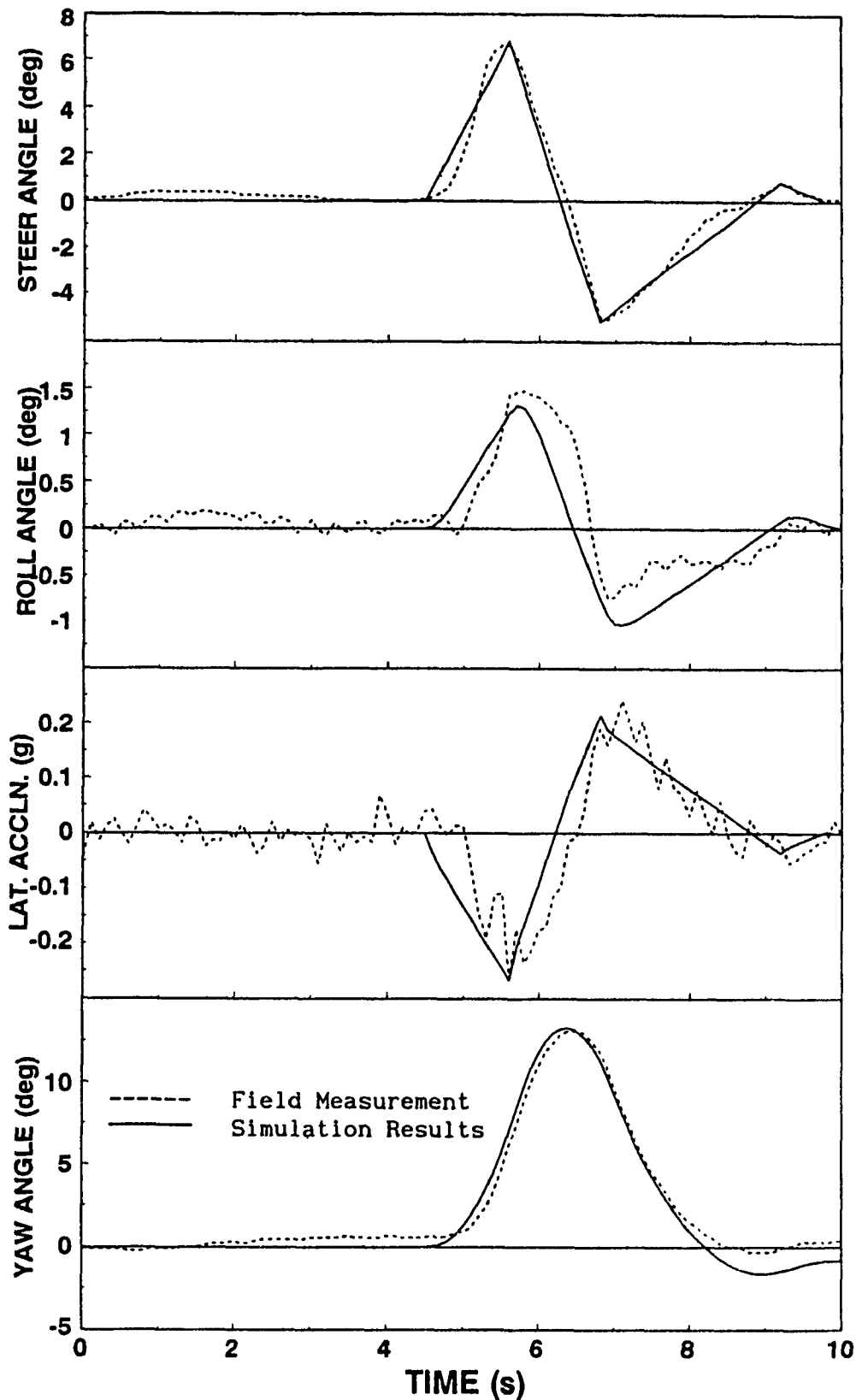


Figure 7.13 Comparison of experimental and simulation response of the 50% filled tank vehicle at a vehicle speed of 35 km/h, during a 15m lane change manoeuvre

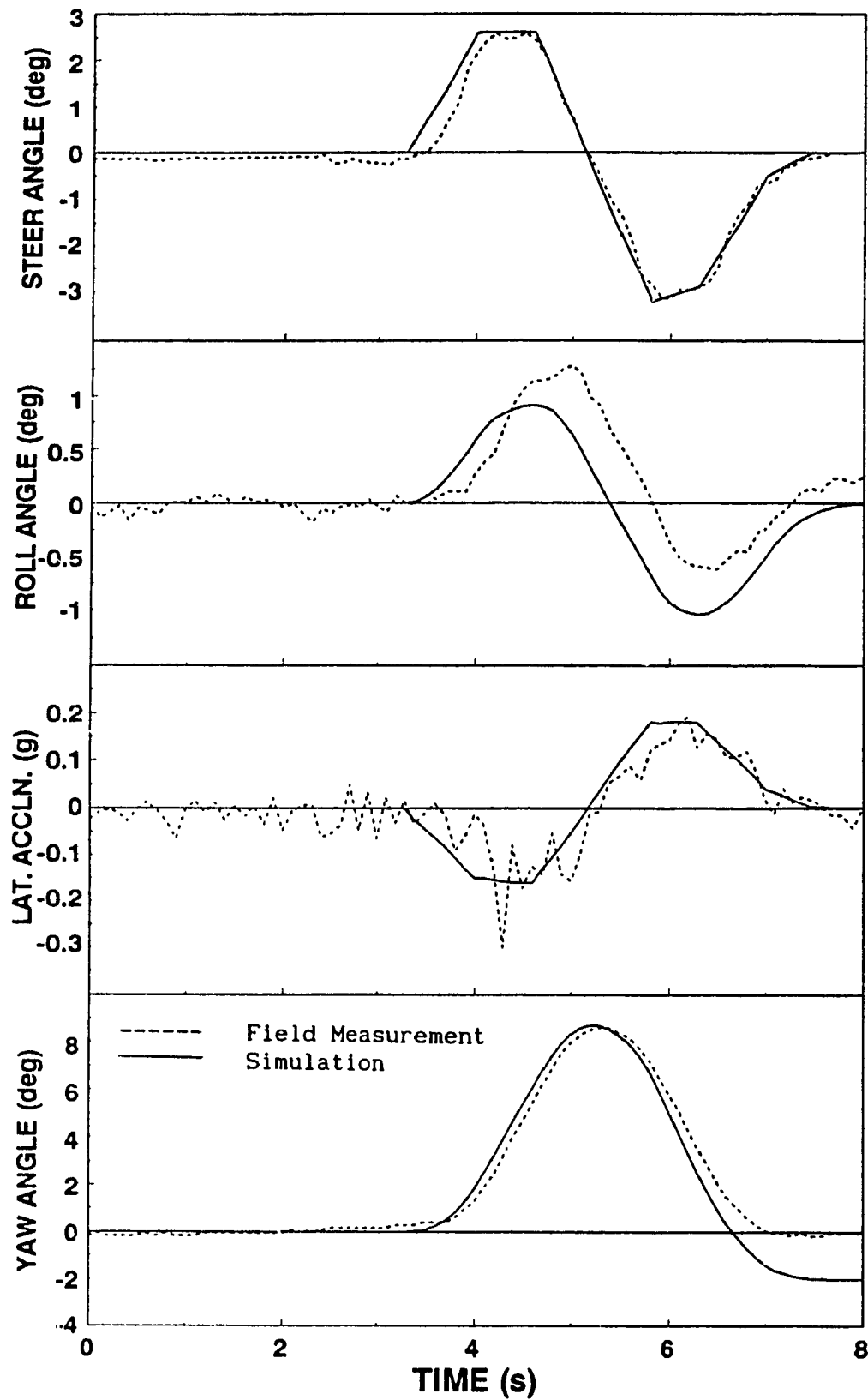


Figure 7 14 Comparison of experimental and simulation response of the 50% filled tank vehicle at a vehicle speed of 45 km/h, during a 21m lane change manoeuvre

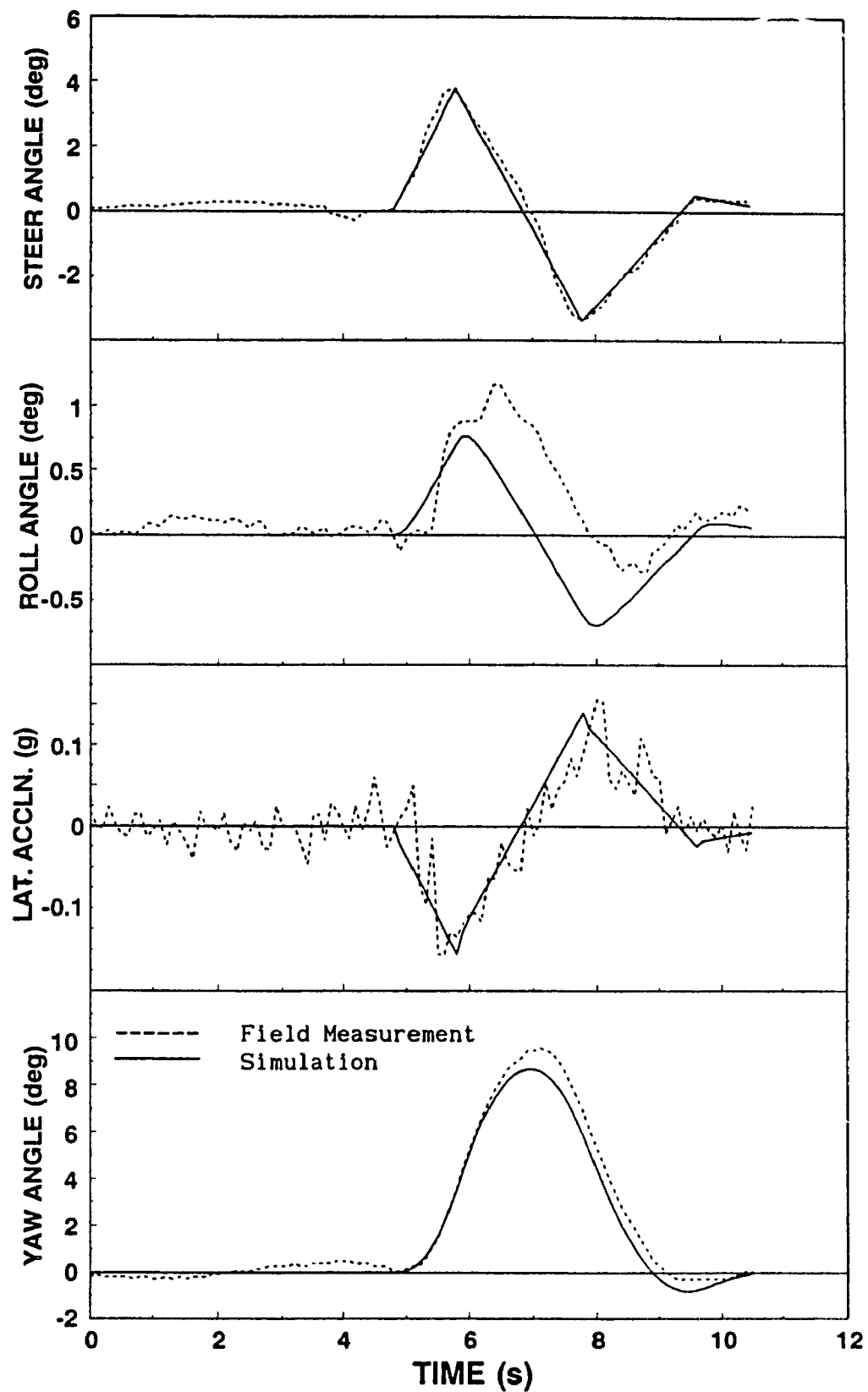


Figure 7.15 Comparison of experimental and simulation response of the 50% filled tank vehicle at a vehicle speed of 35 km/h, during a 21m lane change manoeuvre

The directional response characteristics of the 70% filled tank vehicle established via computer simulations are compared to those established from the field tests for a 15.0 m (50 feet) lane change manoeuvre conducted at a vehicle speed of 45 km/h, as shown in Figure 7.16. The field test response characteristics correlate very well with the simulation results, as indicated in Figure 7.16. Comparison of figures 7.12 and 7.16 reveals that the increase in the fill condition from 50% to 70% does not reveal a significant change in the response values due to the fact that the increase in the total payload as well as the change in the overall centre of mass height does not change very much. Further, the simulation vehicle experiences a small increase in the yaw angle while the test vehicle experiences a decrease in its response as the fill level is increased, indicating a possibility of an error in zero offsetting of the yaw angle during the test run.

7.5 Summary

The test vehicle, associated instrumentation and the test courses are briefly described. The field tests were conducted on a two-axle tractor equipped with a cylindrical tank made of a translucent plastic material. The test data obtained from the field were then imported into the "LOTUS" spread sheet along with the tank truck simulation results. The field test data is analyzed to examine the repeatability of the test and to validate the analytical vehicle model, developed in Chapter 4. The simulation results are compared to those established from the field tests. The comparison indicated a very good correlation for various fill conditions, vehicle speed, and manoeuvres. This correlation provides the necessary confidence to depend on the analytical models developed to study the tank vehicle dynamics.

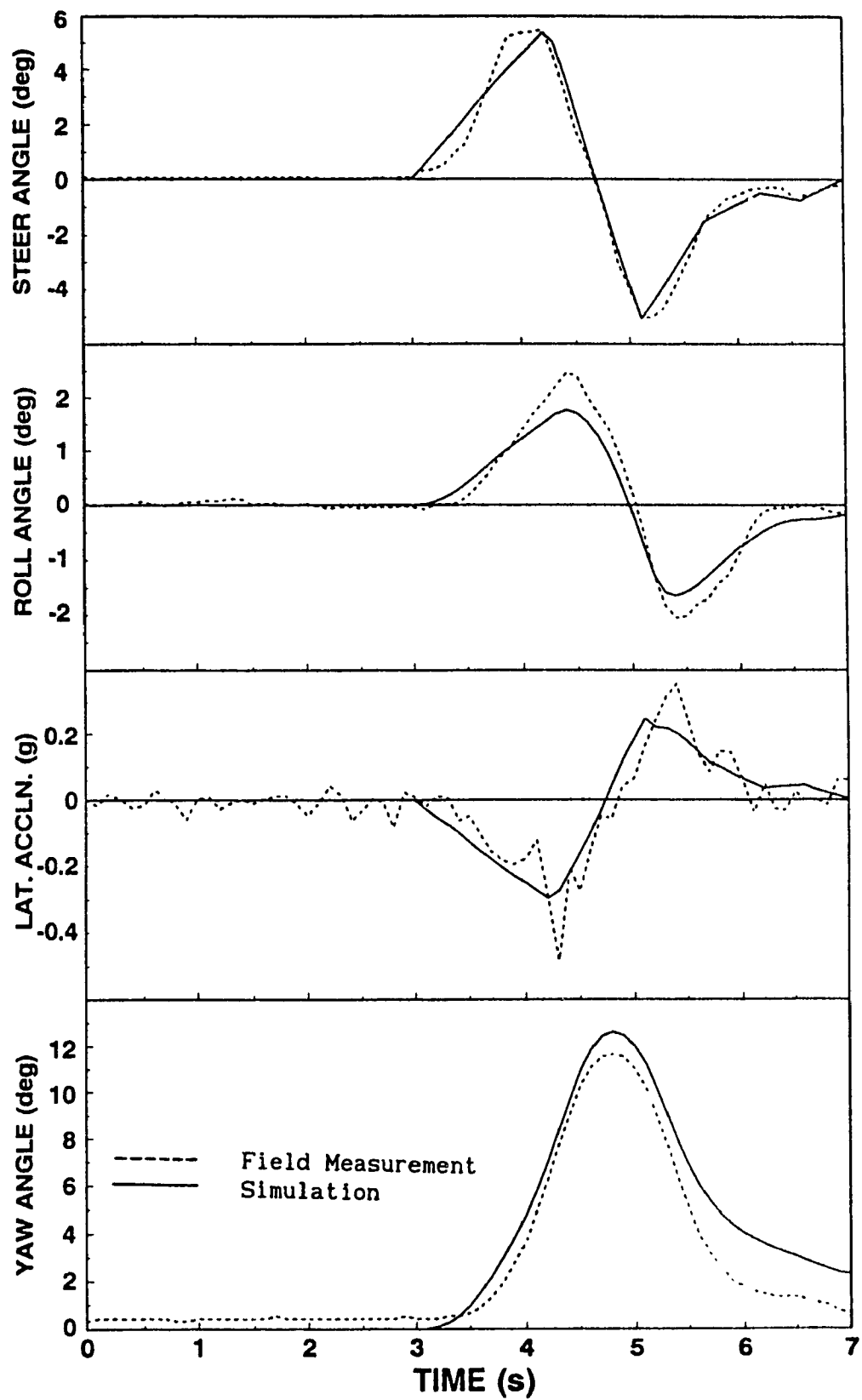


Figure 7.16 Comparison of experimental and simulation response of the 70% filled tank vehicle at a vehicle speed of 45 km/h, during a 15m lane change manoeuvre

REFERENCES FOR CHAPTER 7

1. Winkler, C.B., "Report on testing of the front and rear suspensions of a 1976 Ford L9000 truck", submitted to Ministry of Transportation for Ontario, April 1989.
2. Ervin, R.D., "RTAC study on Weights and Dimensions", Report on Test I, Aug. 1984.
3. Billing, J.R. et al, "Tests of a B-Train Converter Dolly", Ontario Ministry of Transportation and Communications Report No. TVS-CV-82-111, May 1983.

CHAPTER 8

CONCLUSIONS AND SUGGESTIONS FOR FUTURE RESEARCH

8.1 General

The adverse influence of liquid motion within a partially filled tank vehicle on roll stability and directional response characteristics is investigated through computer simulation. This study investigates the steady turning rollover threshold and the dynamic response characteristics of partially filled tank vehicles. The study focuses on quantifying the influence of the slosh forces and moments, arising from a partially filled tank, on the handling and stability of the tank vehicles. The influence of vehicle and tank design factors on the performance of the tank vehicles are also investigated. Three computer models are developed in order to analyze the static and dynamic stability of tank vehicles. The models include:

- (i) Steady turning (kineto-static) roll plane model for evaluating the rollover threshold limits of tank vehicles with arbitrary tank geometry.
- (ii) Quasi-dynamic yaw/roll model of tank vehicle incorporating steady-state liquid motion, for evaluating the directional characteristics and dynamic stability of the tank vehicle.
- (iii) A comprehensive vehicle model obtained by integrating the dynamic yaw/roll model of the tank vehicle with a non-linear fluid slosh model for investigating the directional behaviour of the liquid tank vehicle.

The validity of computer models is demonstrated by comparing the response characteristics obtained from computer simulation to those of the field measurements.

8.2 Highlights of the Investigation and Conclusions

Various tank vehicle combinations used for hauling dangerous goods across Canada were identified through a survey, to select the baseline vehicle configurations for the study. The survey revealed that the tractor-semitrailer tank vehicles (either 5- or 6-axles) are most often used on Canadian highways, followed by 7- or 8-axle B-Train tank vehicle combinations. The survey also identified the various tank cross-sections used in general purpose transportation.

8.2.1 Steady-Turning Stability Analysis

A kineto-static roll plane model of a partially filled arbitrarily shaped tank cross-section is developed and integrated to the roll plane model of the tank vehicle to investigate the steady turning stability of liquid tank vehicles. Tanks of various geometry are investigated for their load shift characteristics during steady turning. The load shift occurring in a partially filled tank vehicle during a steady turning is considerably influenced by the tank geometry, fill level, and lateral acceleration levels. The magnitude of lateral and vertical translation of the centre of mass of liquid within a partially filled tank increases with reduced fill levels. The lateral shift of liquid within a modified oval and square tanks is considerably larger than that in a circular tank. The vertical translation of the C.G. of liquid is relatively small compared to the lateral translation, and is relatively insignificant in the case of modified oval tanks.

The overturning limits of partially filled tank vehicles are considerably lower than those of equivalent rigid cargo vehicles. Tank vehicles exhibit lowest static rollover threshold limits around 40% fill conditions, compared to the equivalent rigid cargo vehicles. Tanks with

modified oval and square cross-sections yield lower values of overturning limits, due to the associated large lateral load shift. Under constant axle loading conditions, overturning limits of tank vehicles decrease when the fill level is reduced. The overturning limits of vehicles with equivalent rigid cargo, however, increases with reduced fill level for constant axle loading conditions.

Computer simulation of steady turning characteristics of a four compartmented tank of arbitrary geometry is also carried out. The effect of compartmenting of tank on the rollover limits is also established. The order of emptying the various compartments is established in order to obtain highest values of rollover threshold acceleration.

8.2.2 Directional Stability Analysis

The kineto-static roll plane model of the tank vehicle was followed by a quasi-dynamic yaw/roll model of the tank vehicle incorporating a steady-state fluid motion. The directional response characteristics of tank vehicle combinations, computed for constant and transient steer inputs, are compared to those of equivalent rigid cargo vehicles to demonstrate the influence of liquid load shift. Parametric sensitivity analyses are conducted in order to study the influence of fill level, axle loads, and vehicle speed on the directional response of tank vehicle combinations. The increase in vertical load on the outer track, due to the liquid load shift, develops unequal distribution of cornering forces between the two tracks, leading to considerable deviation in the path of the liquid tank vehicle compared to an equivalent rigid cargo vehicle. The distribution of the tire vertical loads during a dynamic manoeuvre depends on the fill level, steer input, and vehicle speed.

During a constant steer manoeuvre, the increase in vehicle speed from 60 km/h to 90 km/h, leads to increased roll and lateral acceleration response of the five-axle tractor tank semitrailer and possible rollover, while the equivalent rigid cargo vehicle exhibits stable characteristics.

A comparison of the dynamic characteristics of 5-axle and 6-axle tractor semitrailer tank vehicles, carrying maximum permissible load, reveals that the 6-axle tank vehicle is more stable compared to the 5-axle tank semitrailer vehicle. The partially filled tank vehicles as well as the equivalent rigid cargo vehicles exhibit stable behaviour during lane change manoeuvre, at typical highway speeds. The roll and lateral acceleration response of the partially filled tank vehicles, however, are considerably higher than those of the equivalent rigid cargo vehicles.

Partially filled tank vehicles are less stable compared to their equivalent rigid cargo vehicles in an emergency or an obstacle avoidance type of manoeuvre performed at highway speeds. The excessive load shift occurring during the evasive manoeuvre can lead to wheel lift-off and possible vehicle rollover. The roll and lateral acceleration amplification factors for a B-train tank vehicle computes the magnification of the dynamic response parameters of the rearmost trailer compared to the tractor. The amplification factors indicate the likelihood of trailer rollover.

8.2.3 Directional Stability Analysis incorporating Dynamic Fluid Slosh

The lateral and vertical load shifts computed using the steady-state fluid model is validated through a dynamic fluid slosh model. The dynamic fluid slosh model utilizes a finite difference

scheme to solve the non-linear fluid equations to compute the slosh forces and moments arising due to the fluid motion within the tank. The directional response characteristics of the tank vehicle, incorporating the dynamic liquid slosh model are compared to those of the vehicle incorporating the steady-state liquid model, in order to demonstrate the influence of dynamic slosh forces on the vehicle stability.

Computer simulations of tank vehicle model incorporating the dynamic fluid slosh model for a steady steer input indicate the directional response oscillates at its fundamental mode of vibration around a mean value. The frequency of oscillation lies close to the value derived using a linear theory. The directional response characteristics estimated using the quasi-dynamic vehicle model are found to be slightly higher than the mean value corresponding to the response estimated from the dynamic fluid slosh model. The simulation results reveal that the quasi-dynamic vehicle model can predict the directional response quite close to that evaluated from the comprehensive fluid slosh model. The quasi-dynamic model, however, overestimates the response characteristics in case of low frequency steer inputs, while a high degree of correlation is obtained for steer frequencies corresponding to typical highway manoeuvres.

8.2.4 Validation of Analytical Models

The computer simulation models are validated through experimental results obtained from field tests conducted on a tank truck equipped with a cylindrical tank. Results are obtained for a typical right turn and lane change manoeuvres at various vehicle speeds and compared to those obtained from the analytical models. Computer simulation results correlated well with field testing for various fill conditions, speed

and manoeuvres. This correlation provides the necessary confidence to depend on the analytical models.

8.3 Suggestions for Future Research

The investigations performed in this dissertation can be expanded further to enhance the capabilities of the tank vehicle models. A number of suggestions for future research are recommended here:

- (i) The assumption of composite axles considered in case of the steady turning (kineto-static) roll plane model can lead to errors in estimating rollover threshold limits of wide spread multi-axle semitrailers and semitrailer axles with different suspension characteristics. The model can be modified in order to represent the trailer and tractor suspensions and axles independently so that the rollover threshold of widely spaced tri- and quad-axle tractor-trailer combinations can be investigated.
- (ii) The yaw/roll model of the vehicle can be expanded further to include the simulation of braking, and combined braking and steering manoeuvres. The modification requires an additional longitudinal degree of freedom for the sprung masses and comprehensive tire models to incorporate the influence of the longitudinal slip on the forces and moments developed at the tire-road interface. Such a vehicle model will enable the study of jackknife instability. In order to investigate the influence of fluid slosh on the braking performance and vehicle jackknife, it is recommended to develop a three-dimensional model of the partially filled tank. The quasi-dynamic modeling technique can be applied to determine the magnitude of the longitudinal and lateral load shift, and the corresponding pitch and roll moments.

It is further recommended to investigate the slosh frequencies during acceleration/braking and braking in a turn, in order to examine the validity of the quasi-dynamic model of the tank vehicle for such manoeuvres.

- (iii) The influence of grade and cross-slope of the highway on the load transfer and the rollover threshold can also be investigated.
- (iv) Influence of longitudinal compartments on the roll stability performance of the vehicle should be investigated.
- (v) It is also recommended to investigate the anti-slosh devices, such as pressurized bladders to minimize the dynamic slosh.
- (vi) The influence of tire-road adhesion properties on wet and icy surfaces, on the dynamic stability of the tank vehicles should be investigated.
- (vii) The tire scrub arising during low-speed manoeuvres can be overcome using steerable axles. The influence of such axles on the dynamic response qualities of the articulated tank vehicles can be simulated by modifying the axle and constraint equations in the yaw/roll model.
- (viii) The study can be further expanded to include pre- and post-processors for the various models using graphical inputs.

APPENDIX I

DERIVATION OF EQUATIONS OF MOTION FOR THE KINETO-STATIC ROLL PLANE MODEL OF AN ARTICULATED TANK VEHICLE

I.1 General

The articulated tank vehicle is represented by a three composite axle vehicle model as shown in Figure I.1. The forces and moments acting on the roll plane of the vehicle are presented in Figure I.2. A total of 15 algebraic equations are required to define the roll plane equations of the articulated vehicle. The 15 equations are obtained from balancing roll moments and forces :

- (1) Roll moments acting on the sprung weights;
- (2) Roll moments acting on the unsprung weights;
- (3) Vertical suspension forces;
- (4) Vertical tire forces; and
- (5) Lateral tire forces.

The equations of motion for the roll plane model of an articulated tank vehicle are presented in the following section.

I.2 Roll Moments Acting on the Sprung Weights

The roll equilibrium equations are obtained from balancing the moments of all the forces acting on the sprung mass. The articulated tank vehicle is modeled as three sprung masses: tractor front and tractor rear sprung masses coupled through the torsional compliance of the tractor frame, and the trailer sprung mass coupled to the tractor rear sprung mass through the torsional compliance of the fifth wheel. The liquid bulk within the tank is modeled as a rigid bulk moving under the influence of the tank-trailer roll and lateral acceleration. The gradient of the free surface and hence the centre of gravity of the

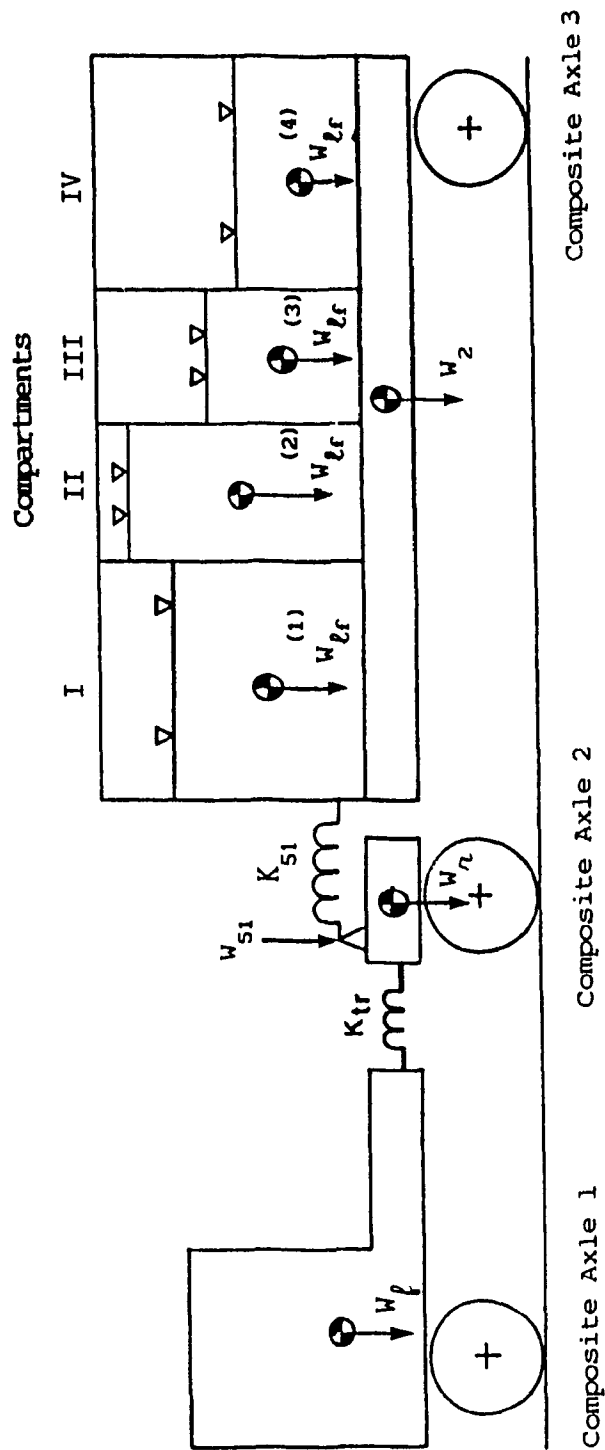


Figure 1.1 Representation of the tractor-tank semitrailer and the axles

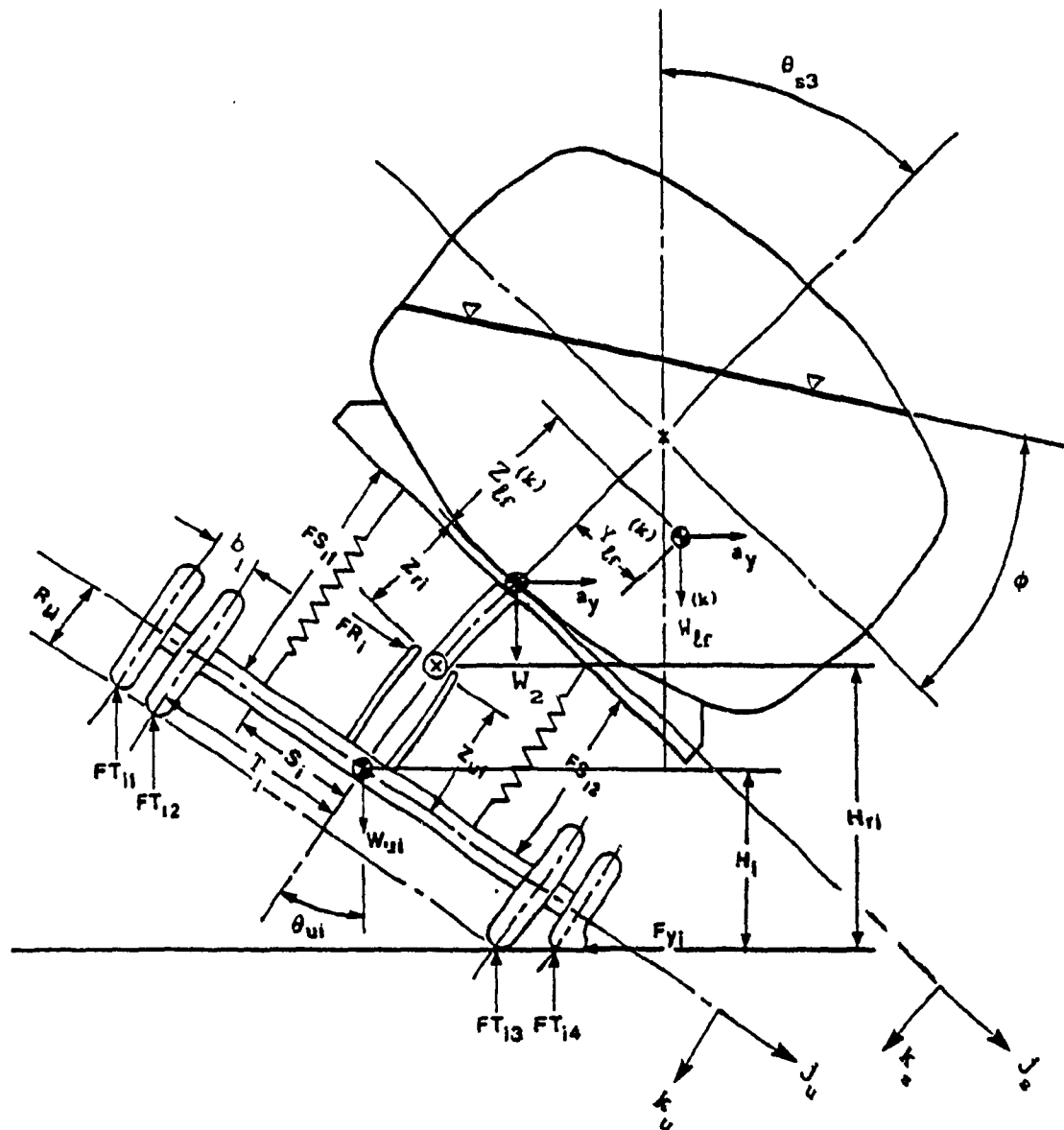


Figure 1.2 Forces and moments acting on the roll plane of a tank vehicle

liquid bulk is determined from the tank cross-section, fill condition, as explained in Chapter 2.

The roll moments acting on the sprung weights include moments due to the suspension forces, the lateral forces at the roll centre, torsional compliance of the tractor frame and the tank-semitrailer structure, the tractor frame shear force, lateral component of the sprung weight, and roll moments due to translation of liquid load in each compartment. Thus the equation of the sprung weights is obtained as:

$$\begin{aligned} (FS_{11} - FS_{12})s_1 + (FS_{11} + FS_{12})Z_{r1}(\theta_{s1} - \theta_{u1}) + F_{r1}Z_{r1} \\ + \alpha_1 + \beta_1 + \gamma_1 + \delta_1 + \xi_1 = 0 ; i = 1, 2, 3 \end{aligned} \quad (1.1)$$

where, FS_{ij} , is the suspension force due to all j springs on the i th axle, given by

$$FS_{ij} = K_{ij} \left[Z_{u1} + (-1)^j s_1 (\theta_{s1} - \theta_{u1}) \right] ; j = 1, 2 \quad (1.2)$$

F_{r1} , the force acting through the roll centre in direction parallel to j_u axis, is expressed by:

$$F_{r1} = W_{s1}(a_y - \theta_{u1}) \quad (1.3)$$

where

$$\begin{aligned} W_{s1} &= W_f + W_{fr} \\ W_{s2} &= W_r + W_{s1} - W_{fr} \\ W_{s3} &= W_2 + \sum_{k=1}^n W_{\ell r}^{(k)} - W_s \end{aligned}$$

and α_1 , β_1 , γ_1 , δ_1 and ξ_1 are the moments due to torsional compliance of

tractor frame (K_{tr}), shear force acting on the tractor frame (W_{fr}), vertical load on the fifth wheel (W_{s1}), torsional compliance of the fifth wheel and tank-semitrailer structure (K_{s1}), and the liquid load ($W_{lf}^{(k)}$), respectively acting on the i th composite axle ($i = 1, 2, 3$). They are expressed by:

$$\alpha_i = \begin{cases} (-1)^{i+1} K_{tr} (\theta_{s2} - \theta_{s1}) ; i = 1, 2 \\ 0 ; i = 3 \end{cases} \quad (I.4)$$

$$\beta_i = \begin{cases} (-1)^{i+1} W_{fr} (a_y - \theta_{s1}) Z_{f1} ; i = 1, 2 \\ 0 ; i = 3 \end{cases} \quad (I.5)$$

$$\gamma_i = \begin{cases} 0 ; i = 1 \\ (-1)^i W_{s1} Z_{s1} (a_y - \theta_{s1}) ; i = 2, 3 \end{cases} \quad (I.6)$$

$$\delta_i = \begin{cases} 0 ; i = 1 \\ (-1)^i K_{s1} (\theta_{s3} - \theta_{s2}) ; i = 2, 3 \end{cases} \quad (I.7)$$

$$\epsilon_i = \begin{cases} 0 ; i = 1, 2 \\ \sum_{k=1}^n W_{lf}^{(k)} [Y_{lf}^{(k)} (1 + a_y \theta_{s1}) + Y_{lf}^{(k)} (a_y \theta_{s1} + a_y \theta_{s1})] - \\ \sum_{k=1}^n W_{lf}^{(k)} [Z_{lf}^{(k)} (\theta_{s1} - a_y) + Z_{lf}^{(k)} (\theta_s - a_y)] ; i = 3 \end{cases} \quad (I.8)$$

The sprung weight roll equilibrium equation for small variation in

the sprung mass roll angle is expressed as:

$$\begin{aligned} & (K_{11} - K_{12})s_1 \Delta Z_{u1} - (K_{11} + K_{12})s_1^2 (\Delta \theta_{s1} - \Delta \theta_{u1}) + \\ & W_{s1} (\Delta a_y - \Delta \theta_{u1}) Z_{r1} + \Delta \alpha_1 + \Delta \beta_1 + \Delta \gamma_1 + \Delta \delta_1 \\ & \Delta \xi_i = 0; \text{ for } i = 1, 2, 3 \end{aligned} \quad (I.9)$$

I.3 Roll Moments Acting on Unsprung Weights

The equation for roll moments of the unsprung weights includes moments arising from suspension and tire forces, lateral forces acting through the roll centre, and lateral forces developed at the tires. The equation of roll equilibrium for the i th unsprung mass can be expressed as:

$$\begin{aligned} & (FS_{11} - FS_{12})s_1 + (FT_{11} - FT_{14})(T_1 + b_1) - (FT_{13} + FT_{14})y_1 \\ & + (FT_{12} - FT_{13})T_1 + F_{r1}Z_{u1} + F_{y1}H_1 + \left(\sum_{j=1}^4 FT_{1j} \right) R_{t1} \theta_{u1} = 0 \end{aligned} \quad (I.10)$$

FT_{1j} , the vertical force acting on the tires can be expressed as:

$$\begin{aligned} FT_{1j} &= KT_{1j} \left[\left\{ T_1 + (2 - j)b_1 \right\} \theta_{u1} - H_1 \right]; j = 1, 2 \\ FT_{1j} &= KT_{1j} \left[\left\{ T_1 + (j - 3)b_1 - y_1 \right\} \theta_{u1} + H_1 \right]; j = 3, 4 \end{aligned} \quad (I.11)$$

and F_{y1} , the total lateral force at the tire-road interface, is given by:

$$F_{y1} = (W_{s1} + W_{u1}) a_y \quad (I.12)$$

The unsprung weight roll equilibrium equation is expressed by

summing up all the moments for small variations in sprung mass roll angles :

$$\begin{aligned}
 & (K_{11} + K_{12})s_1^2(\Delta\theta_{s1} - \Delta\theta_{u1}) + (K_{11} - K_{12})s_1 \Delta Z_{u1} + \\
 & W_{s1}(a_y - \theta_{u1})\Delta Z_{u1} + (W_{s1} + W_{u1})(a_y \Delta H_{u1} + R_{t1} \Delta\theta_{u1}) \\
 & + W_{s1} Z_{u1} \Delta\theta_{u1} + (\Delta FT_{11} - \Delta FT_{14})(T_1 + b_1) \\
 & - (\Delta FT_{13} + \Delta FT_{14})y_1 - (FT_{13} + FT_{14})\Delta y_1 \\
 & + (\Delta FT_{12} - \Delta FT_{13})T_1 ; \text{ for } i = 1, 2, 3
 \end{aligned} \tag{I.13}$$

I.4 Forces Acting through the Suspension Springs

The forces generated by the compression/extension of the suspension springs must satisfy the following equilibrium equation :

$$FS_{11} + FS_{12} = W_{s1}(1 + a_y \theta_{u1}) \tag{I.14}$$

Upon substituting for suspension forces from (I.2), the vertical suspension force balance is expressed as:

$$(K_{11} + K_{12})Z_{u1} - (K_{11} + K_{12})s_1(\theta_{s1} - \theta_{u1}) - W_{s1}(1 + \theta_{u1} a_y) = 0 \tag{I.15}$$

For small variations in the vehicle parameters, the equation (I.15) is rewritten as :

$$\begin{aligned}
 & (K_{11} + K_{12})\Delta Z_{u1} - (K_{11} + K_{12})s_1(\Delta\theta_{s1} - \Delta\theta_{u1}) \\
 & - W_{s1}(\Delta\theta_{u1} a_y + \theta_{u1} \Delta a_y) = 0 ; i = 1, 2, 3
 \end{aligned} \tag{I.16}$$

I.5 Vertical Forces Generated by the Tires

The vertical load carried by each composite axle is assumed to remain constant, neglecting influence of grade and vehicle pitch. Thus, the following equilibrium equation must be satisfied:

$$(W_{s1} + W_{u1}) = \sum_{j=1}^4 FT_{1j} \tag{I.17}$$

Substituting for FT_{ij} from equation (I.11) and for small variations in the vehicle parameters, the tire forces are expressed as:

$$\begin{aligned} & [(-KT_{i1} + KT_{i4})(T_i + b_i) + (-KT_{i2} + KT_{i4})T_i \\ & - (KT_{i3} + KT_{i4})y_i] \Delta\theta_{ui} + (KT_{i1} + KT_{i2} + KT_{i3} + KT_{i4}) \Delta H_i \\ & + (KT_{i3} + KT_{i4}) \theta_{ui} \Delta y_i = 0 ; i = 1, 2, 3 \end{aligned} \quad (I.18)$$

I.6 Lateral Forces Generated by the Tires

When the lateral acceleration approaches the rollover limit of the tank vehicle, the tires on the outside of the turn carry almost the entire axle load. Thus, a lateral translation of the centroid of the normal pressure, acting between a tire and the road surface, is experienced. For a dual tire set, the lateral force experienced by the i th axle is expressed as:

$$F_{yi} = (KY_{i3} + KY_{i4}) y_i \quad (I.19)$$

The lateral force, F_{yi} is given by the inertial component, as shown in equation (I.12). Combining equations (I.12) and (I.19), and rewriting for small variations in vehicle parameters, we get

$$(KY_{i3} + KY_{i4}) \Delta y_i = (W_{si} + W_{ui}) \Delta a_y ; i = 1, 2, 3 \quad (I.20)$$

Equations (I.9) through (I.20) constitute the 15 equations required to describe the roll equilibrium of the tank vehicle during a steady turning manoeuvre.

APPENDIX II

DERIVATION OF EQUATIONS OF MOTION FOR THE DYNAMIC YAW/ROLL MODEL

II.1 General

The equations of motion for the dynamic yaw/roll model of an articulated tank vehicle are developed by integrating the equations of steady state fluid motion and the equations of an articulated rigid cargo vehicle [1]. Derivation of equations of motion is organized in the following steps:

- (1) Axis systems
- (2) Equations of motion for the sprung and unsprung masses
- (3) Suspension forces
- (4) Constraint forces and moments
- (5) Tire and spring forces

II.2 Axis System

The equations of motion of the tank vehicle model are developed using the following coordinate systems.

1. An inertial axis system fixed in space (i_n, j_n, k_n)
2. An axis system fixed to each of the sprung weights $(i_s, j_s, k_s)_f$, where $f = 1, \dots, \eta_s$, and η_s , the number of sprung units is given by,

$$\eta_s = \begin{cases} 2; & \text{tractor-semitrailer} \\ 3; & \text{B-train} \end{cases}$$

3. An axis system fixed to each of the unsprung weights $(i_u, j_u, k_u)_i$, where, $i = 1, \dots, \eta_a$, and η_a , the number of unsprung weights is given by,

$$\eta_a = \begin{cases} 5; & \text{five-axle tractor semitrailer} \\ 6; & \text{six-axle tractor semitrailer} \\ 7; & \text{seven-axle B-train} \end{cases}$$

4. An axis system fixed to the floating C.G of liquid $(i_\ell, j_\ell, k_\ell)_f$, $f = 2, \dots, \eta_\ell$, and η_ℓ , the number of liquid mass is given by,

$$\eta_\ell = \begin{cases} 2; \text{ tractor semitrailer} \\ 3; \text{ B-train} \end{cases}$$

II.2.1 Sprung Mass Axis System

The pitch plane and the coordinate system attached to a tank vehicle is presented in Figure II.1. Euler angles are used to define the orientation of the sprung and unsprung weights with respect to the inertial axis system. The instantaneous location of C.G and the moments of inertia of liquid mass are computed with respect to trailer sprung weight C.G. The three Euler angles required to represent the orientation of each of the sprung mass axis system with respect to the spatial inertial coordinates are yaw (ψ_{sf}), pitch (α_{sf}) and roll (θ_{sf}), as shown in Figure II.2. The axis system of each sprung weight is related to the inertial axis system by the following transformation:

$$\begin{Bmatrix} i_s \\ j_s \\ k_s \end{Bmatrix}_f = [D_1]_f^{-1} \begin{Bmatrix} i_n \\ j_n \\ k_n \end{Bmatrix} \quad (II.1)$$

where $f = 1, \dots, \eta_s$ and the transformation matrix $[D_1]_f$ is given by:

$$[D_1]_f = \begin{bmatrix} \cos \psi_s & -\sin \psi_s \cos \theta_s + \cos \psi_s \alpha_s \sin \theta_s & \sin \psi_s \sin \theta_s + \cos \psi_s \alpha_s \cos \theta_s \\ \sin \psi_s & \cos \psi_s \cos \theta_s + \sin \psi_s \alpha_s \sin \theta_s & -\cos \psi_s \sin \theta_s + \sin \psi_s \alpha_s \cos \theta_s \\ -\alpha_s & \sin \theta_s & \cos \theta_s \end{bmatrix}_f \quad (II.2)$$

II.2.2 Sprung Mass Angular Velocities

The equations of each sprung mass f are written in terms of the

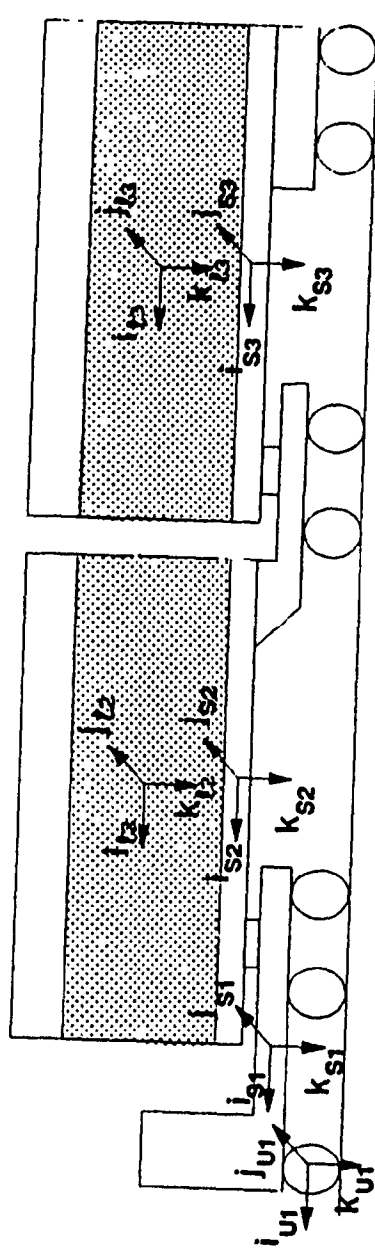
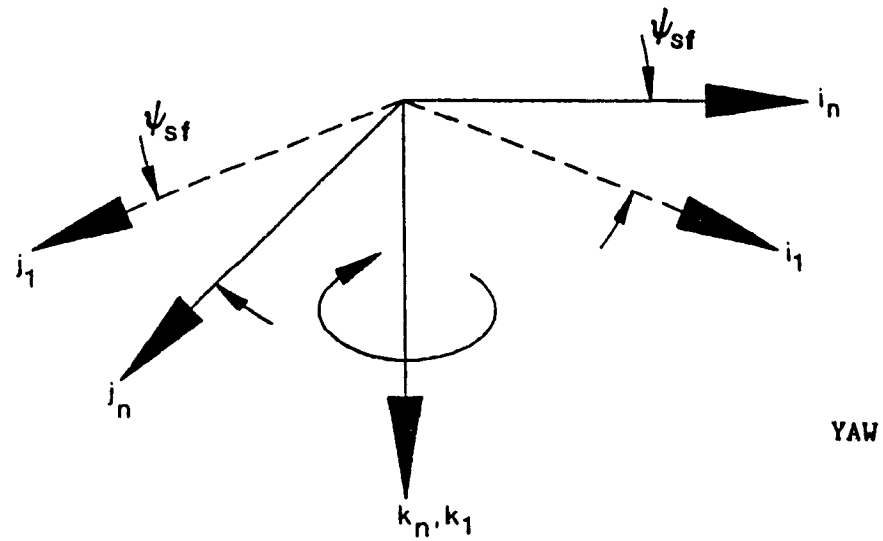
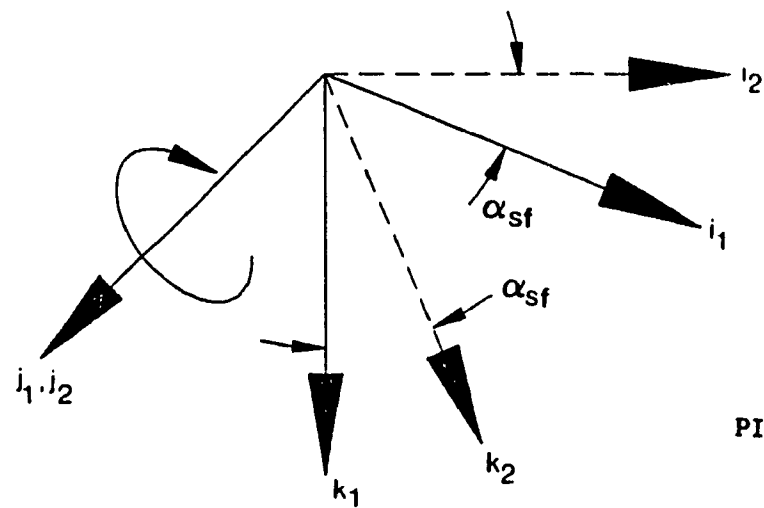


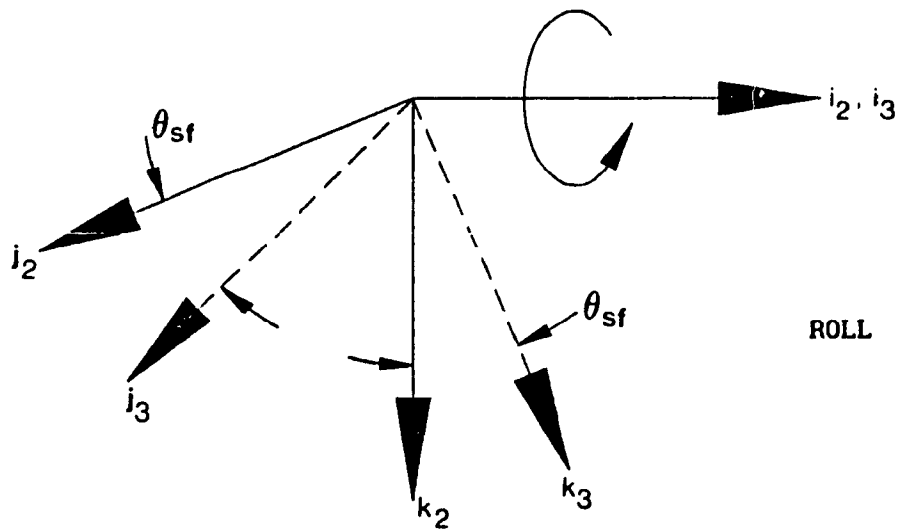
Figure II.1 Pitch plane and the coordinate system attached to an articulated tank vehicle



YAW



PITCH



ROLL

Figure II.2 Euler angle representation of the sprung mass axis system

body fixed angular velocities (p_f, q_f, r_f) and their derivatives. The Euler angles are computed via numerical integration of the Euler angular velocities ($\dot{\theta}_{sf}, \dot{\alpha}_{sf}, \dot{\psi}_{sf}$), expressed in terms of the body fixed velocities. The Euler angular velocities are expressed along the coordinates ($\vec{i}_s, \vec{j}_2, \vec{k}_n$). Therefore, equating the body fixed velocities to the Euler angular velocities and transforming them to a single coordinate frame, we get

$$\dot{\theta}_{sf} = p_f + \alpha_{sf}(q_f \sin\theta_{sf} + r_f \cos\theta_{sf}) \quad (II.3)$$

$$\dot{\alpha}_{sf} = q_f \cos\theta_{sf} - r_f \sin\theta_{sf} \quad (II.4)$$

$$\dot{\psi}_{sf} = q_f \sin\theta_{sf} + r_f \cos\theta_{sf} \quad (II.5)$$

Equations (II.3) to (II.5) are integrated numerically to solve for the Euler angles at any time during the simulation.

II.2.3 Unsprung Mass Axis System

Each unsprung mass is permitted to roll and bounce with respect to the sprung mass to which it is attached. Hence the orientation of the unsprung mass with respect to the sprung mass axis system can be defined by the following transformation (Figure II.3):

$$\begin{Bmatrix} i_u \\ j_u \\ k_u \end{Bmatrix}_i = [D_2]_i^{-1} \begin{Bmatrix} i_s \\ j_s \\ k_s \end{Bmatrix}_f \quad (II.6)$$

where $i = N_1, \dots, N_2$ for $f = 1, \dots, \eta_s$ and the transformation matrix $[D_2]_i$ is given by:

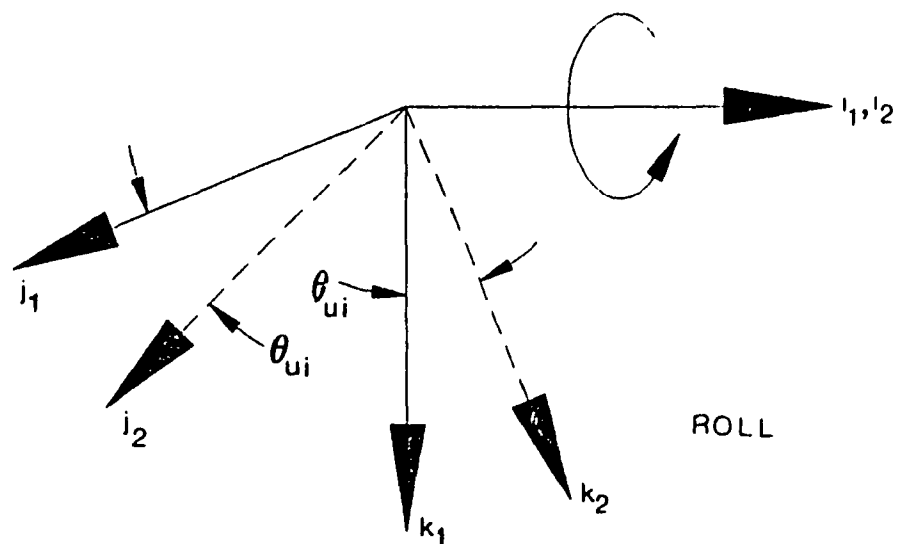
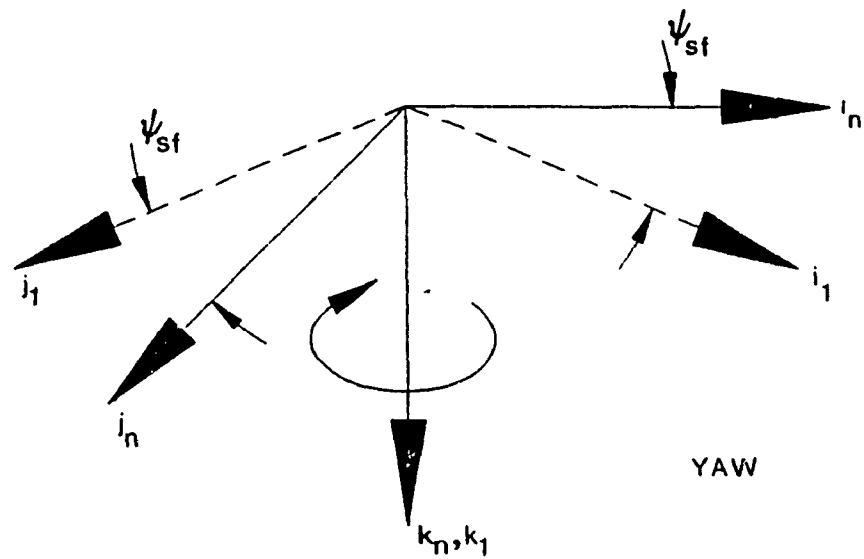


Figure II.3 Euler angle representation of the unsprung mass axis system

$$[D_2]_i = \begin{bmatrix} 1 & -\alpha_{sf} \sin \theta_u & -\alpha_{sf} \cos \theta_u \\ \alpha_{sf} \sin \theta_{sf} & \cos(\theta_{sf} - \theta_u) & \sin(\theta_{sf} - \theta_u) \\ \alpha_{sf} \cos \theta_{sf} & -\sin(\theta_{sf} - \theta_u) & \cos(\theta_{sf} - \theta_u) \end{bmatrix}_i \quad (II.7)$$

$$\text{where } N_1 = \begin{cases} 1 \\ 4 \\ 6 \end{cases}; \quad N_2 = \begin{cases} 3 \\ 5 \\ 7 \end{cases} (6)^1; \quad \text{for } f = \begin{cases} 1 \\ 2 \\ 3 \end{cases} \quad (II.8)$$

II.3 Equations of Motion

Figure II.4 presents the forces and moments acting on the roll plane of an articulated tank vehicle. The motion of each sprung mass is described by five second order differential equations and the motion of each unsprung mass is described by two differential equations.

II.3.1 Equations of Motion for the Sprung Masses

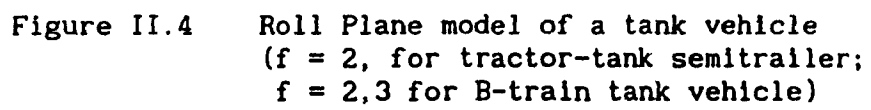
Lateral Force Equations

$$m_f a_{f sf} \vec{j}_{sf} + m_{lf} a_{lf sf} \vec{j}_{sf} = (\text{Lateral forces from the Constraints}) \\ + \sum_{i=N_1}^{N_2} \left[F_{ri} - (FS_{i1} + FS_{i2})(\theta_{sf} - \theta_{ui}) \right] + (m_f + m_{lf}) g \theta_{sf} \quad (II.9)$$

Vertical Force Equations

$$m_f a_{f sf} \vec{k}_{sf} + m_{lf} a_{lf sf} \vec{k}_{sf} = (\text{Vertical forces from the Constraints}) \\ + \sum_{i=N_1}^{N_2} \left[F_{ri} (\theta_{sf} - \theta_{ui}) + (FS_{i1} + FS_{i2}) \right] + (m_f + m_{lf}) g \quad (II.10)$$

¹ for a tri-axle tractor semitrailer



Roll Moment Equations

$$\begin{aligned}
 (I_{xf} + I_{xlf}) \dot{p}_f - (I_{yf} + I_{ylf} - I_{zf} - I_{zlf}) q_f r_f = \\
 \text{(Roll Moments from the Constraints) +} \\
 \sum_{i=N_1}^{N_2} \left[(FS_{i1} + FS_{i2})(\theta_{sf} - \theta_{ui}) Z_{ri} - F_{ri} Z_{ri} + (FS_{i1} + FS_{i2}) s_i \right] \\
 + m_{lf} a_{lf} \vec{j}_{sf} Z_{lf} + m_{lf} a_{lf} \vec{k}_{sf} Y_{lf} + m_{lf} g (\theta_{sf} Z_{lf} + Y_{lf}) \quad (II.11)
 \end{aligned}$$

Pitch Moment Equations

$$\begin{aligned}
 (I_{yf} + I_{ylf}) \dot{q}_f - (I_{zf} + I_{zlf} - I_{xf} - I_{xlf}) p_f r_f = \\
 \text{(Pitch Moments from the Constraints) +} \\
 \sum_{i=N_1}^{N_2} \left[\left\{ (FS_{i1} + FS_{i2}) + F_{ri}(\theta_{sf} - \theta_{ui}) \right\} X_{ui} \right] - m_{lf} a_{lf} \vec{k}_{sf} X_{lf} \\
 - m_{lf} a_{lf} \vec{i}_{sf} Z_{lf} - m_{lf} g (X_{lf} + \alpha_{sf} Z_{lf}) \quad (II.12)
 \end{aligned}$$

Yaw Moment Equations

$$\begin{aligned}
 (I_{zf} + \sum_{i=N_1}^{N_2} I_{zui} + I_{zlf}) \dot{r}_f - (I_{xf} + I_{xlf} - I_{yf} - I_{ylf}) p_f q_f = \\
 \text{(Yaw Moments from the Constraints) +} \\
 \sum_{i=N_1}^{N_2} \left[\left\{ F_{ri} - (FS_{i1} + FS_{i2})(\theta_{sf} - \theta_{ui}) \right\} X_{ui} + \sum_{j=1}^4 AT_{ij} \right] + \\
 m_{lf} a_{lf} \vec{i}_{sf} Y_{lf} + m_{lf} a_{lf} \vec{j}_{sf} X_{lf} \quad (II.13)
 \end{aligned}$$

II.3.2 Equations of Motion for the Unsprung Masses

Roll Moment Equations

$$I_{xui} \dot{p}_{ui} = -(FS_{i1} - FS_{i2})s_i - F_{ri}Z_{ui} - \sum_{j=1}^4 (FT_{ij}\theta_{ui} + FY_{ij})(H_{ri} - Z_{ui}) \\ + (FT_{i2} - FT_{i4})(T_i + y_i) + (FT_{i2} - FT_{i3})T_i \quad (11.14)$$

Vertical Force Equations

$$m_{ui} a_{ui} \vec{k}_{ui} = (FS_{i1} + FS_{i2}) - \sum_{j=1}^4 (FT_{ij} + FY_{ij}\theta_{ui}) + m_{ui}g \quad (11.15)$$

where a_f is the accelerations of the sprung mass f given by:

$$a_f = (\dot{u}_f + q_f w_f - r_f v_f) \vec{i}_{sf} + (\dot{v}_f - p_f w_f + r_f u_f) \vec{j}_{sf} \\ + (\dot{w}_f + p_f v_f - q_f u_f) \vec{k}_{sf} ; f = 1, \dots, \eta_s \quad (11.16)$$

and a_{lf} 's, are the accelerations of the liquid masses expressed by:

$$a_{lf} = a_f + a_{lf/f} ; f = 2, \dots, \eta_l \quad (11.17)$$

where $a_{lf/f}$ is the acceleration of liquid C.G. with respect to the C.G. of the tank trailer f , given by:

$$a_{lf/f} = (\dot{q}_f Z_{lf} - \dot{r}_f Y_{lf} - q_f^2 X_{lf} + p_f q_f Y_{lf} + r_f p_f Z_{lf} - r_f^2 X_{lf}) \vec{i}_{sf} \\ + (-\dot{p}_f Z_{lf} + \dot{r}_f X_{lf} - p_f^2 Y_{lf} + p_f q_f X_{lf} + r_f q_f Z_{lf} - r_f^2 Y_{lf}) \vec{j}_{sf} \\ + (\dot{p}_f Y_{lf} - \dot{q}_f X_{lf} - p_f^2 Z_{lf} + p_f r_f X_{lf} - r_f q_f Y_{lf} + q_f^2 Z_{lf}) \vec{k}_{sf} \quad (11.18)$$

where the linear and rotational velocities of the sprung mass f along the sprung mass coordinates are given by (u_f, v_f, w_f) and (p_f, q_f, r_f) respectively. (X_{lf}, Y_{lf}, Z_{lf}) are the coordinates of the instantaneous center of mass of liquid with respect to the tank trailer C.G. and p_{ui} is the roll velocity of the axle i .

II.4 Suspension Forces

Figure II.4 presents the forces and moments acting on the roll plane of an articulated tank vehicle. The suspension springs are assumed to remain parallel to the \vec{k}_{ul} axis of the unsprung mass, and are capable of transmitting either compressive or tensile forces only. All forces perpendicular to the suspension springs are assumed to act through the roll center, located at a fixed distance Z_{r1} , beneath the sprung mass C.G. and is permitted to slide along the \vec{k}_{ul} axis. The total suspension forces, FS_r transmitted to the sprung mass from the axle i is given by,

$$FS_r = F_{r1} \vec{j}_{ul} - (FS_{11} + FS_{12}) \vec{k}_{ul} \quad (II.19)$$

The suspension forces are defined in the sprung mass coordinate system by applying the coordinate transformation expressed by equations (II.2). Upon applying the transformation, we get:

$$FS_r = F_{r1} [-\alpha_{sf} \sin \theta_{ul} \vec{i}_{sf} + \cos(\theta_{sf} - \theta_{ul}) \vec{j}_{sf} - \sin(\theta_{sf} - \theta_{ul}) \vec{k}_{sf}] - (F_{11} + F_{12}) [-\alpha_{sf} \cos \theta_{ul} \vec{i}_{sf} + \sin(\theta_{sf} - \theta_{ul}) \vec{j}_{sf} + \cos(\theta_{sf} - \theta_{ul}) \vec{k}_{sf}] \quad (II.20)$$

$$FS_r = [-F_{r1} \alpha_{sf} \sin \theta_{ul} + (F_{11} + F_{12}) \theta_{sf} \cos \theta_{ul}] \vec{i}_{sf} + [F_{r1} \cos(\theta_{sf} - \theta_{ul}) - (F_{11} + F_{12}) \sin(\theta_{sf} - \theta_{ul})] \vec{j}_{sf} - [F_{r1} \sin(\theta_{sf} - \theta_{ul}) + (F_{11} + F_{12}) \cos(\theta_{sf} - \theta_{ul})] \vec{k}_{sf} \quad (II.21)$$

The force, F_{r1} , acting through the roll center is an internal force which is eliminated by inspecting the dynamic equilibrium of the axle in the \vec{j}_{ul} direction. The equation for the lateral equilibrium of the axle is given by:

$$m_{u1} [a_{u1} \cdot \vec{j}_{u1}] = -F_{r1} + (FY_{11} + FY_{12} + FY_{13} + FY_{14}) \cos \theta_{u1} - (FT_{11} + FT_{12} + FT_{13} + FT_{14}) \sin \theta_{u1} + m_{u1} g \sin \theta_{u1} \quad (11.22)$$

Rearranging (11.22) to obtain F_{r1} , we get:

$$F_{r1} = -m_{u1} [a_{u1} \cdot \vec{j}_{u1}] + (FY_{11} + FY_{12} + FY_{13} + FY_{14}) \cos \theta_{u1} - (FT_{11} + FT_{12} + FT_{13} + FT_{14}) \sin \theta_{u1} + m_{u1} g \sin \theta_{u1} \quad (11.23)$$

The unknown acceleration of the unsprung mass, a_{u1} is obtained by differentiating the position vector of the axle location with respect to the sprung mass C.G. Hence, a_{ui} , the unsprung mass acceleration is expressed as:

$$a_{ui} = a_f + a_{ri/f} + a_{ui/ri} ; f = 1, \dots, \eta_s ; i = N_1 \text{ to } N_2 \quad (11.24)$$

where $a_{ri/f}$, relative acceleration at the roll center with respect to the C.G. of the sprung mass f and $a_{ui/ri}$, the relative acceleration at the C.G. of axle i with respect to the roll center, are computed by vector differentiation of the lever arm with respect to time

$$\vec{r}_{r1/f} = x_{r1} \vec{i}_{sf} + z_{r1} \vec{k}_{sf} \quad (11.25)$$

$$\dot{\vec{r}}_{r1/f} = \dot{\vec{r}}_{r1/f} = (\dot{z}_{r1} \vec{i}_{sf} + (-\dot{p}_f z_{r1} + x_{r1} \dot{r}_f) \vec{j}_{sf} - x_{r1} \dot{q}_f \vec{k}_{sf}) \quad (11.26)$$

$$a_{r1/f} = \ddot{\vec{r}}_{r1/f} = (\ddot{q}_f z_{r1} - \dot{x}_{r1} \dot{q}_f^2 + \dot{p}_f \dot{r}_f z_{r1} - x_{r1} \dot{r}_f^2) \vec{i}_{sf} + (-\dot{p}_f \dot{z}_{r1} + x_{r1} \ddot{r}_f + z_{r1} \dot{q}_f \dot{r}_f + x_{r1} \dot{q}_f \dot{p}_f) \vec{j}_{sf} + (-\dot{p}_f^2 z_{r1} + x_{r1} \dot{r}_f \dot{p}_f - z_{r1} \dot{q}_f^2 - x_{r1} \dot{q}_f \ddot{q}_f) \vec{k}_{sf} \quad (11.27)$$

Similarly, the term in the equation (11.24), $a_{ui/ri}$ can be derived as

$$\vec{r}_{ul/r1} = z_{ul} \vec{k}_{ul} \quad (II.28)$$

$$\vec{w}_{ul/r1} = \dot{\vec{r}}_{ul/r1} = \dot{z}_{ul} \vec{k}_{ul} - p_{ul} z_{ul} \vec{j}_{ul} \quad (II.29)$$

$$\begin{aligned} \vec{a}_{ul/r1} = \dot{\vec{w}}_{ul/r1} = \ddot{z}_{ul} \vec{k}_{ul} - (\dot{p}_{ul} z_{ul} + 2p_{ul} \dot{z}_{ul}) \vec{j}_{ul} - p_{ul}^2 z_{ul} \vec{k}_{ul} \\ + p_{ul} r_{ul} z_{ul} \vec{i}_{ul} \end{aligned} \quad (II.30)$$

Hence, combining (II.24), (II.27) and (II.30) and transforming the acceleration defined in the sprung mass coordinate system to the unsprung mass coordinates system, the acceleration of the unsprung mass can be obtained. The equation (II.22) then along with the above equations can be used to solve for the roll center forces, F_{r1} . The roll center force is expressed as:

$$\begin{aligned} F_{r1} = -m_{ul} [(\dot{u}_f + q_f w_f - r_f v_f + \dot{q}_f z_{r1} - x_{r1} q_f^2 + p_f r_f z_{r1} + x_{r1} r_f^2) \theta_{sf} \sin \theta_{ul} \\ + (\dot{v}_f + u_f r_f - p_f w_f - \dot{p}_f z_{r1} + x_{r1} \dot{r}_f + z_{r1} q_f r_f + x_{r1} q_f p_f) \cos(\theta_{sf} - \theta_{ul}) \\ - (\dot{w}_f + p_f v_f - q_f u_f - p_f^2 z_{r1} + x_{r1} r_f p_f - z_{r1} q_f^2 - x_{r1} q_f^2) \sin(\theta_{sf} - \theta_{ul}) \\ - (\dot{p}_{ul} z_{ul} - 2p_{ul} \dot{z}_{ul})] + (FY_{11} + FY_{12} + FY_{13} + FY_{14}) \cos \theta_{ul} \\ - (FT_{11} + FT_{12} + FT_{13} + FT_{14}) \sin \theta_{ul} + m_{ul} g \sin \theta_{ul} \end{aligned} \quad (II.31)$$

II.5 Constraint Forces and Moments

The differential equations (II.9) through (II.13), describing the motion of the sprung masses of the tank vehicle combinations, include the forces and the moments arising from the fifth wheel couplings. The constraint forces are evaluated from the kinematic expressions that relate the accelerations at the constraint point due to the sprung masses attached to it. The constraint moments are calculated as a function of the relative angular displacement of the sprung masses. The set of second order differential equations describing the motion of the

tank vehicle combination can be expressed as:

$$M \ddot{\mathbf{x}} = \mathbf{f}_c + N \mathbf{y} \quad (11.32)$$

where M is the inertia matrix, $\ddot{\mathbf{x}}$ is the acceleration vector, \mathbf{f}_c is the force vector comprising of gravitational, suspension and roll center forces, N is a transformation matrix containing vehicle dimensions and velocities, and \mathbf{y} is the vector of unknown constraint forces and moments to be evaluated from the constraint relationships. The kinematic constraint relationships that exist at the various constraint points can be written as follows:

$$a_{5f} = \begin{cases} a_f + a_{5f/f}; \text{ along } (\vec{i}_s, \vec{j}_s, \vec{k}_s)_f \\ \\ a_{f+1} + a_{5f/f+1}; \text{ along } (\vec{i}_s, \vec{j}_s, \vec{k}_s)_{f+1} \end{cases} ; f = 1, \dots, (\eta_s - 1) \quad (11.33)$$

a_{5f} is the acceleration of the fifth wheel constraint connecting the sprung masses f and $f + 1$, and $a_{5f/f}$ is the acceleration of the fifth wheel constraint f with respect to the sprung mass f . Equation (11.33), when transferred to a common sprung mass axis system, can be expressed as follows:

$$C \ddot{\mathbf{x}} = \mathbf{d} \quad (11.34)$$

where C is a matrix of the vehicle dimensions, and \mathbf{d} is a vector, containing displacements \mathbf{x} , velocities $\dot{\mathbf{x}}$, and vehicle dimensions.

The moments on sprung mass f due to the torsional compliance of the articulation c , (MX_{fc} and MY_{fc}) are evaluated from the relative angular displacement between the leading and the trailing units. Figure 11.5 shows the coordinate system attached to the typical fifth wheel arrangement and the relative angular displacements. The leading unit at the constraint point experiences a roll moment while the trailing unit

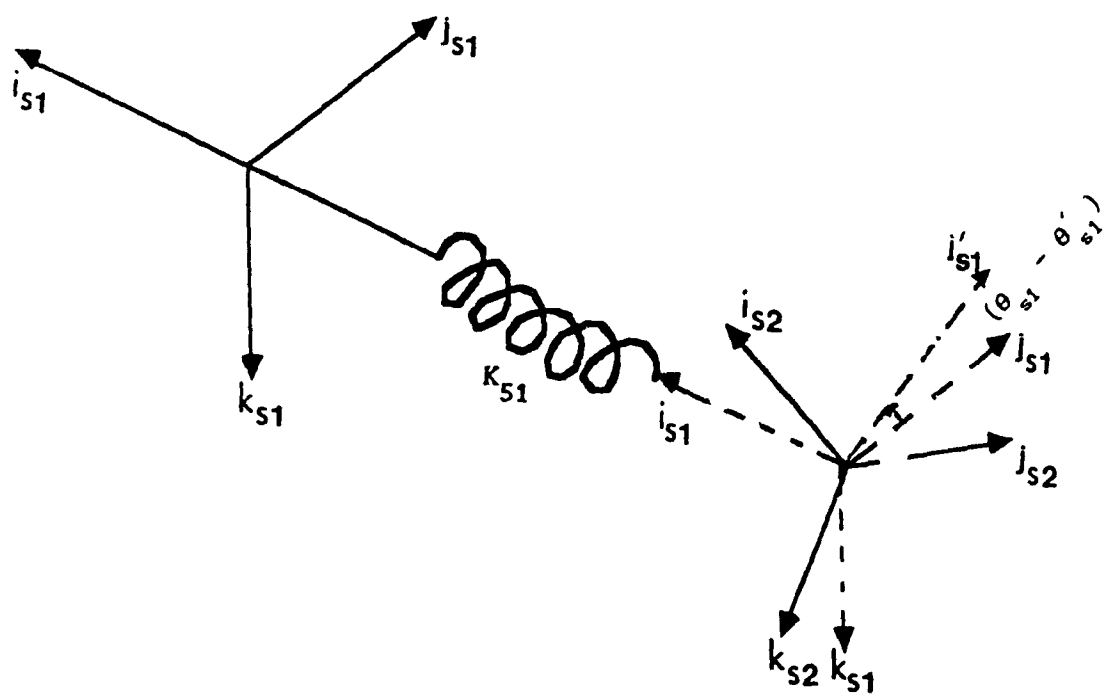


Figure II.5 Coordinate system attached to the fifth wheel arrangement

experiences a roll moment and a pitch moment computed by transforming the roll moments on the leading unit to the trailing unit. The roll moment acting on the tractor unit due to the constraint connecting the tractor and the semitrailer-A, MX_{11} , is computed from the product of the constraint stiffness K_{s1} and relative angular displacement resolved about the \vec{i}_{s1} coordinate, assuming small pitch and roll angles of both the units [2]. The roll and the pitch moments acting on the semitrailer-A, MX_{21} and MY_{21} respectively, are determined by the coordinate transformation of MX_{11} to the coordinates of the semitrailer-A. Similarly the moments acting on the semitrailer-A and semitrailer-B due to the constraint connecting them are expressed by the relative angular displacement. Hence, the net roll and pitch moment on the sprung mass f ($f = 1, \dots, \eta_s$), TMX_f , TMY_f are given by:

$$\begin{aligned} TMX_1 &= MX_{11} ; & TMX_2 &= MX_{21} + MX_{22} ; & TMX_3 &= MX_{32} ; \\ TMY_1 &= MY_{11} ; & TMY_2 &= MY_{21} + MY_{22} ; & TMY_3 &= MY_{32} ; \end{aligned} \quad (II.35)$$

where

$$\begin{aligned} MX_{11} &= K_{s1} \left[\theta_{s2} \cos(\psi_{s2} - \psi_{s1}) - \alpha_{s2} \sin(\psi_{s2} - \psi_{s1}) - \theta_{s1} \right] \\ MY_{11} &= MY_{22} = 0 \\ MX_{21} &= -MX_{11} \left[\cos(\psi_{s2} - \psi_{s1}) + \alpha_{s1} \alpha_{s2} \right] \\ MY_{21} &= -MX_{11} \left[\cos(\psi_{s2} - \psi_{s1}) \alpha_{s2} \sin \theta_{s2} - \alpha_{s1} \sin \theta_{s2} - \sin(\psi_{s2} - \psi_{s1}) \cos \theta_{s2} \right] \\ MX_{22} &= K_{s2} \left[\theta_{s3} \cos(\psi_{s3} - \psi_{s2}) - \alpha_{s3} \sin(\psi_{s3} - \psi_{s2}) - \theta_{s2} \right] \\ MX_{32} &= -MX_{22} \left[\cos(\psi_{s3} - \psi_{s2}) + \alpha_{s2} \alpha_{s3} \right] \\ MY_{32} &= -MX_{22} \left[\cos(\psi_{s3} - \psi_{s2}) \alpha_{s3} \sin \theta_{s3} - \alpha_{s2} \sin \theta_{s3} - \sin(\psi_{s3} - \psi_{s2}) \cos \theta_{s3} \right] \end{aligned} \quad (II.36)$$

The above set of equations can be appropriately reduced for the two sprung mass tractor-semitrailer vehicle combination.

The constraint force vector, y , is solved using equations (II.34) and (II.32). From (II.32),

$$\ddot{x} = M^{-1}f_c + M^{-1}Ny \quad (II.37)$$

Substituting (II.37) in (II.34), we get,

$$CM^{-1}f_c + CM^{-1}Ny = d \quad (II.38)$$

Upon solving (II.38) for the constraint forces, we obtain:

$$y = [CM^{-1}N]^{-1}\{d - CM^{-1}f_c\} \quad (II.39)$$

The set of differential equations given by equations (II.37) are solved by substituting (II.39) into (II.38), by doing so, we obtain:

$$\ddot{x} = M^{-1}f_c + M^{-1}N [CM^{-1}N]^{-1} \{d - CM^{-1}f_c\} \quad (II.40)$$

II.6 Computation of Tire Forces

The cornering forces generated at the tire-road interface are nonlinear function of the side slip angle and the vertical load on the tires. The side slip angle γ_{ij} , of the j th tire on axle i is expressed in terms of the body fixed velocities of the sprung mass f and the axle velocities:

$$\gamma_{ij} = \tan^{-1} \left[\frac{(v_i)_{\text{axle}}}{(u_{ij})_{\text{tire}}} \right] - \delta_i ; j = 1, 2, \dots, 4; \quad (II.41)$$

where the lateral velocity of axle i , $(v_i)_{\text{axle}}$ and the forward velocity of the tire j on axle i , $(u_{ij})_{\text{tire}}$ are expressed by the following equations:

$$\begin{bmatrix} v_i \end{bmatrix}_{\text{axle}} = \begin{bmatrix} v_f - Z_{ri} p_f \end{bmatrix} \cos \theta_{sf} + X_{ui} r_f / \cos \theta_{sf} - p_{ui} H_{ri} \cos \theta_{ui} \quad (11.42)$$

$$\begin{bmatrix} u_{ij} \end{bmatrix}_{\text{tire}} = \begin{cases} u_f + (-1)^j T_i r_f ; & \text{for } j = 2, 3 \\ u_f + (-1)^{j+1} (T_i + b_i) r_f ; & \text{for } j = 1, 4 \end{cases} \quad (11.43)$$

δ_1 is the front wheel steer and $\delta_i = 0$, $i = 2, \dots, 7$.

The vertical load on the j th tire on axle i , FT_{ij} is computed from the linear compliance of the tire KT_{ij} , expressed as:

$$FT_{ij} = KT_{ij} \Delta_{ij} \quad (11.44)$$

where Δ_{ij} is the vertical deflection of the tire j on axle i . The deflection of the outer most left tire on axle i is given by:

$$\begin{aligned} \Delta_{i1} = & \Delta_{i1}^0 + \Delta Z_f - Z_{ri} (1 - \cos \theta_{sf}) + Z_{ui} \cos \theta_{ui} \\ & - Z_{ui}^0 - (T_i + b_i) \sin \theta_{ui} - X_{ui} \alpha_f \end{aligned} \quad (11.45)$$

where Δ_{i1}^0 is the static tire deflection, ΔZ_f is the static deflection of the sprung mass C.G. along the vertical coordinate \vec{k}_n and Z_{ui}^0 is the initial height of the roll centre from the axle C.G. The deflection of the remaining three tires on axle i are given by:

$$\begin{aligned} \Delta_{i2} &= \Delta_{i1} + b_i \sin \theta_{ui} \\ \Delta_{i3} &= \Delta_{i2} + 2T_i \sin \theta_{ui} \\ \Delta_{i4} &= \Delta_{i3} + b_i \sin \theta_{ui} \end{aligned} \quad (11.46)$$

Equations (II.45) and (II.46) yield the vertical load on a given tire which permits the computation of lateral forces (FY_{ij}) and aligning moments (AT_{ij}) corresponding to the prevailing load and slip angles.

II.7 Computation of Spring Forces

The Spring forces acting on the axle i , FS_{i1} and FS_{i2} , are obtained from the vertical deflection of the springs, ξ_{i1} and ξ_{i2} , using the nonlinear force-deflection relationship for the suspension springs. ξ_{i1} and ξ_{i2} are computed as:

$$\begin{aligned}\xi_{i1} &= H_{ri} - H_{ui} - Z_{ui} + \xi_{i1}^0 - s_i \sin(\theta_{sf} - \theta_{ui}) + \Delta Z_f - X_{ui} \theta_{ui} \\ \xi_{i2} &= \xi_{i1} + 2 s_i \sin(\theta_{sf} - \theta_{ui})\end{aligned}\quad (II.47)$$

where ξ_{i1}^0 is the static spring deflection and s_i is half the suspension spread.

II.8 Description of the Closed Loop Driver Model

A closed loop driver model capable of predicting the vehicle steer using preview control, is integrated with the three-dimensional model of the tank vehicle combination in order to simulate the dynamic response characteristics under various highway manoeuvres. The driver model consists of two phases, (i) a prediction phase, in which the future path of the vehicle is estimated from the present state, and the error in the path of the vehicle from the desired path is estimated, (ii) driver reaction phase, which represents the dynamics of the driver. The driver lag is modeled as a dynamic system representing the human delays and dynamics.

The driver model [3] has been used to simulate and study the closed-loop steering control of commercial vehicles. Certain simplifying assumptions are made in order to study the closed-loop steering control of the vehicle: A linearized model of the tractor is used in the estimation of the future vehicle position, neglecting the influence of the roll dynamics and all semitrailer dynamics on the future trajectory of the vehicle. The driver model, always adapts to the linearized static load equivalent of the the nonlinear vehicle model, and does not update the vehicle to account for the nonlinear effects experienced by the vehicle during the simulation. Hence the driver model may not portray the realistic driver control for closed loop manoeuvres at or close to the vehicle limits.

Figure II.6 shows the basic kinematics involved in the preview control method of computing the closed loop steering angle. The dashed line represents the desired path trajectory and the solid line represents the estimated trajectory computed from the present steering control. The error in the position of the vehicle with respect to the desired trajectory is computed at a certain number of equidistant time intervals within the preview time of the vehicle. The steering control of the vehicle is then selected in order to minimize the sum of the squares of the errors:

$$\sum_{i=1}^N e_i^2 \quad (II\ 48)$$

where N is the number of intervals within the preview time and e is the error in the path of the vehicle. The trajectory of the vehicle within the preview time interval is obtained using a linearized yaw-plane model of the tractor. The linear dynamic equations of lateral and yaw motions of the tractor are given by:

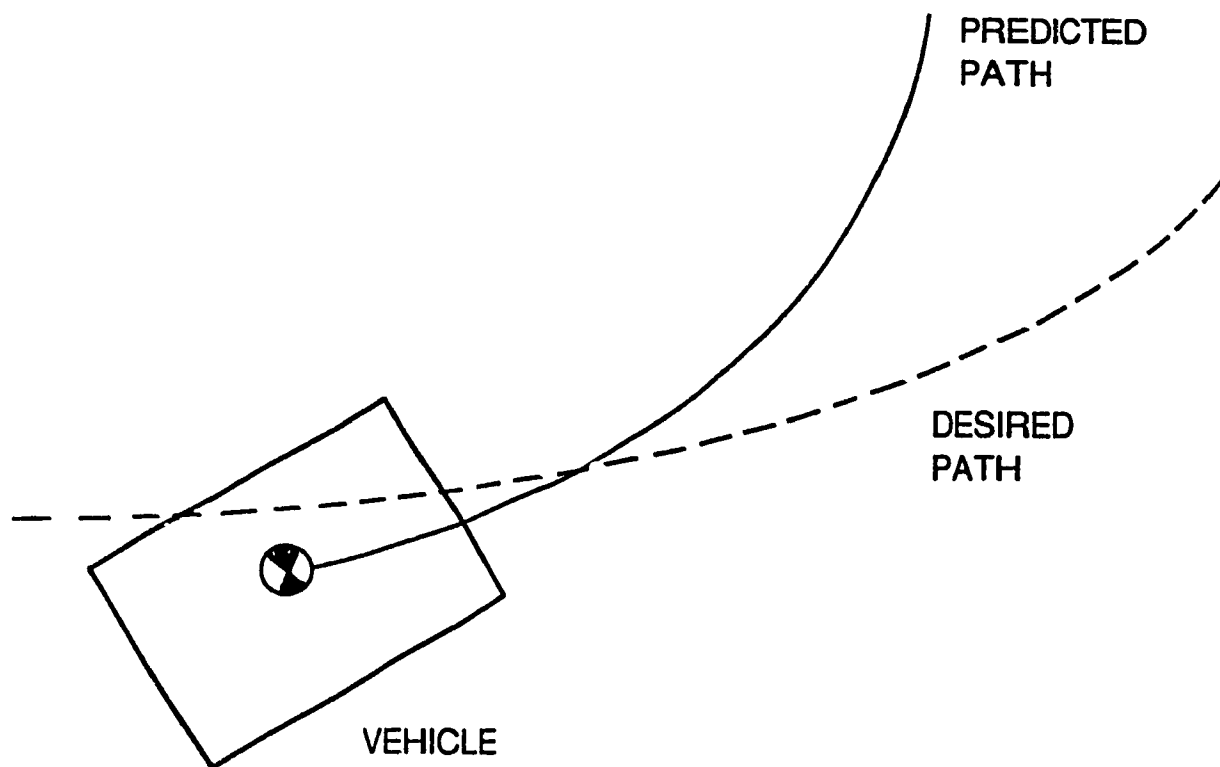


Figure II.6 Typical path geometry used in the preview control driver model

$$\dot{\mathbf{x}} = \mathbf{F}\mathbf{x} + \mathbf{g}\delta \quad (\text{II.49})$$

where

$$\mathbf{x} = \begin{Bmatrix} y \\ v \\ r \\ \Psi \end{Bmatrix} ; \quad \mathbf{g} = \begin{Bmatrix} 0 \\ C_1 \\ C_2 \\ 0 \end{Bmatrix} ; \quad \mathbf{F} = \begin{bmatrix} 0 & 1 & 0 & 0 \\ 0 & A_1 & B_1 & 0 \\ 0 & A_2 & B_2 & 0 \\ 0 & 0 & 1 & 0 \end{bmatrix}$$

and

$$A_1 = -2(C_f + C_r)/MU ; \quad B_1 = 2(bC_r - aC_f)/MU - U ; \quad C_1 = 2C_f/M ;$$

$$A_2 = 2(bC_r - aC_f)/IU ; \quad B_2 = -2(b^2C_r + a^2C_f)/IU ; \quad C_2 = 2aC_f/I ;$$

where

y	lateral displacement of the vehicle mass centre
v	lateral velocity in the vehicle body axis system
r	yaw rate about the body axis
Ψ	vehicle heading angle
δ	front tire steer angle, control variable
U	forward vehicle velocity
C_f, C_r	cornering stiffness of the tires on the front and rear axle
a, b	location of the front and rear tires from the Vehicle C.G
M, I	vehicle mass and the yaw moment of inertia

Figure II.7 shows the closed loop driver preview control model capable of predicting the steer input. The flow chart of preview control driver model implemented with the nonlinear vehicle model in order to compute the dynamic steer input is presented in Figure II.8. The steering control model uses the present lateral position, velocity and acceleration to estimate the future lateral vehicle position, $y(t + T)$, as

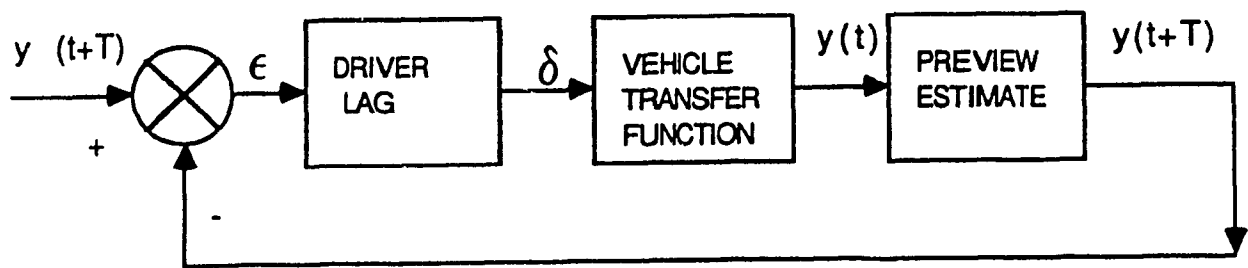


Figure 11.7 Representation of the preview control driver model

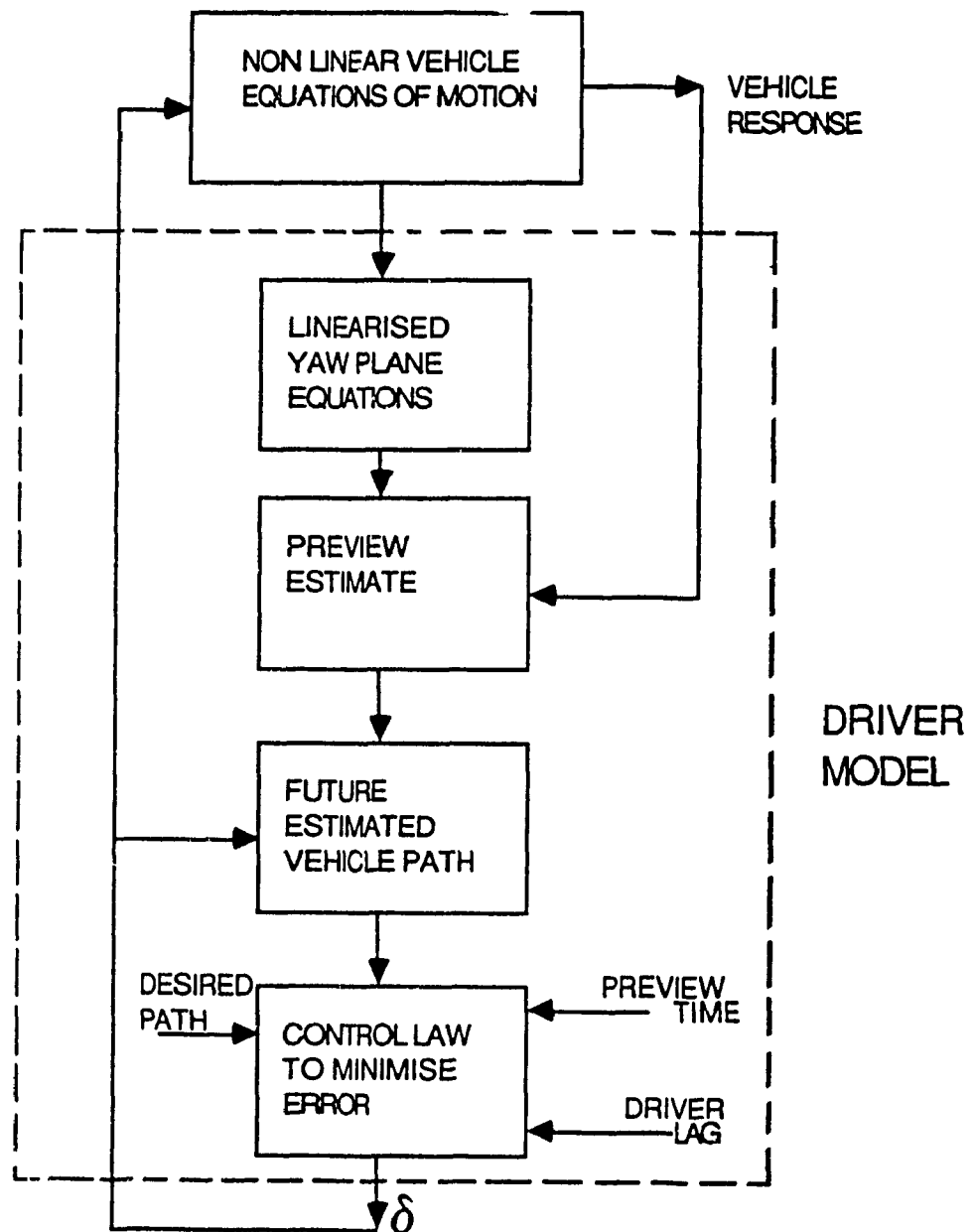


Figure 11.8 Implementation of the driver model in the vehicle simulation

$$y(t + T) = y(t) + \dot{y}(t) T + \ddot{y}(t) T^2/2 \quad (II.50)$$

where t is the current time, $y(t)$, $\dot{y}(t)$, $\ddot{y}(t)$ are the current lateral location, velocity and acceleration respectively. T is the interval of time ahead or the preview time. The closed loop optimal preview control equation for estimation of the steering is given by:

$$\delta(t) = H \varepsilon(t + T) \quad (II.51)$$

Assuming the transfer function H to account for the driver transport lag τ , is expressed by,

$$H = K e^{-s\tau} \quad (II.52)$$

where K , the preview control gain [3] selected to obtain a desired steering performance. The error in the path, $\varepsilon(t+T)$ is expressed as the difference in the vehicle predicted path and the desired path. Hence, the equation for the steering control (II.51) can be written as:

$$\delta(t) = K \left[y_p(t + T) - y(t + T) \right] e^{-s\tau} \quad (II.53)$$

where $y_p(t + T)$ is the actual path of the vehicle to be followed. The driver transport lag $e^{-s\tau}$ is approximated by the first order Padé polynomial as,

$$\frac{1 - \frac{\tau}{2} s}{1 + \frac{\tau}{2} s} \quad (II.54)$$

Equation (II.53) becomes,

$$\dot{\delta}(t) = \frac{2}{\tau} K \left[\varepsilon(t + T) - \frac{\tau}{2} \dot{\varepsilon}(t + T) \right] - \frac{2}{\tau} \delta \quad (II.55)$$

Equation (II.55) along with the equation (II.49) is solved simultaneously to find the steer input to the vehicle.

REFERENCES FOR APPENDIX II

1. Mallikarjunarao, C., "Road Tanker Design: its influence on the risk and economic aspects of transporting gasoline in Michigan", Ph.D. Thesis, University of Michigan, 1982.
2. Mikulcik, E.C., The Dynamics of Tractor-Semitrailer Vehicles: The Jackknifing Problem, SAE paper No. 710045.
3. MacAdam, C.C., "Application of an Optimal Preview Control for Simulation of Closed-loop Automobile Driving", IEEE Trans. on Systems, Man and Cybernetics, Vol. 11, No.6, pp 393-399, 1981.